frontiers | Research Topics

Methods in treating heart failure - device and surgery approach

Edited by
Jamshid Karimov and Antonio Loforte

Published in
Frontiers in Cardiovascular Medicine

ISSN 1664-8714
ISBN 978-2-8325-5400-5
DOI 10.3389/978-2-8325-5400-5

About Frontiers

Frontiers is more than just an open access publisher of scholarly articles: it is a pioneering approach to the world of academia, radically improving the way scholarly research is managed. The grand vision of Frontiers is a world where all people have an equal opportunity to seek, share and generate knowledge. Frontiers provides immediate and permanent online open access to all its publications, but this alone is not enough to realize our grand goals.

Frontiers journal series

The Frontiers journal series is a multi-tier and interdisciplinary set of open-access, online journals, promising a paradigm shift from the current review, selection and dissemination processes in academic publishing. All Frontiers journals are driven by researchers for researchers; therefore, they constitute a service to the scholarly community. At the same time, the *Frontiers journal series* operates on a revolutionary invention, the tiered publishing system, initially addressing specific communities of scholars, and gradually climbing up to broader public understanding, thus serving the interests of the lay society, too.

Dedication to quality

Each Frontiers article is a landmark of the highest quality, thanks to genuinely collaborative interactions between authors and review editors, who include some of the world's best academicians. Research must be certified by peers before entering a stream of knowledge that may eventually reach the public - and shape society; therefore, Frontiers only applies the most rigorous and unbiased reviews. Frontiers revolutionizes research publishing by freely delivering the most outstanding research, evaluated with no bias from both the academic and social point of view. By applying the most advanced information technologies, Frontiers is catapulting scholarly publishing into a new generation.

What are Frontiers Research Topics?

Frontiers Research Topics are very popular trademarks of the *Frontiers journals series*: they are collections of at least ten articles, all centered on a particular subject. With their unique mix of varied contributions from Original Research to Review Articles, Frontiers Research Topics unify the most influential researchers, the latest key findings and historical advances in a hot research area.

Find out more on how to host your own Frontiers Research Topic or contribute to one as an author by contacting the Frontiers editorial office: frontiersin.org/about/contact

Methods in treating heart failure - device and surgery approach

Topic editors
Jamshid Karimov — Cleveland Clinic, United States
Antonio Loforte — University of Turin, Italy

Citation
Karimov, J., Loforte, A., eds. (2024). *Methods in treating heart failure - device and surgery approach*. Lausanne: Frontiers Media SA. doi: 10.3389/978-2-8325-5400-5

Table of contents

frontiers | Frontiers in Cardiovascular Medicine

TYPE Editorial
PUBLISHED 22 May 2024
DOI 10.3389/fcvm.2024.1426133

OPEN ACCESS

EDITED AND REVIEWED BY
Michael Henein,
Umeå University, Sweden

*CORRESPONDENCE
Jamshid H. Karimov
karimoj.cc@gmail.com

RECEIVED 30 April 2024
ACCEPTED 13 May 2024
PUBLISHED 22 May 2024

CITATION
Karimov JH and Loforte A (2024) Editorial: Methods in treating heart failure—device and surgery approach.
Front. Cardiovasc. Med. 11:1426133.
doi: 10.3389/fcvm.2024.1426133

Editorial: Methods in treating heart failure—device and surgery approach

Jamshid H. Karimov[1,2,3]* and Antonio Loforte[4,5]

[1]Department of Biomedical Engineering, Lerner Research Institute, Cleveland Clinic, Cleveland, OH, United States, [2]Cleveland Clinic Lerner College of Medicine, Case Western Reserve University, Cleveland, OH, United States, [3]Kaufman Center for Heart Failure, Heart, Vascular, and Thoracic Institute, Cleveland Clinic, Cleveland, OH, United States, [4]Department of Surgical Sciences, University of Turin, Turin, Italy, [5]Transplant Center, City of Health and Science Hospital Turin, Turin, Italy

KEYWORDS

surgical techniques, heart failure, mechanical circulatory support, device therapies, surgical innovations

Editorial on the Research Topic
Methods in treating heart failure—device and surgery approach

Finding ways to deal with/treat patients with heart failure (HF) is one of the most serious issues facing the healthcare industry today. A primary contributor to cardiovascular mortality that affects approximately 64 million people worldwide, the prevalence of HF, is rising rapidly, even in developing nations (1). Despite exponentially evolving improvements and accelerating technological leaps for all healthcare industry stakeholders, treatment of cardiovascular disease has remained woefully stagnant. In healthcare, HF has held primacy as the most overwhelming burden on both patient morbidity and mortality, arguably driven by high incidence and its considerable detrimental effects. The following acknowledgement of works submitted to this topic, which are all critical works on HF, intend to provide a broad range of medical, therapeutic, and device options and to reflect the present landscape of surgical and technological armaneraium.

Nair addressed the need for improved risk prediction models using artificial intelligence (AI) technology for evaluations of the right ventricular failure after left ventricular device (LVAD) implantation, which remains a major cause of morbidity and mortality in this patient population. Nair provided compelling reviews of existing risk prediction scores, which included primary diagnostic features as well as limitations.

Cardoso et al., summarily reviewed new medical device-based (i.e., mechanical circulatory support) therapies, as well as the various mechanisms for decompensated HF. The article's classification scheme, collectively classified as (DRI_2P_2S), has been proposed to address the advanced device-based therapies by their mechanism of action: **D**ilators (increase venous capacitance), **R**emovers (direct removal of sodium and water), **I**notropes (increase left ventricular contractility), **I**nterstitials (accelerate removal of lymph), **P**ushers (increase renal arterial pressure), **P**ullers (decrease renal venous pressure), and **S**elective (selective intrarenal drug infusion).

Wang et al., reported on the first in-man application of the Liwen RF^{TM} ablation system. This open label, one-arm, prospective, non-randomized study used the system for treatment of drug-resistant hypertrophic obstructive cardiomyopathy. At follow up, amongst those patients excluded from either surgical myectomy (for now, considered

the "gold-standard" treatment for most patients) or alcohol septal ablation, the Liwen RF^{TM} demonstrated a significant reduction in left ventricular outflow obstruction and symptom relief.

Yu et al., described results from *in vivo* studies ($n = 2$) of hemodynamics and potential mechanisms that drive pulmonary circulation in status of ventricular fibrillation. Upon completion of implanting the continuous-flow LVAD (CF-LVAD) in ovine models, the HeartCon Ventricular Assist Device was used. Overall, study-findings underline the importance of the atrial rhythm and function for the circulation maintenance in patients with ventricular fibrillation post-CF-LVAD.

In their original research article, Wang X et al. described their experiences with a minimally invasive, transverse aortic-constriction model (C57BL/6J mice), investigating pressure overload-induced cardiac remodeling and HF. With specifically calibrated instrumentation, this method was found suitable for high-precision aortic contraction in mice that need high reproducibility and low post-operative mortality, holding potentially important research value with regards to cardiac remodeling and HF experimentation.

Funamoto et al. reported the group's early clinical report which shared clinical experience and patient outcomes with the next-gen surgical Impella 5.5. Patients with surgically implanted axillary Impella 5.5 showed optimal short-term survival rates. Axillary placement of the blood pump was used in a multitude of clinical indications (e.g., bridging strategy to durable support, implant LVAD and heart transplant, or perioperative support for high-risk cardiac surgery), all with excellent outcomes.

Zhou et al., investigated the exploratory efficacy of the D-Shant device for interatrial shunting in treating HF with reduced ejection fraction (HFrEF) and HF with preserved ejection fraction (HFpEF). The team of researchers also chose to study the predictive value of biventricular longitudinal strain for functional improvement in such patients. Improvements in both clinical- and functional-status were observed (at 6 months, post-implantation of atrium shunt device).

Schmitto et al. reported on the first clinical use of the left atrial appendage (LAA) for epicardial micrograft transplantation during LVAD implantation (in a 61-year-old male patient with dilated cardiomyopathy). The LAA micrograft transplant was successfully applied epicardially, in conjunction with LVAD implantation. In addition to potential therapeutic benefits, their approach facilitates gathering mechanistic proof of remodeling efficacy at all observed levels (i.e., functional, molecular, and structural).

Lee et al. investigated the differential outcomes of catheter ablation vs. medical treatment in patients with atrial fibrillation (AF) and HF. The cohort study was stratified by different left ventricular ejection fractions (LVEFs), New York Heart Association class ≥II, and different AF-types. Analysis showed improved LVEF, improved 6-min walk distance, less AF recurrence, and lower all-cause mortality. In favor of catheter ablation vs. medical treatment (in AF patients with HF and LVEF of 36%–50%), less HF hospitalization was observed by investigators. This was seen in AF patients with HF and LVEF ≤50% and LVEF ≤35%.

In a retrospective, single-center, observational study, Ma et al. analyzed the feasibility and outcomes of conduction system pacing (CSP) in HF patients with a severely reduced LVEF of less than 30% (HFsrEF). The CSP was found feasible and safe in patients with HFsrEF and was associated with significantly better clinical and echocardiographic outcomes.

With the underlying objective to conduct a dynamic and longitudinal bibliometric analysis of HF, Kuang et al. provided a comprehensive overview of machine learning applications in HF-associated diseases; the perspective of using AI in HF diagnosis and treatment has been emphasized. Dixit and Amsterdam discussed how revascularization should be prioritized at index hospitalization for newly diagnosed HFrEF patients at high risk for coronary artery disease (not presenting with acute coronary syndrome). Ultimately, the authors propose an algorithm for evaluation of ischemic cardiomyopathy in hospitalized patients with newly diagnosed HFrEF, utilizing strategies that could optimize the guidelines and directions of medical therapy outcomes.

Pyka et al., investigated potential benefits of mechanically supported revascularization for heart transplant candidates. The researchers shared a specific case-report, featuring a 53-year-old male heart transplant candidate with type 1 diabetes mellitus. In the study, the subject was initially considered unsuitable for revascularization and had already qualified for heart transplantation. The operating heart team opted for a high-risk mechanically supported percutaneous coronary intervention for revascularization. Several months post-procedure, the patient was no longer listed as a candidate for heart transplant. Overall, their findings suggested that—in select cases—a more thorough assessment of myocardial viability, with potential revascularization strategies, is critical for these patient populations.

Miyagi et al. showed anatomical- and virtual-fittings of two small-sized (i.e., pediatric and infant patients) continuous-flow total artificial heart pumps (CFTAHs) in congenital heart surgery patients. Performed at Cleveland Clinic on pediatric cardiac surgery patients ($n = 40$), the study used 3D-models of pediatric [P-CFTAH] and infant [I-CFTAH] blood pumps. An important landmark in pediatric blood-pump research, the investigators successfully demonstrated optimal dimensions for each of the pumps and proved them to be feasible in all enrolled patients, including those who were under 10 kg at the time of evaluation assessment.

Shen et al. retrospectively analyzed a total of 460 patients to elucidate the prognostic significance of serum albumin and thereby find the creatinine ratio (ACR) in patients receiving heart transplantation for end-stage HF. Their article also discussed efforts to identify potential correlations between ACR and the prognosis of heart transplantation (with optimal cut-off values), purportedly estimating prognosis in this complex patient population.

Overall, the underlying intention of this Frontiers topic was to discuss the HF therapeutics and treatment option landscape. From covering a representative array of sophisticated clinical and engineering tools currently utilized to investigate clinical gaps in treating HF, to discussing the growing number of viable, novel devices, to evaluating the sophisticated surgical approaches, our selected works are representative but by no means conclusive. Further research is needed to determine long-term evolution of any of the devices; for example, the observed shift in patient phenotypes over time would continue to imply that more devices

and treatment strategies should be elaborated. Another such area to examine would be these data points in heart transplant candidates who are less ill and not exclusively at end-stage HF. A regular continuation of research—clinical and data analysis—in addition and development is critical in order to evolve and enable the next generation of surgical techniques and device-based therapies. With time, these research efforts should be able to achieve effective neutralization of device-related complications and to drastically improve overall patient outcomes.

Author contributions

JK: Conceptualization, Writing – original draft, Writing – review & editing. AL: Conceptualization, Writing – original draft, Writing – review & editing.

Conflict of interest

The authors declare that the research was conducted in the absence of any commercial or financial relationships that could be construed as a potential conflict of interest.

Publisher's note

Reference

1. Savarese G, Becher PM, Lund LH, Seferovic P, Rosano GMC, Coats AJS. Global burden of heart failure: a comprehensive and updated review of epidemiology. *Cardiovasc Res*. (2023) 118(17):3272–87. doi: 10.1093/cvr/cvac013. Erratum in: *Cardiovasc Res*. (2023) 119(6):1453. PMID: 35150240.

frontiers | Frontiers in Cardiovascular Medicine

TYPE Opinion
PUBLISHED 14 September 2022
DOI 10.3389/fcvm.2022.848789

OPEN ACCESS

EDITED BY
Giulia Elena Mandoli,
University of Siena, Italy

REVIEWED BY
Cristiano Amarelli,
Azienda Ospedaliera dei Colli, Italy
Massimiliano Meineri,
Helios Kliniken, Germany

*CORRESPONDENCE
Nandini Nair
nandini.nair@gmail.com

SPECIALTY SECTION
This article was submitted to Heart Failure and Transplantation, a section of the journal Frontiers in Cardiovascular Medicine

RECEIVED 05 January 2022
ACCEPTED 25 July 2022
PUBLISHED 14 September 2022

CITATION
Nair N (2022) Use of machine learning techniques to identify risk factors for RV failure in LVAD patients. *Front. Cardiovasc. Med.* 9:848789. doi: 10.3389/fcvm.2022.848789

Use of machine learning techniques to identify risk factors for RV failure in LVAD patients

Nandini Nair*

Division of Cardiology, Department of Medicine, Texas Tech Health Sciences Center (TTUHSC), Odessa, TX, United States

KEYWORDS

left ventricular assist device (LVAD), machine learning, risk prediction models, RV failure, AI technology

Introduction

With increasing use of Mechanical Circulatory Support (MCS) in the last decade and its evolution currently as a standard therapy for patients with end stage heart failure (HF), it is becoming imperative to derive better risk prediction models to improve outcomes. The evolution of MCS and the transition from the older pulsatile-assist devices to the newer continuous flow pumps have ushered in an era of benefits for the HF with reduced ejection fraction population (1–8). However, challenges still persist in post implantation management in the long and short terms. Risk prediction models impact patient selection and, in turn, post-implantation outcomes. One of the most important factors influencing morbidity and mortality in the patients with left ventricular assist device (LVAD) is right ventricular failure (RVF). RVF can occur in ∼10–40% of cases, depending on the definition used to describe such failure (3–8). Several risk prediction models exist in the current literature, which predict RVF in patients with LVAD (9–16). This article attempts to address the need for improved risk prediction models using artificial intelligence (AI) technology.

Impact of RV failure on outcomes in the LVAD population

RVF after LVAD implantation is a major cause of morbidity and mortality in this population. Hence, early recognition of risk factors and taking appropriate steps to prevent RVF remain safest options. RVF occurs due to pre-implantation clinical characteristics of the patient, as well as intraoperative/perioperative issues that occur during these periods.

Preoperative RV dysfunction is a major factor in patients with end-stage HF whether ischemic or non-ischemic. Predisposing factors include development of chronic secondary pulmonary hypertension, mitral regurgitation (MR), and primary disease of the myocardium. Several parameters determined by invasive hemodynamic parameters from preoperative right heart catheterization, such as low RV stroke work

index (RVSWI), central venous pressure (CVP) to the pulmonary capillary wedge pressure (PCWP) ratio, with a ratio >0.63 associated with RV failure and pulmonary arterial pulsatility index (PAPi), are valuable in predicting RVF (11, 14, 17). Additionally, echocardiographic parameters, such as RA/RV size, the RV/LV ratio, left atrium volume index (LAVI), tricuspid annular plane systolic excursion (TAPSE), RV global free wall strain, and RV fractional area change (RVFAC), have all been used to predict RVF and tricuspid regurgitation severity (18).

RVF post LVAD implantation can be classified as acute (<48 h), early (>48 h–<14 days) and late (>14 days). *De novo* RV dysfunction can develop after LVAD implantation, while mild to moderate preoperative RV dysfunction can progress to frank RV failure due to intraoperative and perioperative factors. Cardioplegia leading to relative stunning of the RV myocardium has been noted. Cardiopulmonary bypass can itself initiate cytokine release, systemic inflammatory response syndrome (SIRS), and increased pulmonary vascular resistance (PVR) resulting in RVF.

Additionally, intraoperatively, myocardial ischemia, air embolism, mechanical compression of the PA, tamponade, and impact of LVAD circulation can result in RVF. Increased flow from the LV/LVAD and the consequent increase in venous return to the RV lead to increased RV preload. Loss of the septal contribution to overall RV function with paradoxical septal motion post LVAD implant can contribute to RVF. Despite the decrease in afterload post LVAD implant, the CVP/PCWP ratio worsens early after LVAD due to poor early RV adaptation, which progressively improves with time. Increased venous return to the RV due to rapid stepping up of LVAD speed leads to bulging of the interventricular septum into the LV, causing RV dilation and, therefore, worsening tricuspid regurgitation. Acute hypoxemia and resultant pulmonary vasoconstriction, worsening PVR, will cause RVF. Acute renal failure with increased CVP and metabolic and/or respiratory acidosis contribute to RVF. Increased risk of perioperative bleeding secondary to redo sternotomy and transfusion has been associated with SIRS and worsening RV function. Sustained atrial and ventricular tachyarrhythmias deteriorate RV function in addition.

RVF treatment should include cautious optimization of LVAD speed, diuresis/ultrafiltration, and volume optimization. Inhaled nitric oxide should be provided for pulmonary hypertension and increased RVR or use oral phosphodiesterase-5 inhibitors. Arrythmias should be treated, and, if RVF still persists despite medical management, mechanical support should be provided (RVAD/ECMO). Late RV failure can occur in the presence or absence of normal LVAD function and is difficult to treat with poor long-term outcomes. Body mass index (BMI) >29, BUN >41, and diabetes mellitus were significant predictors of late RVF. Late RVF is associated with worse 5-year posttransplant survival compared with patients who did not develop RVF (19).

LVADs may be designed for long-term hemodynamic support, but RVF still remains a challenge in >30% of patients in the early post LVAD period. RVF causes a significant increase in morbidity and mortality, whether they are bridged to transplantation or are on it as destination therapy. Therefore, RVF should be prevented by robust patient selection using appropriate preoperative risk prediction tools to identify the best LVAD candidates and by efficient perioperative management. Early diagnosis of RVF is the key to improving outcomes. There is, therefore, a need for identifying early predictors of RVF and further refinement of treatment strategies to achieve better outcomes (20).

The effect of RV failure on LVAD outcomes includes increased mortality, deteriorating renal function and longer length of stay in the ICU, all of which contribute to increased morbidity in addition to its effects on mortality (21).

Current risk prediction scores and their limitations

There are a number of risk prediction scores at the present time, all of which have their advantages and limitations. The earliest of the models, which has been the Michigan RVF risk score put forth in 2008, was a single-center retrospective study. Other models have been compared to this. It was the most validated at 16, with a median c-statistic of 0.61. It used 4 binary pre-LVAD clinical variables. There was a higher concern for risk of bias due to variable RVF definition in the validation studies and indication bias due to inclusion of planned BIVAD patients and overfitting resulting in low RVF rates (8, 9).

The EUROMACS model was similarly a retrospective study involving multiple centers using five binary variables for early RVF. It was validated 5 times with a median c-statistic of 0.65. In this model, risk of bias was uncertain because the validation studies had variable definitions of RVF. Registry data were used, which had the inherent problem of missing data. The size of the cohort in the derivation study was large; hence, the applicability concern was low (8, 10).

The Penn model put forth in 2008 was a retrospective single-center study for severe early RVF and used 6 binary variables. It was validated 5 times with a median c-statistic of 0.63. Patients with planned BIVAD resulted in indication bias. RVF definitions varied and the study was impacted by missing data and low RVF risk patients being excluded (8, 11).

The Utah model was a single-center, retrospective study, with eight categorical variables for early RVF. It was validated seven times with a median c-statistic of 0.55. The variables were overfitted, inadequately powered; patients with missing data,

selection bias, and varied RVF definitions were problems with this model too (8, 12).

The CRITT model, which is also a single-center, retrospective study, used central venous pressure >15 mm Hg, severe RV dysfunction, pre-op mechanical ventilation/intubation, severe tricuspid regurgitation, and tachycardia for predicting risk for RVF. It was validated 5 times with a median c-statistic of 0.63. It was a single-center retrospective study. This model had indication bias due to inclusion of planned BIVADs in the derivation study. Applicability was a concern due to large number of pulsatile LVADs in the derivation batch and non-uniform RVF definitions in the validation batches (8, 13).

The model put forth by Kormos et al. used 3 binary variables to predict early RVF. It was validated five times with a median c-statistic of 0.61. This model was derived from a *post-hoc* analysis of a cohort of belonging to the multicenter HeartMate II trial, and, hence, universal applicability was a concern. The model exhibited an inclusion bias because it only included a highly selected population who were all bridged to transplantation. This model had variable RVF definitions and lacked adequate power for analysis (8, 14).

The Pittsburgh Decision Tree uses AI. It was a single-center, retrospective study. It used eight binary variables for early severe RVF. It was validated two times with a median c-statistic of 0.53. Variable RVF definitions and low RVF rates and overfitting were all noted in this model (8, 15).

Overall multiple limitations were noted in all of the existing risk models, making them difficult to be universally applicable for RVF. The definitions for RVF used were highly varied. The percentage of continuous flow pumps was a variable in the different studies, making it less predictable for the present day as pulsatile LVADs have essentially phased out. Not all models reported calibration. Validation groups appear to have not been stringent in patient selection or RVF definition, making them less reliable. Additionally, the type of RVF predicted whether acute, early or late was highly varied. This leads to heterogeneity, depending on the variability from institution to institution of medical vs. device therapies for RVF. Additionally, the existing models have lower-than-ideal c-statistics, ranging from 0.55 to 0.65 (8–15).

Utilizing AI technology to predict risk

Use of machine learning (ML) in developing risk scores for HF mortality seems to have an edge over conventional methods and is currently looking encouraging. The MARKER-HF score has a c-statistic of 0.88 and has been validated in 2 external study cohorts. This model used a boosted decision tree algorithm to derive a model based on automated training using two well-defined cohorts—the low and high groups (22). In another study, telemetry data analyses from a wearable monitor used a general machine learning similarity-based modeling, which was used to predict HF hospitalization. Receiver operating characteristic curves showed a c-statistic of 0.86–89 using the analytics platform. The alert from such prediction models could help clinicians intervene before an HF hospitalization occurs (23). Prediction of mortality post LVAD implantation, in general, has been attempted using Bayesian network analysis with a c-statistic of 0.7 for 1-, 3-, and 12-month mortality (24).

Applications of machine learning algorithms to assess tricuspid annulus excursion on 2-dimensional (2D) and 3-dimensional (3D) echocardiography have been attempted with considerable success in assessment of RV function. Application of an automated segmented model based on neural network architecture was used in a 2D echo image analysis. An ML algorithm was trained and tested in a 6-fold cross validation approach. Tricuspid annular displacement measurements using manual and automated ML segmentation showed that the automated approach was comparable to MRI data. The ROC curves used to test the model showed a c-statistic of 0.69–0.73 in a small population studied. The ML-driven assessment used a deep learning framework and was time efficient with a processing time of <1 s (25). In another study using ML-based algorithms using 3D echocardiographic images, RV volumes and ejection fraction measurements were made with excellent reproducibility, suggesting that automated analysis of data may be more efficient (26).

A Bayesian network analysis-driven model for acute, early, and late RVF post LVAD implantation published in 2016 was based on the INTERMACS registry. The acute, early, and late RVF models comprised of 33, 34, and 33 preoperative variables (from demographics, hemodynamics, laboratory values, and medications), respectively. The performance of this model was superior to earlier models (c-statistic of 0.53–0.65) with c-statistics of 0.9, 0.83, and 0.88 for acute, early, and late RVF, respectively (27). The study had limitations, such as missing data, which are inherent to registry data.

Figure 1 summarizes possible applications of AI technology to develop risk prediction models for RV dysfunction in the LVAD population. Risk prediction helps with improving outcomes if applied to patient selection and management pre-, peri-, and post-device implantation. Incorporating hemodynamic parameters from invasive hemodynamics as well as LVAD parameters and speed can predict RV failure. In a small, single-center study, a new hemodynamic index generated using mean arterial pressure, the ratio of pulmonary artery wedge pressure and central venous pressure, and the ratio of the set pump speed to maximum pump speed in a ramp study showed that this index can be used to predict RV failure. A c-statistic derived from the Area Under the Curve using a Receiver Operative Curve was high at 0.86 (28). A combination of clinical and hemodynamic parameters can be used to generate better and robust risk models. Large databases maybe generated by data pooling from different

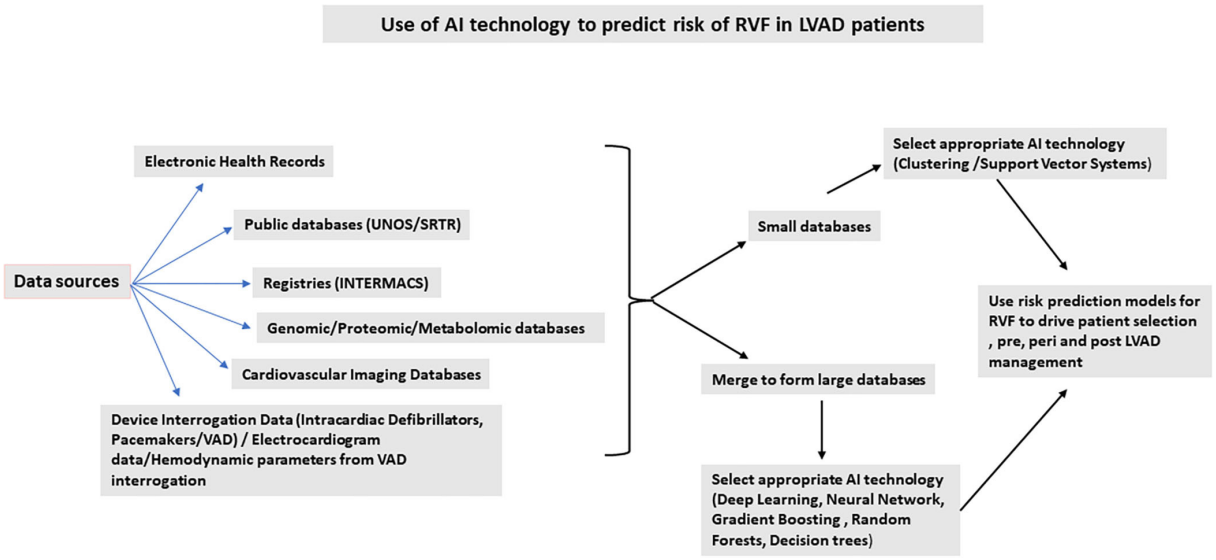

FIGURE 1
Use of AI technology to predict risk of right ventricular failure in left ventricular assist device patients.

smaller databases. AI technology can then be applied following data generation and normalization. The AI technology can then be used to generate risk models for patient selection pre-LVAD, a bridge to transplant and destination populations. The type of AI technology used will depend on the type of database used for analysis. The pros and cons for each different type of AI technology should be considered for each individual analysis undertaken, depending on the size of the database and its tendency to overfit data, time factor, and ease of interpretation. Considering the impact of RVF on post-LVAD outcomes, risk stratification for RV failure is one of the major determinants for patient survival and becomes the most important strategy to improve patient outcomes (29–31).

In summary, the four major aspects of machine learning are collection of data, building an appropriate mathematical model, constructing a learning algorithm, and defining at the final model for decision. Large data sets are ideal, especially for deep learning, which can be derived by combining smaller datasets. The right mathematical model should precisely represent the data and key properties of the problem in question. To achieve best predictive performance flexible models such as those based on the deep neural networks or the Gaussian process should be used. The learning algorithm is then used for computation of variables inherent in the model using the data set. The final process is building the algorithms for precise prediction (32–34).

Discussion

In summary, this review shows that existing literature points to increased efficiency in data analysis and developing risk models using AI technologies. The performance of these models appears to be better than those developed using conventional systems in the present studies, which are largely retrospective. However, testing in larger prospective longitudinal populations still remains to be proven.

Models for prediction of RVF generated by conventional methods have limitations mainly due to universal assumptions of linearity. Regression models are simple and easy to perform as well as understand, but their use in model prediction is not as efficient as ML-based methods. ML methods are based on unbiased classification/clustering of attributes in the setting of a decision tree, neural network or algorithm. Hence, ML technology needs to be used in the setting of a balance between minimal training errors, especially as the models get more complex and its universal applicability. Additionally, recognition of important covariates to be used as input data is another major part of successful generation of risk prediction models. Improving interpretability of machine learning models of prediction is another area to consider.

Future directions and challenges

Standardization of clinical behavior and accuracy of data collection remains a challenge. Algorithms for guideline-derived medical therapy vary across the globe, making it difficult to standardize the data collection. Prospective collection of data is, definitely, a requirement to generate large databases. Generation of large prospective databases will be the crux of generating robust risk prediction models, and validation of results using independent data sets will possibly help develop better risk prediction models. Developments of novel technologies for acquisition of

bio signals and biosensors and secure data transmission could help generate more robust prospective databases contributing toward standardization of input and output variables. Finally, a multimodal approach to data collection will be more powerful in developing risk prediction models. Using powerful risk prediction models will open up new ways of approaching diagnosis and treatment in diverse subpopulations representing different races and socioeconomic strata.

Author contributions

NN is responsible for the entire generation of the manuscript.

Conflict of interest

The author declares that the research was conducted in the absence of any commercial or financial relationships that could be construed as a potential conflict of interest.

Publisher's note

References

1. Basir MB, Schreiber TL, Grines CL, Dixon SR, Moses JW, Maini BS, et al. Effect of early initiation of mechanical circulatory support on survival in cardiogenic shock. *Am J Cardiol.* (2017) 119:845–51. doi: 10.1016/j.amjcard.2016.11.037

2. Slaughter MS, Rogers JG, Milano CA, Russell SD, Conte JV, Feldman D, et al. Advanced heart failure treated with continuous-flow left ventricular assist device. *N Engl J Med.* (2009) 361:2241–51. doi: 10.1056/NEJMoa0909938

3. Kirklin JK, Pagani FD, Kormos RL, Stevenson LW, Blume ED, Myers SL, et al. Eighth annual INTERMACS report: special focus on framing the impact of adverse events. *J Heart Lung Transplant.* (2017) 36:1080–6. doi: 10.1016/j.healun.2017.07.005

4. LaRue SJ, Raymer DS, Pierce BR, Nassif ME, Sparrow CT, Vader JM. Clinical outcomes associated with INTERMACS-defined right heart failure after left ventricular assist device implantation. *J Heart Lung Transplant.* (2017) 36:475–7. doi: 10.1016/j.healun.2016.12.017

5. Kirklin JK, Xie R, Cowger J, de By TMMH, Nakatani T, Schueler S, et al. Second annual report from the ISHLT mechanically assisted circulatory support registry. *J Heart Lung Transplant.* (2018) 37:685–91. doi: 10.1016/j.healun.2018.01.1294

6. Cheng A, Williamitis CA, Slaughter MS. Comparison of continuous-flow and pulsatile-flow left ventricular assist devices: is there an advantage to pulsatility? *Ann Cardiothorac Surg.* (2014) 3:573–81. doi: 10.3978/j.issn.2225-319X.2014.08.24

7. Rogers JG, Aaronson KD, Boyle AJ, Russell SD, Milano CA, Pagani FD, et al. Continuous flow left ventricular assist device improves functional capacity and quality of life of advanced heart failure patients. *J Am Coll Cardiol.* (2010) 55:1826–34. doi: 10.1016/j.jacc.2009.12.052

8. Frankfurter C, Molinero M, Vishram-Nielsen JKK, Foroutan F, Mak S, Rao V, et al. Predicting the risk of right ventricular failure in patients undergoing left ventricular assist device implantation: a systematic review. *Circ Heart Fail.* (2020) 13:e006994. doi: 10.1161/CIRCHEARTFAILURE.120.006994

9. Matthews JC, Koelling TM, Pagani FD, Aaronson KD. The right ventricular failure risk score a pre-operative tool for assessing the risk of right ventricular failure in left ventricular assist device candidates. *J Am Coll Cardiol.* (2008) 51:2163–72. doi: 10.1016/j.jacc.2008.03.009

10. Soliman OII, Akin S, Muslem R, Boersma E, Manintveld OC, Krabatsch T, et al. Derivation and validation of a novel right-sided heart failure model after implantation of continuous flow left ventricular assist devices: the EUROMACS (European registry for patients with mechanical circulatory support) right-sided heart failure risk score. *Circulation.* (2018) 137:891–906. doi: 10.1161/CIRCULATIONAHA.117.030543

11. Fitzpatrick JR III, Frederick JR, Hsu VM, Kozin ED, O'Hara ML, Howell E, et al. Risk score derived from pre-operative data analysis predicts the need for biventricular mechanical circulatory support. *J Heart Lung Transplant.* (2008) 27:1286–92. doi: 10.1016/j.healun.2008.09.006

12. Drakos SG, Janicki L, Horne BD, Kfoury AG, Reid BB, Clayson S, et al. Risk factors predictive of right ventricular failure after left ventricular assist device implantation. *Am J Cardiol.* (2010) 105:1030–5. doi: 10.1016/j.amjcard.2009.11.026

13. Atluri P, Goldstone AB, Fairman AS, MacArthur JW, Shudo Y, Cohen JE, et al. Predicting right ventricular failure in the modern, continuous flow left ventricular assist device era. *Ann Thorac Surg.* (2013) 96:857–63; discussion 863. doi: 10.1016/j.athoracsur.2013.03.099

14. Kormos RL, Teuteberg JJ, Pagani FD, Russell SD, John R, Miller LW, et al. Right ventricular failure in patients with the HeartMate II continuous-flow left ventricular assist device: incidence, risk factors, and effect on outcomes. *J Thorac Cardiovasc Surg.* (2010) 139:1316–24. doi: 10.1016/j.jtcvs.2009.11.020

15. Wang Y, Simon MA, Bonde P, Harris BU, Teuteberg JJ, Kormos RL, et al. Decision tree for adjuvant right ventricular support in patients receiving a left ventricular assist device. *J Heart Lung Transplant.* (2012) 31:140–9. doi: 10.1016/j.healun.2011.11.003

16. Loforte A, Montalto A, Musumeci F, Amarelli C, Mariani C, Polizzi V, et al. Calculation of the ALMA risk of right ventricular failure after left ventricular assist device implantation. *ASAIO J.* (2018) 64:e140–7. doi: 10.1097/MAT.0000000000000800

17. Morine KJ, Kiernan MS, Pham DT, Paruchuri V, Denofrio D, Kapur NK. Pulmonary artery pulsatility index is associated with right ventricular failure after left ventricular assist device surgery. *J Card Fail.* (2016) 22:110–6. doi: 10.1016/j.cardfail.2015.10.019

18. Puwanant S, Hamilton KK, Klodell CT, Hill JA, Schofield RS, Cleeton TS, et al. Tricuspid annular motion as a predictor of severe right ventricular failure after left ventricular assist device implantation. *J Heart Lung Transplant.* (2008) 27:1102–7. doi: 10.1016/j.healun.2008.07.022

19. Takeda K, Takayama H, Colombo PC, Jorde UP, Yuzefpolskaya M, Fukuhara S, et al. Late right heart failure during support with continuous-flow left ventricular assist devices adversely affects post-transplant outcome. *J Heart Lung Transplant.* (2015) 34:667–74. doi: 10.1016/j.healun.2014.10.005

20. Raina A, Patarroyo-Aponte M. Prevention and treatment of right ventricular failure during left ventricular assist device therapy. *Crit Care Clin.* (2018) 34:439–52. doi: 10.1016/j.ccc.2018.03.001

21. Terzic D, Putnik S, Nestorovic E, Jovicic V, Lazovic D, Rancic N, et al. Impact of right heart failure on clinical outcome of left ventricular assist devices (LVAD) implantation: single center experience. *Healthcare.* (2022) 10:114. doi: 10.3390/healthcare10010114

22. Adler ED, Voors AA, Klein L, Macheret F, Braun OO, Urey MA, et al. Improving risk prediction in heart failure using machine learning. *Eur J Heart Fail.* (2020) 22:139–47. doi: 10.1002/ejhf.1628

23. Stehlik J, Schmalfuss C, Bozkurt B, Nativi-Nicolau J, Wohlfahrt P, Wegerich S, et al. Continuous wearable monitoring analytics predict heart failure hospitalization: the LINK-HF multicenter study. *Circ Heart Fail.* (2020) 13:e006513. doi: 10.1161/CIRCHEARTFAILURE.119.006513

24. Kanwar MK, Lohmueller LC, Kormos RL, Teuteberg JJ, Rogers JG, Lindenfeld J, et al. A Bayesian model to predict survival after left ventricular assist device implantation. *JACC Heart Fail.* (2018) 6:771–9. doi: 10.1016/j.jchf.2018.03.016

25. Beecy AN, Bratt A, Yum B, Sultana R, Das M, Sherifi I, et al. Development of novel machine learning model for right ventricular quantification on echocardiography-A multimodality validation study. *Echocardiography.* (2020) 37:688–97. doi: 10.1111/echo.14674

26. Genovese D, Rashedi N, Weinert L, Narang A, Addetia K, Patel AR, et al. Machine learning-based three-dimensional echocardiographic quantification of right ventricular size and function: validation against cardiac magnetic resonance. *J Am Soc Echocardiogr.* (2019) 32:969–77. doi: 10.1016/j.echo.2019.04.001

27. Loghmanpour NA, Kormos RL, Kanwar MK, Teuteberg JJ, Murali S, Antaki JF. A Bayesian model to predict right ventricular failure following left ventricular assist device therapy. *JACC Heart Fail.* (2016) 4:711–21. doi: 10.1016/j.jchf.2016.04.004

28. Montalto A, Amarelli C, Piazza V, Hopkins K, Comisso M, Pantanella R, et al. A new hemodynamic index to predict late right failure in patients implanted with last generation centrifugal pump. *J Card Surg.* (2021) 36:2355–64. doi: 10.1111/jocs.15564

29. Topol EJ. High-performance medicine: the convergence of human and artificial intelligence. *Nat Med.* (2019) 25:44–56. doi: 10.1038/s41591-018-0300-7

30. Krittanawong C, Rogers AJ, Johnson KW, Wang Z, Turakhia MP, Halperin JL, et al. Integration of novel monitoring devices with machine learning technology for scalable cardiovascular management. *Nat Rev Cardiol.* (2021) 18:75–91. doi: 10.1038/s41569-020-00445-9

31. Segar MW, Jaeger BC, Patel KV, Nambi V, Ndumele CE, Correa A, et al. Development and validation of machine learning-based race-specific models to predict 10-year risk of heart failure: a multicohort analysis. *Circulation.* (2021) 143:2370–83. doi: 10.1161/CIRCULATIONAHA.120.053134

32. Ghahramani Z. Probabilistic machine learning and artificial intelligence. *Nature.* (2015) 521:452–9. doi: 10.1038/nature14541

33. LeCun Y, Bengio Y, Hinton G. Deep learning. *Nature.* (2015) 521:436–44. doi: 10.1038/nature14539

34. Sundström J, Schön TB. Machine learning in risk prediction. *Hypertension.* (2020) 75:1165–6. doi: 10.1161/HYPERTENSIONAHA.120.13516

frontiers | Frontiers in Cardiovascular Medicine

TYPE Review
PUBLISHED 21 September 2022
DOI 10.3389/fcvm.2022.962839

OPEN ACCESS

EDITED BY
Kiyotake Ishikawa,
Icahn School of Medicine at Mount Sinai, United States

REVIEWED BY
Cumara Sivathasan,
National Heart Centre Singapore, Singapore
German Ebensperger,
University of Chile, Chile

*CORRESPONDENCE
Abdelmotagaly Elgalad
aelgalad@texasheart.org

SPECIALTY SECTION
This article was submitted to Heart Failure and Transplantation, a section of the journal Frontiers in Cardiovascular Medicine

RECEIVED 06 June 2022
ACCEPTED 01 September 2022
PUBLISHED 21 September 2022

CITATION
de Oliveira Cardoso C, Elgalad A, Li K and Perin EC (2022) Device-based therapy for decompensated heart failure: An updated review of devices in development based on the DRI_2P_2S classification.
Front. Cardiovasc. Med. 9:962839.
doi: 10.3389/fcvm.2022.962839

Device-based therapy for decompensated heart failure: An updated review of devices in development based on the DRI_2P_2S classification

Cristiano de Oliveira Cardoso[1], Abdelmotagaly Elgalad[1]*, Ke Li[1] and Emerson C. Perin[2]

[1]Center for Preclinical Surgical and Interventional Research, Texas Heart Institute, Houston, TX, United States, [2]Center for Clinical Research, Texas Heart Institute, Houston, TX, United States

Congestive heart failure (HF) is a devastating disease leading to prolonged hospitalization, high morbidity and mortality rates, and increased costs. Well-established treatments for decompensated or unstable patients include medications and mechanical cardiac support devices. For acute HF decompensation, new devices are being developed to help relieve symptoms and recover heart and renal function in these patients. A recent device-based classification scheme, collectively classified as DRI_2P_2S, has been proposed to better describe these new device-based therapies based on their mechanism: dilators (increase venous capacitance), removers (direct removal of sodium and water), inotropes (increase left ventricular contractility), interstitials (accelerate removal of lymph), pushers (increase renal arterial pressure), pullers (decrease renal venous pressure), and selective (selective intrarenal drug infusion). In this review, we describe the new class of medical devices with the most current results reported in preclinical models and clinical trials.

KEYWORDS

heart failure, acute heart failure, devices, cardiorenal syndrome, treatment

Introduction

According to the universal definition, "heart failure (HF) is defined as a clinical syndrome with symptoms and/or signs caused by a structural and/or functional cardiac abnormality and corroborated by elevated natriuretic peptide levels and/or objective evidence of pulmonary or systemic congestion" (1). In addition to this broad description, several classification systems for HF can be applied that incorporate stages of risk, the presence of symptoms, the etiology, and the assessment of left ventricular function.

Chronic HF affects about 2% of the adult population worldwide. However, its prevalence is age-dependent, ranging from less than 2% in people < 60 years old to more than 10% in those older than 75 years (2). According

to recent updated data from the American Heart Association, about 6.2 million Americans ≥ 20 years of age were diagnosed with HF between 2013 and 2016 (3). Projections show that the prevalence of HF in the United States will increase 46% from 2012 to 2030, resulting in more than 8 million people with HF (4).

A wide variety of drugs, devices, and procedures are available to improve survival and functional class in patients with HF (5–7). Patients with mild to moderately decompensated HF can usually be stabilized with medical treatment. For those who are extremely ill and unstable (8), various mechanical cardiac support devices can be used to attempt stabilization or as a bridge to transplantation. However, therapeutic options are limited for patients at an intermediate stage, whose HF cannot be controlled with medication but who are not ill enough to benefit from mechanical cardiac support (9).

New device-based treatments are being developed to treat specific pathways in patients with decompensated HF. Although the physiopathology is complex, patients with acute decompensated heart failure (ADHF) (10) present with decreased cardiac contractility and low cardiac output. Low blood pressure leads to deficient perfusion of the organs, which activates the renin-angiotensin-aldosterone system, vasopressin release, and upregulation of the sympathetic nervous system. The neurohormonal changes decrease renal artery pressure and renal blood flow, promoting an increase in sodium and water retention. Fluid overload increases central venous pressures, resulting in systemic congestion and elevated abdominal pressure. Intraabdominal hypertension causes impairment of renal function (11). In addition, the swollen intestine caused by systemic congestion results in poorer absorption of diuretics (12). Rosenblum et al. (13) have proposed a new classification strategy based on seven categories for these devices that act on different mechanisms involved in the pathophysiology of HF. Denoted by the acronym DRI_2P_2S, the classification scheme categorizes the devices according to their mechanism and suggested indication. **Table 1** summarizes the new medical device classification and mechanisms.

Dilators (D–increase venous capacitance)

Around 30% of the blood volume circulates in the arterial circulation, and the rest is confined to the venous system. Because of its large capacitance, the abdominal venous system is the main reservoir for blood volume in the body. In addition, the abdominal venous reservoir responds to sympathetic stimuli by promoting vasoconstriction and shifting fluid from the abdominal system into the circulation. In patients with HF, the shifted volume overloads and worsens peripheral congestion, increases cardiac venous return, and raises cardiopulmonary filling pressures, thus worsening pulmonary congestion.

Vasodilators (nitroprusside and nitrates) dilate venous and arterial vessels. Nitrates act mainly on peripheral veins, whereas nitroprusside affects the arterial and venous systems. Vasodilators reduce the venous return, resulting in less congestion, lower afterload, and a consequent relief of symptoms. Recently, splanchnic nerve modulation has been proposed for treating congestive HF (14). The concept underlying splanchnic nerve modulation is to block the great splanchnic nerve, which carries visceral sympathetic and sensory fibers. The splanchnic nerves, located on both sides of the spine, arise from the sympathetic thoracic trunk to innervate the abdomen. Consequently, a splanchnic nerve block would reduce the response to the abdominal reservoir to the sympathetic tonus, thus reducing the shifting of blood from its cavity to the circulation and decreasing cardiopulmonary filling pressures. Splanchnic nerve block is achieved by using a percutaneous approach under fluoroscopic guidance. First, a spinal needle is positioned to the anterolateral edge of the thoracolumbar spine at the T11–12 level, and then a local anesthetic (lidocaine or ropivacaine) is injected to temporarily block the nerve (unilateral or bilateral).

Two studies (15) have tested this concept in clinical practice. The Splanchnic HF-1 (16, 17) and Splanchnic-HF-2 (18), both small clinical studies, evaluated the physiologic effects of splanchnic nerve block in patients with acute and chronic HF, respectively. Splanchnic HF-1 prospectively assessed 11 patients with HF who had New York Heart Association class III/IV symptoms, reduced ejection fraction, and a pulmonary capillary wedge pressure (PCWP) > 15 mmHg (> 12 mmHg if on inotropes) on baseline right heart catheterization. This

TABLE 1 DRI_2P_2S classification scheme for device-based therapy for heart failure.

Classification scheme	Mechanism of action	Device-based approach
Dilators (D)	Increases venous capacitance	Splanchnic nerve modulation
Removers (R)	Removes sodium and/or water directly	AlfaPump, Reprieve System
Inotropes (I_1)	Improves left ventricular contractility	Cardionomic, NeuroTronik
Interstitial (I_2)	Accelerates lymph removal	WhiteSwell
Pushers (P_1)	Increases renal arterial pressure	Reitan catheter pump, Aortix, Second Heart Assist
Pullers (P_2)	Decreases renal venous pressure	preCardia, Doraya catheter, transcatheter renal decongestion system
Selective (S)	Infuses vasodilator drugs selectively *via* the infrarenal artery	Benephit catheter

Modified from Rosenblum et al. (13).

first-in-human, proof-of-concept study showed that splanchnic nerve block could reduce mean pulmonary arterial pressure, mean arterial pressure, and PCWP, resulting in an increase in cardiac index after the intervention. The Splanchnic-HF-2 trial tested the hypothesis that splanchnic nerve blockade would attenuate the increase in exercise-induced cardiac filling pressures in patients with chronic HF with reduced ejection fraction. In this prospective, open-label, single-arm trial, 15 patients with chronic HF and elevated PCWP underwent exercise testing before and after nerve block with ropivacaine. The findings showed that splanchnic nerve block reduced resting and exercise-induced pulmonary arterial and wedge pressure with favorable effects on cardiac output and exercise capacity, results similar to the Splanchnic HF-1 trial.

Although procedural complications (14) (pneumothorax, chylothorax, bowel perforation, vascular damage, and others) and physiologic changes (diarrhea, orthostatic hypotension, nausea, and vomiting) can occur with nerve block, the procedure was well tolerated and without significant complications in both studies.

Removers (R–direct removal of sodium and water)

Patients with HF have an overload of water and sodium in the extracellular space due to the physiologic and adaptative changes of the failing heart. Although diuretics play an essential role in fluid removal and symptom relief, diuretic resistance may render them non-effective in clinical practice (12).

Water and sodium can be removed from the body *via* ultrafiltration (19). Previous studies have shown that ultrafiltration (20, 21) with either aquapheresis (22) or peritoneal dialysis (23, 24) can be an alternative to diuretics in controlling fluid overload in patients with congestive HF. Because classic ultrafiltration is not the focus of this review, only the newer devices are discussed.

New devices called removers have been used to help treat volume overload in decompensated patients. One of the new devices—the alfapump DSR® (Sequana Medical NV, Belgium)—is implanted subcutaneously in the abdomen and automatically and continuously moves fluid from the abdominal cavity to the bladder, where it is excreted from the body (25). *Via* a surgically implanted port, sodium-free DSR infusate is delivered into the peritoneal cavity; this approach allows for flexible dosing to remove the desired amount of sodium. The DSR infusate remains for a pre-determined time, and it and the extracted sodium are pumped to the bladder and eliminated in the urine (**Figure 1**). In a proof-of-concept study in pigs, the device removed 4.1 ± 0.4 g of sodium from the body in 2 h, with no significant changes in other electrolytes. The ongoing clinical trial SAHARA (NCT04882358) will enroll 24 patients with congestive HF and diuretic resistance. In an interim analysis of six patients in the trial (26), the new device was safe and tolerable, and treated patients showed a mean weight loss of 6 kg compared to baseline and a 30% reduction in NT-proBNP; the estimated glomerular filtration rate (eGFR) was not significantly affected.

The Reprieve System™ (Reprieve Cardiovascular, Milford, MA, USA) is another new decongestion device for improving outcomes for patients with ADHF. The goal in using the Reprieve device is to achieve a target fluid balance. The system comprises a peripheral or central infusion port and a Foley urinary catheter that is connected to an external console. The Reprieve System constantly measures the patient's urine output and infuses a volume of hydration fluid sufficient to maintain a set fluid-balance rate. Two clinical trials provided results on the use of this technology. Target-1 and Target-2 (NCT03897842) trials evaluated the device in 19 patients with congestive HF and preexisting impaired renal function, respectively (27). The findings showed the Reprieve System was safe and tolerable in all patients. In addition, patients treated with the Reprieve System lost weight during hospitalization (−3 kg, $p < 0.001$) and showed improved renal function (baseline creatinine levels of 1.45 ± 0.4 vs. 1.26 ± 0.4 mg/dl at end of therapy, $p = 0.0002$) and decreased CVP (from 15.5 ± 5.3 mmHg at baseline to 12.8 ± 4.8 mmHg at end of therapy; $p = 0.02$).

Inotropes (I_2–increase left ventricular contractility)

The heart is innervated by the cardiac plexus of nerves situated at its base. Cardiac branches are derived from both the sympathetic and parasympathetic nervous systems. In a dog model (28), cardiac plexus stimulation increased cardiac contractility and mean arterial pressure with no changes in heart rate. This concept has been tested in humans with two different devices.

The catheter-based cardiopulmonary nerve stimulation (CPNS, Cardionomic Inc., New Brighton, MN) is a 16-French catheter device that is inserted percutaneously through the right jugular vein and positioned in the right pulmonary artery (**Figure 2**). The CPNS is used to provide endovascular stimulation for up to 5 days in patients with ADHF. In an ongoing clinical trial of CPNS (NCT04814134), initial results (29) in 7 patients showed no adverse events. CPNS therapy increased heart contractility (LV dP/dt max) by 58%, left ventricular relaxation (LV dP/dt min) by 11%, arterial pulse pressure by 20%, and mean arterial pressure by 7%. No significant changes were observed in heart rate. Target enrollment for the trial is 50 patients for evaluating long-term impact.

Using a similar concept, the NeuroTronik CANS Therapy™ System (NCT03169803, NCT02880683, and

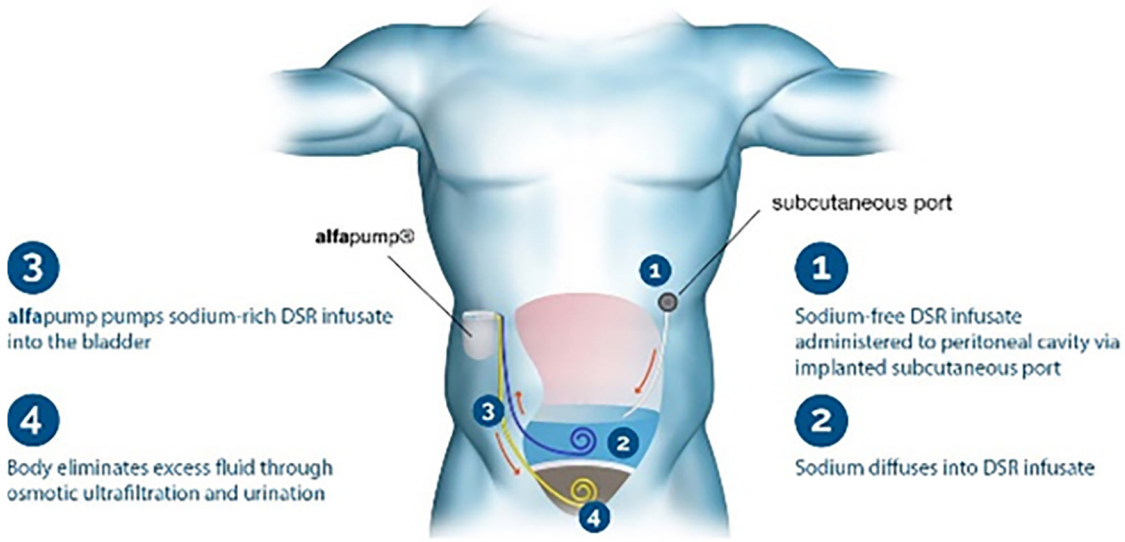

FIGURE 1
Remover device. The Alfapump DSR system for sodium removal. Image used with permission from Sequana Medical.

NCT03542123) is a purpose-built electrical stimulation catheter placed percutaneously in the left brachiocephalic vein *via* left subclavian vein access. The neurostimulator is then connected to the catheter and is used to deliver autonomic nerve stimulation therapy for up to 96 h. At the 2019 Transcatheter Cardiovascular Therapeutics (TCT) symposium (30), investigators presented the initial results of a single-arm study in 12 patients with congestive HF (at least two signs and symptoms) and an ejection fraction < 40%. NeuroTronik therapy improved cardiac index (+ 22%) and decreased PCWP (–28%) and systemic vascular resistance (–22%). No significant changes were observed in cardiac rate.

Interstitial (I_2–accelerate removal of lymph)

In healthy people, excess liquid in the interstitial space is removed through the lymphatic system, which collects fluid in these spaces and returns it to the veins *via* the thoracic and lymphatic ducts. As a consequence of HF, lymphatic drainage of edema in the periphery, abdominal organs, and lungs is reduced (31). The WhiteSwell^{TM} therapy system (WhiteSwell, Ireland) is a new device designed to accomplish complete decongestion while preserving renal function. The device comprises a multi-lumen catheter with two compliant balloons of low-durometer urethane. The catheter balloons are positioned across the bifurcation of the jugular and innominate veins and isolate the thoracic duct outflow when inflated. The system produces a decrease in the local pressure (between both inflated balloons) and reduces venous pressures in the thoracic duct outflow area, thus facilitating drainage of the thoracic duct (**Figure 3**).

In a sheep model of HF, Abraham et al. (32) conducted a proof-of-concept study of the WhiteSwell device. Dilated cardiomyopathy was created by serial coronary embolization, and fluid overload was used to create decompensated HF with pulmonary congestion. The WhiteSwell device was activated for up to 3 h in the four treated sheep; 3 served as controls. Extravascular lung water volume was decreased in treated sheep as compared to controls. The authors also reported a case of an 82-year-old woman who is part of an ongoing clinical trial (NCT02863796) on the safety and feasibility of the WhiteSwell device. She had presented with HF with preserved ejection fraction, hypertension, chronic atrial fibrillation (treated with novel oral anticoagulants), chronic renal failure, and severe pulmonary hypertension. After receiving standard clinical therapy, she was treated with the WhiteSwell device, which was introduced *via* the left internal jugular vein under fluoroscopy guidance. Device treatment significantly increased urine output rate and reduced central venous pressure during the therapy. Results of the ongoing trial have not been published.

Pushers (P1–increase renal arterial pressure)

The close interaction between the kidney and heart in patients with HF has been called cardiorenal syndrome (CRS) (33, 34). CRS is a complex entity that involves both organs and neurohormonal mechanisms, with a physiopathology

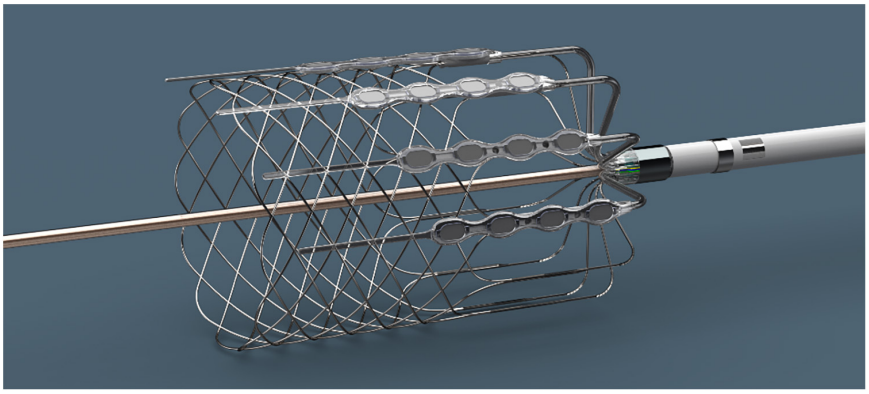

FIGURE 2
Inotrope device. The Cardionomic Cardiac Pulmonary Nerve Stimulation (CPNS). Image used with permission from Cardionomic, Inc.

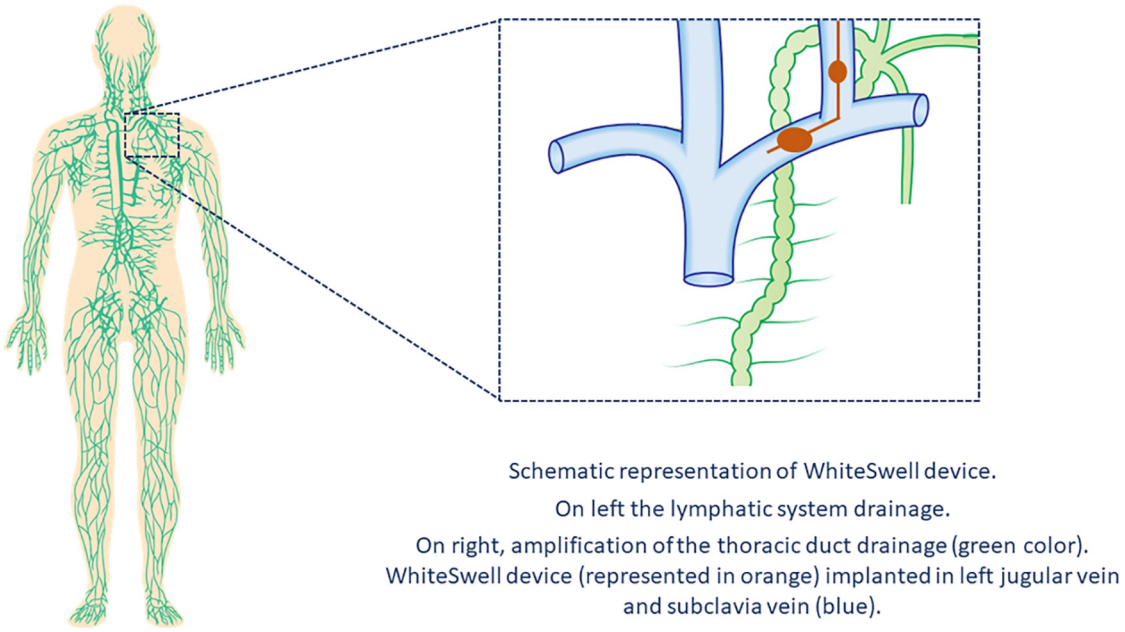

FIGURE 3
Interstitial device. The WhiteSwell device.

characterized by low cardiac output leading to decreased renal perfusion. New devices are being developed to increase renal output in HF. These devices, called pushers, are intended to be temporarily implanted in the descending aorta above the renal arteries and are supposed to increase the flow toward the renal arteries to promote better perfusion in the kidneys. In addition, pushers can also decrease left ventricle afterload. **Figure 4** illustrates the concept of the new pusher devices: Reitan catheter (35), Aortix (36), and Second Heart Assist.

The Reitan catheter pump (Cardiobridge, Germany) was first tested in nine patients requiring mechanical circulatory support during complex percutaneous coronary intervention (PCI) (37). The propeller was set to rotate around 10,000 rpm, promoting a gradient between the radial-femoral pressure of around 10 mmHg. The main finding was that using the device reduced creatine levels by an average of 11 ± 8 μmol/l (P = 0.004) from before to after the procedure. In a larger prospective, observational study (38), 18 patients admitted with decompensated HF, an ejection fraction < 30%, and a cardiac index < 2.1 L/min/m^2 who were in need of inotropic/mechanical support received the device-based therapy. The mean running time of the Reitan device was 18.3 h, and treated patients showed an increase in diuresis, renal function, and cardiac index.

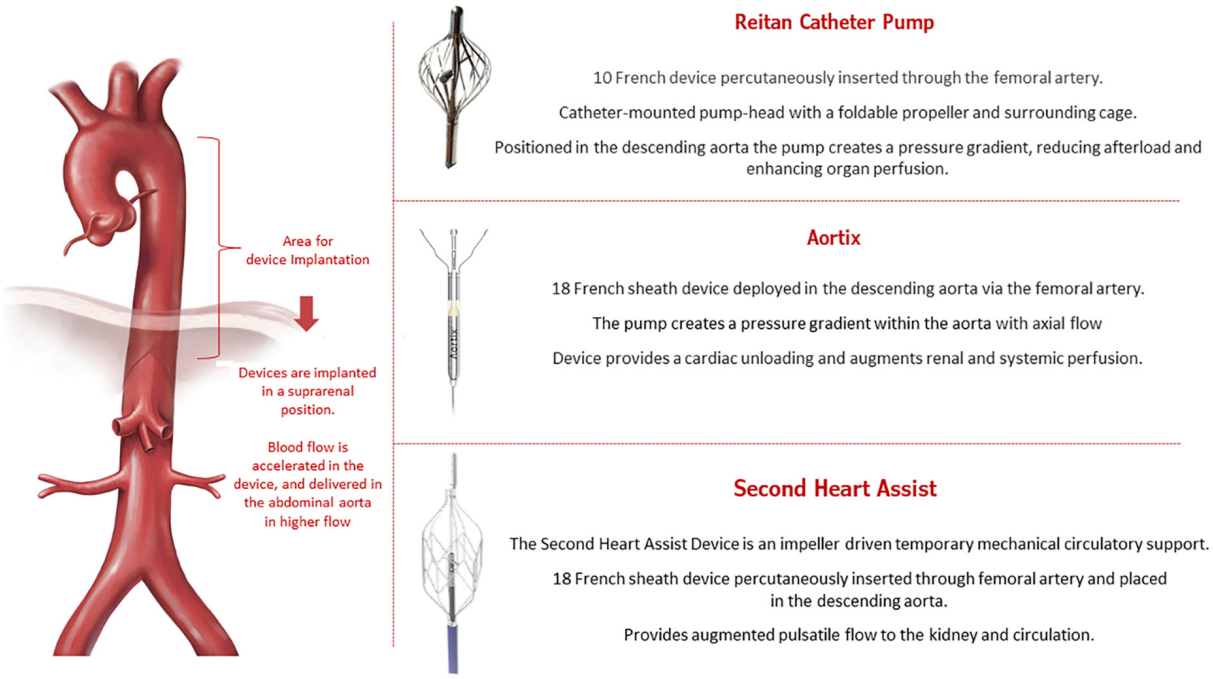

FIGURE 4
Pusher devices for heart failure.

The Aortix (Procyrion, Inc., Houston, TX, USA) is an axial-flow pump that is positioned in the aorta to provide short-term hemodynamic support. The device functions to promote a higher pressure in the distal abdominal aorta (39, 40). The first-in-human study was conducted by Vora et al. (41) and enrolled six patients with renal dysfunction to receive the device during high-risk PCI. Aortix was implanted for a mean time of 70 min with no severe complications. In addition, device support improved urine output (10-fold) and eGFR (mean increase, 6.95 ± 8.09 mL/min). Another case in which this device was successfully implanted was presented at the 2021 TCT symposium (42).

Second Heart Assist (Second Heart Assist, Salt Lake City, UT, USA) is another investigational device that promotes circulatory support for patients with decompensated HF and CRS who are at high-risk for PCI. This stent-based impeller pump is percutaneously inserted (*via* the femoral artery) and enables better flow to the kidneys. No clinical data have been published, but the preclinical data are encouraging.

Although all of the devices in this category have the potential risk for hemolysis, infection, and thromboembolic complications, no serious adverse events have been reported for any of them. However, it is important to be cautious about the potential risk that any invasive device confers in terms of hemocompatibility complications and possible infection. Before being tested in a clinical setting, new devices should be examined in depth for these potential hazards.

Pullers (P_2–decrease renal venous pressure)

Devices in the pullers category are used to reduce cardiac volume overload and filling pressures at the superior/inferior vena cava (IVC) or venous congestion at the abdominal cavity.

The preCARDIA balloon catheter device (Abiomed, Danvers, MA, USA) is placed in the superior vena cava (SVC) for intermittent occlusion. Controlled by a pump, the preCARDIA device unloads the heart, decreasing its filling pressures and helping to achieve decongestion in HF patients (**Figure 5**). In a proof-of-concept study, Kapur et al. (43) demonstrated that transient occlusion of the SVC reduces cardiac filling pressures without significant changes in cardiac output and blood pressure. In their study, eight patients with decompensated HF underwent intermittent balloon occlusion in the SVC; the procedure was well-tolerated and reduced cardiac filling pressure. The VENUS-HF trial (44) (NCT03836079), an early feasibility study, was a multicenter, prospective, single-arm trial of patients who were treated for 12–24 h with the preCARDIA system. Compared with baseline values, right atrial pressure decreased by 34%, PCWP declined by 27%, and urine output and net fluid balance increased by 130 and 156%, respectively. Similarly, intermittent occlusion of the IVC has also effectively reduced cardiac filling pressures (45, 46).

10.3389/fcvm.2022.962839

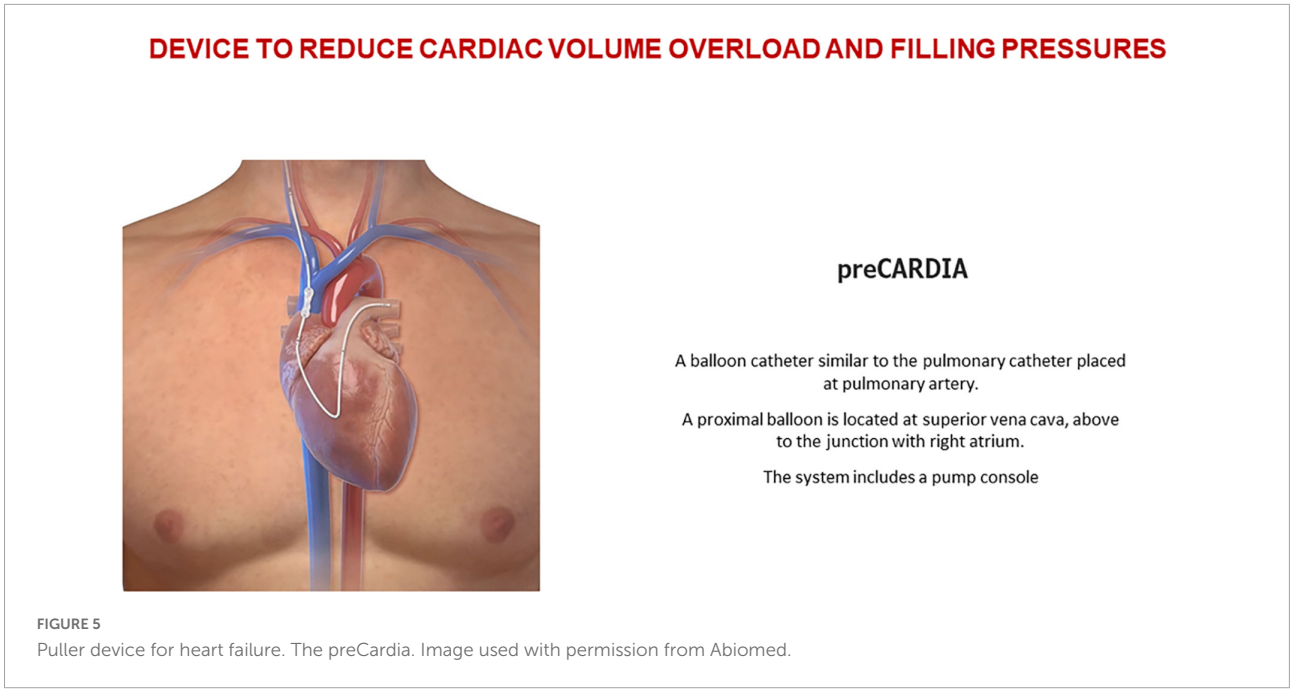

FIGURE 5
Puller device for heart failure. The preCardia. Image used with permission from Abiomed.

As a result of systemic congestion, patients with HF have elevated central venous and intraabdominal pressure (IAP). Moreover, venous congestion is emerging as an important cause of renal dysfunction in patients with CRS, and the term "congestive nephropathy" has been proposed for this new concept (47). Animal studies (48–50) have shown that an elevated IAP is related to renal dysfunction. In a study of pigs with induced pneumoperitoneum, Toens et al. (51) demonstrated that IAP $>$ 40 cmH_2O led to renal dysfunction caused by tubular epithelial necrosis. In clinical medicine, an elevated IAP ($\geq$ 8 mmHg) has also been correlated to renal dysfunction (52) and to an increase in 1-year mortality when IAP $>$ 12 mmHg for more than 72 h after admission (53).

Different devices can be placed below, above, or even within the kidney to reduce kidney congestion. For example, the Doraya catheter (Revamp Medical Ltd., 5 Mefi, Netania, Israel) is a manageable flow-reducing device implanted in the infrarenal IVC for up to 12 h. The temporary mechanical obstruction of flow reduces central venous pressure, renal afterload, and venous returns, thus relieving congestion on the heart, lungs, and kidneys. Two published cases (54) have demonstrated that the Doraya device could promote cardiac decongestion and improve diuretics resistance. A clinical trial of the Doraya catheter for the treatment of acute HF (AHF) (NCT03234647) has been completed, but no published results are available. Another device called Transcatheter Renal Venous Decongestion^{TM} (TRVD) System (Magenta Medical, Kadima, Israel) is designed to reduce the pressure in both renal veins through a catheter-based approach by using an axial-flow pump-head positioned in the IVC. Two sealing elements are placed above and below the kidneys to compartmentalize the renal segment of the IVC and allow selective reduction of renal venous pressures. The TRVD System is intended to be placed shortly after hospital admission to mechanically unload the kidneys for 1–3 days. The first-in-human trial (NCT03621436) tested the concept (55) in 13 patients with HF and low ejection fraction. After TRVD therapy, renal venous pressure decreased (from 19.2 $\pm$ 4.1 to 10.5 $\pm$ 3.3 mmHg, $p < 0.00001$) as did right atrial pressure. The clinical trial is completed, but no results are available.

Selective (S–selective intrarenal drug delivery)

Decreased renal perfusion and vasoconstriction trigger tubular hypoxia and are part of the complex mechanism of kidney function impairment in patients with HF (56). Vasodilator drugs are used to prevent renal vasoconstriction and reduce kidney dysfunction. Although clinical trials have shown that low doses of dopamine or nesiritide (57) did not improve renal function in HF patients, the concept is still being studied in different clinical scenarios. Teirstein et al. (58) tested a selective infusion of fenoldopam (a dopamine 1 receptor agonist that decreases peripheral vascular resistance primarily in renal capillary beds) into the kidneys with a Benephit catheter (Angiodynamics, Latham, NY) during coronary angiography. The Benephit is a bifurcated catheter percutaneously inserted through the femoral artery for selective infusion in both renal arteries. In a randomized, open-label, partial crossover

design trial in 33 patients, the use of the Benephit catheter for the selective renal infusion of fenoldopam was safe and produced some benefit in renal function. In a post-market registry (59), the use of the Benephit catheter system to infuse fenoldopam was examined in 501 patients at high-risk for contrast-induced nephropathy during coronary or peripheral angiography/intervention or cardiovascular surgery. The study showed this approach was safe and resulted in a lower incidence of contrast-induced nephropathy than predicted by the Mehran score. Although this intra-renal selective infusion therapy has demonstrated some benefit during coronary interventions, it has not been tested in the specific clinical scenario of HF; therefore, comments and preliminary results should be cautiously considered.

Discussion

AHF, defined as the rapid development of new symptoms and signs of HF, can be differentiated into ADHF and *de novo* AHF (60). AHF is a presentation caused by an acute heart injury (e.g., myocardial infarction or myocarditis), whereas ADHF is commonly seen in patients with a history of HF who have an imbalance due either to volume redistribution or to overload. The classic clinical presentations of ADHF are signs and symptoms of congestion and volume overload (dyspnea, orthopnea, lower limb edema, ascites). Accounting for most cases of acute decompensation, ADHF is seen often in older patients and has higher mortality rates and more comorbidities than AHF (61).

In addition to the underlying mechanisms of the acute decompensation (disease progression or secondary factor triggering the decompensation), patients with ADHF have changes in myocardial heart contraction and pulmonary function as well as renal dysfunction and intraabdominal changes. Combined, these factors make HF a complex disease to manage, and compensating for these changes with medications is challenging. A multidisciplinary HF management program is mandatory for evaluating patients; this approach ensures that the correct investigations are conducted and that an accurate diagnosis is made. Then, the appropriate evidence-based therapy may be initiated to treat the mechanism that is identified as the primary cause of the acute decompensation. A team approach for HF care has been demonstrated to reduce mortality and hospitalizations in high-risk patients (62), and these strategies play an important role in HF treatment. In addition, new approaches such as telemedicine support and wearable devices can be integrated into the treatment regimen. The new devices described in this review are not meant to replace current HF treatment. Few treatment options are available for the group of patients in whom decompensation cannot be treated with medications but who are not unstable enough to qualify for mechanical support; these new devices may offer an alternative therapeutic option to fill that gap. It is important to emphasize that the devices do not specifically address the mechanisms leading to decompensation. Rather, they support the heart and kidneys to improve preload, afterload, and renal perfusion and function. It is expected that the new devices will help to reverse the decompensation episode because each device acts specifically on the pathway that is exacerbating the decompensation. Thus, patients will benefit by more precisely addressing the mechanisms causing the symptoms during a decompensation episode. If needed, specific heart and kidney support may be possible with the new-device based therapy.

HF has an enormous impact on quality of life. Regardless of the status of left ventricular function (preserved, borderline, and reduced ejection fraction), the risk-adjusted analyses for the composite of mortality and rehospitalization are similar for all groups (63). Because patients with HF frequently see a worsening in their functional class and experience subsequent hospitalizations due to decompensation episodes, economic costs are significantly increasing due to frequent hospitalization and rehospitalization and the related comorbidities. Furthermore, costs related to HF place a heavy economic burden on our medical system. In a recent meta-analysis, the annual median total medical costs for HF care was $24,383 per patient; HF-specific hospitalizations contributed greatly to these costs (median, $15,879 per patient) (64). New types of devices will undoubtedly increase the economic costs of HF. New technologies require a learning curve that involves training requirements and related expenses. Additionally, device-related complications may add extra expenditure on the health care system. Currently, most devices discussed here are in the proof-of-concept phase, early feasibility studies, or first-in-human clinical trials. After early phase studies are completed, the safety of new devices must be examined in clinical trials. Safety is a key point in testing new technology, but cost-effectiveness must also be proved before implementing new devices into clinical practice. The economic burden on the US health care system is increasing (4, 65), and costs are predicted to rise to $70 billion dollars by 2030. Thus, any new medical device must be safe and cost-effective to promote benefit to the patients without superfluous costs to the health care system.

Another crucial step related to safety and efficacy is the quality of the clinical trials performed for testing new devices. Conducting a relevant clinical trial obviously involves a straightforward research question, adequate inclusion/exclusion criteria, randomization, placebos/shams, a reasonable sample size, and planning for interim analyses. However, researchers must focus on appropriate and applicable outcomes for clinical problems that will benefit patients. The use of surrogate endpoints, such as laboratory markers, might lead to inconclusive results or futile benefits that are not clinically relevant. An interim analysis focused on safety and efficacy should be performed because it allows for making evaluations

and decisions during the study and confirms safety endpoints (66). Our perspective is that new trials should focus on a pragmatic approach with broad inclusion criteria and recruitment, minimal organization or resources required, flexibility to deliver the intervention, a primary outcome relevant to patients, and analyses based on intention-to-treat principles (67). Only a pragmatic trial with clinically relevant endpoints will bring tangible benefits to patients, without adding costs and unnecessary interventions.

New technologies can be challenging from the beginning because the precise indication for use and the success and failure criteria are not completely defined. The devices mentioned in this review compose a new class; therefore, specific criteria must be established to avoid their empirical evaluation. For example, a comparable situation was seen in cardiology with definitions for stent thrombosis (68) and transcatheter aortic valve replacement (69). Discrepancies in classifications from different research teams can be standardized by the Academic Research Definition. Accurate and universal definitions are important because they create a uniform understanding of the challenges associated with consistency among endpoints used in reporting clinical trial results. Using standardized clinical endpoints is beneficial as a practical language for communication among researchers, health care providers, and patients. In addition, standardized endpoints are important for regulatory agencies in approving new devices, monitoring outcomes, and dealing with healthcare reimbursement. We believe that standardized criteria are needed to avoid being too liberal or too strict in identifying indications. Likewise, medical societies should be agile enough to introduce those criteria with new technologies before their approval and integration into clinical practice.

Finally, in this review, we discuss future devices that will help treat decompensated HF. Although this device-based therapy is not intended to replace current HF treatments, each one is expected to act at specific pathways of the decompensation, thus improving patient outcomes.

Author contributions

CO and KL made substantial contributions to literature research, conception and design, interpretation of data, and drafting the manuscript. AE and EP contributed to revising the manuscript critically for important intellectual content. All authors read and approved the final version.

Acknowledgments

Rebecca Bartow, PhD, of Scientific Publications at the Texas Heart Institute, contributed to the editing of the manuscript.

Conflict of interest

The authors declare that the research was conducted in the absence of any commercial or financial relationships that could be construed as a potential conflict of interest.

Publisher's note

References

1. Bozkurt B, Coats AJS, Tsutsui H, Abdelhamid CM, Adamopoulos S, Albert N, et al. Universal definition and classification of heart failure: a report of the Heart Failure Society of America, Heart Failure Association of the European Society of Cardiology, Japanese Heart Failure Society and Writing Committee of the Universal Definition of Heart Failure: Endorsed by the Canadian Heart Failure Society, Heart Failure Association of India, Cardiac Society of Australia and New Zealand, and Chinese Heart Failure Association. *Eur J Heart Fail.* (2021) 23:352–80. doi: 10.1002/ejhf.2115

2. Metra M, Teerlink JR. Heart failure. *Lancet.* (2017) 390:1981–95. doi: 10.1016/S0140-6736(17)31071-1

3. Tsao CW, Aday AW, Almarzooq ZI, Alonso A, Beaton AZ, Bittencourt MS, et al. Heart disease and stroke statistics-2022 update: a report from the American Heart Association. *Circulation.* (2022) 145:e153–639.

4. Heidenreich PA, Albert NM, Allen LA, Bluemke DA, Butler J, Fonarow GC, et al. Forecasting the impact of heart failure in the United States: a policy statement from the American Heart Association. *Circ Heart Fail.* (2013) 6:606–19. doi: 10.1161/HHF.0b013e318291329a

5. Writing C, Maddox TM, Januzzi JL Jr, Allen LA, Breathett K, Butler J, et al. 2021 update to the 2017 ACC expert consensus decision pathway for optimization of heart failure treatment: answers to 10 pivotal issues about heart failure with reduced ejection fraction: a report of the american college of cardiology solution set oversight committee. *J Am Coll Cardiol.* (2021) 77:772–810. doi: 10.1016/j.jacc.2020.11.022

6. Dryer C, Cotter EK, Flynn B. Overview of the 2021 update to the 2017 ACC expert consensus decision pathway for optimization of heart failure with reduced ejection fraction. *J Cardiothorac Vasc Anesth.* (2021) 35:2249–52.

7. Yancy CW, Jessup M, Bozkurt B, Butler J, Casey DE Jr, Colvin MM, et al. 2017 ACC/AHA/HFSA focused update of the 2013 ACCF/AHA guideline for the management of heart failure: a report of the American College of Cardiology/American Heart Association task force on clinical practice guidelines

and the heart failure society of America. *J Card Fail.* (2017) 23:628–51. doi: 10.1161/CIR.0000000000000509

8. Truby LK, Rogers JG. Advanced heart failure: epidemiology, diagnosis, and therapeutic approaches. *JACC Heart Fail.* (2020) 8:523–36. doi: 10.1016/j.jchf.2020.01.014

9. DeVore AD, Patel PA, Patel CB. Medical management of patients with a left ventricular assist device for the non-left ventricular assist device specialist. *JACC Heart Fail.* (2017) 5:621–31. doi: 10.1016/j.jchf.2017.06.012

10. Boorsma EM, Ter Maaten JM, Damman K, Dinh W, Gustafsson F, Goldsmith S, et al. Congestion in heart failure: a contemporary look at physiology, diagnosis and treatment. *Nat Rev Cardiol.* (2020) 17:641–55. doi: 10.1038/s41569-020-0379-7

11. ter Maaten JM, Valente MA, Damman K, Hillege HL, Navis G, Voors AA. Diuretic response in acute heart failure-pathophysiology, evaluation, and therapy. *Nat Rev Cardiol.* (2015) 12:184–92. doi: 10.1038/nrcardio.2014.215

12. Felker GM, Ellison DH, Mullens W, Cox ZL, Testani JM. Diuretic therapy for patients with heart failure: JACC state-of-the-art review. *J Am Coll Cardiol.* (2020) 75:1178–95. doi: 10.1016/j.jacc.2019.12.059

13. Rosenblum H, Kapur NK, Abraham WT, Udelson J, Itkin M, Uriel N, et al. Conceptual considerations for device-based therapy in acute decompensated heart failure: DRI2P2S. *Circ Heart Fail.* (2020) 13:e006731. doi: 10.1161/CIRCHEARTFAILURE.119.006731

14. Fudim M, Ponikowski PP, Burkhoff D, Dunlap ME, Sobotka PA, Molinger J, et al. Splanchnic nerve modulation in heart failure: mechanistic overview, initial clinical experience, and safety considerations. *Eur J Heart Fail.* (2021) 23:1076–84. doi: 10.1002/ejhf.2196

15. Fudim M, Patel MR, Boortz-Marx R, Borlaug BA, DeVore AD, Ganesh A, et al. Splanchnic nerve block mediated changes in stressed blood volume in heart failure. *JACC Heart Fail.* (2021) 9:293–300. doi: 10.1016/j.jchf.2020.12.006

16. Fudim M, Ganesh A, Green C, Jones WS, Blazing MA, DeVore AD, et al. Splanchnic nerve block for decompensated chronic heart failure: splanchnic-HF. *Eur Heart J.* (2018) 39:4255–6. doi: 10.1093/eurheartj/ehy682

17. Fudim M, Jones WS, Boortz-Marx RL, Ganesh A, Green CL, Hernandez AF, et al. Splanchnic nerve block for acute heart failure. *Circulation.* (2018) 138:951–3. doi: 10.1161/CIRCULATIONAHA.118.035260

18. Fudim M, Boortz-Marx RL, Ganesh A, DeVore AD, Patel CB, Rogers JG, et al. Splanchnic nerve block for chronic heart failure. *JACC Heart Fail.* (2020) 8:742–52. doi: 10.1016/j.jchf.2020.04.010

19. Chen HY, Chou KJ, Fang HC, Chen CL, Hsu CY, Huang WC, et al. Effect of ultrafiltration versus intravenous furosemide for decompensated heart failure in cardiorenal syndrome: a systematic review with meta-analysis of randomized controlled trials. *Nephron.* (2015) 129:189–96. doi: 10.1159/000371447

20. Costanzo MR, Guglin ME, Saltzberg MT, Jessup ML, Bart BA, Teerlink JR, et al. Ultrafiltration versus intravenous diuretics for patients hospitalized for acute decompensated heart failure. *J Am Coll Cardiol.* (2007) 49:675–83. doi: 10.1016/j.jacc.2006.07.073

21. Bart BA, Goldsmith SR, Lee KL, Givertz MM, O'Connor CM, Bull DA, et al. Ultrafiltration in decompensated heart failure with cardiorenal syndrome. *N Engl J Med.* (2012) 367:2296–304. doi: 10.1056/NEJMoa1210357

22. Costanzo MR, Negoianu D, Jaski BE, Bart BA, Heywood JT, Anand IS, et al. Aquapheresis versus intravenous diuretics and hospitalizations for heart failure. *JACC Heart Fail.* (2016) 4:95–105. doi: 10.1016/j.jchf.2015.08.005

23. Nunez J, Gonzalez M, Minana G, Garcia-Ramon R, Sanchis J, Bodi V, et al. Continuous ambulatory peritoneal dialysis as a therapeutic alternative in patients with advanced congestive heart failure. *Eur J Heart Fail.* (2012) 14:540–8. doi: 10.1093/eurjhf/hfs013

24. Grossekettler L, Schmack B, Meyer K, Brockmann C, Wanninger R, Kreusser MM, et al. Peritoneal dialysis as therapeutic option in heart failure patients. *ESC Heart Fail.* (2019) 6:271–9. doi: 10.1002/ehf2.12411

25. Rao VS, Turner JM, Griffin M, Mahoney D, Asher J, Jeon S, et al. First-in-human experience with peritoneal direct sodium removal using a zero-sodium solution: a new candidate therapy for volume overload. *Circulation.* (2020) 141:1043–53. doi: 10.1161/CIRCULATIONAHA.119.043062

26. Sequana Medical. *Sequana Medical Announces Positive Interim Results of SAHARA DESERT, the alfapump DSR® Study in Heart Failure Patients with Persistent Congestion*. Ghent: Globe Newswire (2021).

27. Biegus J, Zymlinski R, Siwolowski P, Testani J, Szachniewicz J, Tycinska A, et al. Controlled decongestion by reprieve therapy in acute heart failure: results of the TARGET-1 and TARGET-2 studies. *Eur J Heart Fail.* (2019) 21:1079–87. doi: 10.1002/ejhf.1533

28. Kobayashi M, Sakurai S, Takaseya T, Shiose A, Kim HI, Fujiki M, et al. Effects of percutaneous stimulation of both sympathetic and parasympathetic cardiac autonomic nerves on cardiac function in dogs. *Innovations.* (2012) 7:282–9. doi: 10.1177/155698451200700409

29. Mickelsen SRMC, Ebner A, Cuchiara M. Catheter-based cardiopulmonary nerve stimulation impacts left ventricular contractility and relaxation: first in human experience. *Heart Rhythm.* (2021) 18:S353–4. doi: 10.1016/j.hrthm.2021.06.876

30. Marin y Kall C, Boehmer J, Cowie M, Cuchiara M. TCT-86 Cardiac autonomic nerve stimulation improves hemodynamics and clinical status in advanced heart failure patients. *J Am Coll Cardiol.* (2019) 74:B86. doi: 10.1016/j.jacc.2019.08.127

31. Itkin M, Rockson SG, Burkhoff D. Pathophysiology of the lymphatic system in patients with heart failure: JACC state-of-the-art review. *J Am Coll Cardiol.* (2021) 78:278–90. doi: 10.1016/j.jacc.2021.05.021

32. Abraham WT, Jonas M, Dongaonkar RM, Geist B, Ueyama Y, Render K, et al. Direct interstitial decongestion in an animal model of acute-on-chronic ischemic heart failure. *JACC Basic Transl Sci.* (2021) 6:872–81. doi: 10.1016/j.jacbts.2021.09.008

33. Kumar U, Wettersten N, Garimella PS. Cardiorenal syndrome: pathophysiology. *Cardiol Clin.* (2019) 37:251–65. doi: 10.1016/j.ccl.2019.04.001

34. Rangaswami J, Bhalla V, Blair JEA, Chang TI, Costa S, Lentine KL, et al. Cardiorenal syndrome: classification, pathophysiology, diagnosis, and treatment strategies: a scientific statement from the American Heart Association. *Circulation.* (2019) 139:e840–78. doi: 10.1161/CIR.0000000000000664

35. Regamey J, Barras N, Rusca M, Hullin R. A role for the Reitan catheter pump for percutaneous cardiac circulatory support of patients presenting acute congestive heart failure with low output and renal dysfunction? *Future Cardiol.* (2020) 16:159–64. doi: 10.2217/fca-2019-0080

36. Kapur NK, Esposito ML, Whitehead E. Aortix: a novel intra-aortic entrainment pump. *Future Cardiol.* (2021) 17:283–91. doi: 10.2217/fca-2020-0057

37. Smith EJ, Reitan O, Keeble T, Dixon K, Rothman MT. A first-in-man study of the Reitan catheter pump for circulatory support in patients undergoing high-risk percutaneous coronary intervention. *Catheter Cardiovasc Interv.* (2009) 73:859–65. doi: 10.1002/ccd.21865

38. Keeble TR, Karamasis GV, Rothman MT, Ricksten SE, Ferrari M, Hullin R, et al. Percutaneous haemodynamic and renal support in patients presenting with decompensated heart failure: a multi-centre efficacy study using the Reitan Catheter Pump (RCP). *Int J Cardiol.* (2019) 275:53–8. doi: 10.1016/j.ijcard.2018.09.085

39. Annamalai SK, Esposito ML, Reyelt LA, Natov P, Jorde LE, Karas RH, et al. Abdominal positioning of the next-generation intra-Aortic Fluid Entrainment Pump (Aortix) improves cardiac output in a swine model of heart failure. *Circ Heart Fail.* (2018) 11:e005115. doi: 10.1161/CIRCHEARTFAILURE.118.005115

40. Shabari FR, George J, Cuchiara MP, Langsner RJ, Heuring JJ, Cohn WE, et al. Improved hemodynamics with a novel miniaturized intra-aortic axial flow pump in a porcine model of acute left ventricular dysfunction. *ASAIO J.* (2013) 59:240–5. doi: 10.1097/MAT.0b013e31828a6e74

41. Vora AN, Schuyler Jones W, DeVore AD, Ebner A, Clifton W, Patel MR. First-in-human experience with Aortix intraaortic pump. *Catheter Cardiovasc Interv.* (2019) 93:428–33. doi: 10.1002/ccd.27857

42. Heuring, J, Grafton G, Tita C, Fain E, Neely B, Shah P, et al. *TCT 539 – Use of Percutaneous Intra-aortic Mechanical Circulatory Support to Treat Acute Decompensated Heart Failure With Worsening Renal Function 2021*. (2021). Available online at: https://tct2021.crfconnect.com/challenging-cases/6280494947001 (accessed February 16, 2022).

43. Kapur NK, Karas RH, Newman S, Jorde L, Chabrashvili T, Annamalai S, et al. First-in-human experience with occlusion of the superior vena cava to reduce cardiac filling pressures in congestive heart failure. *Catheter Cardiovasc Interv.* (2019) 93:1205–10. doi: 10.1002/ccd.28326

44. Kapur NK, Kiernan MS, Gorgoshvili I, Yousefzai R, Vorovich EE, Tedford RJ, et al. Intermittent occlusion of the superior vena cava to improve hemodynamics in patients with acutely decompensated heart failure: the VENUS-HF early feasibility study. *Circ Heart Fail.* (2022) 15:e008934. doi: 10.1161/CIRCHEARTFAILURE.121.008934

45. Herrera JE, Herrera JA, Palacios IF. TCT-428 first percutaneous transluminal caval flow restriction in a patient with congestive heart failure. *J Am Coll Cardiol.* (2014) 64:B125–6. doi: 10.1016/j.jacc.2014.07.479

46. Kaiser D, Kaiser C, Canfield J, Patel R, Goar FS. TCT-339 partial inferior vena cava occlusion during exercise in heart failure patients prevents left ventricular pressure overload, improves exercise times, and reduces respiratory rate: mechanical "balancing" of biventricular function as a novel therapy for heart failure qualify of life. *J Am Coll Cardiol.* (2019) 74:B336. doi: 10.1016/j.jacc.2019.08.420

47. Husain-Syed F, Grone HJ, Assmus B, Bauer P, Gall H, Seeger W, et al. Congestive nephropathy: a neglected entity? Proposal for diagnostic criteria and future perspectives. *ESC Heart Fail.* (2021) 8:183–203. doi: 10.1002/ehf2.13118

48. Caldwell CB, Ricotta JJ. Changes in visceral blood flow with elevated intraabdominal pressure. *J Surg Res.* (1987) 43:14–20. doi: 10.1016/0022-4804(87)90041-2

49. Masey SA, Koehler RC, Ruck JR, Pepple JM, Rogers MC, Traystman RJ. Effect of abdominal distension on central and regional hemodynamics in neonatal lambs. *Pediatr Res.* (1985) 19:1244–9. doi: 10.1203/00006450-198512000-00004

50. Shimada S, Hirose T, Takahashi C, Sato E, Kinugasa S, Ohsaki Y, et al. Pathophysiological and molecular mechanisms involved in renal congestion in a novel rat model. *Sci Rep.* (2018) 8:16808. doi: 10.1038/s41598-018-35162-4

51. Toens C, Schachtrupp A, Hoer J, Junge K, Klosterhalfen B, Schumpelick V. A porcine model of the abdominal compartment syndrome. *Shock.* (2002) 18:316–21. doi: 10.1097/00024382-200210000-00005

52. Mullens W, Abrahams Z, Skouri HN, Francis GS, Taylor DO, Starling RC, et al. Elevated intra-abdominal pressure in acute decompensated heart failure: a potential contributor to worsening renal function? *J Am Coll Cardiol.* (2008) 51:300–6.

53. Rubio-Gracia J, Gimenez-Lopez I, Sanchez-Marteles M, Josa-Laorden C, Perez-Calvo JI. Intra-abdominal pressure and its relationship with markers of congestion in patients admitted for acute decompensated heart failure. *Heart Vessels.* (2020) 35:1545–56. doi: 10.1007/s00380-020-01634-9

54. Dierckx R, Vanderheyden M, Heggermont W, Goethals M, Verstreken S, Bartunek J. Treatment of diuretic resistance with a novel percutaneous blood flow regulator: concept and initial experience. *J Card Fail.* (2019) 25:932–4. doi: 10.1016/j.cardfail.2019.08.017

55. Vanderheyden M, Bartunek J, Neskovic AN, Milicic D, Keffer J, Kafedzic S, et al. TRVD therapy in acute HF: proof of concept in animal model and initial clinical experience. *J Am Coll Cardiol.* (2021) 77:1481–3. doi: 10.1016/j.jacc.2021.01.029

56. Schefold JC, Filippatos G, Hasenfuss G, Anker SD, von Haehling S. Heart failure and kidney dysfunction: epidemiology, mechanisms and management. *Nat Rev Nephrol.* (2016) 12:610–23. doi: 10.1038/nrneph.2016.113

57. Chen HH, Anstrom KJ, Givertz MM, Stevenson LW, Semigran MJ, Goldsmith SR, et al. Low-dose dopamine or low-dose nesiritide in acute heart failure with renal dysfunction: the ROSE acute heart failure randomized trial. *JAMA.* (2013) 310:2533–43.

58. Teirstein PS, Price MJ, Mathur VS, Madyoon H, Sawhney N, Baim DS. Differential effects between intravenous and targeted renal delivery of fenoldopam on renal function and blood pressure in patients undergoing cardiac catheterization. *Am J Cardiol.* (2006) 97:1076–81. doi: 10.1016/j.amjcard.2005.10.053

59. Weisz G, Filby SJ, Cohen MG, Allie DE, Weinstock BS, Kyriazis D, et al. Safety and performance of targeted renal therapy: the Be-RITe! registry. *J Endovasc Ther.* (2009) 16:1–12. doi: 10.1583/08-2515.1

60. Xanthopoulos A, Butler J, Parissis J, Polyzogopoulou E, Skoularigis J, Triposkiadis F. Acutely decompensated versus acute heart failure: two different entities. *Heart Fail Rev.* (2020) 25:907–16. doi: 10.1007/s10741-019-09894-y

61. Younis A, Mulla W, Goldkorn R, Klempfner R, Peled Y, Arad M, et al. Differences in mortality of new-onset (De-Novo) acute heart failure versus acute decompensated chronic heart failure. *Am J Cardiol.* (2019) 124:554–9. doi: 10.1016/j.amjcard.2019.05.031

62. Morton G, Masters J, Cowburn PJ. Multidisciplinary team approach to heart failure management. *Heart.* (2018) 104:1376–82. doi: 10.1136/heartjnl-2016-310598

63. Shah KS, Xu H, Matsouaka RA, Bhatt DL, Heidenreich PA, Hernandez AF, et al. Heart failure with preserved, borderline, and reduced ejection fraction: 5-year outcomes. *J Am Coll Cardiol.* (2017) 70:2476–86. doi: 10.1016/j.jacc.2017.08.074

64. Urbich M, Globe G, Pantiri K, Heisen M, Bennison C, Wirtz HS, et al. A systematic review of medical costs associated with heart failure in the USA (2014-2020). *Pharmacoeconomics.* (2020) 38:1219–36. doi: 10.1007/s40273-020-00952-0

65. Virani SS, Alonso A, Benjamin EJ, Bittencourt MS, Callaway CW, Carson AP, et al. heart disease and stroke statistics-2020 update: a report from the American Heart Association. *Circulation.* (2020) 141:e139–596. doi: 10.1161/CIR.0000000000000746

66. Kumar A, Chakraborty BS. Interim analysis: a rational approach of decision making in clinical trial. *J Adv Pharm Technol Res.* (2016) 7:118–22. doi: 10.4103/2231-4040.191414

67. Haff N, Choudhry NK. The promise and pitfalls of pragmatic clinical trials for improving health care quality. *JAMA Netw Open.* (2018) 1:e183376. doi: 10.1001/jamanetworkopen.2018.3376

68. Cutlip DE, Windecker S, Mehran R, Boam A, Cohen DJ, van Es GA, et al. Clinical end points in coronary stent trials: a case for standardized definitions. *Circulation.* (2007) 115:2344–51. doi: 10.1161/CIRCULATIONAHA.106.685313

69. VARC-3 Writing Committee, Genereux P, Piazza N, Alu MC, Nazif T, Hahn RT, et al. Valve academic research consortium 3: updated endpoint definitions for aortic valve clinical research. *J Am Coll Cardiol.* (2021) 77:2717–46.

frontiers | Frontiers in Cardiovascular Medicine

TYPE Original Research
PUBLISHED 09 November 2022
DOI 10.3389/fcvm.2022.1028763

OPEN ACCESS

EDITED BY
Lilei Yu,
Wuhan University, China

REVIEWED BY
Dennis Lawin,
Bielefeld University, Germany
Ran Dong,
Capital Medical University, China
Lei Zuo,
Fourth Military Medical University, China

*CORRESPONDENCE
Liwen Liu
liuliwen@fmmu.edu.cn
Rui Hu
yiruyan007@126.com

†These authors have contributed equally to this work and share first authorship

SPECIALTY SECTION
This article was submitted to General Cardiovascular Medicine, a section of the journal Frontiers in Cardiovascular Medicine

RECEIVED 30 August 2022
ACCEPTED 24 October 2022
PUBLISHED 09 November 2022

CITATION
Wang Z, Zhao R, Sievert H, Ta S, Li J, Bertog S, Piayda K, Zhou M, Lei C, Li X, Liu J, Xu B, Feng B, Hu R and Liu L (2022) First-in-man application of Liwen RF^{TM} ablation system in the treatment of drug-resistant hypertrophic obstructive cardiomyopathy.
Front. Cardiovasc. Med. 9:1028763.
doi: 10.3389/fcvm.2022.1028763

First-in-man application of Liwen RF^{TM} ablation system in the treatment of drug-resistant hypertrophic obstructive cardiomyopathy

Zihao Wang[1†], Rong Zhao[2†], Horst Sievert[3], Shengjun Ta[1], Jing Li[1], Stefan Bertog[3,4], Kerstin Piayda[3], Mengyao Zhou[1], Changhui Lei[1], Xiaojuan Li[1], Jiani Liu[1], Bo Xu[2], Bo Feng[2], Rui Hu[1*] and Liwen Liu[1*]

[1]Xijing Hypertrophic Cardiomyopathy Center, Department of Ultrasound, Xijing Hospital, Fourth Military Medical University, Xi'an, China, [2]Xijing Hypertrophic Cardiomyopathy Center, Department of Cardiac Surgery, Xijing Hospital, Fourth Military Medical University, Xi'an, China, [3]CardioVascular Center, Frankfurt, Germany, [4]Minneapolis Veterans Affairs Medical Center, Minneapolis, MN, United States

Objectives: This study sought to evaluate the clinical applicability of the Liwen Liu RF^{TM} ablation system for percutaneous intramyocardial septal radiofrequency ablation (PIMSRA).

Background: Data on new cardiac radiofrequency ablation devices for the treatment of hypertrophic obstructive cardiomyopathy (HOCM) are limited.

Materials and methods: From July 2019 to July 2020, a total of 68 patients with drug-resistant HOCM, who underwent PIMSRA with the Liwen RF^{TM} ablation system, which has an ablation electrode of stepless adjustable length, were prospectively enrolled. Safety endpoints included, amongst others, the occurrence of pericardial effusion and/or hemorrhage, cardiac arrhythmias, device failure and procedural death. The reduction in left ventricular outflow tract (LVOT) gradients at 12 months follow-up were used as a surrogate marker for device efficacy.

Results: All procedures were technically successful. The total energy output time of the system was 75.8 (IQR: 30.0) min, and the average power was 43.61 ± 13.34 watts. No ablation system error occurred. The incidence of pericardial effusion or hemorrhage, transient arrhythmia and resuscitation was 8.8, 39.7, and 1.5% during procedure, respectively. None of the patients died. During 30-day follow-up, there were no complications with the exception of a pericardial effusion in one patient (1.5%). No further complications were reported after 30 days. The patients' resting [baseline: 75 (IQR: 48) *vs.* 12-months: 12 (IQR: 19) mmHg, $p < 0.001$] and provoked [baseline: 122 (IQR: 53) *vs.* 12-months: 41 (IQR: 59) mmHg, $p < 0.001$] LVOT gradients decreased significantly during follow-up.

Conclusion: In this study, we demonstrate the safety and feasibility of the Liwen RF^{TM} ablation system to treat HOCM. The system allows for significant and sustainable LVOT gradient reduction during 12-months of follow-up. Hence, the Liwen RF^{TM} ablation system is a promising new device that has the potential to become an alternative to existing septal reduction concepts in HOCM patients.

KEYWORDS

hypertrophic obstructive cardiomyopathy, percutaneous intramyocardial septal radiofrequency ablation, radiofrequency ablation system, conformal ablation, first-in-man application, Liwen RF

Introduction

Hypertrophic cardiomyopathy is a common hereditary cardiomyopathy, with an incidence of about 2–5 per 1,000 in the adult population (1–3). Asymmetrical left ventricular hypertrophy is the main manifestation and cannot be explained by other cardiac diseases (4, 5). About two-thirds of patients have resting and/or provoked left ventricular outflow tract (LVOT) obstruction, known as hypertrophic obstructive cardiomyopathy (HOCM) (6, 7) which is associated with increased morbidity and limited life-expectancy (1, 8, 9). For HOCM patients with significant symptoms that do not respond to medical treatment, septal reduction therapies are a treatment option. Surgical myectomy (SM) is considered to be the gold standard (10, 11), and alcohol septal ablation (ASA) a less invasive alternative (12). There is evidence that in specialized high-volume centers, the LVOT gradient of patients after SM is generally less than 10 mmHg, and over 90% of patients experience long-term relief of symptoms after surgery (13, 14). Likewise, in an experienced ASA team, nearly 95% of treated patients had a gradient reduction of at least 50% as compared to baseline, with symptom improvement and in-hospital mortality less than 1% (15, 16).

In recent years, the development of percutaneous intramyocardial septal radiofrequency ablation (PIMSRA, Liwen procedure^{TM}) has emerged as a new option for the interventional treatment of HOCM (17). Exploratory results in a small cohort of patients, who could not tolerate thoracotomy and did not choose ASA because of contraindications or unacceptable risks, with a strong willingness to accept minimally invasive treatment, showed a good safety profile and significant and sustainable LVOT gradient reduction (18). Additionally, the feasibility of PIMSRA combined with transcatheter aortic valve replacement (TAVR) for aortic stenosis with LVOT obstruction was demonstrated in a case report (19). However, the radiofrequency needle electrode of the Cool-tip system used in previous trials cannot match the intended ablation range perfectly. We, therefore, developed a new radiofrequency ablation system, the Liwen RF^{TM} system (Hangzhou Nuo Cheng Medical Instrument Co., Ltd., Hangzhou, Zhejiang, China), with an ablation electrode of stepless adjustable length, to achieve adequate and accurate ablation at different anatomical sites of interventricular septum (IVS), referred to as "conformal ablation". Different from the emphasis on tumor ablation that "tumor tissues of different shapes and adjacent normal tissues should be included as much as possible", conformal ablation for HOCM requires strict control of ablation scope within the IVS to avoid perforation and ensure a safe distance between ablation boundary and endocardium to protect the conduction system from damage. This is achieved by adjusting the exposure length of the needle electrode, which we call the "Working section length". This study aims to prove that the Liwen RF ablation system can be used safely and effectively in the treatment of drug-resistant HOCM.

Materials and methods

Patients

This is an open label, one-arm, prospective, non-randomized study. Patients with HOCM and severe LVOT obstruction and refractory symptoms despite adequate medication were eligible for trial participation. Treatment options were discussed with the patient, and cases were presented in a multi-disciplinary heart team. Patients provided written informed consent. **Table 1** lists the inclusion and exclusion criteria for this study. Patients with a higher sudden

Abbreviations: ASA, Alcohol septal ablation; HOCM, Hypertrophic obstructive cardiomyopathy; IVS, Interventricular septum; LVEF, Left ventricular ejection fractions; LVOT, Left ventricular outflow tract; MAE, Major adverse events; NYHA, New York Heart Association; PIMSRA, Percutaneous intramyocardial septal radiofrequency ablation; SAM, Systolic anterior motion; SCDI, Sudden cardiac death index; SM, Surgical myectomy; TTE, Transthoracic echocardiography; VF, Ventricular fibrillation.

TABLE 1 Inclusion and exclusion criteria of patients.

Inclusion criteria:
(1) Age between 18 and 70
(2) Resting or provoked LVOT gradient ≥ 50 mmHg
(3) Septal thickness of at least 15 mm
(4) Refractoriness to medical therapy with a beta-blocker, and/or CCB
(5) Symptoms attributed to HOCM
(6) NYHA functional class ≥ II
(7) Informed consent and agreement to complete follow-up
Exclusion criteria:
(1) Pregnancy or breast-feeding
(2) Non-obstructive hypertrophic cardiomyopathy
(3) Septal thickness ≥ 30 mm
(4) SCDI ≥ 10
(5) Presence of concomitant heart disease requiring surgery
(6) Symptomatic heart failure at rest despite maximal guideline directed medical therapy and LVEF < 40%

CCB, calcium channel blocker; HOCM, hypertrophic obstructive cardiomyopathy; LVEF, left ventricular ejection fractions; NYHA, New York Heart Association; SCDI, sudden cardiac death index.

cardiac death index (SCDI) were thought to be more likely to have an accident during ablation, so SCDI ≥ 10 was considered a contraindication or patient exclusion criterion.

The study was registered at chictr.org (ChiCTR2000031936) and was conducted in accordance with the ethical standards of the Helsinki Declaration. The protocol was approved by the Ethics Committee of Xijing Hospital (KY-20192076-F-1).

Equipment

The Liwen RF ablation system consists of the following components:

- Liwen RF ablation electrode kit (RFET02A): sterile packaged for single use. As the core device of the Liwen RF system, the ablation electrode is also the most important part of the equipment. It has been specifically developed for radiofrequency ablation of the ventricular septal myocardium.
- Liwen RF ablation generator (RFGR100): Reuse unit. Used to generate radiofrequency energy and output to the electrode needle. The generator incorporates an algorithm designed for cardiac ablation that will simultaneously detect the impedance and temperature of the electrode needle for energy output management. The equipment is operated by an engineer.
- System cooling pump (RFPP01): Reuse unit. This is used to cool the electrode needle and prevent overheating in the ablation area. The device should be kept on during the energy output. The refrigerant is sterile water placed in an ice bucket during procedure.
- Patient circuit electrode: Disposable non-sterile consumables. It is used to form a loop with the ablation electrode and the patient's tissue which is connected to the generator by a cable attached to the ablation electrode kit.

The Liwen RF ablation electrode kit must be used in conjunction with other parts of the Liwen RF ablation system for PIMSRA. It mainly includes the following items: puncture needle (17G), electrode needle (18G), inflow tube, outflow tube, needle tube positioning parts and negative plate connecting cable. It should be noted that except for the patient circuit electrode connection cable, all other items are sterile. The exposed length of the needle electrode, that is, the working section length of Liwen RF, can be adjusted freely within 10∼30 mm by the slider on the handle. As shown in **Figure 1**, five scales are displayed, corresponding to the length of exposed electrode in increments of 5 mm. Nevertheless, in the actual adjustment process, the control of working section length is stepless. The longer the working section length is, the greater the ablation area length, width and thickness will be. Therefore, with the help of imaging equipment, the exposed length of the needle electrode and its position in the IVS should be adjusted according to the degree of cardiac hypertrophy and the desired ablation range.

Before ablation begins, the electrode needle detects the initial impedance of the surrounding tissue. According to our data, the impedance of the septal tissue before ablation ranged from 92 to 115 ohms, with a mean impedance of 103.20 ± 9.13 ohms. With the progress of ablation, the impedance decreased slowly at first, and then gradually increased after a plateau. When the impedance rises sharply to 150% of the initial value, the system enters a "Hibernation state", at which time the system will suspend energy output for 15 s. After that, the system restarts and repeats the process of impedance detection until the next hibernation. Frequent hibernation indicates that the local tissue has been sufficiently ablated. In our experience, the number of cycles for ablation and hibernation is typically three.

Assessments

Philips EPIQ 7C (Philips Medical Systems, Bothell, WA, USA) ultrasound imaging system was used for transthoracic echocardiography (TTE). Septal thickness, LVOT gradient, left ventricular ejection fractions (LVEF), and systolic anterior motion (SAM) of the mitral valve were assessed. SAM is classified into four grades on M-mode echocardiography. Grade 0: No systolic anterior motion of the mitral valve; Grade 1: Brief systolic anterior motion without septal contact; Grade 2: Systolic anterior motion with septal contact lasting < 1/3 of the systolic period; Grade 3: Systolic anterior motion with septal

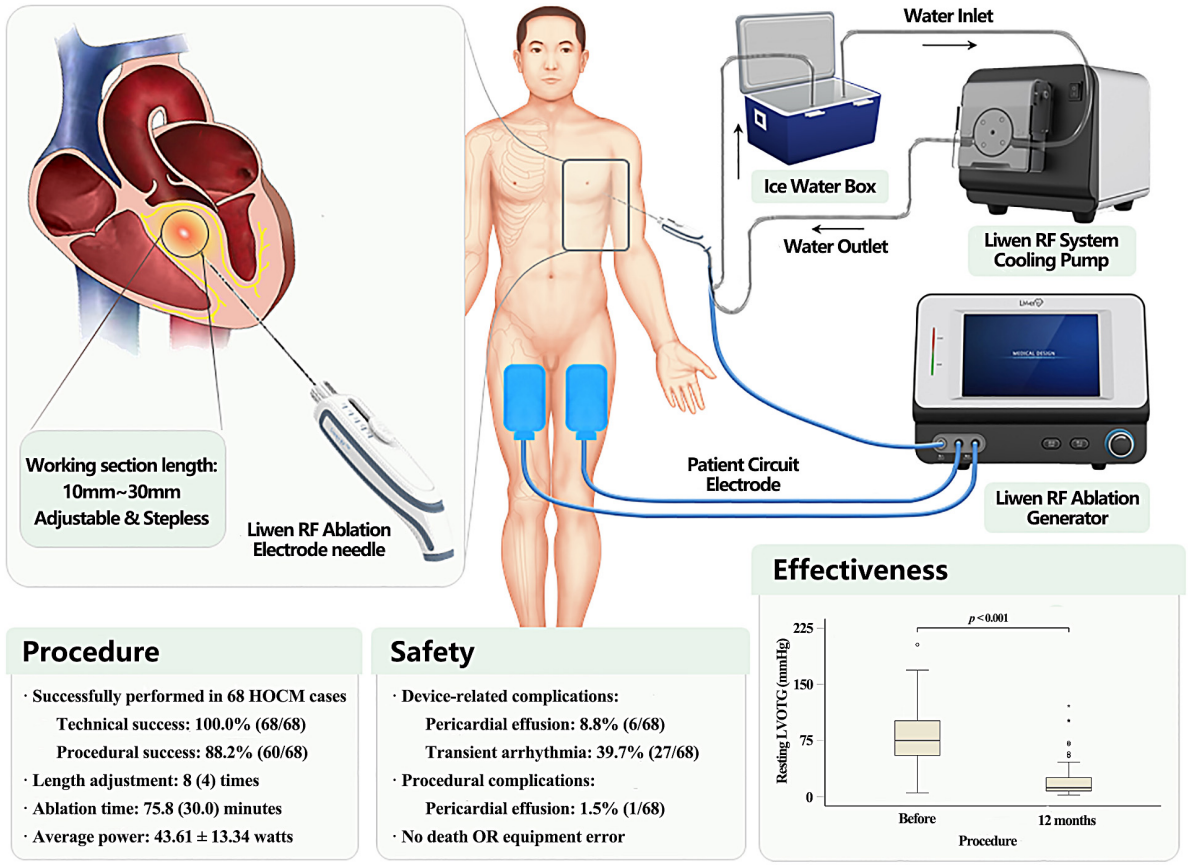

FIGURE 1
Description of Liwen RF^{TM} ablation system and main findings. Liwen RF^{TM} (Hangzhou Nuo Cheng Medical Instrument Co., Ltd., Hangzhou, Zhejiang, China) is a novel radiofrequency ablation system with a stepless adjustable length needle electrodes for percutaneous intramyocardial septal radiofrequency ablation (PIMSRA). The device is an integrated system, comprising ablation electrode kit, ablation generator, cooling system, and patient circuit.

contact lasting ≥ 1/3 of the systolic period (20). Continuous wave doppler guided by color signal was used to measure the LVOT gradient (21, 22). The gradient under exercise stress was provoked by supine cycling (Semi-recumbent and tilting bicycle Ergometer, Lode BV, Groningen, Netherlands) and measured according to a standardized protocol (23). All sections and measurements were obtained in accordance with the recommendations of the American Society of Echocardiography for HOCM (24). The results of genetic tests were interpreted for pathogenicity according to the guidelines of the American College of Medical Genetics and Genomics (25).

Procedure

The use of Liwen RF can be described through four workflow steps: device deployment, puncture, ablation, and withdrawal. Setup and removal of the device are performed jointly by the engineer and the physician. The only conductor on the needle, the working section, releases a high-frequency current in the myocardium which excites ions to generate heat. The local tissue temperature recorded by the electrode tip can reach above 80°C. As a result, the tissue become dehydrated, coagulates, and areas of necrosis are formed. At the same time, the occlusion of the surrounding vessels blocks the blood supply of the hypertrophic myocardium. All procedures follow the requirements of PIMSRA (18, 26). Temporary pacemaker placement is required for patients with pre-procedural right bundle branch block or left bundle branch block. During the procedure, which is performed in general anesthesia, the patient is placed on the left side at 30 to 45 degrees. Then ECG and Liwen RF system are connected. Under echocardiography guidance, the puncture needle is inserted through the guide frame, and reaches the front end of the area, which is thought to be ablated. Then, the needle is pulled out of the core and the electrode needle inserted into the body and pushed to the target area under echocardiography guidance. The ablation generator is turned on. The initial power is 20 watts and gradually increased to 70∼80 watts at 10∼20 watts increments. Ablation

continues for 10 to 12 min. After adjusting the working section length and position of the needle electrode, the aforementioned steps are repeated. The number and location of the ablations are tailored to the expected ablation range. Dehydrated, coagulated tissue that has been completely ablated appears as a hyperechoic area on TTE. Ablation was considered satisfactory when the area was 30∼40 mm along both the long and short axes of the IVS and the thickness reached 2/3 of it. At this point, as shown in **Figure 1**, 3∼5 mm of unablated area must be maintained bilaterally with respect to the endocardium. If prolonged heart block or tachyarrhythmias were detected by ECG, ablation was suspended until normal rhythm was restored spontaneously or after lidocaine treatment. After all ablations are complete, the electrode needle is removed and pressure to the puncture point applied for 5–10 min. Vital signs were closely monitored for at least 15 min, during which TTE was performed to assess the range of ablation, cardiac structure, and hemodynamics. If the rhythm and hemodynamics were stable, the patients were transferred to the ICU for at least 24 h of monitor and recovery.

Process monitoring and energy calculation

Throughout the procedure, an engineer continuously monitors system performance and records equipment errors. The ablation generator, the host of the system, has a touchable display for setting and viewing device parameters. According to the procedure situation, the engineer records the energy output time and maximum power of each ablation, and feedback to the operator. After the procedure, the generator calculates the average power of the entire ablation process. The average power and the ablation time are multiplied to obtain the total output energy.

Endpoints

The primary endpoint is the occurrence of major adverse events (MAE) within 30 days. It is defined as any device or procedure related complication, including but not limited to death, emergency surgery, severe cardiac tamponade requiring pericardiocentesis or surgery, bleeding, and procedure-related stroke. We define device-related and procedural complications as follows: complications that occur while the ablation needle is in the body are considered device-related complications. After the device is removed, if new complications occur or existing complications change, they are classified as procedural complications. Secondary endpoints include: (i) Technical success: the ablation needle enters the myocardium smoothly and leaves completely at the end, and the system has no error throughout the procedure; (ii) Procedural success: Reduction of the resting or provoked LVOT gradient to < 30 mmHg or by $\geq 50\%$ 12 months after procedure.

Statistical analysis

The Shapiro-Wilk test was used to evaluate the data set for normal distribution. Quantitative data of normal distribution were expressed as mean ± standard deviation (SD), and the paired-sample *t*-test was used for comparison. Non-normally distributed quantitative data were represented by medians and interquartile range (IQR), and the Wilcoxon signed rank test was used for comparison. Qualitative data were expressed as absolute counts and percentages of total, and compared using the Pearson χ^2 test. A *P*-value < 0.05 was considered statistically significant. The analyses were performed with SPSS software 26.0 (SPSS Inc., Chicago, IL, USA).

Results

Baseline characteristics

A total of 68 patients were consecutively enrolled from July 2019 to July 2020. During the study, all patients were treated with the same equipment. Baseline characteristics are summarized in **Table 2**. The average age was 47.74 ± 13.85 years, and 29.4% (20/68) were female. According to the prediction model (1), the overall risk of sudden cardiac death was intermediate to high because a median SCDI of $\geq$ 4% was present. Among the 68 patients, the IVS thickness was 23.56 ± 4.55 mm, and the resting LVOT gradient was 78 ± 39 mmHg, accompanied by typical clinical symptoms. All patients underwent genetic testing before the procedure. A total of 31 patients were identified with pathogenic variants in sarcomere protein and related genes, while the genetic profile of the remaining 37 cases has not yet been completely elucidated. Among patients with definite mutations, the proportion of myosin heavy chain (MYH7) gene mutation was 51.6% (16/31), and that of myosin binding protein C (MYBPC3) gene was 38.7% (12/31). Interestingly, one patient had a dual mutation of both MYBPC3 and MYH7. Other pathogenic variants include genes encoding cardiac troponin I (TNNI3) and the protein tyrosine phosphatase non-receptor-type 11 (PTPN11).

Equipment feasibility and procedure data

According to our success definition, all 68 patients achieved satisfactory treatment results. The application success rate of Liwen RF ablation system in the treatment of drug-resistant HOCM was 100%. A series of procedure related parameters and possible technical errors are listed in **Table 3**. During the 68 procedures, the operator had to start/stop the ablation device 8 (IQR: 4) times to adjust the position and working section length to achieve the designed ablation range. The total energy output

TABLE 2 Baseline characteristics of patients.

Group	Value
Age (years)-mean ± SD	47.74 ± 13.85
Female-n (%)	20 (29.4)
BSA (m^2)-mean ± SD	1.80 ± 0.19
SCDI (%)-median (IQR)	4.28 (3.67)
Complicating disease-n (%)	
Hypertension	18 (26.5)
Coronary heart disease	4 (5.9)
Type 2 diabetes mellitus	4 (5.9)
Gene mutation site-n (%)	
MYH7	16 (23.5)
MYBPC3	12 (17.6)
TNNI3	1 (1.5)
PTPN11	1 (1.5)
MYBPC3 and MYH7*	1 (1.5)
Unknown sites	37 (54.4)
NYHA functional class ≥ III-n (%)	18 (26.5)
6-min walk test distance (m)-mean ± SD	451.5 ± 86.0
Symptom-n (%)	
Chest pain	66 (97.1)
Shortness of breath	54 (79.4)
Syncope/pre-syncope	31 (45.6)
LVEF (%)-median (IQR)	58 (4)
IVS (mm)-mean ± SD	23.56 ± 4.55
Mitral valve SAM†-n (%)	
Grade 0	5 (7.4)
Grade 1	2 (2.9)
Grade 2	30 (44.1)
Grade 3	31 (45.6)
Resting LVOTG (mmHg)-mean ± SD	78 ± 39
Provoked LVOTG (mmHg)-mean ± SD	126 ± 44

*Double mutation; †Measured at rest. BSA, body surface area; IQR, interquartile range; IVS, interventricular septum; LVEF, left ventricular ejection fractions; LVOTG, left ventricular outflow tract gradient; NYHA, New York heart association functional class; SAM, systolic anterior motion; SCDI, sudden cardiac death index.

TABLE 3 Data of equipment and procedure.

Group	Value
Technical success-n (%)	68 (100)
Procedural success-n (%)	60 (88.2)
Time of ablation (minutes)-median (IQR)	75.8 (30.0)
Ablation times-median (IQR)	8 (4)
Range of ablation (mm)-median (IQR)	
Length	40 (9)
Width	40 (13)
Thickness	16 (4)
Maximum power (W)-mean ± SD	64 ± 18
Average power (W)-mean ± SD	43.61 ± 13.34
Total energy (kJ)-median (IQR)	186.02 (114.97)
Equipment error-n (%)	
Device power cannot be turned on	0 (0.0)
No power output	0 (0.0)
No impedance reading	0 (0.0)
No RF connection	0 (0.0)
Cooling pump be stationary	0 (0.0)
No coolant flow or insufficient flow	0 (0.0)
Needle fracture	0 (0.0)
Power supply interruption	0 (0.0)
Needle bending-n (%)	7 (10.3)

IQR, interquartile range; RF, radiofrequency.

time was 75.8 (IQR: 30.0) min, and the cumulative energy release 186.02 (IQR: 114.97) kilojoules. The maximum and average power were 64 ± 18 and 43.61 ± 13.34 watts, respectively. There was no interruption or failure of the procedure caused by the error of the ablation system. Although we were fully prepared and formulated corresponding solutions and treatment plans, no error occurred during this period. The integrity of the ablation needle was routinely examined after the procedure. Needle fracture did not occur in any of the interventions. Interestingly, in 7 (10.3%) patients, the needles were bent after removal. The degree of bending varies from patient to patient and ranges from 5 to 60°. Further analysis showed that needle bending was not associated with complications or efficacy. Therefore, we do not consider it a type of equipment error.

Major adverse events and safety

All MAE are listed in Table 4. Most complications occurred during the intervention. Pericardial effusion/hemorrhage was noted in six patients (8.8%) during ablation or needle removal and was treated successfully with pericardiocentesis. There were no recurrences at follow-up. At routine examination 1 month after the procedure, one patient (1.5%) presented with pericardial effusion and was treated successfully with pericardiocentesis. None of the patients hat to undergo cardiac surgery. Nineteen patients (27.9%) experienced transient idioventricular rhythm during the procedure and recovered after a brief pause in ablation. One patient (1.5%) had complete left bundle branch block (CLBBB), and six patients (8.8%) had complete right bundle branch block (CRBBB). Their heart rhythm gradually returned to normal during subsequent ablations, and all the blocks were transient and resolved at the end of the procedure. None of the seven patients had a permanent heart block during follow-up. Ventricular fibrillation (VF) with hypotension occurred in one (1.5%) patient. The needle was removed, and the procedure was terminated prematurely. The patient underwent immediate cardiopulmonary resuscitation and VF could be terminated by defibrillation to sinus rhythm. Subsequently, the patient's hemodynamics remained stable and without any neurologic deficit and this complication was without any further sequelae.

TABLE 4 Major adverse events within 30 days.

Group-n (%)	Device-related complications	Procedural complications
Pericardial effusion	6 (8.8)	1 (1.5)
Cardiac tamponade	0 (0.0)	0 (0.0)
Pleural effusion	0 (0.0)	0 (0.0)
Transient idioventricular rhythm	19 (27.9)	0 (0.0)
VT (> 120 bpm)	0 (0.0)	0 (0.0)
CLBBB	1 (1.5)	0 (0.0)
CRBBB	6 (8.8)	0 (0.0)
AVB	0 (0.0)	0 (0.0)
CHB	0 (0.0)	0 (0.0)
VF	1 (1.5)	0 (0.0)
Hypotension	1 (1.5)	0 (0.0)
Ventricular septal pseudoaneurysm	0 (0.0)	0 (0.0)
Ventricular septal perforation	0 (0.0)	0 (0.0)
Infection	0 (0.0)	0 (0.0)
Stroke	0 (0.0)	0 (0.0)
Recovery after SCD	1 (1.5)	0 (0.0)
Death	0 (0.0)	0 (0.0)

AVB, atrial ventricular block; CHB, complete heart block; CLBBB, complete left bundle branch block; CRBBB, complete right bundle branch block; SCD, sudden cardiac death; VF, ventricular fibrillation; VT, ventricular tachycardia.

Importantly, there were no MAE in this patient at 30-day, follow-up.

Effectiveness

Post-procedure characteristics are shown in **Figure 2**. The procedural success was 88.2% (60/68). At 12-months follow-up, the resting LVOT gradient was significantly lower than at baseline [75 (IQR: 48) *vs.* 12 (IQR: 19) mmHg, $p < 0.001$] and there was a significant reduction in the provoked LVOT gradient under physical exercise [122 (IQR: 53) *vs.* 41 (IQR: 59) mmHg, $p < 0.001$]. Two patients (2.9%) experienced paradoxical increases of resting and provoked LVOT gradients, and 1 patient (1.5%) had increases in provoked LVOT gradients. The maximum thickness of the IVS decreased from 23.56 ± 4.55 mm before the procedure to 16.53 ± 3.23 mm after the procedure ($p < 0.001$). Moreover, 17 patients (25.0%) presented with SAM (grade 2 and above) at rest after treatment, as compared to 61 patients (89.7%) before the procedure ($p < 0.001$). There were significant improvements in functional capacity: patients with New York Heart Association (NYHA) functional class $\geq$ III decreased from 18 (26.5%) patients at baseline to 3 (4.4%) at 12 months follow-up ($p = 0.143$). At the same time, the incidence of chest pain [66 (97.1%) *vs.* 11 (16.2%), $p < 0.001$], shortness of breath [54 (79.4%) *vs.* 11 (16.2%), $p < 0.001$] and syncope/pre-syncope [31 (45.6%) *vs.* 4 (5.9%), $p < 0.001$] all decreased at 12-month follow-up.

Discussion

The Liwen RF ablation system has been evaluated in a small series of patients for the treatment of symptomatic HOCM which is resistant to medical management. In this study, a total of 68 patients who underwent septal reduction therapy with the Liwen technology between 2019 and 2020 were included. To our knowledge, this is the first, larger-scale study to report the application of conformal ablation in HOCM patients. This study shows that the application of the new system has been successful in all patients.

Current invasive treatment methods, SM and ASA, can relieve symptoms and improve prognosis by removing LVOT obstruction. It is worth noting that myectomy is an arduous challenge for patients, requiring thoracotomy and cardiopulmonary bypass with a heart-lung machine (27, 28), and the recovery time after the operation is quite long. Obstructions in the ventricular cavity and apex are often difficult to eliminate. In addition, the procedural success is dependent on the surgeon's experience. ASA is less traumatic, compared to myectomy. However, the anatomical variation of the blood vessels supplying the IVS causes variable results regarding target ablation area and clinical results (gradient reduction) (29–31). Importantly, due to the presence of collateral vessels, the infarction area after alcohol injection may be larger than intended and can have serious consequences including large myocardial infarctions, complete atrial ventricular block (AVB) and/or sudden death (15). Endocardial radiofrequency ablation of septal hypertrophy (ERASH) is another transcatheter septal reduction therapy used as an alternative to SM and ASA intolerance (32, 33). It takes a vascular approach and reaches the myocardium through the endocardium. Despite successful LVOT gradient reduction and symptomatic improvement, current reports of ERASH complications and reduction of IVS thickness are inconsistent (34, 35). Given these outcomes, ERASH requires further study.

As for PIMSRA, the new device could change previous protocols for IVS ablation. In previous procedures, the choice of working section length is a delicate issue. Usually, one chooses between two types of needles (ablation needles with 1 or 2 cm electrode length). The longer the electrode is which is used for the procedure, the greater the energy output per unit time. A large area of the myocardium covered by ablation also means a reduced ability of control. Ventricular septal hypertrophy caused by HOCM is usually irregular and the site of hypertrophy may show great variation (36). Larger size ablation needles are often difficult to handle at thickened boundaries. To be safe, including protection of the conduction system and

10.3389/fcvm.2022.1028763

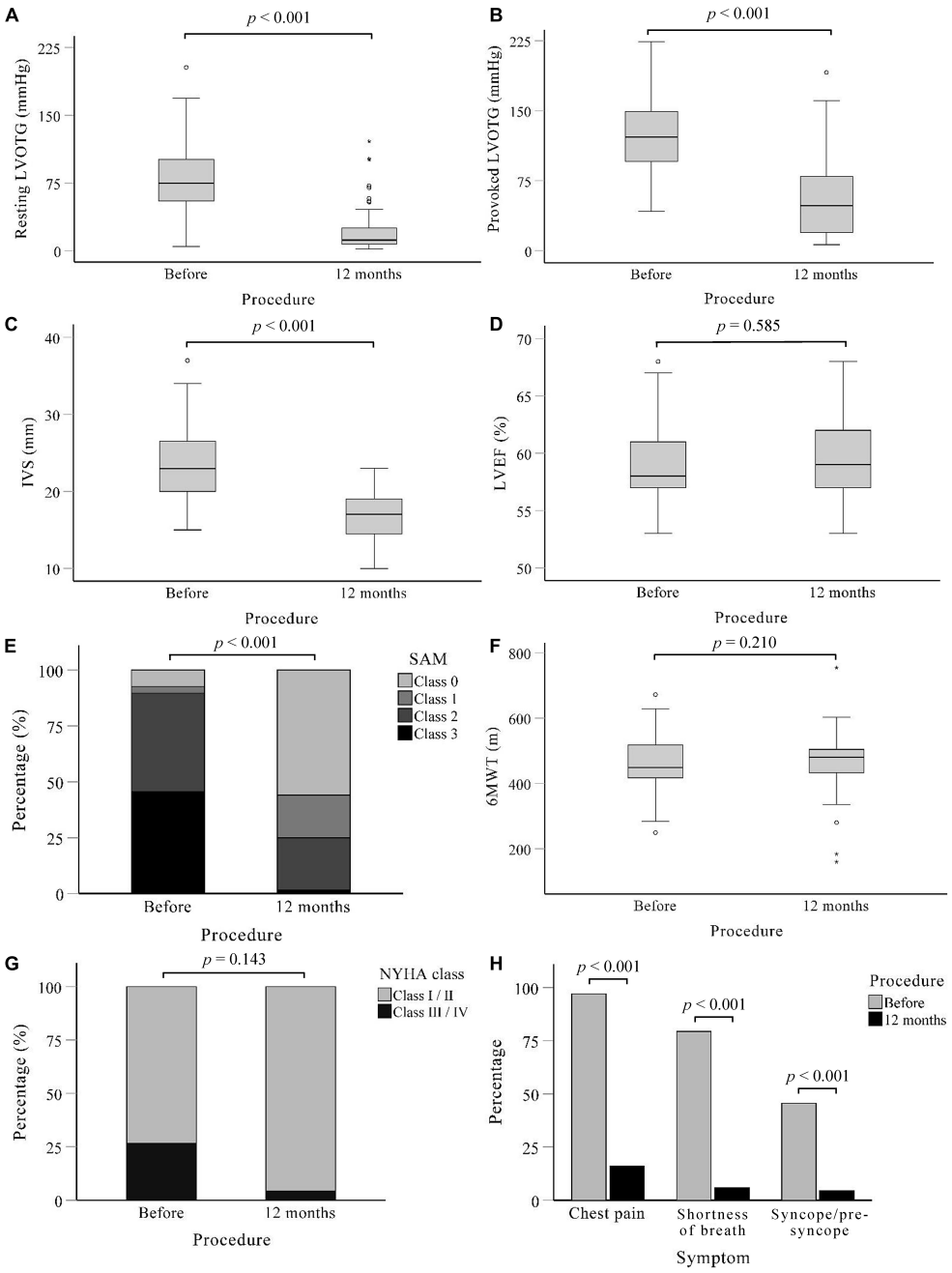

FIGURE 2
Post-procedure characteristics of patients. A systematic evaluation at 12 months after procedure showed that Liwen RF^{TM} was effective in relieving outflow tract obstruction and symptoms compared to baseline. **(A)** Left ventricular outflow tract gradient under calm state. **(B)** Left ventricular outflow tract gradient under provocation of treadmill motion. **(C–E)** Measured in calm state. **(C)** Maximum thickness of interventricular septum. **(D)** Change in left ventricular ejection fractions. **(E)** Grades of mitral valve systolic anterior motion. **(F)** Results of the 6-min walk test. **(G)** The distribution of NYHA function class among patients. **(H)** Incidence of the three main symptoms of chest pain, shortness of breath, and syncope/pre-syncope. IVS, Interventricular septum; LVEF, Left ventricular outflow tract; LVOTG, Left ventricular outflow tract gradient; NYHA, New York heart association; SAM, systolic anterior motion; 6MWT, 6-min walk test.

avoidance of septal perforation, we suggest that the smallest device possible should be used for the procedure, even if thicker LV parts may enable larger device sizes in certain LV areas. Because of this, the ablation may not be fully completed in one cycle, and it is often time-consuming and labor-intensive. The Liwen RF eliminates this hassle completely, with the ablation needle featuring a stepless adjustable electrode. With only one puncture, that is, without changing the needle type, it can

handle IVS of different thickness in different parts. A matching ablation generator adjusts the output according to the electrode's endurance and the changes in impedance resulting from the surrounding myocardial necrosis.

With the concept of conformal ablation, we conducted a preliminary trial using Liwen RF in 68 HOCM patients under the premise of ensuring safety. Three operators performed the procedure in this study. Prior to this, they performed a total of 126 PIMSRA procedures. Regarding safety, pericardial effusion or bleeding occurred mostly because of active hemorrhage of the IVS vessels from coronary vein injury. This apical approach results in small vessel injury and myocardial bleeding along the needle pathway, which is the main cause of pericardial effusion, thus attributable in part to learning curve and pre-procedural planning. The new insertion protocol considers pre-procedural CTA/MRI and intra-operative color Doppler flow imaging. Optimization of needle entry site and direction minimizes vascular injury. In all 68 patients, there was no cardiac tamponade or emergency sternotomy. The PIMSRA procedure uses a 17/18G needle, which remains intra-myocardial. Thus, the injury to myocardium from the needle is limited. In our experience, the use of adjustable needles on the Liwen RF under echocardiographic guidance can effectively reduce the incidence of bleeding. The ablation needle produces a local thermal effect through a high-frequency current. If the ablation boundary is too close to the endocardium, the subendocardial conduction system may be stimulated/injured by the RF energy. We speculate that this is a possible cause of conduction block, ventricular arrhythmias, and even VF. The arrhythmias we encountered were all temporary, thanks to accurate positioning and precise control of the ablation range (working section length). We encountered one patient in need of defibrillation for ventricular fibrillation, which taught us that we need a safe distance from the ablation boundary to the endocardium. There were no secondary abnormalities in the cardiac structure (ventricular septal perforation or ventricular septal pseudoaneurysm). All other patients had stable hemodynamics. We did not find any ablation system error including needle breakage, so we confirmed the stability of the system and the structural strength of the needle. At the same time, we observed that the needle was bent after removal in seven cases. These patients reported no adverse outcomes such as myocardial tears or bleeding. In our analysis, the flexion occurred *in vivo* at the costal margin rather than in the myocardium. The site of puncture and the degree of myocardial fibrosis may explain this phenomenon. Despite the excellent strength of the electrode needle, excessive bending is not recommended during use.

The 12-month follow-up provided insight into the effectiveness of the system. The procedure using Liwen RF can be considered effective. We observed an improvement in cardiac function after procedure. The incidence of chest pain, shortness of breath, and syncope/pre-syncope decreased significantly after LVOT obstruction was resolved, reflecting improvements in patients' quality of life. Due to the increase of cardiac output and the improvement of systemic perfusion, the proportion of patients with NYHA function greater than class 2 decreased after the procedure. With the remission of symptoms, the 6-min walk distance also showed an increasing trend. On echocardiography, hemodynamic findings objectively improved. The absorption of necrotic tissue and myocardial remodeling after radiofrequency ablation reduced the maximum thickness of IVS. The LVOT gradient at rest decreased significantly consistent with a relief of obstruction. The LVOT gradient under provocation of treadmill exercise decreased after the procedure, indicating no obstruction of blood flow during a high dynamic state. The LVOT gradient reduction can diminish the anterior motion of the anterior mitral valve leaflet, thereby further improving the outflow tract gradient. The paradoxical increase in obstruction may be due to insufficient ablation and unintended cardiac remodeling. There was no significant change in LVEF because ventricular filling was limited before obstruction relief. Ventricular end-diastolic volume and stroke volume increased after the procedure. Due to limitations of the formula, the increased cardiac output was not reflected.

Although the procedures were performed with Liwen RF, we tend to attribute the results to the optimization of the needle rather than the procedure itself. The use of this stepless adjustable needle makes it possible for our operators to achieve conformal ablation. Since this is a study of the first-in-man application, it is not meaningful to compare Liwen RF and Cool-Tip, given the differences in treatment procedures between the two systems. We can expect that with the development of a new generation of Liwen RF ablation system, operators will be able to perform more complete and accurate ablations while avoiding complications as much as possible.

Limitations

Patients with septal thickness of 30 mm or more were not included in our study. The safety and effectiveness of the device cannot be verified for use in this population. Subsequent upgrades or new models may remedy this deficiency.

Since this is a newly developed device, the accumulation of time spent by the operators and the learning curve of the doctors may have influenced the results. In addition, this was a preliminary study and the number of cases included in the study was limited. There may be rare complications and specific uses that have not been recognized. More conclusions about safety and applicability need to be answered by further multicenter, prospective studies. We were unable to compare the safety and efficacy of the two system. After the feasibility of the new device is confirmed, large-scale randomized controlled trials will be conducted to fill this gap.

Conclusion

The Liwen RF is a novel device with a stepless adjustable electrode length. It is used to ablate hypertrophic IVS accurately and safely according to its irregular shape in the treatment of drug-resistant HOCM. For patients who cannot undergo SM or ASA, this device demonstrated a significant reduction in LVOT obstruction and alleviation of clinical symptoms during follow-up. The incidence of intraprocedural and postprocedural complications was low. This study demonstrates the feasibility of the Liwen RF ablation system for the treatment of drug-resistant HOCM.

Data availability statement

The original contributions presented in the study are included in the article/supplementary material, further inquiries can be directed to the corresponding authors.

Ethics statement

The studies involving human participants were reviewed and approved by the Ethics Committee of Xijing Hospital. The patients/participants provided their written informed consent to participate in this study.

Author contributions

ZW drafted the article. ST, RH, and LL designed the study. HS, ST, SB, KP, and MZ revised the manuscript. ZW and RH designed figures. RZ, JnL, CL, XL, JaL, BX, and BF were responsible for patient management and data collection. All authors read and approved the final manuscript.

Funding

This study was supported by the National Natural Science Foundation of China (Grant Nos. 82071932 and 82001831); Shaanxi Province Key Project (2017ZDXM-SF-058); and Xijing Hospital Medical Specialty Enhancement Project (Grant No. XJZT18Z03).

Acknowledgments

We thank the participating patients and their families as well as the multi-disciplinary heart team for making this study possible. We also thank to Qi Ming medical team for providing equipment and technical support for this study.

Conflict of interest

HS has received institutional honoraria, travel expenses, and consulting fees from 4tech Cardio, Abbott, Ablative Solutions, Ancora Heart, Append Medical, Bavaria Medizin Technologie GmbH, Bioventrix, Boston Scientific, Carag, CardiacDimensions, Cardimed, Celonova, Comed B.V., Contego, CVRx, Dinova, Edwards Lifesciences, Endologix, Hemoteq, Hangzhou Nuomao Medtech, Holistick Medical, Lifetech, Maquet Getinge Group, Medtronic, Mokita, Occlutech, Recor, RenalGuard, Terumo, Vascular Dynamics, Vectorious Medtech, Venus, Venock, and Vivasure Medical.

The remaining authors declare that the research was conducted in the absence of any commercial or financial relationships that could be construed as a potential conflict of interest.

The reviewer LZ declared a past collaboration with one of the author LL to the handling editor.

Publisher's note

All claims expressed in this article are solely those of the authors and do not necessarily represent those of their affiliated organizations, or those of the publisher, the editors and the reviewers. Any product that may be evaluated in this article, or claim that may be made by its manufacturer, is not guaranteed or endorsed by the publisher.

References

1. Ommen SR, Mital S, Burke MA, Day SM, Deswal A, Elliott P, et al. 2020 AHA/ACC guideline for the diagnosis and treatment of patients with hypertrophic cardiomyopathy: executive summary: a report of the American college of cardiology/American heart association joint committee on clinical practice guidelines. *J Am Coll Cardiol.* (2020) 76:3022–55. doi: 10.1016/j.jacc.2020.08.044

2. Maron BJ, Gardin JM, Flack JM, Gidding SS, Kurosaki TT, Bild DE. Prevalence of hypertrophic cardiomyopathy in a general population of young adults. echocardiographic analysis of 4111 subjects in the cardia study. Coronary artery risk development in (young) adults. *Circulation.* (1995) 92:785–9. doi: 10.1161/01.cir.92.4.785

3. Semsarian C, Ingles J, Maron MS, Maron BJ. New perspectives on the prevalence of hypertrophic cardiomyopathy. *J Am Coll Cardiol.* (2015) 65:1249–54. doi: 10.1016/j.jacc.2015.01.019

4. Davies MJ, McKenna WJ. Hypertrophic cardiomyopathy–pathology and pathogenesis. *Histopathology.* (1995) 26:493–500. doi: 10.1111/j.1365-2559.1995.tb00267.x

5. Shapiro LM, McKenna WJ. Distribution of left ventricular hypertrophy in hypertrophic cardiomyopathy: a two-dimensional echocardiographic study. *J Am Coll Cardiol.* (1983) 2:437–44. doi: 10.1016/s0735-1097(83)80269-1

6. Maron MS, Olivotto I, Betocchi S, Casey SA, Lesser JR, Losi MA, et al. Effect of left ventricular outflow tract obstruction on clinical outcome in hypertrophic cardiomyopathy. *N Engl J Med.* (2003) 348:295–303. doi: 10.1056/NEJMoa021332

7. Elliott P, Gimeno J, Tome M, McKenna W. Left ventricular outflow tract obstruction and sudden death in hypertrophic cardiomyopathy. *Eur Heart J.* (2006) 27:3073. doi: 10.1093/eurheartj/ehl383

8. Gimeno JR, Tome-Esteban M, Lofiego C, Hurtado J, Pantazis A, Mist B, et al. Exercise-induced ventricular arrhythmias and risk of sudden cardiac death in patients with hypertrophic cardiomyopathy. *Eur Heart J.* (2009) 30:2599–605. doi: 10.1093/eurheartj/ehp327

9. Guttmann OP, Rahman MS, O'Mahony C, Anastasakis A, Elliott PM. Atrial fibrillation and thromboembolism in patients with hypertrophic cardiomyopathy: systematic review. *Heart.* (2014) 100:465–72. doi: 10.1136/heartjnl-2013-304276

10. Morrow AG, Brockenbrough EC. Surgical Treatment of idiopathic hypertrophic subaortic stenosis: technic and hemodynamic results of subaortic ventriculomyotomy. *Ann Surg.* (1961) 154:181–9. doi: 10.1097/00000658-196108000-00003

11. Morrow AG. Hypertrophic subaortic stenosis. Operative methods utilized to relieve left ventricular outflow obstruction. *J Thorac Cardiovasc Surg.* (1978) 76:423–30.

12. Sigwart U. Non-surgical myocardial reduction for hypertrophic obstructive cardiomyopathy. *Lancet.* (1995) 346:211–4. doi: 10.1016/s0140-6736(95)91267-3

13. Mohr R, Schaff HV, Puga FJ, Danielson GK. Results of operation for hypertrophic obstructive cardiomyopathy in children and adults less than 40 years of age. *Circulation.* (1989) 80(3 Pt 1:I191–6.

14. Maron BJ, Dearani JA, Ommen SR, Maron MS, Schaff HV, Nishimura RA, et al. Low operative mortality achieved with surgical septal myectomy: role of dedicated hypertrophic cardiomyopathy centers in the management of dynamic subaortic obstruction. *J Am Coll Cardiol.* (2015) 66:1307–8. doi: 10.1016/j.jacc.2015.06.1333

15. Veselka J, Jensen MK, Liebregts M, Januska J, Krejci J, Bartel T, et al. Long-term clinical outcome after alcohol septal ablation for obstructive hypertrophic cardiomyopathy: results from the Euro-Asa registry. *Eur Heart J.* (2016) 37:1517–23. doi: 10.1093/eurheartj/ehv693

16. Nishimura RA, Seggewiss H, Schaff HV. Hypertrophic obstructive cardiomyopathy: surgical myectomy and septal ablation. *Circ Res.* (2017) 121:771–83. doi: 10.1161/CIRCRESAHA.116.309348

17. Liu L, Liu B, Li J, Zhang Y. Percutaneous intramyocardial septal radiofrequency ablation of hypertrophic obstructive cardiomyopathy: a novel minimally invasive treatment for reduction of outflow tract obstruction. *EuroIntervention.* (2018) 13:e2112–3. doi: 10.4244/eij-d-17-00657

18. Liu L, Li J, Zuo L, Zhang J, Zhou M, Xu B, et al. Percutaneous intramyocardial septal radiofrequency ablation for hypertrophic obstructive cardiomyopathy. *J Am Coll Cardiol.* (2018) 72:1898–909. doi: 10.1016/j.jacc.2018.07.080

19. Li YJ, Feng Y, Li X, Zuo L, Gu T, Liu LW, et al. Case report: minimally invasive therapy by transcatheter aortic valve replacement and percutaneous intramyocardial septal radiofrequency ablation for a patient with aortic stenosis combined with hypertrophic obstructive cardiomyopathy: two-year follow-up results. *Front Cardiovasc Med.* (2021) 8:735219. doi: 10.3389/fcvm.2021.735219

20. Pollick C, Rakowski H, Wigle ED. Muscular subaortic stenosis: the quantitative relationship between systolic anterior motion and the pressure gradient. *Circulation.* (1984) 69:43–9. doi: 10.1161/01.cir.69.1.43

21. Panza JA, Petrone RK, Fananapazir L, Maron BJ. Utility of continuous wave doppler echocardiography in the noninvasive assessment of left ventricular outflow tract pressure gradient in patients with hypertrophic cardiomyopathy. *J Am Coll Cardiol.* (1992) 19:91–9. doi: 10.1016/0735-1097(92)90057-t

22. Sasson Z, Yock PG, Hatle LK, Alderman EL, Popp RL. Doppler echocardiographic determination of the pressure gradient in hypertrophic cardiomyopathy. *J Am Coll Cardiol.* (1988) 11:752–6. doi: 10.1016/0735-1097(88)90207-0

23. Lancellotti P, Pellikka PA, Budts W, Chaudhry FA, Donal E, Dulgheru R, et al. The clinical use of stress echocardiography in non-ischaemic heart disease: recommendations from the European association of cardiovascular imaging and the American society of echocardiography. *J Am Soc Echocardiogr.* (2017) 30:101–38. doi: 10.1016/j.echo.2016.10.016

24. Lang RM, Badano LP, Mor-Avi V, Afilalo J, Armstrong A, Ernande L, et al. Recommendations for cardiac chamber quantification by echocardiography in adults: an update from the American society of echocardiography and the European association of cardiovascular imaging. *J Am Soc Echocardiogr.* (2015) 28:1–39.e14. doi: 10.1016/j.echo.2014.10.003

25. Richards S, Aziz N, Bale S, Bick D, Das S, Gastier-Foster J, et al. Standards and guidelines for the interpretation of sequence variants: a joint consensus recommendation of the American college of medical genetics and genomics and the association for molecular pathology. *Genet Med.* (2015) 17:405–24. doi: 10.1038/gim.2015.30

26. Liu LW, Zuo L, Zhou MY, Li J, Zhou XD, He GB, et al. Efficacy and safety of transthoracic echocardiography-guided percutaneous intramyocardial septal radiofrequency ablation for the treatment of patients with obstructive hypertrophic cardiomyopathy. *Zhonghua Xin Xue Guan Bing Za Zhi.* (2019) 47:284–90. doi: 10.3760/cma.j.issn.0253-3758.2019.04.005

27. Smedira NG, Lytle BW, Lever HM, Rajeswaran J, Krishnaswamy G, Kaple RK, et al. Current effectiveness and risks of isolated septal myectomy for hypertrophic obstructive cardiomyopathy. *Ann Thorac Surg.* (2008) 85:127–33. doi: 10.1016/j.athoracsur.2007.07.063

28. Iacovoni A, Spirito P, Simon C, Iascone M, Di Dedda G, De Filippo P, et al. A contemporary European experience with surgical septal myectomy in hypertrophic cardiomyopathy. *Eur Heart J.* (2012) 33:2080–7. doi: 10.1093/eurheartj/ehs064

29. Chan W, Williams L, Kotowycz MA, Woo A, Rakowski H, Schwartz L, et al. Angiographic and echocardiographic correlates of suitable septal perforators for alcohol septal ablation in hypertrophic obstructive cardiomyopathy. *Can J Cardiol.* (2014) 30:912–9. doi: 10.1016/j.cjca.2014.04.008

30. Cooper RM, Shahzad A, McShane J, Stables RH. Alcohol septal ablation for hypertrophic obstructive cardiomyopathy: safe and apparently efficacious but does reporting of aggregate outcomes hide less-favorable results, experienced by a substantial proportion of patients? *J Invasive Cardiol.* (2015) 27:301–8.

31. Kim LK, Swaminathan RV, Looser P, Minutello RM, Wong SC, Bergman G, et al. Hospital volume outcomes after septal myectomy and alcohol septal ablation for treatment of obstructive hypertrophic cardiomyopathy: US nationwide inpatient database, 2003-2011. *JAMA Cardiol.* (2016) 1:324–32. doi: 10.1001/jamacardio.2016.0252

32. Lawrenz T, Borchert B, Leuner C, Bartelsmeier M, Reinhardt J, Strunk-Mueller C, et al. Endocardial radiofrequency ablation for hypertrophic obstructive cardiomyopathy: acute results and 6 months' follow-up in 19 patients. *J Am Coll Cardiol.* (2011) 57:572–6. doi: 10.1016/j.jacc.2010.07.055

33. Kong L, Zhao Y, Pan H, Ma J, Qian J, Ge JA. Modified endocardial radiofrequency ablation approach for hypertrophic obstructive cardiomyopathy guided by transthoracic echocardiography: a case series. *Ann Transl Med.* (2021) 9:1006. doi: 10.21037/atm-21-2783

34. Crossen K, Jones M, Erikson C. Radiofrequency septal reduction in symptomatic hypertrophic obstructive cardiomyopathy. *Heart Rhythm.* (2016) 13:1885–90. doi: 10.1016/j.hrthm.2016.04.018

35. Liu Q, Qiu H, Jiang R, Tang X, Guo W, Zhou K, et al. Selective interventricular septal radiofrequency ablation in patients with hypertrophic obstructive cardiomyopathy: who can benefit? *Front Cardiovasc Med.* (2021) 8:743044. doi: 10.3389/fcvm.2021.743044

36. Hughes SE. The pathology of hypertrophic cardiomyopathy. *Histopathology.* (2004) 44:412–27. doi: 10.1111/j.1365-2559.2004.01835.x

frontiers | Frontiers in Cardiovascular Medicine

TYPE Brief Research Report
PUBLISHED 09 January 2023
DOI 10.3389/fcvm.2022.1000352

OPEN ACCESS

EDITED BY
Matteo Cameli,
University of Siena, Italy

REVIEWED BY
Valentina Barletta,
Pisana University Hospital, Italy
Charles Hoopes,
University of Alabama at Birmingham,
United States

*CORRESPONDENCE
Zhi-Gang Liu
✉ liuzg@tedaich.com

SPECIALTY SECTION
This article was submitted to
Heart Failure and Transplantation,
a section of the journal
Frontiers in Cardiovascular Medicine

RECEIVED 22 July 2022
ACCEPTED 19 December 2022
PUBLISHED 09 January 2023

CITATION
Yu X-Y, Shi J-W, Rong Y-S, Chen Y-L, Liu T-W, Zang Y-R, Fu Z-A, Zhang J-M, Han Z-F and Liu Z-G (2023) The role of atria in ventricular fibrillation after continuous-flow left ventricular assist device implantation in ovine model. *Front. Cardiovasc. Med.* 9:1000352. doi: 10.3389/fcvm.2022.1000352

The role of atria in ventricular fibrillation after continuous-flow left ventricular assist device implantation in ovine model

Xin-Yi Yu[1], Jian-Wei Shi[1], Yan-Sheng Rong[2], Yuan-Lu Chen[3], Tian-Wen Liu[4], Yi-Rui Zang[1], Ze-An Fu[1,5], Jie-Min Zhang[4], Zhi-Fu Han[6] and Zhi-Gang Liu[1,5]*

[1]Department of Cardiovascular Surgery, TEDA International Cardiovascular Hospital, Chinese Academy of Medical Sciences & Peking Union Medical College, Tianjin, China, [2]Department of Anesthesiology, TEDA International Cardiovascular Hospital, Chinese Academy of Medical Sciences & Peking Union Medical College, Tianjin, China, [3]Department of Cardiac Electrophysiology, TEDA International Cardiovascular Hospital, Chinese Academy of Medical Sciences & Peking Union Medical College, Tianjin, China, [4]Laboratory Animal Center, TEDA International Cardiovascular Hospital, Chinese Academy of Medical Sciences & Peking Union Medical College, Tianjin, China, [5]Cardiovascular Clinical College of Tianjin Medical University, Tianjin, China, [6]ROCOR Medical Technology Co., Ltd., Tianjin, China

Objectives: This study attempted to explore the hemodynamics and potential mechanisms driving pulmonary circulation in status of ventricular fibrillation (VF) following continuous-flow left ventricular assist device (CF-LVAD) implantation.

Methods: An ovine CF-LVAD model was built in small-tailed Han sheep, with the pump speed set as 2,400 rpm. VF was induced following ventricular tachycardia using a temporary pacemaker probe to stimulate the right and left ventricular free walls. The central venous pressure (CVP), pump flow (PF), pulmonary artery flow (PAF) and other major indicators were observed and recorded after VF.

Results: Low-flow systemic and pulmonary circulation could be sustained for 60 min under VF with sinus atrial rhythm after CF-LVAD implantation. The CVP gradually increased. The mean PF declined from 1.80 to 1.20 L/min, and the mean PAF decreased from 1.62 L/min to 0.87 L/min. Under VF with atrial fibrillation, the systemic and pulmonary circulation couldn't be sustained. The CVP jumped from the 5 mmHg baseline to 12 mmHg, the mean PF

rapidly decreased from 3.45 L/min to 0.79 L/min, and the PAF declined from 3.94 L/min to 0.77 L/min.

Conclusion: The atrial rhythm and function might be essential for the circulation maintenance in patients with VF after CF-LVAD implantation.

KEYWORDS

left ventricular assist device (LVAD), ventricular fibrillation (VF), atria, arrhythmia, atrial function

1. Introduction

Mechanical circulatory support (MCS) with continuous-flow left ventricular assist device (CF-LVAD) has been preferably used as a "bridge" device before a heart transplantation and regarded as one of the long-term treatment options for patients with end-stage heart failure. Nonetheless, ventricular arrhythmias (VA) including ventricular fibrillation (VF) which is common in malignant arrhythmias, are frequent after CF-LVAD implantation with an incidence of about 20–60% (1, 2). Under normal physiological status, VF is considered as the main causative factor of sudden cardiac death, as it leads to disappearance of ventricular systolic function and complete loss of cardiac output resulting in severe hemodynamic collapse. Likewise, the VF following CF-LVAD implantation remains to be associated with a risk of low cardiac output or perfusion stop of vital organs and tissues due to the absence of MCS support to the right ventricle (3).

The right heart function is still crucial after CF-LVAD implantation given its role in driving pulmonary blood return to the left heart, which is important for the systemic circulation, even though the CF-LVAD can substitute for the left ventricle to perform the systolic function thereby sustaining the systemic circulation. Theoretically, the VF following CF-LVAD implantation is accompanied by complete loss of the right ventricular squeezing, leading to reductions in CF-LVAD preload and cardiac output, which eventually results in circulatory collapse. To the contrary, no clinical signs of serious circulatory failure are found in VF patients with CF-LVAD in the shorter term, instead some non-specific symptoms such as fatigue, chest tightness or drowsiness (4–7).

Currently, the hemodynamics of VF after CF-LVAD implantation remains elusive. In this study, an acute ovine CF-LVAD model was devised in small tail Han sheep. The systemic and pulmonary circulation was observed and the potential mechanism driving the pulmonary circulation was explored, which may provide possible theoretical explanations for the VF after CF-LVAD implantation.

Abbreviations: CF-LVAD, continuous-flow left ventricular assist device; MCS, mechanical circulatory support; VA, ventricular arrhythmias; VF, ventricular fibrillation; HR, heart rate; AOP, aortic pressure; CVP, central venous pressure; LVP, left ventricular pressure; PF, pump flow; PAF, pulmonary arterial flow; ABG, arterial blood gas; LVEF, left ventricular ejection fraction; RVEF, right ventricular ejection fraction; VT, ventricular tachycardia; RAP, right atrial pressure; LAP, left atrial pressure; RVP, right ventricular pressure; AF, atrial fibrillation.

2. Materials and methods

2.1. Experimental device

HeartCon Ventricular Assist Device (ROCOR Medical Technology Co. Ltd., Tianjin, China) was applied as the CF-LVAD, with the body made with titanium alloy and a maximum auxiliary flow of 10 L/min (8).

2.2. Animal model

Two healthy adult male Small Tail Han sheep, each aged 16- and 18-month and weighed 56 and 58 kg, were used as model A and model B. All the two sheep were purchased from Xi'an Dilepu Biology & Medicine Co., Ltd (SCXK [Shanxi] 2014-004). All the two sheep were housed in separate cages for 2 weeks, and no abnormal clinical signs or blood indicators were observed. All protocols and experimental procedures were approved by the Institutional Animal Care and Use Committee of TEDA International Cardiovascular Hospital. Animal experiments were performed in accordance with the National Institutes of Health guidelines for the Care and Use of Laboratory Animals and the Regulations for the Administration of Affairs Concerning Experimental Animals (2017.03.01 edition) published by the State Council of the People's Republic of China. At the end of the experiment, the animals were euthanized by injection of high concentrations of potassium chloride under anesthesia.

2.3. Surgical preparation and operative procedures

The two sheep were subjected to 24-h fasting and 20-h water deprivation prior to operation. After animal sedation by intramuscular injection of xylazine (1.0 mg/kg), the surgical site was exposed, and the neck skin was prepared. Vascular access was obtained through the great saphenous vein, and an intravenous bolus of propofol (60–200 mg) was injected. Tracheal intubation was then performed with parameters including tidal volume 8–12 ml/kg/min, frequency 12–20 times/min, inspired oxygen concentration 40–100%, positive end-expiratory pressure 5–10 mmHg (1 mmHg = 0.133 kPa) and sevoflurane inhalation 2–4%. A nasogastric tube was inserted for decompression. The arterial puncture was achieved through the left ear to obtain arterial access, and central venous access was obtained via puncture of the left internal jugular vein. Anesthesia was maintained by continuous infusion of dexmedetomidine (0.5–1 mg/kg/h) and succinylcholine (50–100 mg/h).

A thoracotomy was performed at the left fifth intercostal space, and a lidocaine drip (2 mg/min) was initiated to prevent arrhythmias. The pericardium was incised from the apex to the pulmonary artery, and the heart was suspended in a pericardial cradle. The site for pump placement was determined according to the apex position. After obtaining a whole-blood clotting time greater than 450s by intravenous bolus injection of 1.0 mg/kg heparin, the descending thoracic aorta was dissected for outflow graft anastomosis. A partial occlusion clamp was applied, and the pump's 10-mm outflow graft was sewn end-to-side to the descending aorta with 4-0 Prolene sutures. Hemostasis of the anastomotic site was obtained to reduce the effect of excessive bleeding on capacity loading. The sewing ring was attached to the left ventricular apex with 8 interrupted sutures. The left pleural cavity was filled with warm normal saline. A cruciform incision was made on the beating heart. Then a ventricular punch was advanced through the ventricular sewing ring, the left ventricular core was removed, and the pump was inserted into the left ventricular cavity and secured. The pump was started at 2,000 rpm; then, the artificial blood vessel was opened after full gas exhausting. In the context of circulatory stability, a temporary pacemaker electrode was implanted in the free wall of the right ventricle and left ventricle, respectively.

2.4. Research methods

The pump speed was adjusted to 2,400 rpm, and baseline data were recorded after stable vital signs and circulatory stability were obtained. The ventricular rate was controlled by pacing, with the initial rate as 180 beats/min at an increasing rate of 20 beats/min. Rates at 180 beats/min, 200 times/min, 220 times/min and above were recorded and the corresponding circulatory conditions were studied.

A multi-channel physiological recorder (MP150 Biopac, USA) was used to record the heart rate (HR), aortic pressure (AOP) (the measurement point was aortic root), central venous pressure (CVP) (right atrial pressure here), left atrial pressure (LAP) and left ventricular pressure (LVP) etc. A double-channel ultrasonic flowmeter (Transonic, USA) was operated to obtain real-time pump flow (PF) (the measurement point was pump outflow graft) and pulmonary arterial flow (PAF). A blood gas analyzer (IL-1430, USA) was applied to perform arterial blood gas (ABG) analysis every 10–15 min. A color doppler ultrasound (Philips5500, Netherlands) was used to calculate right/left ventricular ejection fraction (RVEF/LVEF) and assess aortic valve function by cardiac surface ultrasound every 10–15 min.

3. Results

3.1. Baseline data of sheep with CF-LVAD

The baseline pump speed of both model A and model B was 2,400 rpm. Supported by CF-LVAD, the LVEF and RVEF respectively were 65 and 48% in model A while 72 and 64% in model B; the mean PF and PAF respectively were 1.80 and 1.62 L/min in model A while 3.54 and 3.94 L/min in model B; the CVP was 6 mmHg in model A and 5 mmHg in model B (**Supplementary Figures 1A, B**). The baseline ABG results of model A and model B are exhibited in **Supplementary Table 1**.

3.2. VT after CF-LVAD implantation

Under ventricular tachycardia (VT) following CF-LVAD implantation, CVP showed a gradual upward trend while PAF exhibited a downward trend with the increase in ventricular rate (**Figure 1**). When the ventricular rate reached 280 beats/min, the rate of PAF decline began to gradually slow down. The PAF and CVP basically changed reversely during the whole process.

The cardiac electrical activity, PF, PAF and atrial/ventricular pressure of the animal models are described in **Supplementary Figure 2**. With the increase in ventricular rate, right atrial pressure (RAP) gradually increased while LAP was relatively stable. In addition, RVP, LVP, PF, and PAF reduced with the increase in ventricular rate.

3.3. VF after CF-LVAD implantation

Ventricular fibrillation was induced in both the model A and model B when the ventricular rate reached 320 beats/min, while

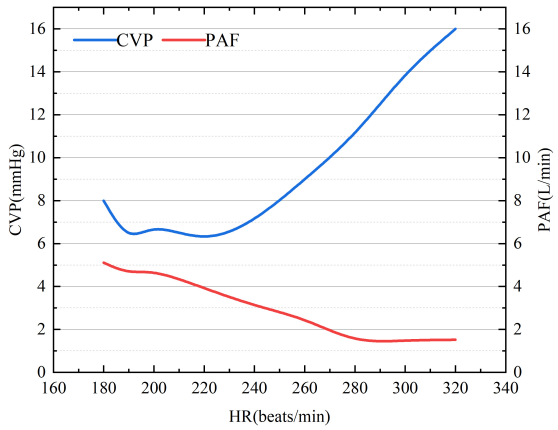

FIGURE 1
The association of ventricular rate with CVP and PAF under VT after CF-LVAD implantation. CVP, central venous pressure (right atrial pressure here); PAF, pulmonary artery flow.

there was distinct difference. In model A, VF occurred with sinus atrial rhythm and is accompanied by gradually increased CVP (from 6 mmHg baseline to 10 mmHg at 10 min, 11 mmHg at 30 min and 12 mmHg at 60 min) and waveform amplitude (from 3 mmHg baseline to 7 mmHg at 60 min) with increasing duration. Both LVP and AOP were lower than the normal baseline after VF. Both mean PF and PAF went down while were kept at 1.20 and 0.87 L/min, respectively, during the whole process of VF. The cardiac electrical activity, PF, PAF, CVP, and LVP/AOP after VF were detailed in **Figure 2**. The ABG results at each time point were shown in **Supplementary Table 2**. LVEF was always 0 while RVEF was kept at around 36%. At 60 min of VF, sinus rhythm was successfully restored by defibrillation (25 J) (**Figure 2F**), PF, PAF, LVP, and AOP restored to baseline or slightly higher levels, CVP declined to baseline and the waveform amplitude decreased (**Figure 2F**).

In model B, VF occurred with AF, accompanied by rapid increase in the mean CVP (from 5 mmHg baseline to 12 mmHg) along with irregular waveform and reduced amplitude. In the meantime, the mean PF (3.54–0.79 L/min) and PAF (3.94–0.77 L/min) declined rapidly with the loss of regular waveform. The LVP and RVP also dropped rapidly, and the RVP fell to nearly 0 mmHg. The cardiac electrical activity, PF, PAF, and LVP/RVP after VF were detailed in **Figure 3**. The data of ABG were listed in **Supplementary Table 3**. Circulation of the model B could not be sustained and administration of drugs such as norepinephrine (NE) was ineffective. Besides, immediate defibrillation at 25–50 J failed to restore the sinus rhythm. Both the LVEF and RVEF were 0 on cardiac ultrasound.

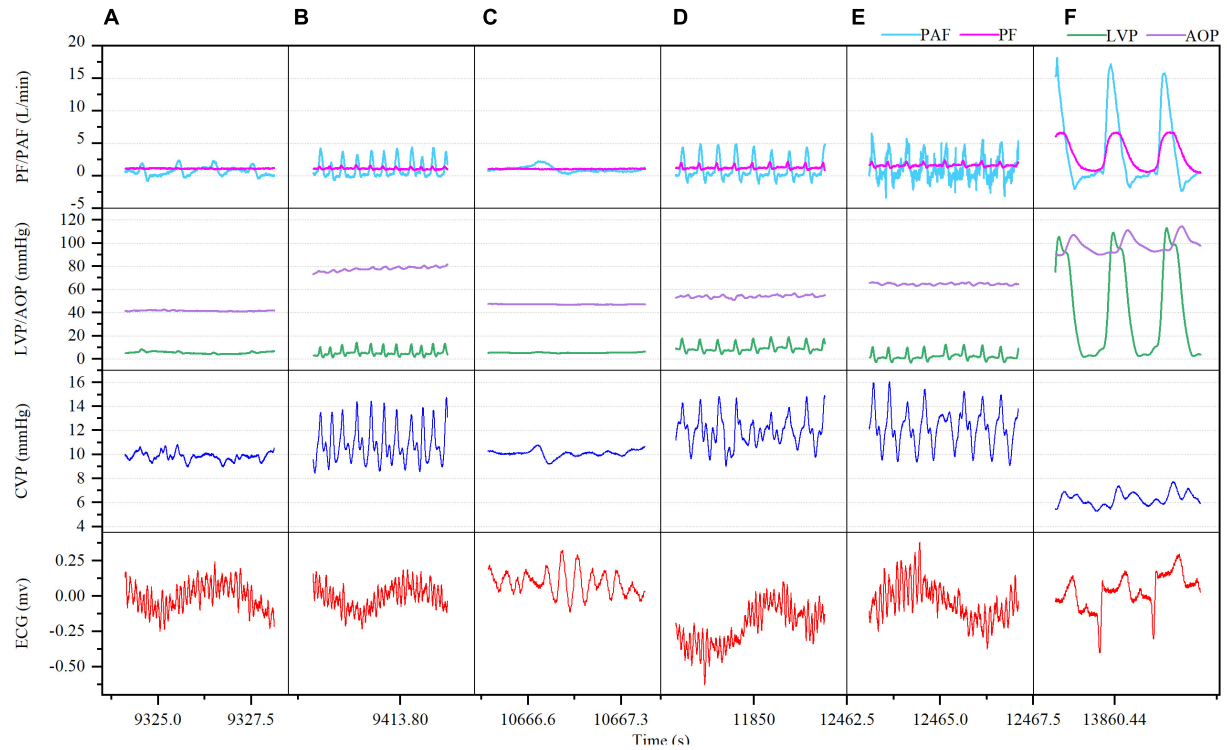

FIGURE 2
Ventricular fibrillation (VF) with sinus rhythm after CF-LVAD implantation (Model A). **(A)** VF 5 min; **(B)** VF 10 min; **(C)** VF 30 min; **(D)** VF 50 min; **(E)** VF 60 min; **(F)** after defibrillation. PF, pump flow; PAF, pulmonary artery flow; LVP, left ventricular pressure; AOP, aortic pressure.

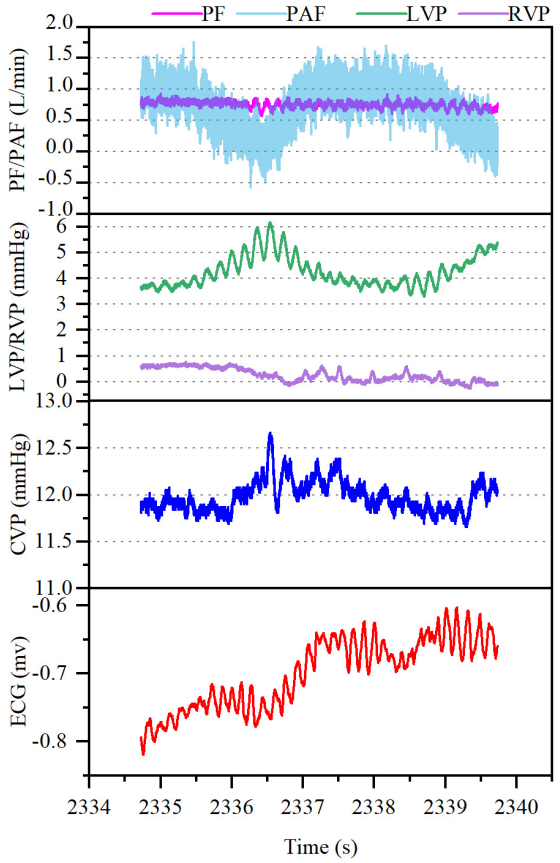

FIGURE 3
Ventricular fibrillation (VF) with atrial fibrillation after CF-LVAD implantation (Model B). PF, pump flow; PAF, pulmonary artery flow; LVP, left ventricular pressure; RVP, right ventricular pressure.

4. Discussion

Ventricular tachycardia commonly occurs with hemodynamic disorders, together with accelerated ventricular rate and dramatically shortened period of ventricular diastole with deceased filling pressures, resulting in cardiac output reduction. VF is the major cause of sudden cardiac death immediately followed by severe hemodynamic disorders, systemic and pulmonary circulation arrest, and significantly depressed myocardial contractility caused by hypoxia and acidosis. CF-LVAD is mainly developed as an additional pump to the left ventricle to maintain the pumping function. Meanwhile, the native right ventricle remains important for maintaining the normal function of CF-LVAD, as it is responsible for complete pulmonary circulation, which is essential for the maintenance of hemodynamics and provides sufficient preload for CF-LVAD. Theoretically, VF occurs with the stop of native right ventricular contraction instantly followed by pulmonary circulation arrest, resulting in CF-LVAD dysfunction due to insufficient preload. However, patients with CF-LVAD support can survive with less severe clinical symptoms during onset VF, and in short period there may be no serious signs of hemodynamic failure (4–7, 9, 10).

In this study, a CF-LVAD was implanted in small tail Han sheep and VF was induced by increasing ventricular rate using a temporary pacemaker. Our observational study demonstrate that both the model A and model B exhibited stable hemodynamics when VT occurred. In the meantime, with the increase in the ventricular rate, the RAP increased and the RAF decreased, while the PAF was eventually stable at a certain low level. When the ventricular rate reached 320 beats/min, VF was induced in both the models with distinct difference. In model A, VF occurred with sinus atrial rhythm, accompanied by gradual increase in the RAP and the difference between right atrial systolic and diastolic blood pressures while reductions in the LVP, PF, and PAF. However, the reductions in PF and PAF were not significant. Circulation could be sustained and there was no significant acid-base disorder. During the whole process (60 min), the right ventricular ejection was still effective (RVEF, 36%). In model B, VF occurred with AF, resulting in rapid increase in the RAP while reduction in the difference between right atrial systolic and diastolic blood pressures. Additionally, the LVP and RVP rapidly decreased to nearly 0 mmHg, while the PF and PAF also showed a significant downward trend. The circulation under this circumstance could not be sustained.

Dib et al. (5) and Jakstaite et al. (7) considered that the hemodynamics under VF after LVAD implantation was similar to Fontan circulation through case analysis. The Fontan operation is used as a surgical strategy for functional single ventricle, with the venous blood from the superior and inferior vena cava directly drained to the pulmonary artery (**Figure 4A**). In that way, CVP should be equal to or greater than the pulmonary arterial pressure within a range of 12–14 mmHg. Consistently, the current comparative study also found that the hemodynamics under VF following CF-LVAD implantation resembled but was not identical to the Fontan circulation.

Firstly, under normal physiological conditions, Fontan circulation requires negative thoracic pressure. For surgical reasons, the negative thoracic pressure in the animal model was lost in the present study. As a result, the right atrium and right ventricle are not simply conduits for blood flow under VF following CF-LVAD implantation (**Figure 4B**). Upon ventricular systolic dysfunction, the atrial rhythm and function may be necessary for circulation maintenance after VF. Under normal circumstances, the left atrium serves as a reservoir, conduit and pump, which is responsible for about 25% left ventricular filling (11, 12). In the present study, the model A had increased amplitude of the RAP waveform after VF, which might be caused by the certain compensatory increase in the right atrial contractility according to the Frank-Starling law.

Moreover, to maintain the hemodynamics after VF following CF-LVAD implantation, RAP should be also equal to

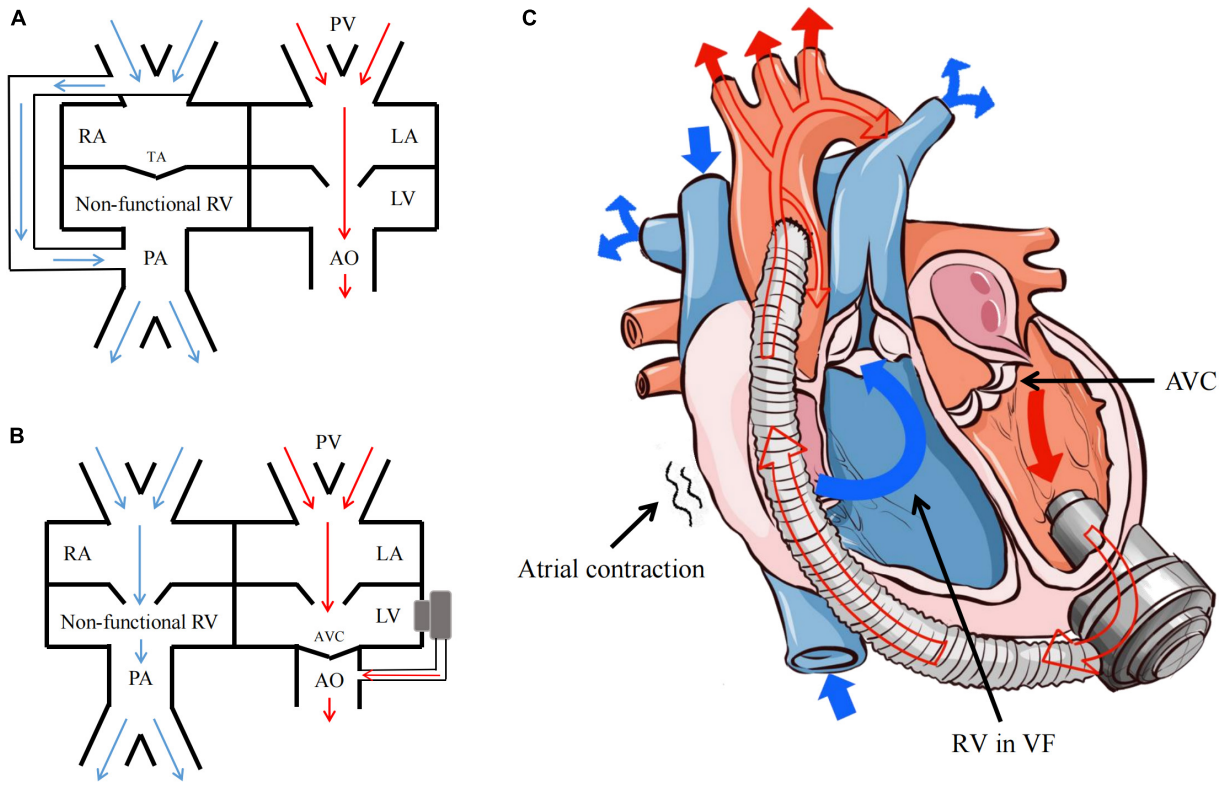

FIGURE 4
Fontan circulation and the hemodynamics of VF after CF-LVAD implantation. **(A)** Fontan circulation; **(B)** the hemodynamics of VF after CF-LVAD implantation; **(C)** the model diagram of hemodynamics in the VF state after CF-LVAD implantation. RA, right atrium; RV, right ventricle; LA, left atrium; LV, left ventricle; PA, pulmonary artery; PV, pulmonary vein; TA, tricuspid atresia; AVC, aortic valve closure.

or greater than the pulmonary arterial pressure as the Fontan circulation, while the value might be lower than 12 mmHg. Different from the dependence of Fontan circulation on pulmonary vascular development, CF-LVAD implantation can reduce pulmonary vascular resistance, i.e., afterload of the right heart. In addition, the CF-LVAD will fully replace the left ventricle after VF to complete pulmonary circulation with the right atrium via cooperating with the left atrium with sinus rhythm to reduce pulmonary vascular resistance.

Combining the findings mentioned above, the present study believed that sustained atrial sinus rhythm is the hemodynamic characteristic under non-typical VF after CF-LVAD implantation. We found that the RAP and compensation in the right atrial contractility increased after blood return to the right atrium from the superior and inferior vena cava, which directly drove the blood flow from the non-functional right ventricle to the pulmonary artery and subsequently to the non-functional left ventricle through the pulmonary vein and left atrium. Finally, the blood was pumped into the systemic circulation by the CF-LVAD (**Figure 4C**). During the whole process, the LVP reduced due to the preload reduction of the left atrium and the complete closure of aortic valves and opening of mitral valve as result of loss of left ventricular contractility. Similar hemodynamic characteristics were found in the context of VT after CF-LVAD implantation, except for the "weak" participation of the ventricular systolic function.

Presently, the cause of VF after CF-LVAD implantation remains undetermined. Besides, routine ECG or ECG monitoring is not able to clearly illustrate the atrial rhythm under a VF condition after implantation. Hence, patients with CF-LVAD implantation might present VF with sinus atrial rhythm as described in the current study. Based on our findings and previous research (13), for those CF-LVAD-planted patients with atypical symptoms of VF, abnormal ventricular activation induced by mechanical stimulus or aberrant repolarization of the local cardiomyocytes might be a predisposing factor for VF, with the atrial rhythm and function not be affected.

There are some limitations to this study. First, the present study does not allow causal interpretation because it is an observational case study with a small sample size, although the now present findings serve as a sound basis for further mechanistic studies. Second, the VF with CF-LVAD model in this study was acute and without negative thoracic pressure, different with the chronic VF in clinical practice. However, the hemodynamics of the two types is supposed to be

similar. Further larger-scale experimental studies and chronic animal experiment should be devised to explore the effect of long-term/recurrent VF on the hemodynamics and multi-organ functions.

5. Conclusion

The hemodynamics in the context of VF after CF-LVAD implantation resembled but was not identical to the Fontan circulation. The atrial rhythm and function might be necessary for maintenance of the pulmonary and systemic circulation under VF after implantation.

Data availability statement

The original contributions presented in this study are included in the article/**Supplementary material**. Requests to access the datasets should be directed to Z-GL, liuzg@tedaich.com.

Ethics statement

The animal study was reviewed and approved by Institutional Animal Care and Use Committee of TEDA International Cardiovascular Hospital.

Author contributions

X-YY and J-WS: drafting article, design, data collection, data analysis, data interpretation, and critical revision of manuscript. Y-SR, Y-LC, T-WL, J-MZ, and Z-FH: concept/design, data collection, and data interpretation. Y-RZ and Z-AF: data collection. Z-GL: concept/design, data interpretation, critical revision of manuscript, and approval of manuscript. All authors contributed to the article and approved the submitted version.

Funding

This work was sponsored by Tianjin Health Research Project (grant/award number: TJWJ2022XK045) and Tianjin Key Medical Discipline (Specialty) Construction Project (grant/award number: TJYXZDXK-019A).

Acknowledgments

The illustration (**Figure 4C**) in this manuscript was provided by Xiang-Yu Xu.

Conflict of interest

Z-FH is employed by ROCOR Medical Technology Co., Ltd., Tianjin, China.

The remaining authors declare that the research was conducted in the absence of any commercial or financial relationships that could be construed as a potential conflict of interest.

Publisher's note

Supplementary material

The Supplementary Material for this article can be found online at: https://www.frontiersin.org/articles/10.3389/fcvm.2022.1000352/full#supplementary-material

References

1. Shi J, Yu X, Liu ZA. Review of new-onset ventricular arrhythmia after left ventricular assist device implantation. *Cardiology.* (2022) 147:315–27.

2. Kadado A, Akar J, Hummel J. Arrhythmias after left ventricular assist device implantation: incidence and management. *Trends Cardiovasc Med.* (2018) 28:41–50. doi: 10.1016/j.tcm.2017.07.002

3. Gopinathannair R, Cornwell W, Dukes J, Ellis C, Hickey K, Joglar J, et al. Device therapy and arrhythmia management in left ventricular assist device recipients: a scientific statement from the American heart association. *Circulation.* (2019) 139:e967–89. doi: 10.1161/CIR.0000000000000673

4. Eyituoyo H, Aben R, Arinze N, Vu D, James E. Ventricular fibrillation 7 years after left ventricular assist device implantation. *Am J Case Rep.* (2020) 21:e923711. doi: 10.12659/AJCR.923711

5. Dib E, Grayburn P, Bindra A. Asymptomatic ventricular fibrillation in peripartum cardiomyopathy with a left ventricular assist device. *Proceedings.* (2020) 34:180–1. doi: 10.1080/08998280.2020.1829947

6. Smith M, Moak J. Asymptomatic ventricular fibrillation in continuous flow left-ventricular assist device. *Am J Emerg Med.* (2021) 49:130–2. doi: 10.1016/j.ajem.2021.05.065

7. Jakstaite A, Luedike P, Wakili R, Kochhauser S, Ruhparwar A, Rassaf T, et al. Case report: incessant ventricular fibrillation in a conscious left ventricular assist device patient. *Eur Heart J Case Rep.* (2021) 5:ytab337. doi: 10.1093/ehjcr/ytab337

8. Yu X, Shi J, Zang Y, Zhang J, Liu Z. Factors influencing the functional status of aortic valve in ovine models supported by continuous-flow left ventricular assist device. *Artif Organs.* (2022) 46:1334–45. doi: 10.1111/aor.14207

9. Busch M, Haap M, Kristen A, Haas C. Asymptomatic sustained ventricular fibrillation in a patient with left ventricular assist device. *Ann Emerg Med.* (2011) 57:25–8. doi: 10.1016/j.annemergmed.2010.05.023

10. Patel P, Williams J, Brice J. Sustained ventricular fibrillation in an alert patient: preserved hemodynamics with a left ventricular assist device. *Prehosp Emerg Care.* (2011) 15:533–6. doi: 10.3109/10903127.2011.598616

11. Economou D, Xanthopoulos A, Papamichalis M, Chamaidi A, Dimos A, Tavoularis D, et al. Left atrial systolic function in acute coronary syndromes. *Hellenic J Cardiol.* (2020) 61:291–2. doi: 10.1016/j.hjc.2019.10.005

12. Henein M, Mondillo S, Cameli M. Left atrial function. *Anatol J Cardiol.* (2019) 22:52–3. doi: 10.14744/AnatolJCardiol.2019.31036

13. Nakahara S, Chien C, Gelow J, Dalouk K, Henrikson C, Mudd J, et al. Ventricular arrhythmias after left ventricular assist device. *Circ Arrhythm Electrophysiol.* (2013) 6:648–54. doi: 10.1161/CIRCEP.113.000113

frontiers | Frontiers in Cardiovascular Medicine

TYPE Original Research
PUBLISHED 20 February 2023
DOI 10.3389/fcvm.2023.1110032

OPEN ACCESS

EDITED BY
Maria Monsalve,
Autonomous University of Madrid,
Spain

REVIEWED BY
Anzhu Wang,
Xiyuan Hospital, China Academy of Chinese Medical Sciences, China
Xinyu Weng,
Fudan University, China

*CORRESPONDENCE
Aijuan Qu
✉ aijuanqu@ccmu.edu.cn

SPECIALTY SECTION
This article was submitted to General Cardiovascular Medicine, a section of the journal Frontiers in Cardiovascular Medicine

RECEIVED 28 November 2022
ACCEPTED 19 January 2023
PUBLISHED 20 February 2023

CITATION
Wang X, Zhu X, Shi L, Wang J, Xu Q, Yu B and Qu A (2023) A time-series minimally invasive transverse aortic constriction mouse model for pressure overload-induced cardiac remodeling and heart failure.
Front. Cardiovasc. Med. 10:1110032.
doi: 10.3389/fcvm.2023.1110032

A time-series minimally invasive transverse aortic constriction mouse model for pressure overload-induced cardiac remodeling and heart failure

Xia Wang[1,2,3], Xinxin Zhu[2,3], Li Shi[2,3], Jingjing Wang[4], Qing Xu[5], Baoqi Yu[2,3] and Aijuan Qu[2,3]*

[1]Beijing Key Laboratory for HIV/AIDS Research, Center for Infectious Diseases, Beijing Youan Hospital, Capital Medical University, Beijing, China, [2]Department of Physiology and Pathophysiology, School of Basic Medical Sciences, Capital Medical University, Beijing, China, [3]Key Laboratory of Remodeling-Related Cardiovascular Diseases, Ministry of Education, Beijing Key Laboratory of Metabolic Disorder-Related Cardiovascular Diseases, Beijing, China, [4]Laboratory of Animal Facility, Capital Medical University, Beijing, China, [5]Core Facility Centre, Capital Medical University, Beijing, China

Transverse aortic constriction (TAC) is a widely-used animal model for pressure overload-induced cardiac hypertrophy and heart failure (HF). The severity of TAC-induced adverse cardiac remodeling is correlated to the degree and duration of aorta constriction. Most studies of TAC are performed with a 27-gauge needle, which is easy to cause a tremendous left ventricular overload and leads to a rapid HF, but it is accompanied by higher mortality attributed to tighter aortic arch constriction. However, a few studies are focusing on the phenotypes of TAC applied with a 25-gauge needle, which produces a mild overload to induce cardiac remodeling and has low post-operation mortality. Furthermore, the specific timeline of HF induced by TAC applied with a 25-gauge needle in C57BL/6J mice remains unclear. In this study, C57BL/6J mice were randomly subjected to TAC with a 25-gauge needle or sham surgery. Echocardiography, gross morphology, and histopathology were applied to evaluate time-series phenotypes in the heart after 2, 4, 6, 8, and 12 weeks. The survival rate of mice after TAC was more than 98%. All mice subjected to TAC maintained compensated cardiac remodeling during the first two weeks and began to exhibit heart failure characteristics after 4 weeks upon TAC. At 8 weeks post-TAC, the mice showed severe cardiac dysfunction, hypertrophy, and cardiac fibrosis compared to sham mice. Moreover, the mice raised a severe dilated HF at 12 weeks. This study provides an optimized method of the mild overload TAC-induced cardiac remodeling from the compensatory period to decompensatory HF in C57BL/6J mice.

KEYWORDS

heart failure, cardiac remodeling, cardiac hypertrophy, cardiac fibrosis, transverse aortic constriction

Introduction

Heart failure (HF) is a consequence of various cardiovascular diseases and is still one of the leading causes of mortality worldwide, which remains a major clinical and public health problem (1–3). The development of HF is characterized by a process of adverse cardiac remodeling (4), and it is mainly attributed to increased pressure overload such as hypertension (5, 6). Therefore, it is important to uncover the cellular and molecular mechanisms of HF for better understanding and new therapeutic targets.

Transverse aortic constriction (TAC) has been the preferred murine model of adverse cardiac remodeling induced by pressure overload, which plays an important role in preclinical studies (7–11) since it was first built by Rockman et al. (12). The severity of adverse cardiac remodeling induced by TAC largely depends on the degree of aorta constriction and the duration of constriction. Therefore, there is considerable variability in TAC during the cardiac remodeling progression to an overt HF (13). At present, several minimal invasiveness TAC models with low mortality have been developed (9–11, 14–17), which has made the TAC model more effective and accurate. The mice subjected to TAC go through cardiac hypertrophy, cardiac fibrosis, and inflammation, and eventually develop cardiac dilation and HF. The progression of cardiac remodeling and HF induced by TAC relies on the degree and duration of constriction of the aorta (13). Although increasing the degree of aortic constriction, frequently using a 27-gauge needle, can increase the severity of pressure response in the left ventricular wall and increase the probability of more animal transition from compensated cardiac hypertrophy to HF, the mortality rate is higher than expected (7, 8, 18).

The TAC conducted with a 25-gauge needle presents a mild cardiac remodeling progression with lower mortality (19). Therefore, a 25-gauge needle can cause a much milder constriction of the aorta arch and could be very useful for studying hypertensive cardiac remodeling in mice, or studies with more susceptibility to mortality. In addition to the severity of constriction, its duration is also responsible for the variation of TAC response. Moreover, few studies have focused on time-series phenotypes of TAC models induced by different durations of aortic constriction (20). In C57BL/6 J mice, the potential time-series of adverse cardiac remodeling induced by TAC applied with a 25-gauge needle at different durations of constriction also remains unknown. Although C57BL/6 J mice are one of the most used strains, their susceptibility to HF development is also controversial (20, 21). Therefore, generating a reproducible murine cardiac remodeling model is instrumental for investigating the mechanisms of HF progress.

In this study, a simple and less invasive TAC method was performed. The procedure involves the fewest apparatuses and less damage to the mice. This TAC method neither requires cutting of the ribs and intercostal muscles nor tracheal intubation with a ventilation setup. Moreover, TAC surgery with a 25-gauge needle has a greater survival rate, above 98%, and its operation time is only 10–15 min. Then, time-series cardiac remodeling phenotypes induced by a much milder TAC applied with a 25-gauge needle were analyzed in C57BL/6 J mice. The phenotype results indicate that HF and cardiac dilation raised in 8 weeks or later in TAC mice. This study provides a deep insight into a 25-gauge TAC-induced cardiac remodeling from the compensatory period to the decompensatory stage and leads to HF in C57BL/6 J mice.

Materials and methods

Animals

C57BL/6 J mice were purchased from Charles River Company (Beijing, China). All mice were kept under specific pathogen-free conditions, a standard 12-h light/dark cycle in individually ventilated cages, and free access to a normal chow diet and water. All experimental procedures were in accordance with the U.S. National Institutes of Health Guidelines for the Care and Use of Laboratory Animals. All animal studies were approved under the project license AEEI-2018-127 granted by the ethics board of Capital Medical University.

Minimally invasive transverse aortic constriction surgery

A minimally invasive transverse aortic constriction (TAC) method without standard chest opening has been established (17). In this study, the 10~12-week-old male C57BL/6 J mice (23~27 g) were randomized to be subjected to TAC or sham surgery. All mice were anesthetized with a single intraperitoneal injection of supersaturated 2,2,2-tribromoethanol (T48402, Sigma-Aldrich, St. Louis, MO, United States) saline solution at a dose of 10~13 $\mu L\,g^{-1}$ and fixed on an operation plate. Adequate sedation was determined by the lack of toe-pinch reflex. A topical depilatory agent was applied to the neck and chest, and the area was cleaned with 75% alcohol.

Before the surgery, several 25-gauge blunt needles and a simple retractor made of paper clip were prepared (Figure 1). Under a dissecting microscope (Model SZ2-ILST, OLYMPUS Corporation, TOKYO, Japan), the mouse was placed in the supine position, the skin was opened, and a 1.5~2 cm incision at the midline of the neck and chest was made (Figure 2A). The thyroid gland was pulled toward the head by gently separating connective tissues. Then, the sternocleidomastoid muscle layer on the trachea was separated toward both sides. Next, the sternum stem was cut along the midline and slightly separated (Figure 2B), and the thymus covering the aortic arch was separated from it. Finally, the aortic arch and two carotid arteries were fully exposed by the simple retractor (Figure 2C).

A 25-gauge curved needle with a 7-0 suture, as shown in Figure 1A, was placed under the arch and pushed to perforate between the vessel wall and connective tissue on the other side (Figure 2D). Then, the suture was pulled out of the curved needle (Figure 2E), and it was immediately taken out from the aortic arch and placed above it as a spacer for ligation (Figure 2F). Finally, the knotted position was retracted successfully, and the spacer was gently withdrawn (Figure 2G). When the needle was removed, the diameter of the aortic arch was narrowed to 0.5 mm. The end of the suture was cut, and the skin was closed with a 4–0 suture in a continuous suture pattern. After surgery, all mice were allowed to recover on a warming pad until they were fully awake. The sham surgery was subjected to an identical operation in which the aortic arch was visualized but not banded.

All TAC and sham mice were randomly divided into five groups for the experiment: 2 weeks group (2 W), 4 weeks group (4 W), 6 weeks group (6 W), 8 weeks group (8 W), and 12 weeks group (12 W). All groups were observed after 1 week of surgery.

Echocardiography

After 3~7 days of surgery, aortic flow peak velocity (AV Peak Vel) at the TAC constriction band site was measured using color and pulsed-wave Doppler (Vevo2100; VisualSonics, Inc., Toronto, ON, Canada). Briefly, mice were shaved and anesthetized with isoflurane (2%–4% for induction and 1%–1.5% for maintenance) and were placed in the supine position on a heated platform with ECG electrodes attached to monitor the heart rate (>550 bpm). The pulsed-wave Doppler was used to measure blood speed in either TAC (total 50) or sham (total 25) mice, and the peak pressure was also calculated.

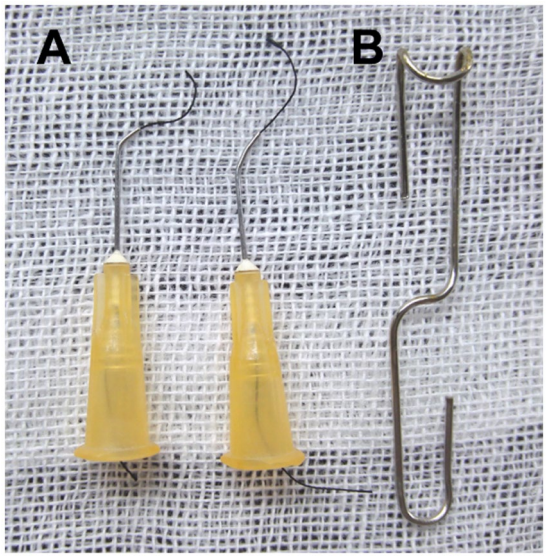

FIGURE 1
Homemade surgical instruments. **(A)** Creating the ligation spacer and curved needle with suture: bend the blunt 25-gauge needle 30°~45° with a needle holder. **(B)** Making a simple surgical retractor with the paper clip, as illustrated previously.

Cardiac function was evaluated at a time-series by echocardiography using a high-resolution small animal imaging system (Vevo 2100; VisualSonics, Toronto, ON, Canada) as described (22, 23). B-Mode and M-Mode of parasternal long and short axis were measured at the level of the papillary muscles (Sham 2 W group, $n = 22$; TAC 2 W group, $n = 34$; Sham 4 W group, $n = 16$; TAC 4 W group, $n = 22$; Sham 6 W group, $n = 18$; TAC 6 W group, $n = 19$; Sham 8 W group, $n = 19$; TAC 8 W group, $n = 26$; Sham 12 W group, $n = 12$; TAC 12 W group, $n = 24$). By using Vevo LAB 2.1.0 software, the following parameters were measured digitally from the M-mode tracings as follows: heart rate, diastolic and systolic left ventricular anterior wall, diastolic and systolic left ventricular internal dimensions, and diastolic and systolic left ventricular posterior wall. Based on these measurements, diastolic and systolic left ventricular volume, left ventricular mass, left ventricular ejection fraction (EF%), and left ventricular fractional shortening (FS%) were also calculated.

Morphological analyses

Mice were euthanized at 2, 4, 6, 8, and 12 W after operation, respectively. Hearts were fixed in 10% phosphate-buffered formalin, embedded in paraffin, and sectioned (4 μm). Hematoxylin and eosin (H&E), Masson's trichrome, and wheat germ agglutinin (WGA) staining were performed on the sections using standard procedures as previously described (23). Images were obtained using a high-capacity digital slide scanner (Pannoramic SCAN, 3DHISTECH, Budapest, HUN). The fibrotic area (collagen area/total area) was dyed by Masson's trichrome staining (Sham 2 W group, $n = 10$; TAC 2 W group, $n = 15$; Sham 4 W group, $n = 8$; TAC 4 W group, $n = 8$; Sham 6 W group, $n = 8$; TAC 6 W group, $n = 8$; Sham 8 W group, $n = 10$; TAC 8 W group, $n = 15$; Sham 12 W group, $n = 8$; TAC 12 W group, $n = 8$) and cross-sectional area of the cardiomyocytes (Sham 2 W group, $n = 10$; TAC 2 W group, $n = 10$; Sham 4 W, $n = 10$; TAC 4 W group, $n = 14$; Sham 6 W group, $n = 8$; TAC 6 W group, $n = 11$; Sham 8 W group, $n = 14$; TAC 8 W group, $n = 15$; Sham 12 W group, $n = 10$; TAC 12 W group, $n = 12$) was determined using Image-Pro Plus 6.0 software (Media Cybernetics, Rockville, MD, United States).

Quantitative real-time PCR

Total RNA in the heart tissues was extracted by the TRIzol reagent (Invitrogen, New York, United States). The first cDNA strand was synthesized from 2 μg of total RNA using the GoScript™ Reverse Transcription System (Promega, Southampton, United Kingdom). Quantitative real-time (qPCR) was performed using SYBR Green Master Mix (TaKaRa, Tokyo, Japan) with CFX Connect Real-Time System (Bio-Rad, Hercules, CA). Amplification was performed as follows: 95°C for 3 min, 95°C for 30 s, and 60°C for 45 s for each step of 40 cycles. The expression of hypertrophic genes *Anf*, *Bnp*, and *Myh7* and fibrotic genes *Col1a2* and *Col3a1* (Sham 2 W group, $n = 10$; TAC 2 W group, $n = 20$; Sham 4 W, $n = 8$; TAC 4 W group, $n = 14$; Sham 6 W group, $n = 9$; TAC 6 W group, $n = 15$; Sham 8 W group, $n = 13$; TAC 8 W group, $n = 19$; Sham 12 W group, $n = 10$; TAC 12 W group, $n = 17$) were measured using qPCR. mRNA levels were normalized to the level of the endogenous housekeeping gene *Actb* and calculated with the comparative cycle threshold method (ΔΔCT).

Primers sequences are as follows: *Anf* (Forward: CACAGATCTGATGGATTTCAAGA, Reverse: CCTCATCTTCTA CCGGCATC); *Bnp* (Forward: 5′-GAAGGTGCTGTCCCAGATGA-3′, Reverse: 5′-CCAGCAGCTGCATCTTGAAT-3′); *Myh7* (Forward: 5′-GATGTTTTTGTGCCCGATGA-3′, Reverse: 5′-CAGTCACCGTC TTGCCATTCT-3′); *Col1a2* (Forward: 5′-AGTCGATGGCTGCTCC AAAA-3′, Reverse: 5′-AGCACCACCAATGTCCAGAG-3′); *Col3a1* (Forward: 5′-TCCTGGTGGTCCTGGTACTG-3′, Reverse: 5′-AGGAG AACCACTGTTGCCTG-3′); *Actb* (Forward: 5′-ATGGAGGGGAAT ACAGCCC-3′, Reverse: 5′-TTCTTTGCAGCTCCTTCGTT-3′).

Statistical analysis

All data in the study are expressed as mean ± S.E.M and were calculated and plotted using GraphPad Prism 8.0 software (GraphPad Software, La Jolla, CA). For statistical comparisons, the determination of normal distribution was first evaluated. Then, potentially similar variances were evaluated in normally distributed data. Student's *t*-test was performed for two group comparisons and ANOVA for the comparison of groups for which similar variance tests were passed. Nonparametric tests were used where data were not normally distributed. Log-rank (Mantel–Cox) test and Gehan–Breslow–Wilcoxon test were performed for the survival rate of mice after TAC 12 W (Sham 12 W group, $n = 43$; TAC 12 W group, $n = 70$). In all cases, significance was attributed to differences for which the two-tailed probability was <0.05.

Results

TAC induces significant pressure overload of the heart

Compared to the traditional open-chest TAC, this minimally invasive TAC procedure is simpler and easier to perform, time, and

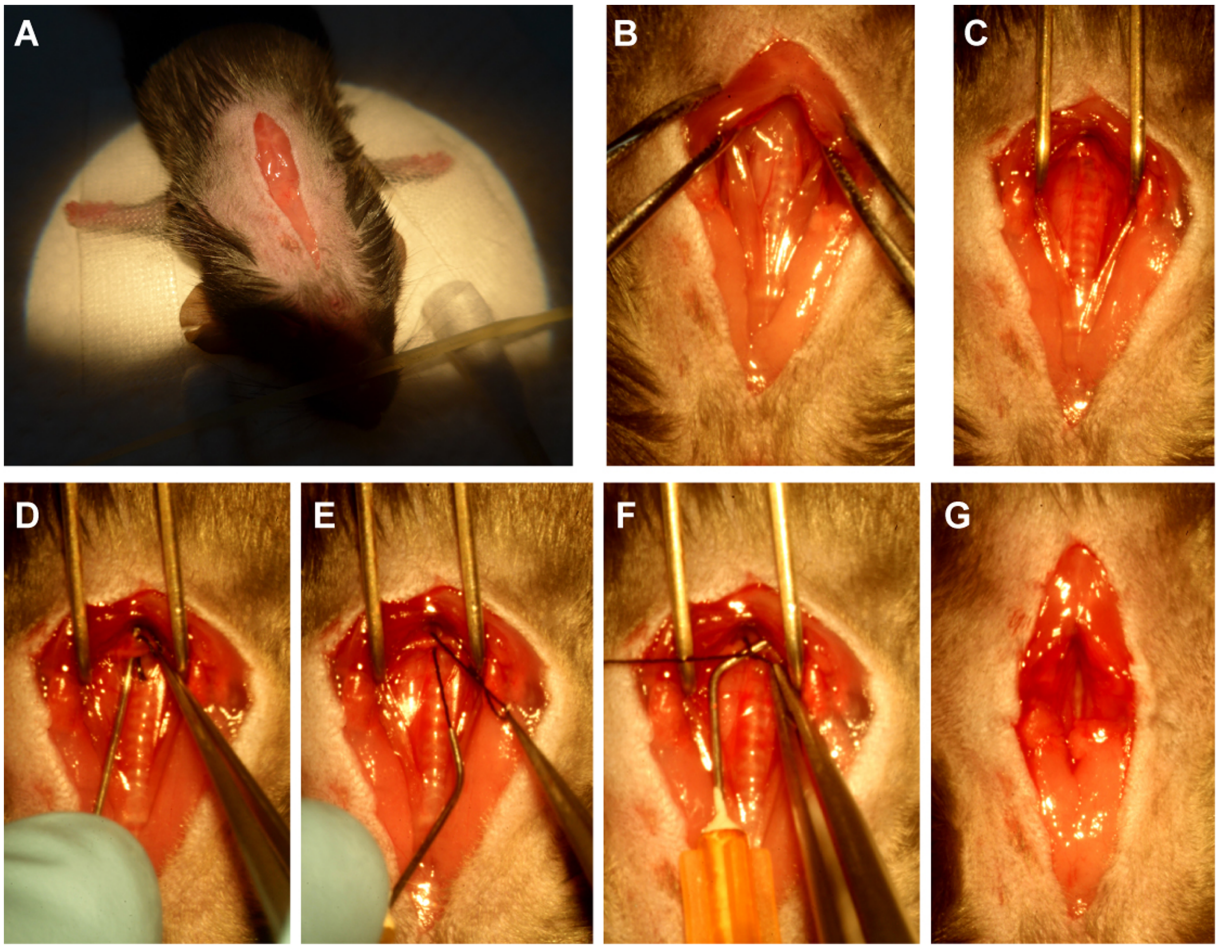

FIGURE 2
The procedure of minimally invasive TAC. **(A)** Open a 1.5~2cm incision at the midline of the neck and chest. **(B)** Cut the sternum stem about 3~5mm. **(C)** Separate the aortic arch from the nearby connective tissue by using the above-mentioned simple surgical retractor. **(D)** Guide the suture under the aortic arch by using the above-mentioned curved needle with suture. **(E)** Pull out of the suture from the curved needle. **(F)** Binding a constriction of the desired diameter with the above-mentioned 25-gauge curved needle. **(G)** Completed constriction.

labor-saving. As shown in Figure 1, the preparation of the primary tools for this surgery is simple and minimal, requiring 2~3 bent, 25-gauge blunt needles, and a simple retractor made with a paper clip. Once the thyroid had been retracted, the sternum was cut, and the thymus was moved to fully expose the aortic arch. Subsequent ligation of the aortic arch was very simple and easy (Figure 2).

Color Doppler and pulsed-wave Doppler were used to verifying the success of aortic arch constriction and determine the flow velocities of the aortic arch (24, 25). However, many studies may not have confirmed the success of aortic contraction (13). In this study, the constricted transverse aorta could be clearly visualized by color Doppler (Figure 3A), 7 days after surgery. Also, by using pulsed-wave Doppler, it was possible to verify that the flow velocity peak was increased at the contraction site. In the banding site of TAC mice, a successful constriction could be clearly observed which was shown by a significant increase in AV flow velocity peak (>2,800 mm/s) compared to a sham mouse with no constriction (Figure 3B). Moreover, the AV pressure peak was used to assess TAC severity. The pressure peak (>40 mmHg) was able to overload the left ventricular wall (Figure 3C). These results show that the TAC applied with a 25-gauge needle successfully produced left ventricular wall pressure overload in C57BL/6 J mice.

TAC induces time-series cardiac remodeling in mice subjected to surgery with a 25-gauge needle

TAC-treated mice develop cardiac hypertrophy, cardiac fibrosis, inflammation, and eventually cardiac dilation and HF. The progression of this adverse cardiac remodeling induced by TAC is associated with the duration of aortic constriction (9, 13). However, very few studies observed a time-series cardiac remodeling phenotype induced by TAC (11, 20, 21), especially in C57BL/6 J mice applied with a 25-gauge needle. In this study, echocardiography was used to evaluate the cardiac morphology and function changes by analyzing the left ventricle wall thickness and systolic functional parameters at 2, 4, 6, 8, and 12 weeks after TAC surgery in C57BL/6 J mice. During echocardiography, all mice were posited on a heated platform with ECG electrodes attached, to monitor the heart rate > 550 bpm. Compared to the sham group, all mice subjected to TAC surgery successfully developed adverse cardiac remodeling (Figure 4A). First, the echocardiography results showed that the left ventricular wall thickness was increased in all TAC groups. Further analysis showed time-series changes in the left ventricular

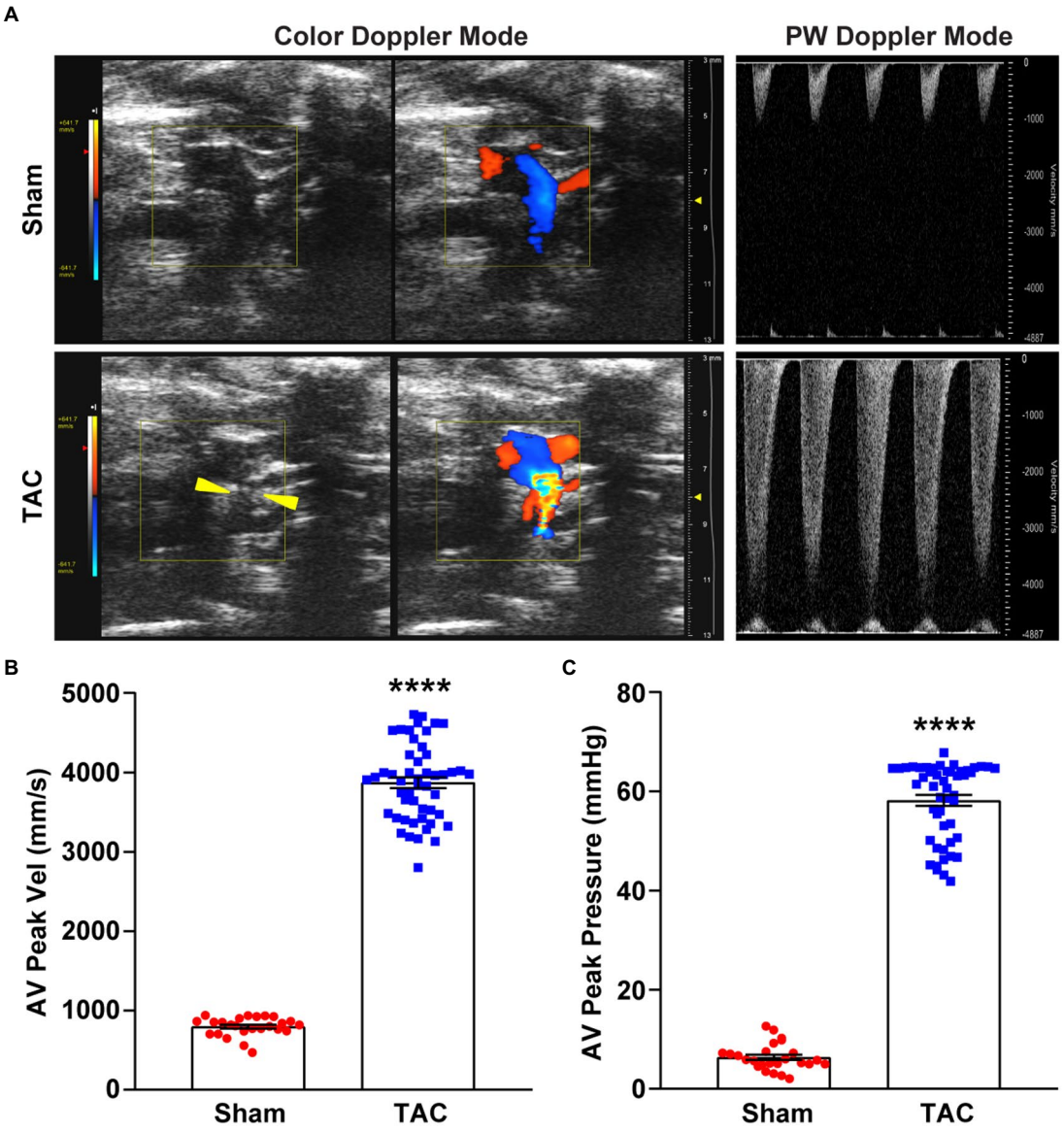

FIGURE 3
Color and pulsed-wave Doppler ultrasound. **(A)** Representative color Doppler imaging of an aortic flow velocity peak of the non-ligated (sham) mouse (top) and the ligated (TAC) mouse (bottom). The constriction between the two carotid arteries on the aortic arch is visible (yellow arrowheads). **(B)** Quantification of the AV peak velocity after surgery. **(C)** AV peak pressure was calculated by doppler velocities. n=25~50. Unpaired t-test for two-group comparisons, ****p<0.0001 vs. Sham.

anterior wall (LVAW) among the five TAC groups. Within 6 weeks, the LVAW thickness of TAC mice gradually thickened, but it began to become thinner after 8 weeks, and by the end of 12 weeks the LVAW thickness was even thinner (Figures 4B,C). Similar results were also observed for the thickness of the left ventricular posterior wall (LVPW; Figures 4D,E). Moreover, left ventricular mass (LV mass) was also calculated in the study, which is one of the most important parameters of cardiac remodeling. Results showed that when compared to sham mice, the LV mass of TAC mice increased in a time-series (Figure 4F). Second, compared to the sham group, left ventricular systolic function analysis showed that the ejection fraction (EF) and fractional shortening (FS) increased compensatory within 2 weeks after TAC, but they gradually decreased on week 4, and significantly decreased over 8 weeks, especially at week 12 (Figures 4G,H). Third, the left ventricular internal dimensions (LVID) and left ventricular volume (LV vol), which are important parameters for left ventricular remodeling and cardiac dysfunction, were also analyzed. Compared to sham mice, the diastolic LVID and systolic LVID in TAC mice were decreased at week 2 and then progressively increased within 4~12 weeks after TAC (Figures 4I,J). Similar results for the diastolic LV vol and systolic LV vol (Figures 4K,L) were also observed. During the echocardiography, mice were placed on a heated platform with ECG electrodes attached to monitor the heart rate > 550 bpm, and there was no significant difference among all groups (Figure 4M).

Taken together, C57BL/6J mice subjected to TAC applied with a 25-gauge needle maintained a compensated state with increased EF and FS in 2 weeks post-surgery and gradually developed to the decompensatory period over 4 weeks after TAC. At 4 weeks, TAC mice were in the early phase of cardiac dysfunction, but they developed serious cardiac dysfunction with extremely low EF and FS and extremely increased cardiac diameters and volumes over 8 weeks post-TAC and even congestion at week 12.

In our study, mice survival after TAC surgery was also analyzed for 12 weeks and found that mice subjected to a 25-gauge TAC had >98%

10.3389/fcvm.2023.1110032

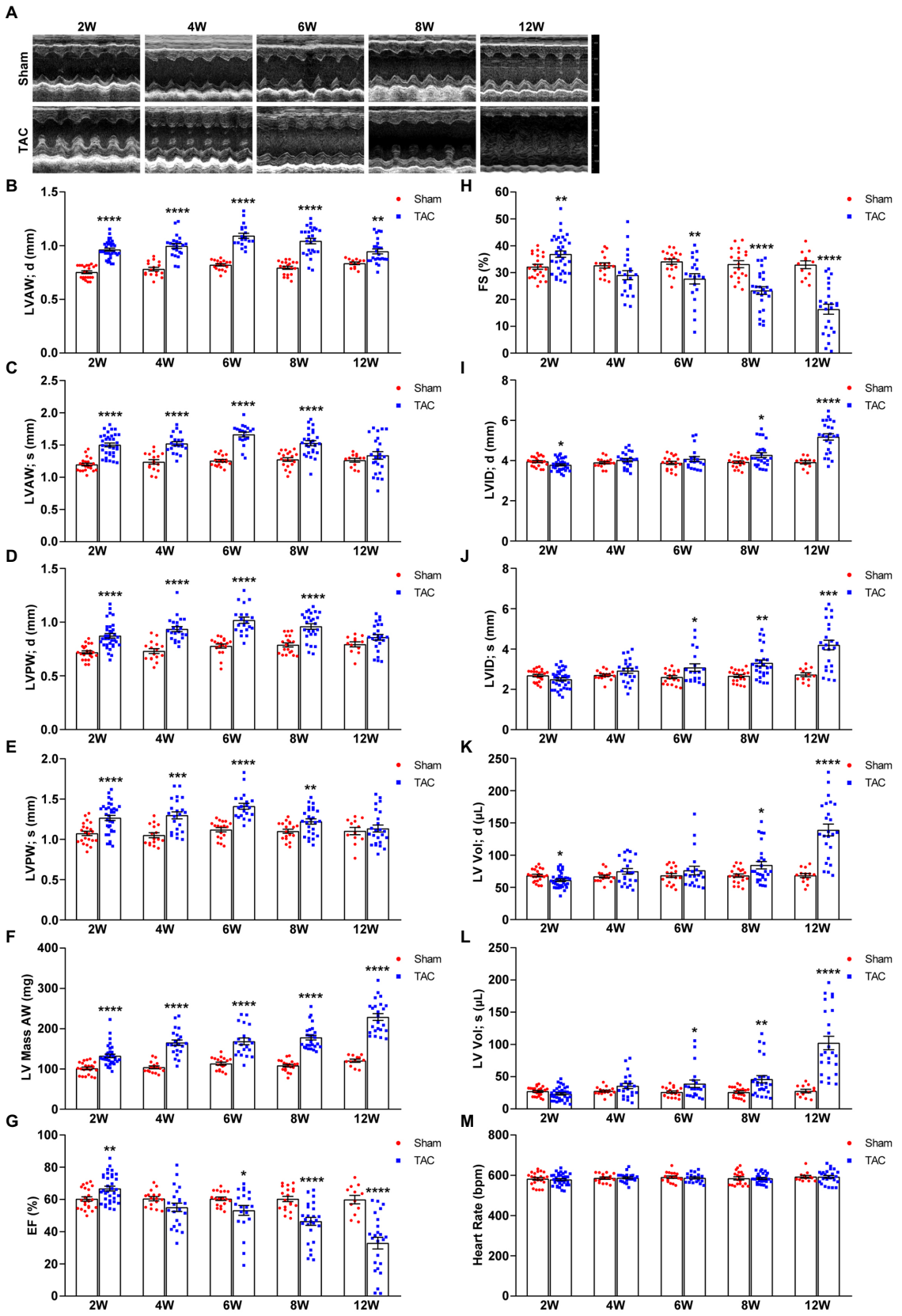

FIGURE 4
Echocardiography at various time points after surgery. **(A)** Representative two-dimensional guided M-mode echocardiogram of the various groups. **(B)** The thickness of the diastolic left ventricular anterior wall. **(C)** Systolic left ventricular anterior wall. **(D)** Diastolic left ventricular posterior wall. **(E)** Systolic left ventricular posterior wall. **(F)** Left ventricular mass AW. **(G)** Quantification of ejection fraction (EF). **(H)** Quantification of fractional shortening (FS). **(I)** Diastolic left ventricular internal dimensions. **(J)** Systolic left ventricular internal dimensions. **(K)** Diastolic left ventricular volume. **(L)** Systolic left ventricular volume. **(M)** Heart rate. n=12~34. Unpaired t-test for two-group comparisons, *p<0.05, **p<0.01, ***p<0.001, ****p<0.0001 vs. corresponding Sham.

survival in the perioperative period (24 h) and 1 week after surgery (Figure 5). Moreover, the survival of 8 weeks and 12 weeks after TAC was 88.57% and 82.86%, respectively. Taken together, this TAC method applied with a 25-gauge needle greatly improves the survival rate after operation in C57BL/6 J mice.

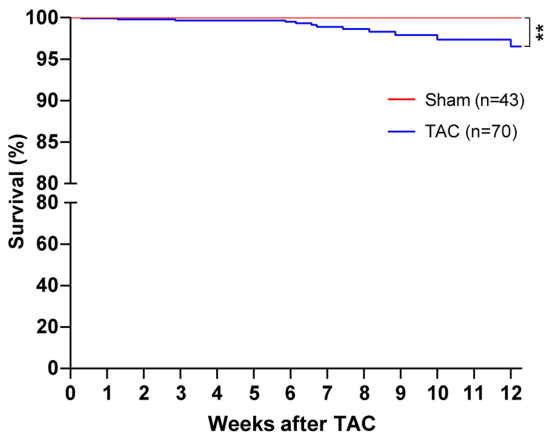

FIGURE 5
Survival of mice after TAC surgery. C57BL/J mice were randomized to TAC with a 25-gauge needle or sham surgery. The survival of mice was monitored for 12weeks after surgery. Log-rank (Mantel–Cox) test and Gehan–Breslow–Wilcoxon test were performed for the survival rate of mice after TAC. $^{**}p<0.01$ vs. Sham.

A 25-gauge needle TAC induces cardiac hypertrophy

In accordance with the echocardiographic data, the heart of the TAC mouse also presented a significantly time-series enlarged and deformed heart (Figure 6A). Accordingly, the heart weight normalized to body weight (HW/BW) and tibia length (HW/TL) were also significantly increased in TAC mice compared to the sham group (Sham 2 W group, $n = 20$; TAC 2 W group, $n = 27$; Sham 4 W group, $n = 12$; TAC 4 W group, $n = 15$; Sham 6 W group, $n = 10$; TAC 6 W group, $n = 17$; Sham 8 W group, $n = 19$; TAC 8 W group, $n = 27$; Sham 12 W group, $n = 10$; TAC 12 W group, $n = 20$; Figures 6B,C). Cardiomyocyte area was also significantly increased in TAC mice compared to the sham group. Further analysis showed that the duration of constriction and cardiomyocyte area of TAC mice gradually increased before 8 weeks, but it had a reduction over 12 weeks (Figure 7).

The hypertrophic genes atrial natriuretic factor (*Anf*), brain natriuretic peptide (*Bnp*), and β-myosin heavy chain (*Myh7*) were also examined. Results show that the expression of *Anf*, *Bnp*, and *Myh7* had a gradual time-series increase in the TAC mouse heart compared to the sham group (Figures 8A–C). Taken together, these results show that a

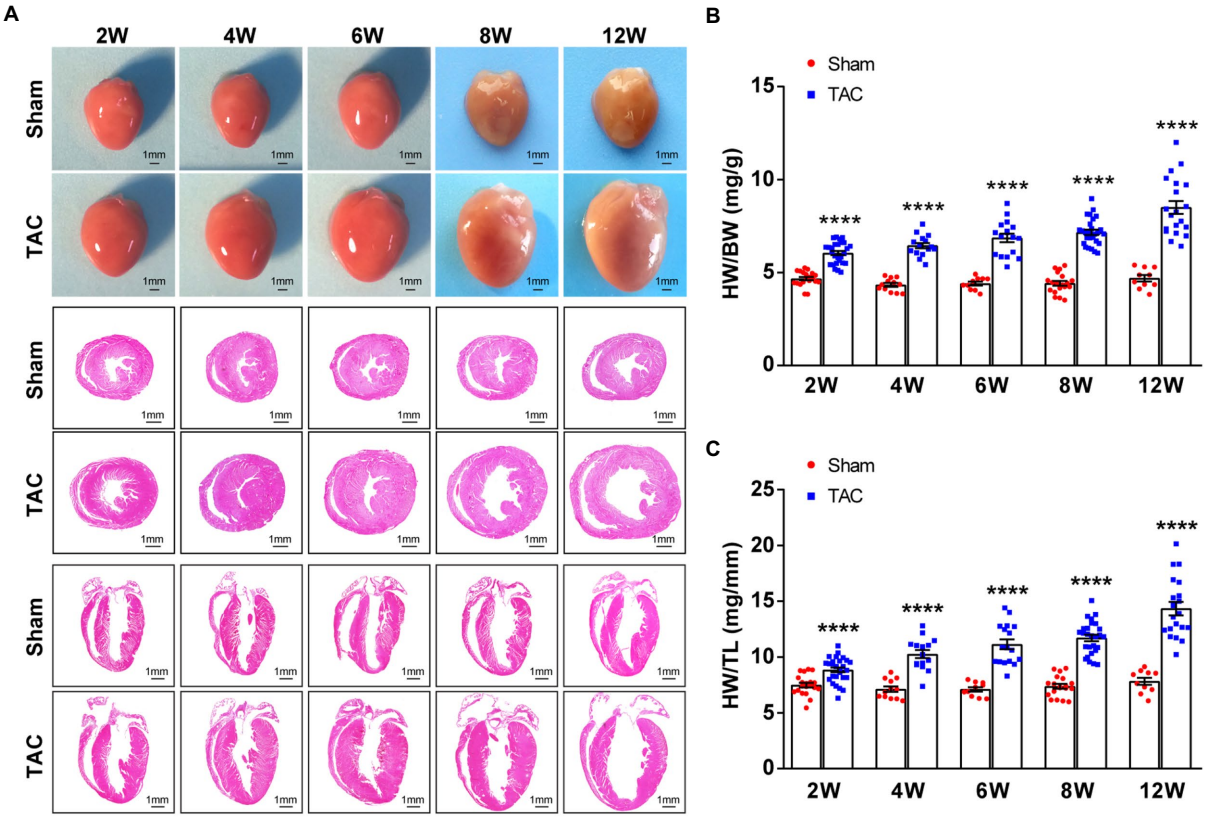

FIGURE 6
Mouse heart weight and size had a time-series increase after TAC. **(A)** Representative gross heart of mice at various times upon surgery (top), representative images of hematoxylin and eosin (H&E) staining of heart section across the heart's short axis (transverse section) at various times upon surgery (middle), and representative images of H&E staining of heart section along the heart's long axis (coronal section) at various times upon surgery (bottom). **(B)** HW/BW ratios at various times upon surgery. **(C)** HW/TL ratios at various times upon surgery. n=10~27. Unpaired t-test for two-group comparisons, $^{****}p<0.0001$ vs. the corresponding sham.

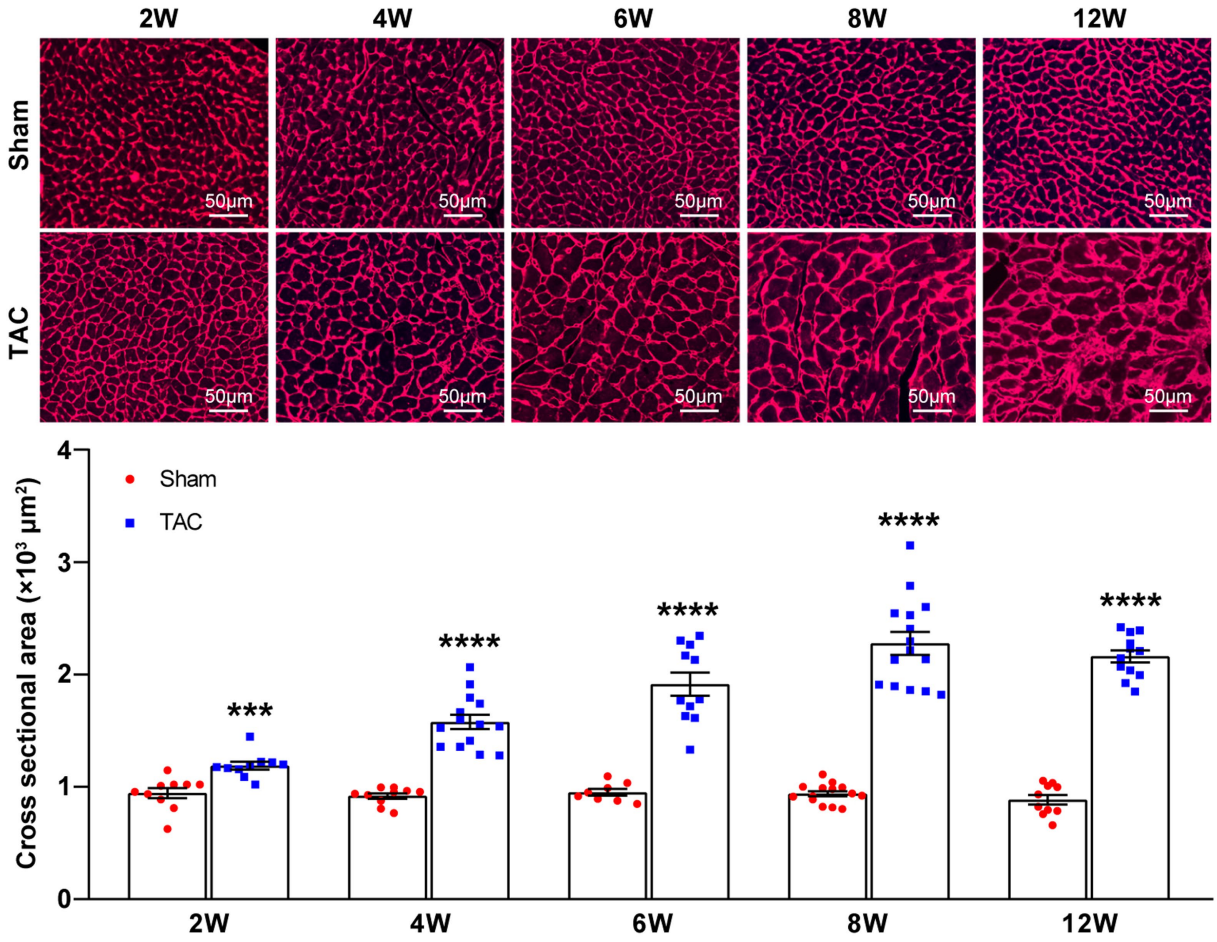

FIGURE 7
Cardiomyocyte area during TAC-induced time-series cardiac remodeling. Representative images of wheat germ agglutinin staining of heart sections (top). Quantification of cross-sectional areas of cardiomyocytes (bottom), n=8~15. Unpaired t-test for two-group comparisons, ***p<0.001, ****p<0.0001 vs. corresponding sham.

25-gauge needle can successfully induce a time-series cardiac remodeling from a compensatory period to a decompensatory period of HF over 8 weeks after TAC.

A 25-gauge needle TAC induces cardiac fibrosis

Cardiac fibrosis plays an important role in the development and progression of HF by causing adverse electrical and mechanical disturbances in diseased hearts (26). Pressure overload-induced cardiac hypertrophy is invariably accompanied by the formation of cardiac fibrosis. Here, the cardiac fibrosis was also analyzed in the mouse heart at different constriction durations by using Masson's trichrome staining. Analysis showed that compared to the sham group, mice subjected to TAC applied with a 25-gauge needle developed significant cardiac fibrosis (Figures 9A,B). Moreover, cardiac fibrosis showed a time-series gradually increasing trend after TAC. Meanwhile, expression of the fibrosis genes collagen type I (*Col1a2*) and collagen type III (*Col3a1*) was also detected in the mouse heart. The level of these genes corresponded to the degree of cardiac fibrosis area (Figure 9C). Taken together, C57BL/6 J mice subjected to TAC applied with a 25-gauge needle had a time-series increase in cardiac fibrosis that was confirmed by the analysis of Masson's trichrome staining and fibrosis-related gene expression over 12 weeks after TAC. These results confirm the importance of cardiac fibrosis in the development and progression of HF.

Discussion

Transverse aortic constriction is a widely used pressure overload model for studying adverse cardiac remodeling and heart failure, and it has been widely used and modified to be minimally invasive since it was first devised to study the mechanisms of cardiac hypertrophy by Rockman in 1991 (7, 12, 14–17, 27, 28). Minimally invasive TAC is a more desirable method for the construction of the aorta arch in mice. It is performed without intubation, ventilation, and entering the chest cavities of mice, involves significantly fewer apparatuses and less damage to mice, leading to a more rapid recovery, and a greater survival rate after surgery. However, the popularity of this minimally invasive TAC method in the study of cardiac remodeling is not high (13). In addition, the degree of constriction resulting from this method is also variable.

The constriction degree of the aorta arch is the most important factor affecting the phenotypes of TAC-induced cardiac remodeling. The constriction diameter of the needles used for TAC varied from 17-gauge to 30-gauge, but a 27-gauge needle has been the most common needle

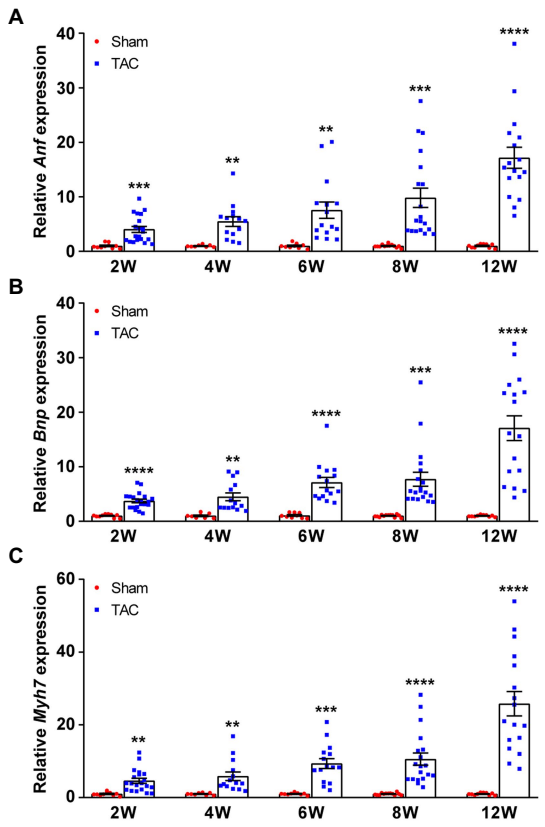

FIGURE 8
Expression of fetal genes during TAC-induced time-series cardiac remodeling. Expression of the *Anf* **(A)**, *Bnp* **(B)**, and *Myh7* **(C)** in mouse hearts was quantified by qPCR at various times upon surgery. n=8~20. Unpaired t-test for two-group comparisons, $^{**}p<0.01$, $^{***}p<0.001$, $^{****}p<0.0001$ vs. the corresponding sham.

size (>70%) for constriction in TAC study (9, 10, 13, 16, 28). Several studies have compared the resulting phenotypes to different needles, including 25-gauge, 26-gauge, and 27-gauge needles (9, 11). It is reported that the three degrees of tightness TAC models all induced significant, severity-dependent left ventricular hypertrophy and cardiac dysfunction compared to sham mice for 4 weeks. Mice subjected to 27-gauge TAC had the most severe cardiac hypertrophy, cardiac dysfunction, and cardiac fibrosis, and most quickly display features of heart failure compared to 25-gauge and 26-gauge needles. Moreover, it is critical that the suture around the aorta is not too tight during the surgery, because it may lead to a tremendous left ventricular overload and cause a fatal reduction of blood flow to other critical organs, such as the kidneys (11). Taken together, compared to bigger size needles, smaller needles can create a narrower constriction, which results in tremendous left ventricular overload and higher mortality (18). According to the aforementioned reports, a 27-gauge needle is not the best choice for the TAC model, which may be attributable to a too-tight constriction of the aortic arch. However, a 25-gauge needle can cause a much milder constriction of the aorta arch, which is more suitable for the studies of cardiac remodeling in mice, and even studies of more susceptibility to mortality.

Besides the constriction degree of the aorta arch, the duration of aortic constriction is also correlated to the phenotypes of adverse cardiac remodeling (13). However, a time-series of cardiac remodeling phenotypes, induced by TAC applied with a 25-gauge needle in C57BL/6 J mice model, has not been reported. There are cardiac hypertrophy, cardiac dysfunction, cardiac fibrosis, and HF characteristics in TAC-induced cardiac remodeling. Different durations of aortic constriction in mice can induce distinct cardiac remodeling phenotypes and the heart experiences from a compensatory period to an HF period. After TAC surgery, most experiments used a follow-up time of 28 days (16), some followed up by 7, 14, or 56 days (9, 11, 13, 16, 17, 23), and rarely 84 days (20). Moreover, when part of the mice subjected to TAC still showed compensated cardiac hypertrophy, some mice developed HF (29). Therefore, understanding this time-series variability involved in a TAC model is crucial to appropriate study design and interpretation, particularly when investigating the effects of conditional expression of genetic interventions or pharmacologic agents.

Furthermore, C56BL/6 J mice subjected to 25-gauge TAC surgery in studies were reported to be in a compensatory cardiac hypertrophy stage at 4 weeks after TAC, but the specific timeline for the development of heart failure still was not clear (11). In our study, this question has been answered. At 2 weeks after TAC, mice subjected to TAC applied with a 25-gauge needle were in a compensatory period of cardiac remodeling, and the cardiac dysfunction began to appear 4 weeks after surgery. Most of the mice had developed cardiac dysfunction at 6 weeks after TAC. Over 8 weeks, the mice subjected to TAC had developed to the stage of decompensatory HF. Moreover, there was a dilated HF at 12 weeks after TAC. These results are different from that in a study of congestive heart failure (20). Moreover, this method greatly shortens the time of HF induced by pressure overload in C56BL/6 J mice (30).

In this study, the minimally invasive TAC mice model was applied to pressure overload-induced cardiac remodeling and HF in C57BL/6 J mice. Compared to conventional TAC (12), this operation was easier to perform and improved the survival rate. Furthermore, the 2,2,2-tribromoethanol anesthetic and a 25-gauge needle constriction were used to replace the ketamine/xylazine anesthetics and a 27-gauge ligation needle, which were mostly used in reports (9, 13, 16, 17). A 25-gauge needle produced a much milder pressure overload on the left ventricular and had higher survival in this TAC study compared to the effects of a 27-gauge needle (9, 11). Therefore, a 25-gauge needle is much more suitable for studying hypertensive heart diseases. In addition, the time-series of TAC-induced cardiac remodeling phenotypes were observed due to different durations of left ventricular pressure overload by a 25-gauge ligation needle in C57BL/6 J mice. Results showed that the mice subjected to TAC were in the compensatory period of cardiac hypertrophy 2 weeks after the operation, accompanied by the trend of increased cardiac function. Then, the transition from compensatory hypertrophy to early cardiac insufficiency was reflected in the continuous decline of cardiac function within 4~8 weeks. Finally, TAC mice showed an obvious characteristic of heart failure at 8 weeks after TAC and they developed to the stage of dilated heart failure at 12 weeks after the operation. Therefore, in C57BL/6 J mice, TAC applied with 25-gauge needles induced a time-series phenotype of cardiac remodeling with the duration of constriction, and the stage of HF was successfully induced after 8 weeks or later post-TAC. These results are slightly different from previous reports (11, 20).

Despite the homogeneity in experimental design, the TAC model contains a substantial degree of heterogeneity in the outcome measures. Moreover, most studies do not report the mouse number used for each outcome measure (13). This is mainly due to the individual differences among mice in the study and the considerable variability within the same strain (30, 31). This variability within the experiment affects the sample size required to detect the effects of treatment or genetic alterations. Therefore, increasing the experimental sample size is a good way to solve this phenomenon. It is reported that 16%–17% of studies

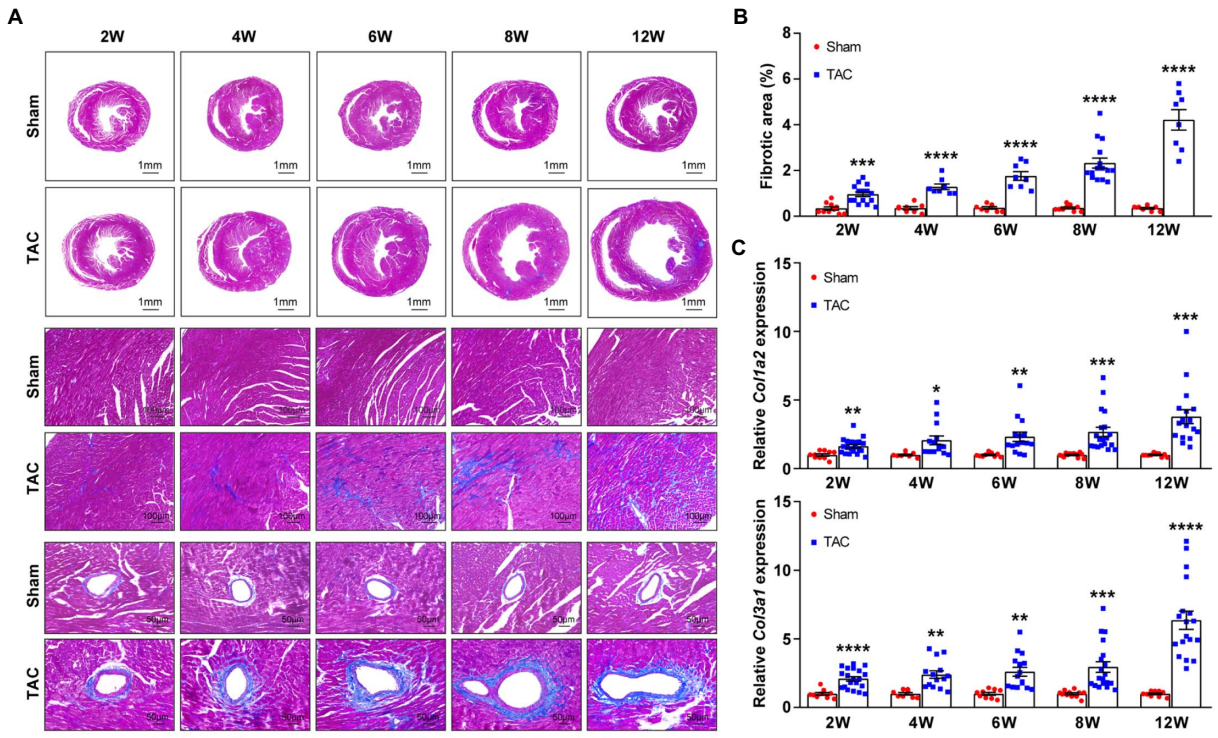

FIGURE 9
Time-series cardiac fibrosis induced by TAC. **(A)** Representative images of Masson's trichrome staining of heart sections (top). **(B)** Quantification of the fibrotic area (bottom), n=8~15. **(C)** Expression of *Col1a2* and *Col3a1* in mouse heart was detected by qPCR at various times upon surgery, n=8~20. Unpaired t-test for two-group comparisons, *p<0.05, **p<0.01, ***p<0.001, ****p<0.0001 vs. corresponding sham.

used ≤5 animals in the TAC group, and most articles did not report the number of animals used for each parameter measure, thus, the reproducibility of these results might be of concern (13, 29). In view of the very low number of animals in previous TAC studies, the sample size of each group in this study was increased to adequate numbers (>8) to ensure the reliability of the evaluation parameters, especially the numbers in TAC groups, which is imperative for interventions or pharmacologic agent study in future. Moreover, excepting for histomorphology analysis, the other analysis results in this study, especially survival rate, also collected experimental data from other C57BL/6 J TAC models in our laboratory (these data will not be used in future), which were conducted by the same operator in our team.

In summary, the present study provides a comprehensive analysis of the time-series cardiac remodeling phenotypes induced by different durations of the TAC model applied with a 25-gauge needle in C57BL/6 J mice. Moreover, this TAC method is suitable for high-precision aortic contraction in mice that need high reproducibility and low post-operative mortality. These data have important guiding significance and research value for the research of cardiac remodeling and heart failure in the future. However, there are still some limitations in the current study. The TAC surgery is also affected by the sex, strain, and age of animals, therefore, the data in the present study may not apply to females, other strains, or different age mice.

Data availability statement

The original contributions presented in the study are included in the article/supplementary material, further inquiries can be directed to the corresponding author.

Ethics statement

The animal study was reviewed and approved by the Ethics Board of the Capital Medical University.

Author contributions

XW designed the study, performed the experiments, and wrote the manuscript. XZ, LS, and BY performed the experiments and analyzed the data. JW participated in the mice breeding and management. QX participated in the echocardiography. AQ conceived the study, supervised the study, and wrote the manuscript. All authors contributed to the article and approved the submitted version.

Funding

This study was supported by the National Natural Science Foundation of China (81800233 and 82070474), the China Postdoctoral Science Foundation (2017M620830), the Beijing Postdoctoral Research Foundation (2018-22-113), and the Key Science and Technology Project of Beijing Municipal Institutions (KZ202010025032).

Conflict of interest

The authors declare that the research was conducted in the absence of any commercial or financial relationships that could be construed as a potential conflict of interest.

Publisher's note

References

1. Roger, VL. Epidemiology of heart failure: a contemporary perspective. *Circ Res*. (2021) 128:1421–34. doi: 10.1161/CIRCRESAHA.121.318172

2. Heidenreich, PA, Bozkurt, B, Aguilar, D, Allen, LA, Byun, JJ, Colvin, MM, et al. 2022 AHA/ACC/HFSA guideline for the Management of Heart Failure: executive summary: a report of the American College of Cardiology/American Heart Association joint committee on clinical practice guidelines. *Circulation*. (2022) 145:e876–94. doi: 10.1161/CIR.0000000000001062

3. Ambrosy, AP, Fonarow, GC, Butler, J, Chioncel, O, Greene, SJ, Vaduganathan, M, et al. The global health and economic burden of hospitalizations for heart failure: lessons learned from hospitalized heart failure registries. *J Am Coll Cardiol*. (2014) 63:1123–33. doi: 10.1016/j.jacc.2013.11.053

4. Frantz, S, Bauersachs, J, and Ertl, G. Post-infarct remodelling: contribution of wound healing and inflammation. *Cardiovasc Res*. (2009) 81:474–81. doi: 10.1093/cvr/cvn292

5. Kannan, A, and Janardhanan, R. Hypertension as a risk factor for heart failure. *Curr Hypertens Rep*. (2014) 16:447. doi: 10.1007/s11906-014-0447-7

6. Di Palo, KE, and Barone, NJ. Hypertension and heart failure: prevention, targets, and treatment. *Heart Fail Clin*. (2020) 16:99–106. doi: 10.1016/j.hfc.2019.09.001

7. Wang, X, Ye, Y, Gong, H, Wu, J, Yuan, J, Wang, S, et al. The effects of different angiotensin II type 1 receptor blockers on the regulation of the ACE-AngII-AT1 and ACE2-Ang(1-7)-mas axes in pressure overload-induced cardiac remodeling in male mice. *J Mol Cell Cardiol*. (2016) 97:180–90. doi: 10.1016/j.yjmcc.2016.05.012

8. Yu, Y, Hu, Z, Li, B, Wang, Z, and Chen, S. Ivabradine improved left ventricular function and pressure overload-induced cardiomyocyte apoptosis in a transverse aortic constriction mouse model. *Mol Cell Biochem*. (2019) 450:25–34. doi: 10.1007/s11010-018-3369-x

9. Deng, H, Ma, LL, Kong, FJ, and Qiao, Z. Distinct phenotypes induced by different degrees of transverse aortic constriction in C57BL/6N mice. *Front Cardiovasc Med*. (2021) 8:641272. doi: 10.3389/fcvm.2021.641272

10. Li, H, Liu, Q, Wang, S, Huang, L, Huang, S, Yue, Y, et al. A new minimally invasive method of transverse aortic constriction in mice. *J Cardiovasc Transl Res*. (2022) 15:635–43. doi: 10.1007/s12265-021-10170-4

11. Richards, DA, Aronovitz, MJ, Calamaras, TD, Tam, K, Martin, GL, Liu, P, et al. Distinct phenotypes induced by three degrees of transverse aortic constriction in mice. *Sci Rep*. (2019) 9:5844. doi: 10.1038/s41598-019-42209-7

12. Rockman, HA, Ross, RS, Harris, AN, Knowlton, KU, Steinhelper, ME, Field, LJ, et al. Segregation of atrial-specific and inducible expression of an atrial natriuretic factor transgene in an in vivo murine model of cardiac hypertrophy. *Proc Natl Acad Sci U S A*. (1991) 88:8277–81. doi: 10.1073/pnas.88.18.8277

13. Bosch, L, de Haan, JJ, Bastemeijer, M, van der Burg, J, van der Worp, E, Wesseling, M, et al. The transverse aortic constriction heart failure animal model: a systematic review and meta-analysis. *Heart Fail Rev*. (2021) 26:1515–24. doi: 10.1007/s10741-020-09960-w

14. Eichhorn, L, Weisheit, CK, Gestrich, C, Peukert, K, Duerr, GD, Ayub, MA, et al. A closed-chest model to induce transverse aortic constriction in mice. *J Vis Exp*. (2018):134. doi: 10.3791/57397

15. Liu, B, Li, A, Gao, M, Qin, Y, and Gong, G. Modified protocol for a mouse heart failure model using minimally invasive transverse aortic constriction. *STAR Protoc*. (2020) 1:100186. doi: 10.1016/j.xpro.2020.100186

16. Tavakoli, R, Nemska, S, Jamshidi, P, Gassmann, M, and Frossard, N. Technique of minimally invasive transverse aortic constriction in mice for induction of left ventricular hypertrophy. *J Vis Exp*. (2017):127. doi: 10.3791/56231

17. Zaw, AM, Williams, CM, Law, HK, and Chow, BK. Minimally invasive transverse aortic constriction in mice. *J Vis Exp*. (2017):121. doi: 10.3791/55293

18. Furihata, T, Kinugawa, S, Takada, S, Fukushima, A, Takahashi, M, Homma, T, et al. The experimental model of transition from compensated cardiac hypertrophy to failure created by transverse aortic constriction in mice. *Int J Cardiol Heart Vasc*. (2016) 11:24–8. doi: 10.1016/j.ijcha.2016.03.007

19. Calamaras, TD, Baumgartner, RA, Aronovitz, MJ, McLaughlin, AL, Tam, K, Richards, DA, et al. Mixed lineage kinase-3 prevents cardiac dysfunction and structural remodeling with pressure overload. *Am J Physiol Heart Circ Physiol*. (2019) 316:H145–59. doi: 10.1152/ajpheart.00029.2018

20. Tannu, S, Allocco, J, Yarde, M, Wong, P, and Ma, X. Experimental model of congestive heart failure induced by transverse aortic constriction in BALB/c mice. *J Pharmacol Toxicol Methods*. (2020) 106:106935. doi: 10.1016/j.vascn.2020.106935

21. Barrick, CJ, Rojas, M, Schoonhoven, R, Smyth, SS, and Threadgill, DW. Cardiac response to pressure overload in 129S1/SvImJ and C57BL/6J mice: temporal- and background-dependent development of concentric left ventricular hypertrophy. *Am J Physiol Heart Circ Physiol*. (2007) 292:H2119–30. doi: 10.1152/ajpheart.00816.2006

22. Wang, X, Wang, HX, Li, YL, Zhang, CC, Zhou, CY, Wang, L, et al. MicroRNA let-7i negatively regulates cardiac inflammation and fibrosis. *Hypertension*. (2015) 66:776–85. doi: 10.1161/HYPERTENSIONAHA.115.05548

23. Wang, X, Zhu, XX, Jiao, SY, Qi, D, Yu, BQ, Xie, GM, et al. Cardiomyocyte peroxisome proliferator-activated receptor alpha is essential for energy metabolism and extracellular matrix homeostasis during pressure overload-induced cardiac remodeling. *Acta Pharmacol Sin*. (2022) 43:1231–42. doi: 10.1038/s41401-021-00743-z

24. Scherrer-Crosbie, M, and Thibault, HB. Echocardiography in translational research: of mice and men. *J Am Soc Echocardiogr*. (2008) 21:1083–92. doi: 10.1016/j.echo.2008.07.001

25. Hartley, CJ, Reddy, AK, Madala, S, Michael, LH, Entman, ML, and Taffet, GE. Doppler estimation of reduced coronary flow reserve in mice with pressure overload cardiac hypertrophy. *Ultrasound Med Biol*. (2008) 34:892–901. doi: 10.1016/j.ultrasmedbio.2007.11.019

26. Schelbert, EB, Fonarow, GC, Bonow, RO, Butler, J, and Gheorghiade, M. Therapeutic targets in heart failure: refocusing on the myocardial interstitium. *J Am Coll Cardiol*. (2014) 63:2188–98. doi: 10.1016/j.jacc.2014.01.068

27. Martin, TP, Robinson, E, Harvey, AP, MacDonald, M, Grieve, DJ, Paul, A, et al. Surgical optimization and characterization of a minimally invasive aortic banding procedure to induce cardiac hypertrophy in mice. *Exp Physiol*. (2012) 97:822–32. doi: 10.1113/expphysiol.2012.065573

28. Schnelle, M, Catibog, N, Zhang, M, Nabeebaccus, AA, Anderson, G, Richards, DA, et al. Echocardiographic evaluation of diastolic function in mouse models of heart disease. *J Mol Cell Cardiol*. (2018) 114:20–8. doi: 10.1016/j.yjmcc.2017.10.006

29. Mohammed, SF, Storlie, JR, Oehler, EA, Bowen, LA, Korinek, J, Lam, CS, et al. Variable phenotype in murine transverse aortic constriction. *Cardiovasc Pathol*. (2012) 21:188–98. doi: 10.1016/j.carpath.2011.05.002

30. Melleby, AO, Romaine, A, Aronsen, JM, Veras, I, Zhang, L, Sjaastad, I, et al. A novel method for high precision aortic constriction that allows for generation of specific cardiac phenotypes in mice. *Cardiovasc Res*. (2018) 114:1680–90. doi: 10.1093/cvr/cvy141

31. Hermans, H, Swinnen, M, Pokreisz, P, Caluwe, E, Dymarkowski, S, Herregods, MC, et al. Murine pressure overload models: a 30-MHz look brings a whole new "sound" into data interpretation. *J Appl Physiol*. (1985) 2014:563–71. doi: 10.1152/japplphysiol.00363.2014

frontiers | Frontiers in Cardiovascular Medicine

TYPE Original Research
PUBLISHED 28 February 2023
DOI 10.3389/fcvm.2023.1018203

OPEN ACCESS

EDITED BY
Matteo Pagnesi,
ASST Spedali Civili di Brescia, Italy

REVIEWED BY
Mario Gramegna,
San Raffaele Hospital (IRCCS), Italy
Maurizio Bertaina,
Ospedale San Giovanni Bosco,
Italy

*CORRESPONDENCE
Masaki Funamoto
✉ Masaki.Funamoto@hcahealthcare.com;
✉ mskarudy@gmail.com

SPECIALTY SECTION
This article was submitted to Structural Interventional Cardiology, a section of the journal Frontiers in Cardiovascular Medicine

RECEIVED 16 August 2022
ACCEPTED 13 January 2023
PUBLISHED 28 February 2023

CITATION
Funamoto M, Kunavarapu C, Kwan MD, Matsuzaki Y, Shah M and Ono M (2023) Single center experience and early outcomes of Impella 5.5.
Front. Cardiovasc. Med. 10:1018203.
doi: 10.3389/fcvm.2023.1018203

Single center experience and early outcomes of Impella 5.5

Masaki Funamoto[1]*, Chandra Kunavarapu[2], Michael D. Kwan[2], Yuichi Matsuzaki[1], Mahek Shah[2] and Masahiro Ono[1]

[1]Department of Cardiothoracic Surgery, Methodist Hospital, San Antonio, TX, United States, [2]Advanced Heart Failure and Transplant Cardiology, Methodist Hospital, San Antonio, TX, United States

Background: Acute decompensated heart failure (HF) and cardiogenic shock (CS) frequently are refractory to conservative treatment and require mechanical circulatory support (MCS). We report our early clinical experience and evaluate patient outcomes with the newer generation surgical Impella 5.5.

Methods: Seventy patients that underwent Impella 5.5 implantation between October 2019 and December 2021 at a single center were enrolled in this study. Pre-operative characteristics, peri-operative clinical course information, and post-operative outcomes were retrospectively collected.

Results: Fifty-seven (81%) patients survived to discharge, and 51 (76%) patients survived at the time of the first 30days post-discharge visit. Thirty-one patients (44%) received Impella support for a bridge to advanced surgical heart failure therapy (transplant or durable left ventricular assist device [LVAD]), 27 (39%) cases were used for a bridge to recovery/decision and 12 (17.1%) cases was used for planned perioperative support for high-risk cardiac surgery procedure.

Conclusion: Our results suggest that Impella 5.5 provides favorable survival in the management of HF and CS, particularly used for a bridge to heart transplant or LVAD. Early extubation and mobilization with high flow circulatory support allowed effective tailoring of MCS approaches from peri-operative support for high-risk cardiac surgery, bridge to recovery, and to advanced surgical heart failure therapy.

KEYWORDS

cardiogenic shock, Impella, temporary mechanical circulatory support, bridge to recovery, bridge to transplant, bridge to LVAD, high risk cardiac surgery

Introduction

Cardiogenic shock (CS) is associated with in-hospital mortality rates ranging from 27 to 51%, and management remains challenging despite advances in therapies (1–4). Cardiogenic shock is caused by severe impairment of the myocardium that results in diminished cardiac output, end-organ hypoperfusion, and hypoxia. While inotropic agents are widely used, mortality is higher with an increased number of prescribed vasopressors. Catecholamine therapy is associated with significant limitations including arrhythmias, increased myocardial oxygen consumption, and inadequate circulatory support (5, 6). Temporary mechanical circulatory support (MCS) is a key component of early patient management for CS with pronounced benefits, including substantial cardiovascular support without increased risk of myocardial ischemia and possible decreased myocardial oxygen demand, which may increase the likelihood of eventual recovery. Registry data indicate that early MCS device use is associated with improved rates of survival rather than deferred use in acute myocardial infarction CS (7, 8). There are various options for acute percutaneous MCS: the intra-aortic balloon pump (IABP), axial flow pumps/catheter-based left ventricular assist device (cVAD; Impella 2.5, Impella CP), left atrial-to-femoral arterial ventricular assist devices (Tandem

Heart), and venous–arterial extracorporeal membrane oxygenation (ECMO) (9–12). These devices are designed for rapid deployment, short term support, requiring bed-rest, which often affects mobility and recovery. IABP can be placed *via* the axillary artery, but often is insufficient to support patients with profound CS, and has not demonstrated an early mortality benefit for patients with CS (1).

Impella 5.5 is a microaxial, surgically implanted heart pump that unloads the left ventricle, reduces ventricular work, and provides the circulatory support necessary to allow recovery and early assessment of residual myocardial function. It is designed for long-duration support and enables ambulation to optimize recovery while using real-time SmartAssist intelligence (13).

In October 2018, a new heart transplant allocation system was implemented with a 6-tiered classification system in the United States. Non-dischargeable mechanical support devices such as IABP, cVADs, and ECMO classified patients as Status 1 or 2, and are prioritized under the new system (13), with ambulatory Impella 5.5 in the spotlight as a favorable bridging strategy for heart transplant. Here, we report early outcomes in patients implanted with the Impella 5.5 at a single-center and current clinical use of axillary Impella in a mid-America tertiary high-volume MCS medical center.

Materials and methods

Study design

Patients that underwent the Impella 5.5 implantation at Methodist Hospital San Antonio, TX, between October 2019 and December 2021 were included in the study. The Surgical Unloading Renal Protections and Sustainable Support Study (SURPASS) registry (NCT05100836) is a database for all surgically implanted Impella procedures that is prospectively maintained by the manufacturer and retrospective collection of data. Clinical and outcome data were obtained from this SURPASS registry and retrospective review of electronic medical records. Patients were followed after hospital discharge for recovery, death, or transition to durable left ventricular assist device (LVAD) or heart transplantation. This study was approved by the Hospital Corporation of American (HCA) Healthcare Institutional Review Board. The investigation conforms with the principles outlined in the Declaration of Helsinki.

Device design, surgical technique, and mechanical circulatory support strategy

The Impella 5.5® with SmartAssist® heart pump is a temporary LVAD intended for longer use, with FDA approval for up to 14 days and CE mark approval for up to 30 days. The device can be inserted either *via* the axillary artery or by direct aortic access with a minimum vessel diameter ≥ 7 mm. The inlet position on the Impella 5.5 differs from earlier models and must be positioned 5 cm below the aortic valve annulus. The device is equipped with optical sensor technology, to be used with echocardiography to facilitate proper device positioning across the aortic valve.

All patients underwent Impella implantation under general anesthesia. The intraoperative echocardiogram and pulmonary artery line was used to monitor cardiac function. The Impella 5.5 was inserted at the axillary artery, which is suitable for longer support without concern of mediastinal infection. If pre-op CT is available, we recommend checking the diameter of the axillary artery to ensure it is 6 mm or more, as well as to examine for calcification, stenotic, or tortuous vessels and arch, and the length of ascending aorta with 7 cm or more for access site evaluation. In addition, use of preoperative transthoracic echocardiogram (TTE) allows visualization of LV cavity size, angle of the LV-aortic root and assessment of aortic valve leaflet calcification/atherosclerosis. Although an infrequent occurrence, aortic valve leaflet calcification/atherosclerosis can cause Impella related aortic insufficiency, thus providing an opportunity to predict the potential device related risk.

For axillary approach, the pectoralis major was divided along with muscle fiber, and the pectoralis minor was retracted laterally without severing muscles to prevent potential bleeding from the muscle surface. The thoracoacromial artery was used as an important anatomical landmark to locate the axillary artery with minimal dissection. After exposing the axillary artery, heparin is administered to obtain an activated clotting time >250s. Our standard surgical approach for Impella 5.5 was established with a 10 mm prosthetic vascular graft, anastomosed in an end-to-side fashion to the right axillary artery. The access site was determined based on a CT scan. We prefer to use right axillary approach for axillary Impella since catheters make a natural curve and go straight down to the ascending aorta and LV in most of the cases. For axillary IABP, the left axillary approach is preferred to avoid excess stress on the intima of ascending aorta/arch vessels, especially for longer term use. However, if the right axillary approach is not feasible or there is any visible tortuous arch vessels *via* CT scan, the left axillary artery approach should be considered, with the ascending aorta or the innominate artery as alternatives for Impella access. Insertion was guided under fluoroscopy and positioning was adjusted using intraoperative transesophageal echocardiography.

Once inserted, at least two views of a TTE, such as parasternal long axis and apical four chamber view, are obtained to confirm the Impella position. Impella 5.5 does not have a pigtail and thus, it is easy to change the position, but as a result there is also higher risk of the device moving from its ideal positioning. Moreover, the device could attach to or push the septum if rotated completely away from the mitral valve and could lead to suction events. Therefore, the Impella pump needs to be away from the LV wall in multiple views (Figure 1).

For patients with cardiogenic shock, MCS utilization is considered when two or more moderate doses of inotropes or vasopressors are needed. We prefer to first use dobutamine, add epinephrine as a second agent, and then use vasopressin/norepinephrine bitartrate as needed to maintain cardiac output and perfusion pressure for cardiogenic shock. The threshold of MCS is lowered if the patient has an arrhythmia issue. After MCS initiation, vasopressors are decreased as much as possible, and inotropes are titrated according to the hemodynamic/perfusion status, but a moderate dose of dobutamine (3–5 mcg/kg/min) is usually maintained for RV support.

The combination of Impella 5.5 and veno-arterial extracorporeal membrane oxygenation (VA-ECMO) is established as a stepped strategy. As such, we do not suggest Impella 5.5 as a rescue device. For profound CS requiring VA-ECMO, Impella CP or IABP are used for LV unloading or afterload reduction at the first line additional support, to be transitioned to Impella 5.5.

Data collection and statistical analysis

Data were collated and tabulated using Microsoft Excel (Microsoft Corporation, Redmond, WA, United States). Normally distributed descriptive statistics are presented as mean (quartile 1 (Q1), quartile 3

10.3389/fcvm.2023.1018203

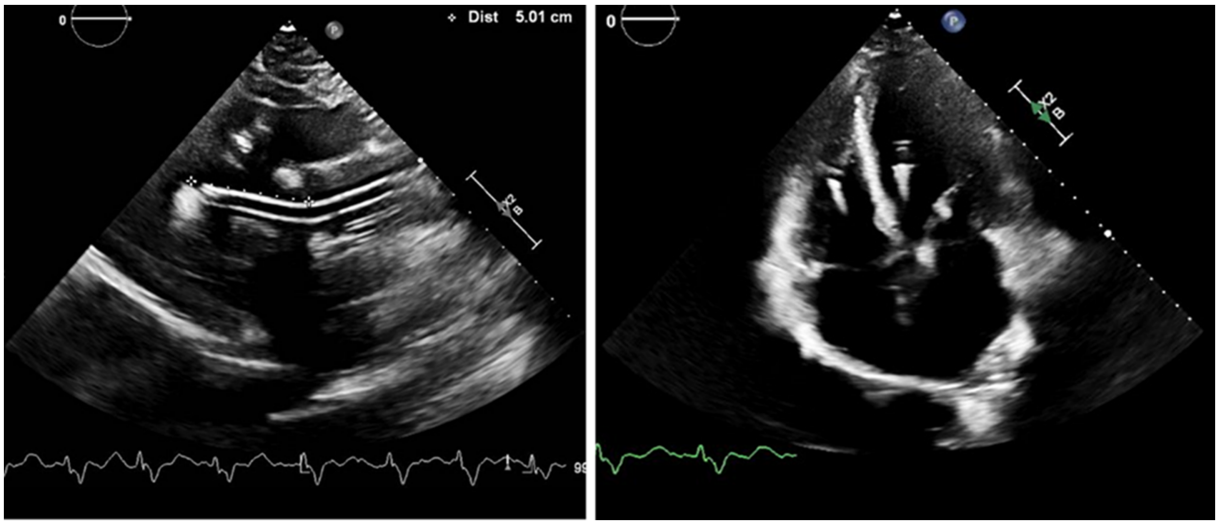

FIGURE 1
Positioning of the Impella 5.5: The bending portion of Impella pump head will be on the level of aortic valve with the tip pointing away from the posterior wall in the parasternal long axis view, and away from septum in the four chamber view. Impella position-related aortic insufficiency could be observed for patients with atherosclerotic aortic valve in the apical view.

(Q3)) for continuous variables and *n* (percent) for categorical variables. Tabular denominators reflect the number with available data for a given data point. Survival analyzes were performed using Kaplan–Meier analyzes. Independent variables with >10% unrecorded or missing values were excluded, with the majority of factors in the tables having no missing data. Statistical analyzes were performed using GraphPad Prism v9 (GraphPad Software Inc., San Diego, CA, United States).

Results

Patient population and procedural characteristics

Patients in our study cohort were 90% male and 55 years of age (Q1–Q3, 48–65). Baseline left ventricular ejection fraction (LVEF) was 20% (Q1–Q3, 15–22) and 48 (69%) patients had at least mild right ventricular dysfunction by TTE. The etiologies requiring MCS were acute myocardial infarction (17%), acute decompensated heart failure (HF, 61%), post-cardiotomy CS (4%), and planned support for high-risk cardiac surgery (17%). The indications of Impella implantation were bridge to decision in 7 (10%), bridge to recovery in 20 (29%), bridge to durable LVAD in 6 (9%) cases, bridge to heart transplant in 25 (36%) cases, and perioperative support for high-risk cardiac surgery in 12 (17%) cases. Fifty patients (71%) had other types of MCS prior to Impella 5.5 implantation. Thirty (44%) patients were upgraded to Impella 5.5 from intra-aortic balloon pump (IABP), 16 (25%) from Impella CP percutaneous LVAD, and 14 (20%) patients were transitioned to 5.5 as a de-escalation from VA-ECMO. Baseline and procedural characteristics are presented in Table 1.

Outcomes

The majority of patients had Impella 5.5 inserted *via* the right axillary artery (96%). The mean duration of Impella support was 10 days (Q1–Q3, 6–12 days). For the cohort, overall survival to discharge was 57 patients (81%). Five patients (7%) were bridged to durable LVAD, 23 patients (33%) received heart transplantation, and 29 patients (41%) achieved cardiac recovery (Table 2). Of the patients in this study, survival to discharge occurred in 13/18 (72%) for bridge to recovery, 4/9 (44%) for bridge to decision, 23/25 (92%) for bridge to heart transplant, 5/6 (83%) for bridge to durable surgical LVAD, and 12/12 (100%) for bridge to recovery from high-risk cardiac surgery. In the group of bridge to recovery/decision and bridge to heart transplant/LVAD, the majority of patients had concomitant RV systolic dysfunction by TTE (70 and 84%, respectively).

Notably, in the bridge to transplant group, 10 patients receiving Impella were bridged from IABP due to support failure. In addition, 44% of patients who underwent Impella 5.5 placement were transitioned from IABP, which includes upgrading for IABP support failure and de-escalation from IABP/VA-ECMO.

With respect to Impella-supported cardiac surgery, seven patients underwent isolated coronary artery bypass grafting, and five cases were valve or combined valve/coronary/aortic procedures. In a total of 10 STS cases, the mean STS scores of mortalities were 5.2% (Q1–Q3, 1.6–7.5%). All patients survived to discharge from the index admission (Table 3).

As shown in Figure 2, Kaplan–Meier analysis demonstrated significant difference in 90 days survival between the groups of bridge to LVAD/heart transplant and non LVAD/heart transplant (native heart recovery, HR 3.71, 95% CI 1.35–10.21; $p = 0.029$). Thirty-two patients (46%) experienced at least one complication while on Impella 5.5 support. Four patients had thrombocytopenia, 6 developed axillary hematomas requiring exploration, 1 had mediastinal bleeding requiring chest washout, 6 had acute kidney injury or required renal replacement therapy, and 2 patients had cerebrovascular accidents. There were 7 patients with transient high plasma free hemoglobin (pf-Hb) level (>20 mg/dL), all of which were resolved with positional or anticoagulation adjustment, and only 1 patient had device dislodgement requiring revision of Impella 5.5 placement. There was one surgical site infection requiring vascular construction. Aortic valve injury, distal limb ischemia, or other vascular complications did not occur (Table 4).

10.3389/fcvm.2023.1018203

TABLE 1 Baseline characteristics and periprocedural data.

Baseline clinical characteristics	All (*n*=70)	Bridge to recovery/ decision (*n*=27)	Bridge to heart transplant/LVAD (*n*=31)	Planned perioperative support (*n*=12)
Age, years	55.4 (48.3, 65.0)	59.0 (57.0, 65.5)	50.4 (37.0, 63.5)	60.2 (56.5, 65.3)
Male, *n* (%)	63 (90)	23 (85)	29 (94)	11 (92)
BMI, kg/m^2	29.0 (25.5, 32.2)	30.5 (25.9, 34.5)	28.5 (25.3, 30.9)	26.7 (25.2, 28.7)
Cardiogenic Shock, *n* (%)	58 (83)	26 (96)	27 (87)	5 (42)
Post-CPR, *n* (%)	13 (19)	11 (41)	2 (7)	0 (0)
ICM, *n* (%)	36 (51)	19 (70)	9 (29)	8 (67)
Baseline LVEF, %	20.1 (5.4, 6.8)	24.0 (17.9, 30.7)	16.2 (14.0, 20.0)	21.1 (16.3, 26.5)
Baseline LVEDD, mm	6.1 (5.4, 6.8)	5.8 (5.0, 6.5)	6.5 (6.0, 6.9)	6.0 (5.3, 6.5)
Severe mitral regurgitation, *n* (%)	16 (23)	7 (26)	7 (23)	2 (17)
RV dysfunction*, *n* (%)	48 (69)	19 (70)	26 (84)	3 (25)
SCAI stages at admission				
A: "At risk"	2 (3)	0 (0)	0 (0)	2 (17)
B: "Beginning" cardiogenic shock	2 (3)	0 (0)	0 (0)	2 (17)
C: "Classic" cardiogenic shock	39 (56)	8 (30)	26 (84)	5 (42)
D: "Deteriorating" cardiogenic shock	15 (21)	8 (30)	4 (13)	3 (25)
E: "Extremis"	12 (17)	11 (16)	1 (3)	0 (0)
Pre-op Creatinine	1.9 (1.1, 2.2)	2.1 (1.2, 2.6)	1.9 (1.3, 2.2)	1.2 (1.0, 1.2)
Pre-op ALT	281.0 (28.3, 134.5)	588.0 (37.5, 280.0)	100.0 (21.5, 105.0)	57.7 (28.8, 67.3)
MCS prior to Impella 5.5, *n* (%)	50 (71)	24 (89)	22 (71)	5 (46)
Impella 5.5 added to VA ECMO, *n* (%)	14 (20)	8 (30)	6 (19)	0 (0)
Upgrade from IABP, *n* (%)	30 (44)	10 (37)	19 (61)	2 (17)
Upgrade from Impella 2.5/CP, *n* (%)	16 (23)	13 (48)	1 (3)	2 (17)
Impella insertion site				
Right Axillary artery, *n* (%)	66 (94)	28 (100)	31 (100)	8 (67)
Ascending aorta, *n* (%)	3 (4)	0 (0)	0 (0)	3 (25)
Innominate artery, *n* (%)	1 (1)	0 (0)	0 (0)	1 (8)

Data is presented as *n* (%) or mean (quartile 1, quartile 3). ALT, alanine transaminase; BMI, body mass index; CPR, cardiopulmonary resuscitation; IABP, intra-aortic balloon pump; ICM, ischemic cardiomyopathy; LVAD, left ventricular assist device; LVEF, left ventricular ejection fraction; MCS, mechanical circulatory support; SD, standard deviation; VA ECMO, venoarterial extracorporeal membrane oxygenation *RV dysfunction was defined if it meets at least one of the following values: (I) tricuspid annular place systolic excursion (TAPSE) < 17 mm; (II) fractional area change (FAC) < 35%; (III) and/or tricuspid annular systolic velocity (s') < 9.5 cm/s, according to the recommendation guidelines from ASE/EAC (14).

TABLE 2 Clinical outcomes on Impella Support.

Clinical outcome on Impella support	All (*n*=70)	Bridge to recovery/ decision (*n*=27)	Bridge to heart transplant/LVAD (*n*=31)	Planned perioperative support (*n*=12)
Duration of Impella 5.5 support, days	10.0 (6.0, 12.0)	7.4 (5.0, 10.5)	13.6 (8.0, 17.0)	6.4 (5.8, 7.3)
Length of hospital stay, days	27.5 (17.0, 34.8)	17.7 (15.0, 21.0)	38.6 (24.5, 42.0)	20.9 (14.8, 25.3)
Survival to discharge, *n*/*N* (%)	57/70 (81)	17/27 (63)	29/31 (94)	12/12 (100)
Post discharge 30 days survival*, *n*/*N* (%)	52/68 (77)	13/26 (50)	29/31 (94)	11/11 (100)

Data is presented as *n* /N (%) or mean (quartile 1, quartile 3). *After the index admission. LVAD, left ventricular assisted device.

Discussion

While studies using Impella devices for CS show reasonable survival for AMI-CS (15), several smaller randomized clinical trials have failed to demonstrate improved outcomes with Impella 2.5 or Impella CP over IABP (9, 15–17). However, the first 200 cases in the US using Impella 5.5 had a rate of overall survival to explant of 74% in patients with CS (18). The current single center study further supports the potential benefit of Impella 5.5 for CS management with 81% of the overall survival to discharge after Impella 5.5 implantation. Of these patients,

TABLE 3 Outcomes for Impella-supported cardiac surgery.

Case	Gender	BMI	SCAI at Admission	RV Failure	Pre-Op Cr	Pre-op LVEF (%)	Pre-op LVED (cm)	Previous MCS Devices	Access Approach	STS Score Mortality (%)	STS Score Major Morbidity (%)	Total ischemic time (min)	Total CPB time (min)	Cardiac Procedure	Duration of support (days)	Post-discharge 30-day survival
1	Male	29.4	B	NO	1.01	16.7	6.5	No	Rt. Axillary	3.65	17.9	68	104	On-pump CABG	8	Yes
2	Male	30.3	A	YES	0.79	32.3	5.8	No	Rt. Axillary	1.30	14.8	93	132	MVR	4	Yes
3	Male	27.0	B	YES	0.86	15.0	4.5	No	Rt. Axillary	2.47	16.3	63	91	On-pump CABG	6	Yes
4	Male	24.5	C	YES	1.00	13.8	6.2	No	Direct Aorta	7.03	30.1	69	122	On-pump CABG	8	Lost to FU
5	Male	28.5	C	NO	1.08	28.0	6.6	No	Direct Aorta	0.61	6.8	84	126	On-pump CABG	7	Yes
6	Male	27.1	C	NO	1.17	23.0	4.7	No	Innominate	N/A	N/A	142	323	AVR; ascending aortic replacement	8	Yes
7	Male	25.7	D	NO	2.09	19.0	6.0	Impella CP	Rt. Axillary	14.24	56.6	49	68	On-pump CABG	7	Yes
8	Male	20.0	C	NO	0.96	19.0	7.8	No	Direct Aorta	N/A	N/A	123	226	MV repair; AVR	7	Yes
9	Male	25.4	A	NO	0.90	29.0	7.0	No	Rt. Axillary	0.97	12.3	67	95	MVR	4	Yes
10	Male	32.2	C	NO	0.98	18.0	5.3	IABP	Rt. Axillary	7.60	74.0	115	147	On-pump CABG; AVR	6	Yes
11	Male	27.1	D	NO	1.87	13.6	6.0	Impella CP	Rt. Axillary	8.70	63.0	79	104	On-pump CABG	7	Yes
12	Female	22.8	D	NO	1.35	26.0	5.1	IABP; Impella 2.5	Rt. Axillary	5.20	42.0	96	121	On-pump CABG	5	Yes

AVR, aortic valve replacement; BMI, body mass index; CABG, coronary artery bypass graft; cm, centimeter; CPB, cardiopulmonary bypass; FU, follow-up; IABP, intra-aortic balloon pump; LVEF, left ventricle ejection fraction; LVED, left ventricular end diastolic; MCS, mechanical circulatory support; min, minute; MVR, mitral valve replacement; N/A, not applicable; Pre-op, pre-operation; RV, right ventricle; SCAI, Society for Cardiovascular Angiography and Interventions; STS, Society of Thoracic Surgeons.

10.3389/fcvm.2023.1018203

10.3389/fcvm.2023.1018203

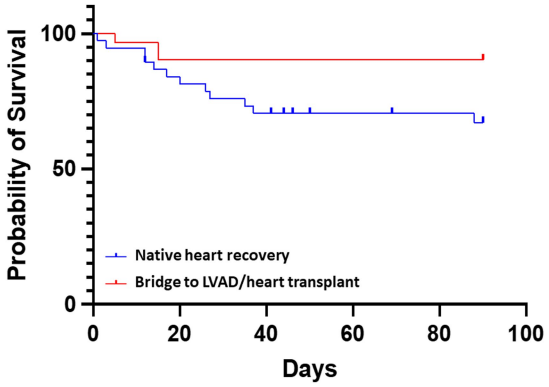

FIGURE 2
Comparative survival for patients receiving Impella 5.5. The probability of survival was greater in patients with a bridge to LVAD/heart transplant vs. bridge to native heart recovery (non LVAD/heart transplant) HR 3.71, 95% CI 1.35–10.21; p=0.029.

TABLE 4 Adverse events related to Impella 5.5.

Complication	*N* (%)
Stroke	2 (2.9)
Acute kidney injury	3 (4.3)
Renal replacement therapy	3 (4.3)
Acute hepatic dysfunction	2 (2.9)
Respiratory failure/dysfunction*	4 (5.7)
Thrombocytopenia**	4 (5.7)
Anemia	10 (14.3)
Bleeding requiring surgery	7 (10.0)
Surgical site infection	1 (1.4)
Valve injury	0 (0)
Cardiac perforation	0 (0)
Ventricular arrhythmia	6 (8.6)
Device dislodgement	1 (1.4)
Hemolysis (Pf-Hb > 20 mg/dL)	7 (10.0)

Pf-Hb: plasma free hemoglobin. *Respiratory failure/dysfunction is defined as the impairment of respiratory function requiring reintubation, tracheostomy or the inability to discontinue ventilatory support 48 h after Impella device explant. This excludes intubation for reoperation or temporary intubation for diagnostic or therapeutic procedures. **Thrombocytopenia is defined as having a platelet count measurement of less than 50,000/mm^3 taken more than 48 h after the Impella implant.

74% had other types of MCS prior to Impella, 44% received Impella support for a bridge to advanced surgical heart failure therapy, 39% of cases were for a bridge to recovery/decision, and 17% cases were perioperative support for high-risk cardiac surgery. Moreover, all patients receiving a heart transplant from Impella 5.5 bridge survived more than 90 days after discharge. Thus, future studies are warranted with the newer Impella devices (5.0/5.5), which have higher flow rates and may provide more sufficient cardiac output to maintain systemic organ perfusion in patients with severe CS or heart failure requiring full hemodynamic support.

Outcomes for CS with medical management without any mechanical circulatory support is poor, particularly for patients with prominent CS, stage D or E according to the Society of Cardiovascular Angiography and Interventions (SCAI) CS classifications (19–21). As such, temporary MCS devices are often used as a bridge until the patient recovers or condition deteriorates needing a long-term assist device or heart transplantation. IABP was often implemented as a first-line temporary MCS for refractory CS and acute decompensated heart failure, due to its quick deployment and less invasive features compared with other MCS devices. As such, IABP did not show survival benefit for cardiogenic shock due to acute myocardial infarction (AMI-CS) (22). However, several observational studies have indicated that the IABPs can improve outcome in cardiogenic shock due to acute decompensated heart failure (HF-CS). Compared to AMI-CS, it has a different underlying pathophysiology and, accordingly, different responses to pharmacological treatments and mechanical support (23, 24). IABP combines a more substantial effect on left ventricular afterload with a modest increase (0.5–1.0 L/min; 25, 26) in cardiac output and would therefore be most suitable in clinical scenarios characterized by a disproportionate increase in afterload without profound hemodynamic compromise. For a bridge to transplant/LVAD, groin IABP is switched to axillary position once stabilized with groin IABP so that patients can ambulate while waiting for transplant/LVAD. However, some patients fail to stabilize with IABP due to insufficient support or multiple dislodgement in axillary IABP. Our study showed benefit of Impella 5.5 following IABP support failure. After the switch to Impella, these patients achieved functional recovery enabling participation in physical therapy, occupational therapy, or ambulation with improved cardiorenal syndrome or improved type 2 pulmonary hypertension, followed by a successful heart transplant, which supports the potential advantages of extensive Impella 5.5 use in this setting.

To date, studies for Impella protected cardiac surgery have been limited to small case series, with the majority reporting no to minimal mortality or morbidity (27–29). Collectively, these studies concluded that prophylactic use of the Impella 5.5 is safe and effective in patients with severe LV dysfunction. Once hemodynamics deteriorates in surgical cases with severe LV dysfunction, RV also fails with significant increase in preload and afterload, and eventually VA-ECMO is required for profound biventricular dysfunction. Unfortunately, the outcome for postcardiotomy cardiogenic shock (PCCS) requiring VA-ECMO is poor with a high rate of complications (30). In contrast, left ventricular unloading with Impella decreases wall tension, improves coronary perfusion favoring myocardial recovery, and could reduce pulmonary congestion and RV afterload with smaller bore access. In line with these data, the current study demonstrates that use of Impella 5.5 was protective and all surgical patients survived to discharge without any major device-related complications in our initial Impella 5.5 experience, despite sick population with 67% of cardiogenic shock status at stage C or D at the time of the cardiac surgery.

Interestingly, patients with CS that received an early pulmonary artery catheter (PAC) prior to MCS had improved short-term mortality and overall survival rates compared to patients without a PAC. This was also associated with lower incidence of short-term mortality, particularly in advanced CS (31, 32). Moreover, PAC-derived hemodynamic parameters such as CPO, pulmonary artery pulsatility index (PAPi), or CVP/PCWP ratio have been used to assess RV function, LV filling status, and guide treatment after Impella implantation. In Impella-supported cardiac surgery, 3–5 days are generally required to stabilize volume status and achieve organ perfusion at which point Impella support can start to be withdrawn. In our study, the mean support time of Impella 5.5 was 6.4 days for the patients that received Impella-supported cardiac surgery. Hemodynamic monitoring with PAC is an essential part of our practice to evaluate and manage both LV and RV

dysfunction appropriately. A low threshold is set for longer MCS support to take advantage of axillary Impella, to reduce the requirement for vasopressors/inotropes, to avoid kidney dysfunction related to organ malperfusion, and to enable early extubation/early ambulation maintaining functional status without cardiac stress.

During critical illness, patients who are immobilized for more than a few days develop neuromuscular weakness despite receiving full supportive care. Thus, early mobilization (EM) of ICU patients is necessary to attenuate critical illness-associated muscle weakness (33) and is especially important to improve functional status for those awaiting heart transplant (34). At our institution, the mobilization protocol includes appropriate pain control with minimal sedation/narcotics; early extubation (in the operating room if possible); early tracheostomy if needed; physical therapy/occupational therapy consultation on post-operative day 0; active/passive range of motion even if intubated; out of bed to chair for all meals, ambulation twice or three times a day on post-operative day 1; cycle ergometer as needed; daily physical therapy/occupational therapy evaluation; and daily nutrition assessment.

Of the 6 cases of Impella access site/axillary wound re-exploration for hematoma, none had any active surgical bleeding at the time of re-exploration. We set a low threshold for wound exploration for hematoma/bleeding with consideration of risk of infection related to hematoma, especially for patients waiting for transplant. This strategy may have contributed to the relatively higher rate of bleeding related complication in this series. Other complications were minimal and included acute kidney injury or required renal replacement therapy (6 patients), transient high pf-Hb level (>20 mg/dL, 7 patients), device dislodgement (1 patient), and cerebrovascular accident (CVA, 2 patients). The CVA complications occurred during urgent Impella exchange cases as a result of significant hemolysis with groin Impella. Both had unclear neurologic status while on the ventilator throughout the procedure. There was left ventricular thrombus at the time of Impella CP insertion, which disappeared on follow-up TTE prior to Impella 5.5 device exchange. Thus, the CVA events likely happened prior to Impella 5.5 placement and were not related to Impella 5.5. Aortic valve injury, distal limb ischemia, or other vascular complications did not occur in this series.

In the current MCS era, tailoring the MCS de-escalation approach according to patient condition is essential for best practices in patients with CS or heart failure (Figure 3). In this single center cohort, patients receiving Impella 5.5 support have meaningful outcomes in the management of profound CS and end-stage heart failure. Impella 5.5 is an important hub MCS device and can be used for up- or downgraded support and to bridge to the next treatment course. This includes LVAD and heart transplant, and the exchange from other temporary MCS inserted *via* the femoral artery (VA-ECMO, IABP or earlier Impella models) for longer duration support with less device-related complications or access site issues. In all indications, early MCS initiation strategy is crucial for maximal treatment effects and to avoid poor outcomes. Impella 5.5 utilization is considered at our institution if the patient needs more than 48-h MCS support at the time of evaluation.

Limitations

Our study is not without limitations as this is a retrospective cohort study without randomization, with a small sample size that consists of a variety of patients with relatively stable CS and profound CS requiring VA-ECMO from a single center, and only reports short-term outcomes from temporary Impella 5.5 support. Additionally, our institution has more males than females that receive advanced surgical heart failure therapy and heart transplants (35). Thus, our institutional gender distribution also affects the gender disparity in this study. Furthermore, our cohort was not compared to patients treated with other MCS, such as IABP alone or other Impella devices (CP/5), or those treated with medical therapy only. Due to the nature of our retrospective study, PAC data and lactate level are not included here as there was a large amount of missing data for those parameters. Given that our cohort had a large number of patients on VA-ECMO and that both hemodynamic parameters and the dose of inotropes/vasopressors are affected by the support level of VA-ECMO, further assessments are deferred to studies

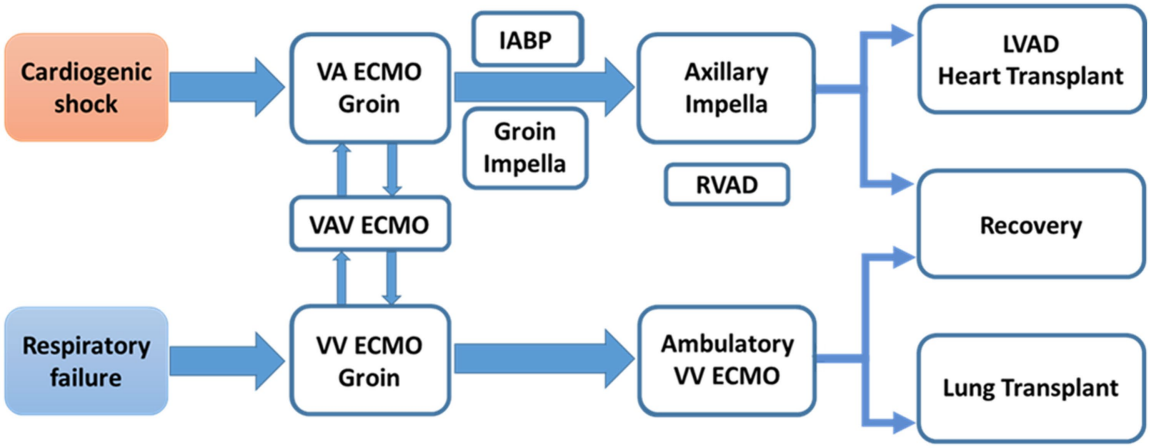

FIGURE 3
MCS de-escalation in patients with CS or heart failure. MCS is not just one time procedure. A team require comprehensive MCS experiences to provide optimal MCS strategy, tailored for patient's status, and maximal survival benefit. IABP, intra-aortic balloon pump; LVAD, left ventricular assist device; MCS, mechanical circulatory support; RVAD, right ventricular assist device; VA-ECMO, veno-arterial extracorporeal membrane oxygenation; VAV ECMO, veno-arterio-venous extracorporeal membrane oxygenation; VV ECMO, veno-venous extracorporeal membrane oxygenation.

with a more focused patient population in a larger cohort. As a result, this analysis is hypothesis generating for future studies.

Conclusion

In this study, patients with surgically implanted axillary Impella 5.5 have encouraging short-term survival rates, specifically in patients with CS or decompensated heart failure, which have historically high early mortality rates. Axillary placement of Impella 5.5 was used in a multitude of clinical indications, such as bridging strategy to durable support, implant LVAD and heart transplant, or perioperative support for high-risk cardiac surgery all with excellent outcomes. The execution of prospective, multicenter, randomized, long-term outcome studies, are warranted to further delineate the optimal patient profile, timing, and management of Impella 5.5 support.

Data availability statement

The raw data supporting the conclusions of this article will be made available by the authors, without undue reservation.

Ethics statement

The studies involving human participants were reviewed and approved by HCA Healthcare Internal Review Board committee members, who determined informed consent was not required for this retrospective study.

Author contributions

MF and MO: study conception and design. MF: data collection, analysis, and interpretation of results. MF, CK, MK, YM, MS, and MO: draft manuscript preparation. All authors reviewed the results and approved the final version of the manuscript.

Acknowledgments

JetPub Scientific Communications LLC, supported by Abiomed, assisted the authors in the preparation of this manuscript, in accordance with Good Publication Practice (GPP3) guidelines.

Conflict of interest

The authors declare that the research was conducted in the absence of any commercial or financial relationships that could be construed as a potential conflict of interest.

Publisher's note

References

1. Thiele, H, Zeymer, U, Neumann, F-J, Ferenc, M, Olbrich, H-G, Hausleiter, J, et al. Intraaortic balloon support for myocardial infarction with cardiogenic shock. *N Engl J Med*. 367:1287–96. doi: 10.1056/NEJMOA1208410

2. Goldberg, RJ, Makam, RCP, Yarzebski, J, McManus, DD, Lessard, D, and Gore, J.M. Decade-Long trends (2001-2011) in the incidence and hospital death rates associated with the in-hospital development of cardiogenic shock after acute myocardial infarction. *Circ Cardiovasc Qual Outcomes*. 9:117–25. doi: 10.1161/CIRCOUTCOMES.115.002359

3. Van Diepen, S, Katz, JN, Albert, NM, Henry, TD, Jacobs, AK, Kapur, NK, et al. Contemporary management of cardiogenic shock: a scientific statement from the American Heart Association. *Circulation*. (2017) 136:e232–68. doi: 10.1161/CIR.0000000000000525

4. Kolte, D, Khera, S, Aronow, WS, Mujib, M, Palaniswamy, C, Sule, S, et al. Trends in incidence, management, and outcomes of cardiogenic shock complicating ST-elevation myocardial infarction in the United States. *J Am Heart Assoc*. (2014) 3:e000590. doi: 10.1161/JAHA.113.000590

5. Vahdatpour, C, Collins, D, and Goldberg, S. Cardiogenic shock. *J Am Heart Assoc*. 8:e011991. doi: 10.1161/JAHA.119.011991

6. Werdan, K, Gielen, S, Ebelt, H, and Hochman, JS. Mechanical circulatory support in cardiogenic shock. *Eur Heart J*. (2014) 35:156–67. doi: 10.1093/EURHEARTJ/EHT248

7. Iannaccone, M, Franchin, L, Hanson, ID, Boccuzzi, G, Basir, MB, Truesdell, AG, et al. Timing of impella placement in PCI for acute myocardial infarction complicated by cardiogenic shock: an updated meta-analysis. *Int J Cardiol*. (2022) 362:47–54. doi: 10.1016/J.IJCARD.2022.05.011

8. Basir, MB, Schreiber, TL, Grines, CL, Dixon, SR, Moses, JW, Maini, BS, et al. Effect of early initiation of mechanical circulatory support on survival in cardiogenic shock. *Am J Cardiol*. (2017) 119:845–51. doi: 10.1016/J.AMJCARD.2016.11.037

9. Ouweneel, DM, Eriksen, E, Sjauw, KD, van Dongen, IM, Hirsch, A, Packer, EJS, et al. Percutaneous mechanical circulatory support versus intra-aortic balloon pump in cardiogenic shock after acute myocardial infarction. *J Am Coll Cardiol*. (2017) 69:278–87. doi: 10.1016/J.JACC.2016.10.022

10. Fincke, R, Hochman, JS, Lowe, AM, Menon, V, Slater, JN, Webb, JG, et al. Cardiac power is the strongest hemodynamic correlate of mortality in cardiogenic shock: a report from the SHOCK trial registry. *J Am Coll Cardiol*. (2004) 44:340–8. doi: 10.1016/J.JACC.2004.03.060

11. O'Neill, WW, Kleiman, NS, Moses, J, Henriques, JPS, Dixon, S, Massaro, J, et al. A prospective, randomized clinical trial of hemodynamic support with Impella 2.5 versus intra-aortic balloon pump in patients undergoing high-risk percutaneous coronary intervention: the PROTECT II study. *Circulation*. (2012) 126:1717–27. doi: 10.1161/CIRCULATIONAHA.112.098194

12. Basir, MB, Schreiber, T, Dixon, S, Alaswad, K, Patel, K, Almany, S, et al. Feasibility of early mechanical circulatory support in acute myocardial infarction complicated by cardiogenic shock: the Detroit cardiogenic shock initiative. *Catheter Cardiovasc Interv*. (2018) 91:454–61. doi: 10.1002/CCD.27427

13. Ramzy, D, Soltesz, E, and Anderson, M. New surgical circulatory support system outcomes. *ASAIO J*. (2020) 66:746–52. doi: 10.1097/MAT.0000000000001194

14. Lang, RM, Badano, LP, Victor, MA, Afilalo, J, Armstrong, A, Ernande, L, et al. Recommendations for cardiac chamber quantification by echocardiography in adults: an update from the American Society of Echocardiography and the European Association of Cardiovascular Imaging. *J Am Soc Echocardiogr*. (2015) 28:1–39.e14. doi: 10.1016/J.ECHO.2014.10.003

15. Schäfer, A, Westenfeld, R, Sieweke, J-T, Zietzer, A, Wiora, J, Masiero, G, et al. Complete revascularisation in Impella-supported infarct-related cardiogenic shock patients is associated with improved mortality. *Front Cardiovasc Med*. (2021) 8:678748. doi: 10.3389/FCVM.2021.678748

16. Ouweneel, DM, Engstrom, AE, Sjauw, KD, Hirsch, A, Hill, JM, Gockel, B, et al. Experience from a randomized controlled trial with Impella 2.5 versus IABP in STEMI patients with cardiogenic pre-shock. Lessons learned from the IMPRESS in STEMI trial. *Int J Cardiol*. (2016) 202:894–6. doi: 10.1016/J.IJCARD.2015.10.063

17. Seyfarth, M, Sibbing, D, Bauer, I, Fröhlich, G, Bott-Flügel, L, Byrne, R, et al. A randomized clinical trial to evaluate the safety and efficacy of a percutaneous left ventricular assist device versus intra-aortic balloon pumping for treatment of cardiogenic shock caused by myocardial infarction. *J Am Coll Cardiol*. (2008) 52:1584–8. doi: 10.1016/J.JACC.2008.05.065

18. Ramzy, D, Anderson, M, Batsides, G, Ono, M, Silvestry, S, D'Alessandro, DA, et al. Early outcomes of the first 200 US patients treated with Impella 5.5: a novel temporary left ventricular assist device. *Innovations (Phila)*. (2021) 16:365–72. doi: 10.1177/15569845211013329

19. Naidu, SS, Baran, DA, Jentzer, JC, Hollenberg, SM, van Diepen, S, Basir, MB, et al. SCAI SHOCK stage classification expert consensus update: a review and incorporation of

validation studies: this statement was endorsed by the American College of Cardiology (ACC), American College of Emergency Physicians (ACEP), American Heart Association (AHA), European Society of Cardiology (ESC) Association for Acute Cardiovascular Care (ACVC), International Society for Heart and Lung Transplantation (ISHLT), Society of Critical Care Medicine (SCCM), and Society of Thoracic Surgeons (STS) in. *J Am Coll Cardiol*. (2022) 79:933–46. doi: 10.1016/J.JACC.2022.01.018

20. Baran, DA, Long, A, Badiye, AP, and Stelling, K. Prospective validation of the SCAI shock classification: single center analysis. *Catheter Cardiovasc Interv*. (2020) 96:1339–47. doi: 10.1002/CCD.29319

21. Schrage, B, Dabboura, S, Yan, I, Hilal, R, Neumann, JT, Sörensen, NA, et al. Application of the SCAI classification in a cohort of patients with cardiogenic shock. *Catheter Cardiovasc Interv*. (2020) 96:E213–9. doi: 10.1002/CCD.28707

22. Thiele, H, Zeymer, U, Neumann, FJ, Ferenc, M, Olbrich, HG, Hausleiter, J, et al. Intra-aortic balloon counterpulsation in acute myocardial infarction complicated by cardiogenic shock (IABP-SHOCK II): final 12 month results of a randomised, open-label trial. *Lancet (London, England)*. (2013) 382:1638–45. doi: 10.1016/S0140-6736(13)61783-3

23. Baldetti, L, Pagnesi, M, Gramegna, M, Belletti, A, Beneduce, A, Pazzanese, V, et al. Intra-aortic balloon pumping in acute decompensated heart failure with Hypoperfusion: from pathophysiology to clinical practice. *Circ Heart Fail*. (2021) 14:e008527. doi: 10.1161/CIRCHEARTFAILURE.121.008527

24. Morici, N, Marini, C, Sacco, A, Tavazzi, G, Saia, F, Palazzini, M, et al. Intra-aortic balloon pump for acute-on-chronic heart failure complicated by cardiogenic shock. *J Card Fail*. (2022) 28:1202–16. doi: 10.1016/J.CARDFAIL.2021.11.009

25. Khan, TM, and Siddiqui, AH (2022). Intra-aortic balloon pump. StatPearls. Available at: https://www.ncbi.nlm.nih.gov/books/NBK542233/ (Accessed November 3, 2022).

26. Scheidt, S, Wilner, G, Mueller, H, Summers, D, Lesch, M, Wolff, G, et al. Intra-aortic balloon counterpulsation in cardiogenic shock. Report of a co-operative clinical trial. *N Engl J Med*. (1973) 288:979–84. doi: 10.1056/NEJM197305102881901

27. Ranganath, NK, Nafday, HB, Zias, E, Hisamoto, K, Chen, S, Kon, ZN, et al. Concomitant temporary mechanical support in high-risk coronary artery bypass surgery. *J Card Surg*. (2019) 34:1569–72. doi: 10.1111/JOCS.14295

28. Masiello, P, Mastrogiovanni, G, Colombino, M, Cafarelli, F, Frunzo, F, Padula, M, et al. Impella-supported cardiac surgery. *Interv Cardiol*. (2020) 12:32–6. doi: 10.37532/FMIC.2020.12(2).650

29. Saito, S, Shibasaki, I, Matsuoka, T, Niitsuma, K, Hirota, S, Kanno, Y, et al. Impella support as a bridge to heart surgery in patients with cardiogenic shock. *Interact Cardiovasc Thorac Surg*. (2022) 35:ivac088. doi: 10.1093/ICVTS/IVAC088

30. Biancari, F, Dalén, M, Fiore, A, Ruggieri, VG, Saeed, D, Jónsson, K, et al. Multicenter study on postcardiotomy venoarterial extracorporeal membrane oxygenation. *J Thorac Cardiovasc Surg*. (2020) 159:1844–1854.e6. doi: 10.1016/J.JTCVS.2019.06.039

31. Frea, S, Pidello, S, Canavosio, FG, Bovolo, V, Botta, M, Bergerone, S, et al. Clinical assessment of hypoperfusion in acute heart failure – evergreen or antique? *Circ J*. (2015) 79:398–405. doi: 10.1253/CIRCJ.CJ-14-1052

32. Bertaina, M, Galluzzo, A, Rossello, X, Sbarra, P, Petitti, E, Prever, SB, et al. Prognostic implications of pulmonary artery catheter monitoring in patients with cardiogenic shock: a systematic review and meta-analysis of observational studies. *J Crit Care*. (2022) 69:154024. doi: 10.1016/J.JCRC.2022.154024

33. Hodgson, CL, Berney, S, Harrold, M, Saxena, M, and Bellomo, R. Clinical review: early patient mobilization in the ICU. *Crit Care*. (2013) 17:207. doi: 10.1186/CC11820

34. Shaw, TB, Blitzer, D, Carter, KT, Lirette, S, Mohammed, A, Copeland, J, et al. Functional status of heart transplant recipients predicts survival. *Clin Transpl*. (2022) 36:e14748. doi: 10.1111/CTR.14748

35. Colvin, M, Smith, JM, Ahn, Y, Skeans, MA, Messick, E, Bradbrook, K, et al. OPTN/SRTR 2020 annual data report: heart. *Am J Transplant*. (2022) 22:350–437. doi: 10.1111/AJT.16977

frontiers | Frontiers in Cardiovascular Medicine

TYPE Original Research
PUBLISHED 17 April 2023
DOI 10.3389/fcvm.2023.1121689

OPEN ACCESS

EDITED BY
Christos Bourantas,
Queen Mary University of London, United Kingdom

REVIEWED BY
Chunyan Ma,
The First Affiliated Hospital of China Medical University, China
Lijun Yuan,
Air Force Medical University, China

*CORRESPONDENCE
Yuman Li
✉ liym@hust.edu.cn
Mingxing Xie
✉ xiemx@hust.edu.cn

†These authors have contributed equally to this work

SPECIALTY SECTION
This article was submitted to Cardiovascular Imaging, a section of the journal Frontiers in Cardiovascular Medicine

RECEIVED 12 December 2022
ACCEPTED 29 March 2023
PUBLISHED 17 April 2023

CITATION
Zhou Y, Li H, Fang L, Wu W, Sun Z, Zhang Z, Liu M, Liu J, He L, Chen Y, Xie Y, Li Y and Xie M (2023) Biventricular longitudinal strain as a predictor of functional improvement after D-shant device implantation in patients with heart failure.
Front. Cardiovasc. Med. 10:1121689.
doi: 10.3389/fcvm.2023.1121689

Biventricular longitudinal strain as a predictor of functional improvement after D-shant device implantation in patients with heart failure

Yi Zhou[1,2,3†], He Li[1,2,3†], Lingyun Fang[1,2,3†], Wenqian Wu[1,2,3], Zhenxing Sun[1,2,3], Ziming Zhang[1,2,3], Manwei Liu[1,2,3], Jie Liu[1,2,3], Lin He[1,2,3], Yihan Chen[1,2,3], Yuji Xie[1,2,3], Yuman Li[1,2,3*] and Mingxing Xie[1,2,3*]

[1]Department of Ultrasound, Union Hospital, Tongji Medical College, Huazhong University of Science and Technology, Wuhan, China, [2]Clinical Research Center for Medical Imaging in Hubei Province, Wuhan, China, [3]Hubei Province Key Laboratory of Molecular Imaging, Wuhan, China

Background: The creation of an atrial shunt is a novel approach for the management of heart failure (HF), and there is a need for advanced methods for detection of cardiac function response to an interatrial shunt device. Ventricular longitudinal strain is a more sensitive marker of cardiac function than conventional echocardiographic parameters, but data on the value of longitudinal strain as a predictor of improvement in cardiac function after implantation of an interatrial shunt device are scarce. We aimed to investigate the exploratory efficacy of the D-Shant device for interatrial shunting in treating heart failure with reduced ejection fraction (HFrEF) and heart failure with preserved ejection fraction (HFpEF), and to explore the predictive value of biventricular longitudinal strain for functional improvement in such patients.

Methods: A total of 34 patients were enrolled (25 with HFrEF and 9 with HFpEF). All patients underwent conventional echocardiography and two-dimensional speckle tracking echocardiogram (2D-STE) at baseline and 6 months after implantation of a D-Shant device (WeiKe Medical Inc., WuHan, CN). Left ventricular global longitudinal strain (LVGLS) and right ventricular free wall longitudinal strain (RVFWLS) were evaluated by 2D-STE.

Results: The D-Shant device was successfully implanted in all cases without periprocedural mortality. At 6-month follow-up, an improvement in New York Heart Association (NYHA) functional class was observed in 20 of 28 patients with HF. Compared with baseline, patients with HFrEF showed significant reduced left atrial volume index (LAVI) and increased right atrial (RA) dimensions, as well as improved LVGLS and RVFWLS, at 6-month follow-up. Despite reduction in LAVI and increase in RA dimensions, improvements in biventricular longitudinal strain did not occur in HFpEF patients. Multivariate logistic regression demonstrated that LVGLS [odds ratio (OR): 5.930; 95% CI: 1.463–24.038; $P = 0.013$] and RVFWLS (OR: 4.852; 95% CI: 1.372–17.159; $P = 0.014$) were predictive of improvement in NYHA functional class after D-Shant device implantation.

Conclusion: Improvements in clinical and functional status are observed in patients with HF 6 months after implantation of a D-Shant device. Preoperative biventricular longitudinal strain is predictive of improvement in NYHA functional class and may be helpful to identify patients who will experience better outcomes following implantation of an interatrial shunt device.

KEYWORDS
HFpEF, HFrEF, D-Shant device, speckle-tracking echocardiography, NYHA functional class

Introduction

Heart failure (HF), whether it occurs with preserved ejection fraction (HFpEF; defined by a left ventricular ejection fraction [LVEF] ≥40%) or with reduced ejection fraction (HFrEF; defined by a LVEF <40%), remains a major public health care burden associated with substantial morbidity and mortality (1). Although HFpEF and HFrEF are heterogeneous with respect to etiology and pathophysiology, elevation of left atrial pressure (LAP) is the common mechanism precipitating worsening symptoms and acute decompensation (2–5). LA decompression, with the goal of limiting the increase in pulmonary venous pressure, may contribute to improved symptoms and outcomes in these patients (6). Percutaneously implanted permanent interatrial shunt devices have recently been developed for the treatment of patients with HF and have produced encouraging early clinical and hemodynamic results (7–12). Identification of quantitative predictors of the impact of an interatrial shunt device on cardiac functional recovery is crucial and may allow appropriate selection of patients. The clinical efficacy of advanced echocardiographic imaging, such as two-dimensional speckle tracking echocardiography (2D-STE), has been supported by various investigations. A number of studies from the past few years have shown that assessing global longitudinal strain may assist in refining the decision-making process in patients with HF (13–17). However, the clinical value of biventricular longitudinal strain, measured *via* 2D-STE, in HF patients following treatment with an interatrial shunt device has not been described. The objective of this study was to determine the exploratory efficacy of the D-Shant device (WeiKe Medical Inc., WuHan, CN) for treatment of patients with HFrEF and HFpEF, and to assess the predictive value of biventricular longitudinal strain in such patients.

Methods

Study population

A total of 34 patients with HFrEF and HFpEF were admitted to the Union Hospital, Tongji Medical College, Huazhong University of Science and Technology in 2020 and 2021. The study was approved by the Ethics Committee of Union Hospital Tongji Medical College, Huazhong University of Science and Technology (20200165). All patients provided written informed consent. The inclusion criteria were: HFpEF (LVEF ≥40%) or HFrEF (LVEF <40%); pulmonary capillary wedge pressure (PCWP) ≥15 mmHg at rest; and New York Heart Association (NYHA) functional class II–IV with chronic heart failure, still experiencing symptoms after at least 4 weeks of standardized drug treatment. The exclusion criteria were: moderate or greater right ventricular (RV) dysfunction; severe liver and kidney damage; recent history of surgery or severe trauma; autoimmune diseases or other serious systemic diseases.

Clinical data

Demographic characteristics, data from laboratory examinations, and comorbidities of the patients were obtained from electronic medical records. The hemodynamics of PCWP, mean right atrial pressure (RAP), and PCWP-RAP were measured using a fluid-filled balloon-tipped catheter. Exercise capacity was assessed using the 6-min walk test (6MWT). Functional status and quality of life were assessed by evaluation of NYHA functional class and administration of the Kansas City Cardiomyopathy Questionnaire (KCCQ).

Intervention

The procedures were performed under general anesthesia. Standard trans-septal puncture of the interatrial septum was carried out by fluoroscopy and transesophageal echocardiography (**Figure 1**). The delivery system was advanced *via* the wire into the LA, the left side of the D-Shant device was opened, and the delivery system was retracted to make contact with the septum on the LA side. The right half of the device was then placed into the right atrial side of the septum. The delivery system and guiding wire were then removed.

Transthoracic echocardiography

Transthoracic echocardiographic examinations were performed in all patients using the EPIQ 7C ultrasound system (Philips Medical Systems, Andover, Massachusetts) at baseline and 6 months after implantation of the D-Shant device. All echocardiographic images were acquired following published American Society of Echocardiography guidelines and analyzed by an experienced investigator who was blinded to the clinical characteristics of the study population. Echocardiographic indices were measured three times, and the mean value was used for the statistical analysis.

Conventional echocardiography analysis

Conventional echocardiographic parameters were measured following the guidelines of the American Society of Echocardiography (18). LV end-diastolic volume index (LVEDVI), LV end-systolic volume index (LVESVI), and LVEF

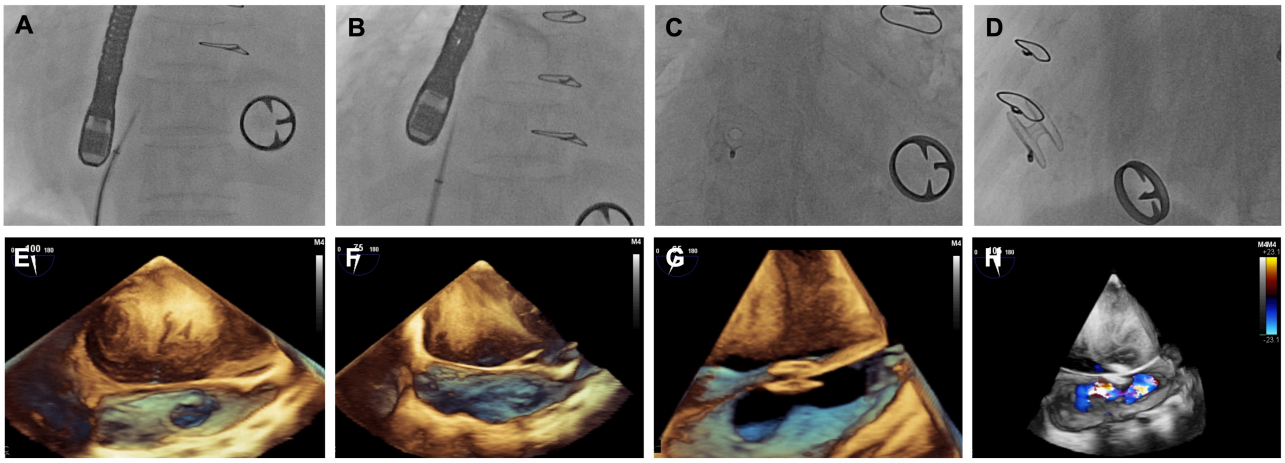

FIGURE 1
Images of D-shant device implantation. (**A**) x-ray and (**E**) transesophageal echocardiography (TEE) show the atrial septal position; (**B**) x-ray and (**F**) TEE guide atrial septal puncture; (**C**) x-ray and (**G**) TEE show release of the D-Shant device; and finally, (**D**) x-ray and (**H**) TEE color Doppler confirm the position of the D-Shant device and left-to-right shunting.

were measured using the biplane Simpson's method. Mitral inflow peak early diastolic velocity (E), peak late diastolic velocity (A), E/A ratio, septal and lateral mitral annular early diastolic velocities (e′), and the E/e′ ratio were used as indices of diastolic function. Multiple echocardiographic windows were employed to screen for tricuspid regurgitation and spectral Doppler velocity. Left atrial volume index (LAVI) was calculated using the area–length method (19) and indexed to body surface area. RA and RV dimensions were determined from the apical 4-chamber view. Tricuspid annulus plane systolic excursion (TAPSE) was measured as the systolic displacement of the tricuspid lateral annulus, as recorded on M-mode imaging. Right ventricular fractional area change (RVFAC) was calculated from the end-diastolic and end-systolic areas derived from the apical 4-chamber view. Tricuspid lateral annular systolic velocity (S′) was assessed using tissue Doppler imaging from the apical 4-chamber view. Finally, valvular regurgitation severity was graded qualitatively according to current recommendations: none/trace (grade 0), mild (grade I), moderate (grade II), or severe (grade III) (20).

2D-STE analysis

2D-STE analysis was conducted according to the recommendations of the American Society of Echocardiography and the European Association of Cardiovascular Imaging (21). Left ventricular global longitudinal strain (LVGLS) and right ventricular free wall longitudinal strain (RVFWLS) were measured using the 2D Auto Strain software package (Qlab13, Philips Healthcare, Andover, Massachusetts). The software tracked the endocardial borders of the left and right ventricles throughout the cardiac cycle, with manual modifications as needed. Images with low tracking quality were excluded. LVGLS was acquired by averaging three apical views (the apical 2-, 3-, and 4-chamber views). RVFWLS was calculated as the mean of the strain values in the three segments of the RV free wall. The average frame rate of the clips used for 2D-STE analysis was 50–70 frames/s.

Intra- and inter-observer reproducibility

Intra-observer and inter-observer reproducibility for the LVGLS and RVFWLS measurements obtained from 28 patients were assessed *via* calculation of intra-class correlation coefficients (ICCs) and Bland–Altman analysis. Intra-observer reproducibility was analyzed by having the same investigator repeat the biventricular longitudinal strain measurements. Inter-observer reproducibility was determined by comparison of measurements to those obtained by a second investigator who was blinded to the results of the first measurements.

Statistical analysis

Statistical analysis was performed using IBM SPSS Statistics version 26.0 (SPSS, Inc). Continuous data are reported in the form mean ± SD if normally distributed data or median (interquartile range) if non-normally distributed. Categorical data are reported in the form percentage (number) and were compared using the chi-square test or Fisher's exact test. Measurements of continuous variables obtained at baseline and 6 months after implantation were compared using the paired Student's *t*-test or the Wilcoxon signed rank test. An independent samples t-test or Mann–Whitney *U* test was used to compare the group who exhibited improvement in NYHA functional class and to the group who did not. Univariate and multivariate logistic regression analyses were performed to identify the predictors of improvement in NYHA functional class

6 months after device implantation. Univariate predictors with $P < 0.10$ were included in a multivariate logistic regression, which was used to determine the independent predictors. Receiver operating characteristic (ROC) curve analysis was used to identify the best parameters for prediction of improvement in NYHA functional class. The best cutoff value was based on the maximum Youden index. All statistical tests were two-sided, and a P value <0.05 was considered to represent statistical significance.

Results

Baseline characteristics

The clinical characteristics of patients with HFrEF and HFpEF at baseline are presented in Table 1. In total, 25 patients with HFrEF and 9 patients with HFpEF were enrolled. The mean age across all patients was 59 ± 11 years, and 18 patients (52.9%) were male. Among all 34 participants, 32 patients (94.1%) were categorized into NYHA functional class III or IV, and the average PCWP was 17.7 ± 4.7 mmHg. Hypertension was present in 7 patients, diabetes in 10 patients, coronary artery disease in 38.2% of patients, and a history of atrial fibrillation or flutter in 4 patients. There were no differences between the HFrEF and HFpEF groups in terms of age, sex, heart rate, systemic or diastolic arterial pressure, incidence of comorbidities (hypertension, diabetes, coronary artery disease, atrial fibrillation or flutter), NYHA functional class, level of hemoglobin, estimated glomerular filtration rate (eGFR), N-terminal pro-B type natriuretic peptide (NT-proBNP), or hemodynamics of the PCWP, RAP, or PCWP-RAP.

TABLE 1 Clinical characteristics of patients with HFrEF and HFpEF at baseline.

	Overall	HFrEF group ($n = 25$)	HFpEF group ($n = 9$)	P-value
Demographics				
Age, y	59 ± 11	59 ± 12	60 ± 11	0.730
Male	52.9% (18/34)	52.0% (13/25)	55.6% (5/9)	>0.999
BMI, kg/m^2	23.0 (20.4, 26.0)	22.7 (19.5, 25.6)	23.5 (21.9, 26.4)	0.140
SBP, mmHg	116 ± 22	115 ± 25	120 ± 10	0.489
DBP, mmHg	75 ± 10	73 ± 11	80 ± 6	0.072
HR, bpm	74 ± 14	74 ± 14	72 ± 15	0.565
Hypertension, % (n)	20.6% (7/34)	16.0% (4/25)	33.3% (3/9)	0.348
Diabetes, % (n)	29.4% (10/34)	32.0% (8/25)	22.2% (2/9)	0.692
Atrial fibrillation or flutter, % (n)	11.8% (4/34)	8.0% (2/25)	22.2% (2/9)	0.281
Coronary artery disease, % (n)	38.2% (13/34)	44.0% (11/25)	22.2% (2/9)	0.429
NYHA functional class				0.591
II	5.9% (2/34)	8.0% (2/25)	0.0% (0/9)	
III	76.5% (26/34)	76.0% (19/25)	77.8% (7/9)	
IV	17.6% (6/34)	16.0% (4/25)	22.2% (2/9)	
Laboratory data				
Hemoglobin, g/L	119.5 (106.0, 132.0)	116.0 (101.0, 131.5)	126.0 (110.5, 134.0)	0.298
eGFR, mL/min	80.1 (66.4, 99.3)	81.2 (66.3, 98.9)	75.6 (51.2, 102.9)	0.869
NT-proBNP, pg/mL	1675.4 (403.0, 3795.0)	2100.0 (490.5, 6215.0)	618.0 (358.4, 2005.0)	0.166
Hemodynamics				
PCWP, mmHg	17.7 ± 4.7	18.1 ± 5.2	16.7 ± 2.6	0.818
RAP, mmHg	4.0 (2.0, 7.0)	4.0 (2.0, 7.0)	5.0 (3.0, 5.5)	0.316
PCWP-RAP, mmHg	13.0 (11.0, 15.3)	13.0 (13.0, 17.5)	12.0 (11.5, 14.0)	>0.999

Values are presented in the form mean ± SD, % (n), or median (interquartile range). BMI, body mass index; SBP, systolic blood pressure; DBP, diastolic blood pressure; HR, heart rate; NYHA, New York Heart Association; eGFR, estimated glomerular filtration rate; NT-proBNP, N-terminal pro-B type natriuretic peptide; PCWP, pulmonary capillary wedge pressure; RAP, right atrial pressure.

Clinical and echocardiographic characteristics after implantation

Sizing specifications for the D-Shant device in each patient are shown in Supplementary Table S1. At 6 months after implantation, 5 patients with HFrEF and 1 patient with HFpEF were lost to follow up. Among the remaining patients, there were sustained improvements in NYHA functional class, with 5 patients (17.9%) now in NYHA functional class IV, 6 (21.4%) in NYHA functional class III, 16 (57.1%) in NYHA functional class II, and 1 [3.6%] in NYHA functional class I (Supplementary Figure S1A). Similarly, significant improvements in KCCQ score (32.1 ± 6.5 vs. 80.3 ± 6.6; $P < 0.001$) and 6 MWT results (333.0 ± 53.5 vs. 367.1 ± 74.3; $P < 0.001$) were observed across all patients (Supplementary Figures S1B,C). Table 2 presents the conventional echocardiographic and 2D-STE parameters at baseline and 6 months after implantation. Color flow Doppler imaging confirmed the presence of an interatrial left-to-right shunt at a follow-up visit. With the creation of a small left-to-right shunt, increased RA dimensions were observed among the HFrEF and HFpEF groups. At 6 months after device implantation, a significant reduction in LAVI was found only in the HFrEF group, whereas tricuspid S′, LVEDVI, LVESVI, LVEF, E/A, E/e′, TAPSE, and RVFAC did not differ from baseline values in either the HFrEF or the HFpEF group.

Compared with baseline measurements, significant improvements in LVGLS and RVFWLS were observed in the HFrEF group (LVGLS: −10.5 [−10.8, −10.2] vs. −14.3 [−14.5, −14.2], $P < 0.001$; RVFWLS: −15.5 [−15.6, −15.2] vs. −18.5 [−19.5, −18.0], $P < 0.001$) (Figure 2), but not in the HFpEF group.

Predictors of functional improvement after implantation of D-shant device

An improvement in NYHA functional class at 6 months after implantation of the D-Shant device was noted in 17 of 20 patients with HFrEF, and in 3 of 8 patients with HFpEF. The baseline echocardiographic characteristics of patients with and without functional improvements in NYHA functional class are shown in Table 3. Compared with patients who did not show

TABLE 2 Echocardiographic characteristics of patients with HFrEF and HFpEF at baseline and 6 months after D-shant device implantation.

Parameter	Overall			HFrEF group ($n = 20$)			HFpEF group ($n = 8$)		
	Baseline	6-month follow-up	*P*-value	Baseline	6-month follow-up	*P*-value	Baseline	6-month follow-up	*P*-value
Left heart									
LAVI, mL/m^2	52.8 (39.7, 72.0)	44.9 (30.2, 52.4)	0.009	51.5 (38.8, 79.4)	47.2 (30.2, 53.1)	0.005	53.3 (42.0, 55.4)	41.0 (29.6, 48.3)	0.161
E/A ratio	1.6 ± 1.1	1.5 ± 0.9	0.523	1.5 ± 1.0	1.2 ± 0.7	0.206	1.6 ± 1.0	1.3 ± 0.7	0.345
E/e′ ratio	12.7 ± 5.2	13.5 ± 5.2	0.641	14.2 ± 6.1	12.7 ± 5.1	0.197	10.5 ± 3.3	12.9 ± 3.7	0.263
Mitral regurgitation, % (n)			0.051			0.627			0.058
None/Trace	14.3% (4/28)	25.0% (7/28)		20.0% (4/20)	20.0% (4/20)		0.0% (0/8)	37.5% (3/8)	
Mild	17.9% (5/28)	17.9% (5/28)		15.0% (3/20)	15.0% (3/20)		25.0% (2/8)	25.0% (2/8)	
Moderate	32.1% (9/28)	39.3% (11/28)		25.0% (5/20)	45.0% (9/20)		50.0% (4/8)	25.0% (2/8)	
Severe	35.7% (10/28)	17.9% (5/28)		40.0% (8/20)	20.0% (4/20)		25.0% (2/8)	12.5% (1/8)	
LVEDVI, mL/m^2	103.7 ± 35.1	106.0 ± 43.7	0.811	121.5 ± 45.2	122.0 ± 50.0	0.938	77.4 ± 22.7	71.1 ± 15.3	0.161
LVESVI, mL/m^2	69.1 ± 30.0	69.5 ± 41.2	0.362	80.3 ± 28.5	77.6 ± 32.9	0.624	41.1 ± 15.2	38.0 ± 15.2	0.161
LVEF, %	34.5 (29.0, 39.7)	35.0 (28.5, 47.9)	0.733	30.2 (29.0, 35.0)	30.8 (26.6, 38.0)	0.072	47.0 (39.9, 51.2)	45.5 (37.3, 58.3)	0.484
LVGLS, %	−10.6 (−11.6, −10.3)	−14.3 (−14.5, −14.2)	<0.001	−10.5 (−10.8, −10.2)	−14.3 (−14.5, −14.2)	<0.001	−12.1 (−12.5, −10.5)	−14.2 (−14.4, −12.4)	0.161
Right heart									
RA dimension, mm	39.2 ± 7.6	43.9 ± 8.0	0. 002	40.1 ± 8.1	43.6 ± 8.1	0. 036	37.0 ± 6.0	44.6 ± 8.1	0.017
RV dimension, mm	39.2 ± 8.5	39.7 ± 7.5	0.346	38.7 ± 8.8	39.5 ± 7.0	0.657	40.4 ± 8.2	40.3 ± 9.1	0.865
Tricuspid regurgitation, % (n)			0.869			0.331			0.655
None/Trace	28.6% (8/28)	17.9% (5/28)		30.0% (6/20)	20.0% (4/20)		25.0% (2/8)	12.5% (1/8)	
Mild	25.7% (10/28)	46.4% (13/28)		40.0% (8/20)	45.0% (9/20)		25.0% (2/8)	50.0% (4/8)	
Moderate	10.7% (3/28)	17.9% (5/28)		5.0% (1/20)	15.0% (3/20)		25.0% (2/8)	25.0% (2/8)	
Severe	25.0% (7/28)	17.9% (5/28)		25.0% (5/20)	20.0% (4/20)		25.0% (2/8)	12.5% (1/8)	
S′ velocity, cm/s	6.0 (4.9, 6.8)	6.2 (5.0, 7.4)	0585	6.1 (4.9, 7.0)	5.8 (5.0, 7.4)	0.561	5.8 (4.8, 6.7)	6.4 (5.1, 8.0)	0.674
TAPSE, mm	17.0 ± 3.1	17.0 ± 2.9	0.652	16.8 ± 3.0	17.0 ± 3.0	0.059	18.0 ± 3.2	17.0 ± 3.4	0.222
RVFAC, %	40.5 ± 11.6	39.0 ± 10.3	0.425	37.7 ± 12.4	38.3 ± 10.4	0.102	46.5 ± 10.3	43.6 ± 6.7	0.263
RVFWLS, %	−15.6 (−17.0, −15.4)	−18.8 (−19.8, −17.9)	<0.001	−15.5 (−15.6, −15.2)	−18.5 (−19.5, −18.0)	<0.001	−17.4 (−17.5, −17.1)	−21.7 (−23.6, −16.3)	0.063

Values are presented in the form mean ± SD, % (n), or median (interquartile range). LAVI, left atrial volume index; E, mitral inflow peak early diastolic velocity; A, peak late diastolic velocity; e′, septal and lateral mitral annular early diastolic velocities; LVEDVI, left ventricular end-diastolic volume index; LVESVI, left ventricular end-systolic volume index; LVEF, left ventricular ejection fraction; LVGLS, left ventricular global longitudinal strain; RA, right atrial; RV, right ventricular; S′, tricuspid lateral annular systolic velocity; RVFAC, right ventricular fractional area change; TAPSE, tricuspid annulus plane systolic excursion; RVFWLS, right ventricular free wall longitudinal strain.

improvement in NYHA functional class, those who did show improvement exhibited lower absolute values of LVGLS and RVFWLS at baseline (Figure 3). However, LAVI, LVEDVI, LVESVI, LVEF, E/A, E/e′, RA and RV dimensions, tricuspid S′, TAPSE, RVFAC, and degree of mitral and tricuspid regurgitation did not differ between the two groups.

To investigate the predictors of improvement in NYHA functional class, we performed univariate and multivariate analyses (Table 4). Univariate logistic regression analysis showed that 6 MWT score [odds ratio (OR): 1.025; 95% CI: 1.003–1.047; $P = 0.028$], LVGLS (OR: 5.788; 95% CI: 1.673–20.029; $P = 0.006$), RVFAC (OR: 4.300; 95% CI: 1.427–12.955; $P = 0.010$), and RVFWLS (OR: 2.640; 95% CI: 1.464–4.762; $P = 0.001$) were predictors of improvement in NYHA functional class at 6-month follow-up after device implantation among all patients with HF. In contrast, age, gender, NT-proBNP, PCWP, LAVI, LVEF, RA and RV dimensions, and TAPSE were not predictive of NYHA functional class improvement. In multivariate models, 6 MWT score and KCCQ score continued to be of prognostic value. LVGLS (OR: 5.930; 95% CI: 1.463–24.038; $P = 0.013$) and RVFWLS (OR: 4.852; 95% CI: 1.372–17.159; $P = 0.014$) were associated with improvement in NYHA functional class.

ROC curve analysis of these variables for use in prediction of improvement in NYHA functional class showed that LVGLS (area under the curve: 0.83) and RVFWLS (area under the curve: 0.81) were associated with NYHA functional class improvement at 6 months after implantation (Figure 4). The optimal cutoff value for LVGLS for prediction of this outcome was −12.15%, with sensitivity of 100% and specificity of 63%; the best cutoff value for RVFWLS was −17.25% (sensitivity: 100%; specificity: 63%).

Reproducibility

Intra-observer and inter-observer reproducibility are shown in Table 5. The inter-observer and intra-observer ICCs for LVGLS and RVFWLS were all greater than 0.90, indicating that both parameters exhibited excellent reproducibility. Inter-observer and

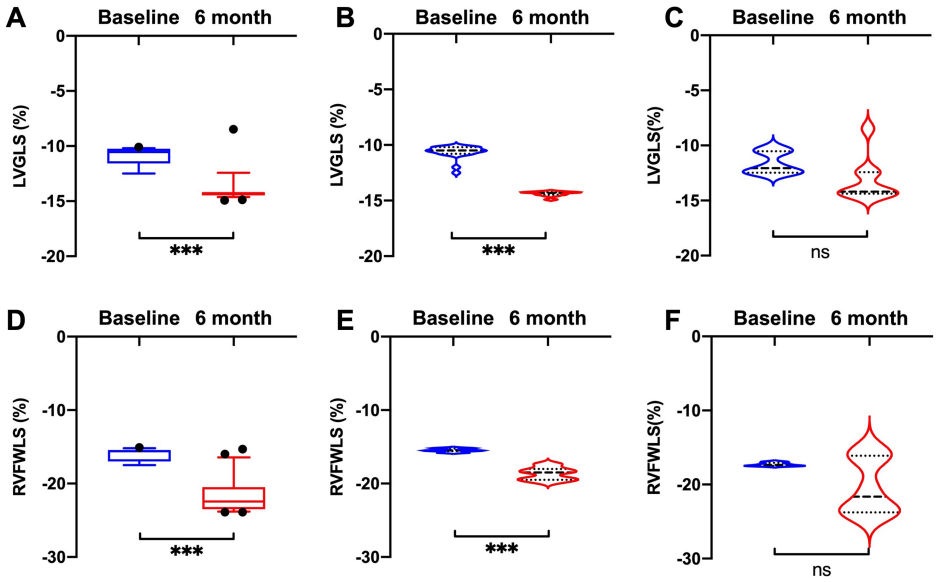

FIGURE 2
Comparisons of LVGLS and RVFWLS values at baseline and 6 months after D-shant device implantation. (**A**) LVGLS and (**D**) RVFWLS in all patients; (**B**) LVGLS and (**E**) RVFWLS in patients with HFrEF; and (**C**) LVGLS and (**F**) RVFWLS in patients with HFpEF. HFpEF, heart failure with preserved ejection fraction; HFrEF, heart failure with reduced ejection fraction; LVGLS, left ventricular global longitudinal strain; RVFWLS, right ventricular free wall longitudinal strain.

intra-observer agreement for LVGLS and RVFWLS were high, as reflected by the small bias values and narrow limits of agreement.

Discussion

This study indicated that preoperative LVGLS and RVFWLS are associated with improvement in the NYHA functional class of patients 6 months after implantation of an interatrial shunt device. Specifically, patients who experienced improvement in their NYHA functional class had lower absolute values of LVGLS and RVFWLS. The significance of these findings is that they suggest these novel parameters could be useful in selecting appropriate patients for atrial shunt device implantation. This could have a significant impact on clinical decision-making, as doctors may now be able to use LVGLS and RVFWLS values to identify patients who are more likely to benefit from this intervention. Additionally, the ability to predict which patients may experience functional improvement following the procedure could help doctors to counsel patients more effectively on the potential benefits and risks of atrial shunt device implantation. Overall, this study contributes new knowledge to the field and has the potential to positively impact patient outcomes.

A significant reduction in LAVI was observed in the HFrEF group at 6-month follow-up, suggesting an adaptive change in LA volume in response to the interatrial shunt device. Previous studies have indicated that LA volume is a predictor of cardiac adverse events in HF patients (22, 23). In addition, an increase in RA size was noted in our study, which could represent an effect of the shunting itself or reflect an increase in circulating volume. These findings were in line with those obtained for the Corvia IASD, which has been shown to be associated with significant enlargement in RA volume at 6 months (9).

Consistent with previous work (10, 24), there was evidence of alleviation of symptoms and improved quality of life at 6-month follow-up. Improvement in NYHA functional class was observed in 85.0% of patients (17/20) with HFrEF, which is in accordance with previous reports (17, 24). In contrast, 62.5% (5/8) of patients with HFpEF were unchanged in terms of NYHA functional class at 6-month follow-up. Similarly to this finding, the REDUCE LAP-HF I trial indicated no significant improvement in NYHA functional class in patients with HFpEF after interatrial shunt device implantation (25). Plausible explanations might be greater myocardial damage and pulmonary disease (9), and further research is warranted to systematically test these results.

2D-STE allows for the semiautomated quantification of myocardial mechanics and helps to refine the decision-making process in patients with HF. However, evidence on the clinical implications of 2D-STE measurements in patients with interatrial shunt device implantation is scarce. Our study has revealed the differentiation in changes in ventricular function response to interatrial shunt device implantation between patients with HFrEF and those with HFpEF. Improvements in LVGLS and RVFWLS were identified in HFrEF patients, but not in the HFpEF group. In patients with HFrEF, LV unloading caused by device implantation could account for the higher value of LVGLS at follow-up (26). Similarly, the greater RVFWLS after implantation of the device can be attributed to compensatory "overwork" of the RV myocardium, owing to the large preload reserve of the RV and pulmonary vascular reserve (27). Patients with HFpEF frequently have biventricular components to their

TABLE 3 Baseline echocardiographic characteristics in patients who did and did not undergo improvement in NYHA functional class after D-shant device implantation.

Parameter	Patients with improvement in NYHA functional class ($n = 20$)	Patients without improvement in NYHA functional class ($n = 8$)	*P*-value
Left heart			
LAVI, mL/m^2	53.1 (41.0, 81.0)	46.6 (33.1, 55.3)	0.237
LVEDVI, mL/m^2	106.9 ± 32.0	95.8 ± 43.3	0.354
LVESVI, mL/m^2	72.9 ± 27.9	59.6 ± 34.8	0.218
LVEF, %	32.7 (29.0, 37.5)	39.5 (30.5, 44.3)	0.123
E/A ratio	1.7 ± 1.2	1.3 ± 0.9	0.262
E/e′ ratio	13.7 ± 5.2	10.2 ± 4.5	0.123
Mitral regurgitation, % (*n*)			0.202
None/Trace	20.0% (4/20)	0.0% (0/8)	
Mild	10.0% (2/20)	37.5% (3/8)	
Moderate	35.0% (7/20)	25.0% (2/8)	
Severe	35.0% (7/20)	37.5% (3/8)	
LVGLS, %	−10.5 (−10.8, −10.2)	−12.4 (−12.5, −10.5)	0.006
Right heart			
RA dimension, mm	40.2 ± 8.1	36.8 ± 5.8	0.237
RV dimension, mm	40.0 ± 9.5	37.1 ± 5.2	0.566
S′ velocity, cm/s	6.0 (4.8, 7.0)	6.1 (5.2, 6.7)	0.862
TAPSE, mm	17.0 ± 3.2	17.1 ± 3.0	0.980
RVFAC, %	37.9 ± 11.6	46.9 ± 9.5	0.070
Tricuspid regurgitation, % (*n*)			0.743
None/Trace	20.0% (4/20)	50.0% (4/8)	
Mild	40.0% (8/20)	25.0% (2/8)	
Moderate	10.0% (2/20)	12.5% (1/8)	
Severe	30.0% (6/20)	12.5% (1/8)	
RVFWLS, %	−15.5 (−15.8, −15.2)	−17.4 (−17.5, −15.5)	0.010

Values are presented in the form mean ± SD, % (*n*), or median (interquartile range). LAVI, left atrial volume index; E, mitral inflow peak early diastolic velocity; A, peak late diastolic velocity; e′, septal and lateral mitral annular early diastolic velocities; LVEDVI, left ventricular end-diastolic volume index; LVESVI, left ventricular end-systolic volume index; LVEF, left ventricular ejection fraction; LVGLS, left ventricular global longitudinal strain; RA, right atrial; RV, right ventricular; S′, tricuspid lateral annular systolic velocity; RVFAC, right ventricular fractional area change; TAPSE, tricuspid annulus plane systolic excursion; RVFWLS, right ventricular free wall longitudinal strain.

cardiomyopathy and virtually always have abnormalities in pulmonary arterial capacitance and some degree of pulmonary vascular remodeling (12, 28, 29), rendering them more sensitive to even minor degrees of RV volume overload. Our findings are novel in that we have identified LVGLS and RVFWLS as predictors of improvement in NYHA functional class after interatrial shunt device implantation. Elshafey et al. have recently documented the significant correlation of LVGLS with NYHA functional class among patients with HFrEF (30). Another study has found that LV segmental longitudinal strain could be a predictor of recovery of cardiac function in patients with reduced LVEF (15). In our cohort, biventricular systolic myocardial deformation may have been associated with recovery of cardiac function after D-Shant device implantation. Myocardial systolic strain has been linked to serum levels of aminoterminal propeptide of procollagen I/III and tissue inhibitor of matrix metalloproteinase-1, both of which are indicators of cardiac fibrosis (31). Biventricular longitudinal strain may prove to be a noninvasive surrogate measure for prediction of NYHA functional class improvement in patients who undergo interatrial shunt device implantation. Although this study suggests an association between biventricular longitudinal strain and recovery of cardiac function, the results should be further tested in a large cohort of patients with HF.

Limitations

Because of the strict exclusion criteria and the fact that this was a small single-center study, the sample size was small. We were unable to include several clinical variables (e.g., cardiovascular diseases, RAP, and PCWP-RAP) in the model due to the small number of cases, which raises the possibility of model overfit. As a result, we were unable to modify our model fully. The current study should be viewed as a proof of concept, and larger multicenter investigations are needed. Additionally, invasive right heart catheterization was not performed in our cohort of patients

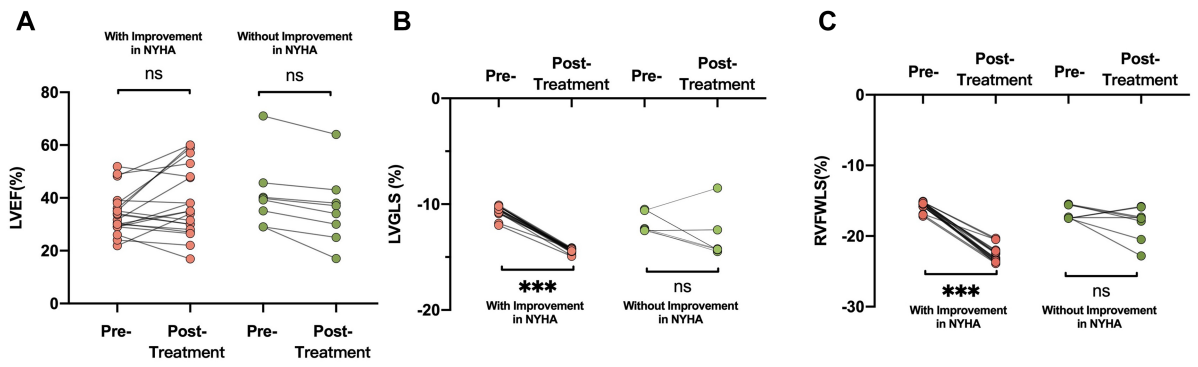

FIGURE 3
Comparisons of (A) LVEF, (B) LVGLS, and (C) RVFWLS in patients who did and did not undergo improvement in NYHA functional class after D-shant device implantation. LVEF, left ventricular ejection fraction; NYHA, New York Heart Association; LVGLS, left ventricular global longitudinal strain; RVFWLS, right ventricular free wall longitudinal strain.

TABLE 4 Univariate and multivariate analyses of factors associated with improvement in NYHA functional class after D-shant device implantation.

	Univariate		Model 1 6 WMT + KCCQ + LVGLS		Model 2 6 WMT + KCCQ + RVFWLS + RVFAC	
	OR (95% CI)	*P*-value	OR (95% CI)	*P*-value	OR (95% CI)	*P*–value
Age	0.920 (0.833–1.016)	0.101				
Gender	0.600 (0.112–3.214)	0.551				
NT-proBNP	1.000 (1.000–1.000)	0.331				
6 MWT	1.025 (1.003–1.047)	0.028	1.023 (1.001–1.046)	0.041		0.254
KCCQ	1.150 (0.999–1.323)	0.052		0.102	1.156 (1.005–1.330)	0.043
PCWP	1.561 (0.913–2.669)	0.104				
LAVI	1.040 (0.990–1.093)	0.117				
LVEF	0.932 (0.850–1.021)	0.128				
LVGLS	5.788 (1.673–20.029)	0.006	5.930 (1.463–24.038)	0.013		
RA dimension	2.073 (0.548–7.846)	0.283				
RV dimension	1.579 (0.535–4.661)	0.408				
TAPSE	0.985 (0.752–1.292)	0.915				
RVFAC	4.300 (1.427–12.955)	0.010				0.074
RVFWLS	2.640 (1.464–4.762)	0.001			4.852 (1.372–17.159)	0.014

Odds ratios are presented with 95% CIs.
LAVI, left atrial volume index; LVEF, left ventricular ejection fraction; LVGLS, left ventricular global longitudinal strain; RA, right atrial; RV, right ventricular; RVFAC, right ventricular fractional area change; TAPSE, tricuspid annulus plane systolic excursion; RVFWLS, right ventricular free wall longitudinal strain; PCWP, pulmonary capillary wedge pressure; NT-proBNP, N-terminal pro-B type natriuretic peptide; 6 MWT, 6-min walk test; KCCQ, Kansas City Cardiomyopathy Questionnaire.

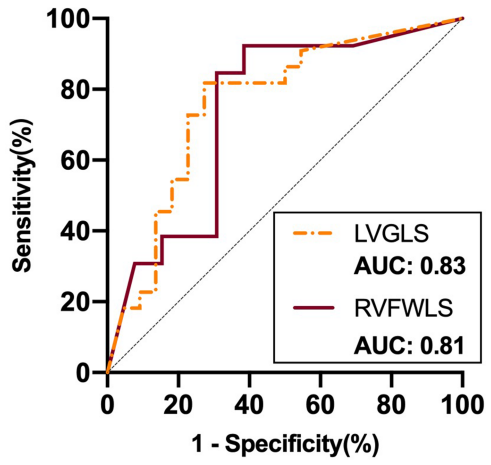

FIGURE 4
ROC curve analysis of STE parameters as predictors of improvement in NYHA functional class after D-shant device implantation. ROC, receiver-operating characteristic; NYHA, New York Heart Association; LVGLS, left ventricular global longitudinal strain; RVFWLS, right ventricular free wall longitudinal strain.

TABLE 5 The reproducibility of LVGLS and RVFWLS measurements.

	ICC (95% CI)	Bias	Limits of agreement
Intra-observer			
LVGLS, %	0.89 (0.82–0.93)	−0.07	−4.07–3.92
RVFWLS, %	0.99 (9.6–0.10)	−0.29	−1.16–0.58
Inter-observer			
LVGLS, %	0.92 (0.87–0.95)	−0.14	−3.43–3.16
RVFWLS, %	0.99 (9.7–1.00)	−0.27	−1.12–0.66

CI, confidence interval; LVGLS, left ventricular global longitudinal strain; ICC, intraclass correlation coefficient; RVFWLS, right ventricular free wall longitudinal strain.

at 6-month follow-up. Although our results indicated biventricular longitudinal strain on echocardiography to be a valuable predictor of NYHA functional class improvement after interatrial shunt device implantation among patients with HFrEF and HFpEF, the diagnostic utility of strain cutoffs as noninvasive markers was not provided owing to the small sample size. Future research is warranted to test this issue, as well as the relative clinical utility of biventricular longitudinal strain in larger-scale epidemiological cohorts.

Conclusions

The findings of this study suggest that biventricular longitudinal strain can be used as a non-invasive surrogate measure for prediction of recovery of cardiac function after implantation of a D-Shant device. This information may have a significant impact on clinical decision-making by enabling physicians to identify patients who are likely to benefit from the device and to make more informed decisions regarding atrial shunt device implantation.

Overall, this study has the potential to improve patient outcomes and reduce morbidity and mortality in heart failure patients, making it a valuable contribution to the field of cardiology.

Data availability statement

The original contributions presented in the study are included in the article/**Supplementary Material**, further inquiries can be directed to the corresponding author/s.

Ethics statement

The studies involving human participants were reviewed and approved by the Ethics Committee of Wuhan Union Hospital [2020 No.(0165)]. The patients/participants provided their written informed consent to participate in this study.

Author contributions

All of the authors named have made a significant, direct, and intellectual contribution to the work and have given their permission for it to be published. All authors contributed to the article and approved the submitted version.

Funding

This work was supported by the National Natural Science Foundation of China (Grant Nos. 82230066, 82001854, 82001852), the Key Research and Development Program of Hubei (2020DCD015, 2021BCA138), and the National Natural Science Foundation of Hubei province (No. 2020CFB781).

Conflict of interest

The authors declare that the research was conducted in the absence of any commercial or financial relationships that could be construed as a potential conflict of interest.

Publisher's note

Supplementary material

The Supplementary Material for this article can be found online at: https://www.frontiersin.org/articles/10.3389/fcvm.2023.1121689/full#supplementary-material.

References

1. Owan TE, Hodge DO, Herges RM, Jacobsen SJ, Roger VL, Redfield MM, et al. Trends in prevalence and outcome of heart failure with preserved ejection fraction. *N Engl J Med*. (2006) 355:251–9. doi: 10.1056/NEJMoa052256

2. Zile MR, Baicu CF, Gaasch WH. Diastolic heart failure–abnormalities in active relaxation and passive stiffness of the left ventricle. *N Engl J Med*. (2004) 350:1953–9. doi: 10.1056/NEJMoa032566

3. Abraham WT, Adamson PB, Bourge RC, Aaron MF, Costanzo MR, Stevenson LW, et al. Wireless pulmonary artery haemodynamic monitoring in chronic heart failure: a randomised controlled trial. *Lancet*. (2011) 377:658–66. doi: 10.1016/s0140-6736(11)60101-3

4. Carson PE, Anand IS, Win S, Rector T, Haass M, Lopez-Sendon J, et al. The hospitalization burden and post-hospitalization mortality risk in heart failure with preserved ejection fraction: results from the I-PRESERVE trial (irbesartan in heart failure and preserved ejection fraction). *JACC Heart Fail*. (2015) 3:429–41. doi: 10.1016/j.jchf.2014.12.017

5. Redfield MM. Heart failure with preserved ejection fraction. *N Engl J Med*. (2016) 375:1868–77. doi: 10.1056/NEJMcp1511175

6. Sambhi MP, Zimmerman HA. Pathologic physiology of lutembacher syndrome. *Am J Cardiol*. (1958) 2:681–6. doi: 10.1016/0002-9149(58)90264-9

7. Del Trigo M, Bergeron S, Bernier M, Amat-Santos IJ, Puri R, Campelo-Parada F, et al. Unidirectional left-to-right interatrial shunting for treatment of patients with heart failure with reduced ejection fraction: a safety and proof-of-principle cohort study. *Lancet*. (2016) 387:1290–7. doi: 10.1016/s0140-6736(16)00585-7

8. Feldman T, Komtebedde J, Burkhoff D, Massaro J, Maurer MS, Leon MB, et al. Transcatheter interatrial shunt device for the treatment of heart failure: rationale and design of the randomized trial to REDUCE elevated left atrial pressure in heart failure (REDUCE LAP-HF I). *Circ Heart Fail*. (2016) 9:e003025. doi: 10.1161/circheartfailure.116.003025

9. Hasenfuß G, Hayward C, Burkhoff D, Silvestry FE, McKenzie S, Gustafsson F, et al. A transcatheter intracardiac shunt device for heart failure with preserved ejection fraction (REDUCE LAP-HF): a multicentre, open-label, single-arm, phase 1 trial. *Lancet*. (2016) 387:1298–304. doi: 10.1016/s0140-6736(16)00704-2

10. Rodés-Cabau J, Bernier M, Amat-Santos IJ, Ben Gal T, Nombela-Franco L, García Del Blanco B, et al. Interatrial shunting for heart failure: early and late results from the first-in-human experience with the V-wave system. *JACC Cardiovasc Interv*. (2018) 11:2300–10. doi: 10.1016/j.jcin.2018.07.001

11. Shang X, Zhang C, Chen S, Chen S, Wang X, Wang B, et al.. Early animal experimental study of atrial shunt device D-shant. *Chin J Intervent Cardiol*. (2020) 28:6. doi: 10.3969/j.issn.1004-8812.2020.06.006

12. Shah SJ, Borlaug BA, Chung ES, Cutlip DE, Debonnaire P, Fail PS, et al. Atrial shunt device for heart failure with preserved and mildly reduced ejection fraction (REDUCE LAP-HF II): a randomised, multicentre, blinded, sham-controlled trial. *Lancet*. (2022) 399:1130–40. doi: 10.1016/s0140-6736(22)00016-2

13. Kaneko A, Tanaka H, Onishi T, Ryo K, Matsumoto K, Okita Y, et al. Subendocardial dysfunction in patients with chronic severe aortic regurgitation and preserved ejection fraction detected with speckle-tracking strain imaging and transmural myocardial strain profile. *Eur Heart J Cardiovasc Imaging*. (2013) 14:339–46. doi: 10.1093/ehjci/jes160

14. Park JH, Kusunose K, Kwon DH, Park MM, Erzurum SC, Thomas JD, et al. Relationship between right ventricular longitudinal strain, invasive hemodynamics, and functional assessment in pulmonary arterial hypertension. *Korean Circ J*. (2015) 45:398–407. doi: 10.4070/kcj.2015.45.5.398

15. Kusunose K, Torii Y, Yamada H, Nishio S, Hirata Y, Seno H, et al. Clinical utility of longitudinal strain to predict functional recovery in patients with tachyarrhythmia and reduced LVEF. *JACC Cardiovasc Imaging*. (2017) 10:118–26. doi: 10.1016/j.jcmg.2016.03.019

16. Morris DA, Krisper M, Nakatani S, Köhncke C, Otsuji Y, Belyavskiy E, et al. Normal range and usefulness of right ventricular systolic strain to detect subtle right ventricular systolic abnormalities in patients with heart failure: a multicentre study. *Eur Heart J Cardiovasc Imaging*. (2017) 18:212–23. doi: 10.1093/ehjci/jew011

17. Moon MG, Hwang IC, Lee HJ, Kim SH, Yoon YE, Park JB, et al. Reverse remodeling assessed by left atrial and ventricular strain reflects treatment response to sacubitril/valsartan. *JACC Cardiovasc Imaging*. (2022) 15:1525–41. doi: 10.1016/j.jcmg.2022.03.019

18. Rudski LG, Lai WW, Afilalo J, Hua L, Handschumacher MD, Chandrasekaran K, et al. Guidelines for the echocardiographic assessment of the right heart in adults: a report from the American society of echocardiography endorsed by the European association of echocardiography, a registered branch of the European society of cardiology, and the Canadian society of echocardiography. *J Am Soc Echocardiogr*. (2010) 23:685–713. doi: 10.1016/j.echo.2010.05.010

19. Lopez L, Colan SD, Frommelt PC, Ensing GJ, Kendall K, Younoszai AK, et al. Recommendations for quantification methods during the performance of a pediatric echocardiogram: a report from the pediatric measurements writing group of the American society of echocardiography pediatric and congenital heart disease

council. *J Am Soc Echocardiogr*. (2010) 23:465–95; quiz 576–467. doi: 10.1016/j.echo.2010.03.019

20. Zoghbi WA, Enriquez-Sarano M, Foster E, Grayburn PA, Kraft CD, Levine RA, et al. Recommendations for evaluation of the severity of native valvular regurgitation with two-dimensional and Doppler echocardiography. *J Am Soc Echocardiogr*. (2003) 16:777–802. doi: 10.1016/S0894-7317(03)00335-3

21. Mor-Avi V, Lang RM, Badano LP, Belohlavek M, Cardim NM, Derumeaux G, et al. Current and evolving echocardiographic techniques for the quantitative evaluation of cardiac mechanics: aSE/EAE consensus statement on methodology and indications. *J Am Soc Echocardiogr*. (2011) 24:277–313. doi: 10.1016/j.echo.2011.01.015

22. Takemoto Y, Barnes ME, Seward JB, Lester SJ, Appleton CA, Gersh BJ, et al. Usefulness of left atrial volume in predicting first congestive heart failure in patients > or=65 years of age with well-preserved left ventricular systolic function. *Am J Cardiol*. (2005) 96:832–6. doi: 10.1016/j.amjcard.2005.05.031

23. Abhayaratna WP, Fatema K, Barnes ME, Seward JB, Gersh BJ, Bailey KR, et al. Left atrial reservoir function as a potent marker for first atrial fibrillation or flutter in persons > or=65 years of age. *Am J Cardiol*. (2008) 101:1626–9. doi: 10.1016/j.amjcard.2008.01.051

24. Paitazoglou C, Özdemir R, Pfister R, Bergmann MW, Bartunek J, Kilic T, et al. The AFR-PRELIEVE trial: a prospective, non-randomised, pilot study to assess the atrial flow regulator (AFR) in heart failure patients with either preserved or reduced ejection fraction. *EuroIntervention*. (2019) 15:403–10. doi: 10.4244/eij-d-19-00342

25. Feldman T, Mauri L, Kahwash R, Litwin S, Ricciardi MJ, van der Harst P, et al. Transcatheter interatrial shunt device for the treatment of heart failure with preserved ejection fraction [REDUCE LAP-HF I (reduce elevated left atrial pressure in patients with heart failure)]: a phase 2, randomized, sham-controlled trial. *Circulation*. (2018) 137:364–75. doi: 10.1161/circulationaha.117.032094

26. Burns AT, La Gerche A, D'hooge J, MacIsaac AI, Prior DL. Left ventricular strain and strain rate: characterization of the effect of load in human subjects. *Eur J Echocardiogr*. (2010) 11:283–9. doi: 10.1093/ejechocard/jep214

27. Eyskens B, Ganame J, Claus P, Boshoff D, Gewillig M, Mertens L. Ultrasonic strain rate and strain imaging of the right ventricle in children before and after percutaneous closure of an atrial septal defect. *J Am Soc Echocardiogr*. (2006) 19:994–1000. doi: 10.1016/j.echo.2006.02.001

28. Shah SJ, Kitzman DW, Borlaug BA, van Heerebeek L, Zile MR, Kass DA, et al. Phenotype-specific treatment of heart failure with preserved ejection fraction: a multiorgan roadmap. *Circulation*. (2016) 134:73–90. doi: 10.1161/circulationaha.116.021884

29. Simmonds SJ, Cuijpers I, Heymans S, Jones EAV. Cellular and molecular differences between HFpEF and HFrEF: a step ahead in an improved pathological understanding. *Cells*. (2020) 9:242. doi: 10.3390/cells9010242

30. Elshafey WEH, Al Khoufi EA, Elmelegy EK. Effects of sacubitril/valsartan treatment on left ventricular myocardial torsion mechanics in patients with heart failure reduced ejection fraction 2D speckle tracking echocardiography. *J Cardiovasc Echogr*. (2021) 31:59–67. doi: 10.4103/jcecho.jcecho_118_20

31. Kang SJ, Lim HS, Choi BJ, Choi SY, Hwang GS, Yoon MH, et al. Longitudinal strain and torsion assessed by two-dimensional speckle tracking correlate with the serum level of tissue inhibitor of matrix metalloproteinase-1, a marker of myocardial fibrosis, in patients with hypertension. *J Am Soc Echocardiogr*. (2008) 21:907–11. doi: 10.1016/j.echo.2008.01.015

frontiers | Frontiers in Cardiovascular Medicine

TYPE Brief Research Report
PUBLISHED 28 April 2023
DOI 10.3389/fcvm.2023.1143886

OPEN ACCESS

EDITED BY
Tomasz Zieliński,
National Institute of Cardiology, Poland

REVIEWED BY
Peter Lee,
Brown University, United States
Philippe Menasché,
Assistance Publique Hopitaux De Paris, France

*CORRESPONDENCE
Esko Kankuri
✉ esko.kankuri@helsinki.fi

RECEIVED 13 January 2023
ACCEPTED 10 April 2023
PUBLISHED 28 April 2023

CITATION
Schmitto JD, Kuuva A, Kronström K, Hanke JS and Kankuri E (2023) Use of left atrial appendage as an autologous tissue source for epicardial micrograft transplantation during LVAD implantation.
Front. Cardiovasc. Med. 10:1143886.
doi: 10.3389/fcvm.2023.1143886

Use of left atrial appendage as an autologous tissue source for epicardial micrograft transplantation during LVAD implantation

Jan D. Schmitto[1], Aleksi Kuuva[2], Kai Kronström[2,3], Jasmin S. Hanke[1] and Esko Kankuri[4]*

[1]Department of Cardiac-, Thoracic-, Transplantation and Vascular Surgery, Hannover Medical School, Hannover, Germany, [2]EpiHeart Oy, Helsinki, Finland, [3]Department of Neuroscience and Biomedical Engineering, Aalto University, Espoo, Finland, [4]Department of Pharmacology, Faculty of Medicine, University of Helsinki, Helsinki, Finland

We report here the first clinical use of the left atrial appendage (LAA) for epicardial micrograft transplantation during left ventricular assist device (LVAD) implantation. Previously, a sample from the right atrial appendage (RAA) has been available for processing and administering micrograft therapy in cardiac surgery. Both LAA and RAA are rich sources of various types of myocardial cells and are capable of providing both paracrine and cellular support to the failing myocardium. The surgical approach of LAA micrografting facilitates epicardial micrograft therapy dose escalation and treatment of larger myocardial areas than done previously. Moreover, as collection of treated vs. untreated tissues from the recipient heart is possible following LVAD implantation at the time of heart transplantation, the evaluation of the therapy's mechanism of action can be further deciphered at cellular and molecular levels. This LAA modification of the epicardial micrografting technique has the overall potential to facilitate the adoption of cardiac cell therapy during heart surgery.

KEYWORDS

autologous cardiac micrografts, cell therapy, epicardial transplantation, left ventricular assist device (LVAD), left atrial appendage (LAA), heart failure

Introduction

Myocardial recovery and device explantation are achieved in 3% of patients receiving mechanical circulatory support by left ventricular assist device (LVAD). It is considered that LVAD-induced cardiac unloading induces reverse cardiac remodeling, which contributes to myocardial recovery (1–4). Further possibilities for inducing structural and functional improvements in the myocardium are offered by cellular therapies, which have been under evaluation for the treatment of heart failure over two decades (5, 6). Despite controversies, cellular therapies remain under investigation for their numerous potential beneficial effects on the heart (7, 8). Theoretically, inducing myocardial regeneration at the cellular level can improve myocardial recovery after LVAD implantation. The high costs of cell therapy manufacturing, extensive culturing, dedicated facilities required, and concerns of mutations due to prolonged extensive

Abbreviations
CABG, coronary artery bypass grafting; LVAD, left ventricular assist device.

expansion and *in vitro* manipulations have attracted the search for alternative possibilities to cell therapy production and administration. During LVAD implantation surgery, autologous cardiac tissue can be harvested for the purpose of cell therapy generation from, for example, atrial appendages and left ventricular tissue. Recent data have shown that epicardial transplantation of autologous right atrial appendage (RAA) micrografts is clinically safe and feasible and is associated with beneficial structural and functional effects on ischemic myocardium (9–11).

As compared to the limited amount of tissue that can be harvested from the RAA for therapy preparation, the left atrial appendage (12, 13) allows for harvesting of a substantially greater amount of tissue and thus serves as a scalable tissue source for autologous therapeutic applications. We provide here the first clinical insight into the feasibility and safety of autologous left atrial appendage (LAA) harvesting, processing, and epicardial micrograft transplantation during LVAD implantation.

Method

A 61-year-old male patient with dilated cardiomyopathy underwent LVAD implantation as destination therapy. Prior to surgery, the patient was provided with information regarding the implantation procedure. The patient provided written informed consent for the procedure and follow-up. For the procedure, a HeartMate 3 LVAD (Abbott, Green Oaks, IL, United States) was implanted *via* full sternotomy. The LAA was then closed (Atriclip, Atricure Inc., Mason, OH, United States), removed, and forwarded for mechanical disaggregation and epicardial graft composition. A set of instrumentation for micrografting including a tissue processing station (EpiHeart Oy, Helsinki, Finland) and micrografting tool (HBW srl, Turin, Italy) were used.

Figure 1 illustrates LAA processing and epicardial LAA micrograft patch application. The harvested LAA tissue (~5 g) was first cut into smaller pieces. Processing into micrografts was carried out from 1 g of LAA tissue with the micrografting tool in four 1-min cycles. Each cycle was followed by micrograft harvesting in 4 ml of cardioplegia into a 50-ml centrifugation tube. To ensure washing in an ample buffer solution volume, fresh cardioplegia was added to the tube to reach a total volume of 25 ml. After centrifugation and removal of the cardioplegia supernatant, the LAA micrograft pellet was suspended in saline-diluted (1:1) fibrinogen component of the Tisseel fibrin sealant (Tisseel, Baxter Healthcare Corp., Westlake Village, CA, United States). The micrografts were then applied onto a decellularized equine pericardium matrix sheet (Auto Tissue Berlin GmbH, Berlin, Germany) spread on a dedicated transplant holder (EpiHeart Oy). The completed transplant was placed on a cooling plate (EpiHeart Oy) on the transplant holder to minimize micrograft metabolic activity before transplantation and to allow for controlled fibrin mesh formation. Saline-diluted (1:30) thrombin component of the fibrin sealant was then used to induce the formation of a fibrin mesh gel to support and fix the LAA micrografts to the matrix sheet. At the end of surgery, the autologous LAA micrograft transplant was fixed onto the epicardial surface with four sutures.

Results

The harvesting, mechanical tissue disaggregation, and preparation of the epicardial graft was carried out in a total of 35 min. Impact of the process on the duration of surgery was an increase of 6 min: 2 min for collecting the atrial appendage and 4 min for fixing and suturing the graft in place on the epicardial surface. The postoperative course was uneventful, and the patient was discharged home on postoperative day 33 with regular outpatient follow-up after approximately 3 months.

Discussion

We report here the first clinical application of intraoperative cardiac tissue micrografting using the LAA. The LAA micrograft transplant was successfully applied epicardially in conjunction with LVAD implantation. In addition to potential therapeutic benefits, this approach facilitates obtaining mechanistic proof of remodeling efficacy at functional, molecular, and structural levels using clinical imaging tools. Importantly, this protocol enables in-depth analytical comparisons of a baseline myocardial sample (available from the apical myocardium removed for LVAD implantation) with samples from treated and untreated myocardial areas available from the discarded host heart at heart transplantation. Such analyses can provide unique insights into intriguing new paracrine and cellular mechanisms of action of epicardial cellular therapies and increase our understanding on the nonthrombogenic roles of the LAA (14). Interestingly, graft-to-myocardium migration of tissue-resident macrophages was associated with myocardial healing after epicardial transplantation of LAA in a mouse model of acute myocardial infarction and heart failure (15). The contribution of graft-to-myocardium cell migration to myocardial healing will be an exciting topic for further research the autologous atrial appendage micrografts.

Similar therapy utilizing a small piece of the RAA has already been evaluated in conjunction with coronary artery bypass grafting (CABG) surgeries (9, 11). With increased amounts of tissue, for example from the LAA, available for processing, larger areas can be treated, and increased doses can be administered. Moreover, additional tissues utilizable for cell therapy are also available from cardiac surgeries. In addition to atrial appendage tissues, even leftover parts of vascular grafts at CABG surgery and apical myocardial tissue removed for the LVAD inlet at LVAD implantation are available for rapid mechanical processing to micrografts and subsequent epicardial transplantation intraoperatively. Such hybrid-tissue micrograft transplants may offer unprecedented therapeutic advances.

The adaptation of epicardial micrografting and the utilization of LAA, as presented here, offer a relatively ample autologous cardiac tissue source for surgical cell therapy. Straightforward

10.3389/fcvm.2023.1143886

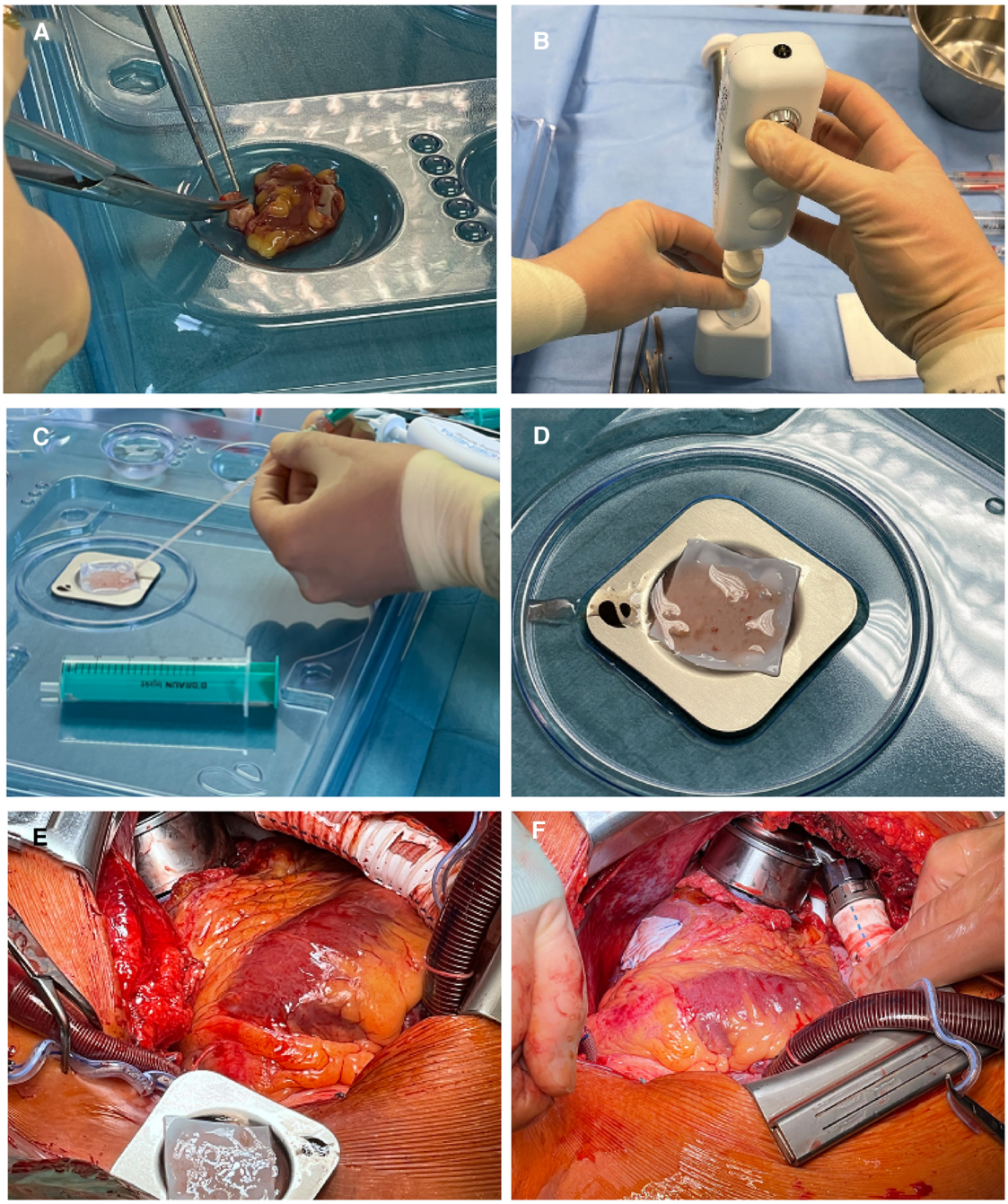

FIGURE 1
Left atrial appendage processing and epicardial transplantation. (**A**) Pieces of LAA are cut for processing. (**B**) Mechanical processing of LAA pieces to micrografts. (**C**) Application of LAA micrografts to the ECM sheet. (**D**) ECM sheet with LAA micrografts waiting for transplantation. (**E**) Transplant in transplant holder for flipping onto the epicardial surface. (**F**) Epicardially applied LAA micrograft patch in place on the left ventricle. LAA, left atrial appendage; ECM, extracellular matrix.

mechanical disaggregation and available regulatory-approved devices are expected to facilitate the adoption of this cardiac cell therapy approach. This, in turn, enables further therapy optimization and provides possibilities to obtain advanced mechanistic understanding of therapy efficacy.

Data availability statement

The original contributions presented in the study are included in the article, further inquiries can be directed to the corresponding author.

Ethics statement

Ethical review and approval was not required for the study on human participants in accordance with the local legislation and institutional requirements. The patient/participant provided his written informed consent to participate in this study.

Author contributions

JDS: Conceptualization, methodology, validation, formal analysis, investigation, resources, writing—review and editing, supervision, and project administration. AK: Methodology, validation, formal analysis, investigation, data curation, writing—original draft, writing—review and editing, and visualization. KK: Conceptualization, methodology, validation, investigation, resources, writing—Original Draft, writing—review and editing, visualization, and project administration. JSH: Validation, investigation, formal analysis, data curation, and writing—review and editing. EK: Conceptualization, methodology, validation, formal analysis, writing—original draft, writing—review and editing, visualization, supervision, and project administration. All authors contributed to the article and approved the submitted version.

Funding

EpiHeart Oy and HBW srl contributed materials to this study. Open access funding was received from EpiHeart Oy. EpiHeart Oy were not involved in the study design, collection, analysis, interpretation of data, the writing of the article or the decision to submit it for publication.

Conflict of interest

EK, AK, and KK are stakeholders of EpiHeart Oy. EK is a scientific advisor for HBW srl.

The remaining authors declare that the research was conducted in the absence of any commercial or financial relationships that could be construed as a potential conflict of interest.

Publisher's note

References

1. Birks EJ. Molecular changes after left ventricular assist device support for heart failure. *Circ Res.* (2013) 113:777–91. doi: 10.1161/CIRCRESAHA.113.301413

2. Birks EJ, Drakos SG, Patel SR, Lowes BD, Selzman CH, Starling RC, et al. Prospective multicenter study of myocardial recovery using left ventricular assist devices (RESTAGE-HF [remission from stage D heart failure]): medium-term and primary end point results. *Circulation.* (2020) 142:2016–28. doi: 10.1161/CIRCULATIONAHA.120.046415

3. Topkara VK, Garan AR, Fine B, Godier-Furnémont AF, Breskin A, Cagliostro B, et al. Myocardial recovery in patients receiving contemporary left ventricular assist devices: results from the interagency registry for mechanically assisted circulatory support (INTERMACS). *Circ Heart Fail.* (2016) 9:e003157. doi: 10.1161/CIRCHEARTFAILURE.116.003157

4. Varshney AS, DeFilippis EM, Cowger JA, Netuka I, Pinney SP, Givertz MM. Trends and outcomes of left ventricular assist device therapy: JACC focus seminar. *J Am Coll Cardiol.* (2022) 79:1092–107. doi: 10.1016/j.jacc.2022.01.017

5. Lampinen M, Vento A, Laurikka J, Nystedt J, Mervaala E, Harjula A, et al. Rational autologous cell sources for therapy of heart failure—vehicles and targets for gene and RNA therapies. *Curr Gene Ther.* (2016) 16:21–33. doi: 10.2174/1566523216666160104141809

6. Bolli R, Solankhi M, Tang XL, Kahlon A. Cell therapy in patients with heart failure: a comprehensive review and emerging concepts. *Cardiovasc Res.* (2022) 118:951–76. doi: 10.1093/cvr/cvab135

7. Kankuri E, Lampinen M, Harjula A. Cellular cardiomyoplasty—challenges of a new era. *Curr Tissue Eng.* (2015) 4:41–6. doi: 10.2174/2211542004666150305235238

8. Marbán E. A phoenix rises from the ashes of cardiac cell therapy. *Nat Rev Cardiol.* (2021) 18:743–4. doi: 10.1038/s41569-021-00625-1

9. Nummi A, Mulari S, Stewart JA, Kivistö S, Teittinen K, Nieminen T, et al. Epicardial transplantation of autologous cardiac micrografts during coronary artery bypass surgery. *Front Cardiovasc Med.* (2021) 8:726889. doi: 10.3389/fcvm.2021.726889

10. Xie Y, Lampinen M, Takala J, Sikorski V, Soliymani R, Tarkia M, et al. Epicardial transplantation of atrial appendage micrograft patch salvages myocardium after infarction. *J Heart Lung Transplant.* (2020) 39:707–18. doi: 10.1016/j.healun.2020.03.023

11. Lampinen M, Nummi A, Nieminen T, Harjula A, Kankuri E. Intraoperative processing and epicardial transplantation of autologous atrial tissue for cardiac repair. *J Heart Lung Transplant.* (2017) 36:1020–2. doi: 10.1016/j.healun.2017.06.002

12. Verma S, Bhatt DL, Tseng EE. Time to remove the left atrial appendage at surgery: LAAOS III in perspective. *Circulation.* (2021) 144:1088–90. doi: 10.1161/CIRCULATIONAHA.121.055825

13. Johnson WD, Ganjoo AK, Stone CD, Srivyas RC, Howard M. The left atrial appendage: our most lethal human attachment! Surgical implications. *Eur J Cardiothorac Surg.* (2000) 17:718–22. doi: 10.1016/s1010-7940(00)00419-x

14. Alkhouli M, Di Biase L, Natale A, Rihal CS, Holmes DR, Asirvatham S, et al. Nonthrombogenic roles of the left atrial appendage: JACC review topic of the week. *J Am Coll Cardiol.* (2023) 81:1063–75. doi: 10.1016/j.jacc.2023.01.017

15. Leinonen JV, Leinikka P, Tarkia M, Lampinen M, Emanuelov AK, Beeri R, et al. Structural and functional support by left atrial appendage transplant to the left ventricle after a myocardial infarction. *Int J Mol Sci.* (2022) 23:4661. doi: 10.3390/ijms23094661

frontiers | Frontiers in Cardiovascular Medicine

TYPE Systematic Review
PUBLISHED 10 May 2023
DOI 10.3389/fcvm.2023.1165011

OPEN ACCESS

EDITED BY
Faisal Syed,
University of North Carolina at Chapel Hill, United States

REVIEWED BY
David Zweiker,
Klinik Ottakring, Austria
Donah Zachariah,
University Hospitals of North Midlands NHS Trust, United Kingdom

*CORRESPONDENCE
Mien-Cheng Chen
✉ chenmien@ms76.hinet.net

RECEIVED 13 February 2023
ACCEPTED 18 April 2023
PUBLISHED 10 May 2023

CITATION
Lee W-C, Fang H-Y, Wu P-J, Chen H-C, Fang Y-N and Chen M-C (2023) Outcomes of catheter ablation vs. medical treatment for atrial fibrillation and heart failure: a meta-analysis. Front. Cardiovasc. Med. 10:1165011. doi: 10.3389/fcvm.2023.1165011

Outcomes of catheter ablation vs. medical treatment for atrial fibrillation and heart failure: a meta-analysis

Wei-Chieh Lee[1,2], Hsiu-Yu Fang[3], Po-Jui Wu[3], Huang-Chung Chen[3], Yen-Nan Fang[3] and Mien-Cheng Chen[3]*

[1]Institute of Clinical Medicine, College of Medicine, National Cheng Kung University, Tainan, Taiwan, [2]Division of Cardiology, Department of Internal Medicine, Chi Mei Medical Center, Tainan, Taiwan, [3]Division of Cardiology, Department of Internal Medicine, Kaohsiung Chang Gung Memorial Hospital, Chang Gung University College of Medicine, Kaohsiung, Taiwan, [4]Division of Cardiology, Department of Internal Medicine, National Cheng Kung University Hospital, College of Medicine, National Cheng Kung University, Tainan, Taiwan

Background: The benefit of catheter ablation vs. medical treatment has been reported to be inconsistent in randomized controlled trials (RCTs) for patients with atrial fibrillation (AF) and heart failure (HF) due to different enrollment criteria. This meta-analysis aimed to decipher the differential outcomes stratified by different left ventricular ejection fractions (LVEFs) and AF types.
Methods: We searched PubMed, Embase, ProQuest, ScienceDirect, Cochrane Library, ClinicalKey, Web of Science, and ClinicalTrials.gov databases for RCTs comparing medical treatment and catheter ablation in patients with AF and HF published before March 31, 2023. Nine studies were included.
Results: When patients were stratified by LVEF, improved LVEF and 6-min walk distance, less AF recurrence, and lower all-cause mortality in favor of catheter ablation were observed in patients with LVEF ≤50% but not in patients with LVEF ≤35%, and short HF hospitalization was observed in patients with LVEF ≤50% and LVEF ≤35%. When patients were stratified by AF types, improved LVEF and 6-min walk distance, better HF questionnaire score, and short HF hospitalization in favor of catheter ablation were observed both in patients with nonparoxysmal AF and mixed AF (paroxysmal and persistent) and less AF recurrence and lower all-cause mortality in favor of catheter ablation were observed in only patients with mixed AF.
Conclusions: This meta-analysis showed improved LVEF and 6-min walk distance, less AF recurrence, and lower all-cause mortality in favor of catheter ablation vs. medical treatment in AF patients with HF and LVEF of 36%–50%. Compared with medical treatment, catheter ablation improved LVEF and had better HF status in patients with nonparoxysmal AF and mixed AF; however, AF recurrence and all-cause mortality in favor of catheter ablation were observed in only HF patients with mixed AF.

KEYWORDS
atrial fibrillation, heart failure, left ventricular ejection fraction, medical treatment, catheter ablation

Introduction

The prevalence of atrial fibrillation (AF) and heart failure (HF) has increased globally (1). Advanced age and underlying structural heart disease are risk factors for AF and HF, which may develop sequentially or coincidentally (2). Patients with both conditions have worse outcomes and a higher risk of adverse clinical events (3, 4). Therefore, appropriate

management of AF and HF is important to reduce morbidity and mortality in patients with AF and HF. One randomized controlled study showed that catheter ablation had a low reported rate of restoring sinus rhythm and did not improve N-terminal pro-B-type natriuretic peptide, 6-min walk distance, or quality of life in patients with persistent AF and HF when compared with rate control (5). However, several randomized controlled studies showed significant benefits from catheter ablation vs. rate control in terms of objective exercise performance, clinical symptoms, neurohormonal status, left ventricular ejection fraction (LVEF), unplanned hospitalization, and mortality in patients with persistent AF and HF (6–8). One randomized controlled trial (RCT) reported that catheter ablation was associated with a significantly lower rate of all-cause mortality or hospitalization for worsening HF than rhythm and rate control therapy in patients with paroxysmal and persistent AF and HF, especially in patients with LVEF ≥ 25% (9). One study reported that timely treatment of arrhythmia-mediated cardiomyopathy might minimize irreversible ventricular remodeling in patients with persistent AF and HF related to LV systolic dysfunction (LVEF ≤ 45%) (10). However, another RCT reported that catheter ablation did not improve LVEF compared with the best medical treatment in HF patients with persistent AF and LVEF ≤ 35% (11). In the subgroup analysis of the CABANA study, catheter ablation produced clinically important improvements in survival, freedom from AF recurrence, and quality of life compared with drug therapy in patients with paroxysmal or persistent AF and clinically stable heart failure with a mean LVEF of 55% (12). However, another open-label study showed no difference in all-cause mortality or HF events between catheter ablation and rate control in patients with high-burden paroxysmal AF or persistent AF and HF symptoms (13). Therefore, the benefit of catheter ablation vs. medical treatment has been reported to be inconsistent in patients with AF and HF regarding clinical symptoms and outcomes. The discrepancy in outcomes between catheter ablation and medical treatment in patients with AF and HF may be due to different inclusion criteria in terms of HF diagnostic criteria and LVEF and AF types. Therefore, this meta-analysis aimed to decipher the differential outcomes of catheter ablation vs. medical treatment in patients with AF and HF, stratified by different LVEFs, New York Heart Association (NYHA) class ≥ II, and different AF types.

Methods

Search strategies, trial selection, quality assessment, and data extraction

Two cardiologists (W-CL and H-YF) performed a systematic literature search of the PubMed, Embase, ProQuest, ScienceDirect, Cochrane Library, ClinicalKey, Web of Science, and ClinicalTrials.gov databases for articles published before March 31, 2023. The databases were searched for relevant studies without language restrictions using the key terms "atrial fibrillation," "heart failure," "catheter ablation," and "medical treatment." Disagreements were resolved by a third reviewer (P-JW). This study included different RCTs that compared the efficacies of catheter ablation and medical treatment in patients with AF and HF. The inclusion criteria were a human study with parallel design and comparison of the efficacy of catheter ablation and medical treatment in patients with AF and HF. The exclusion criteria were case reports or series, animal studies, review articles, conference abstracts, unpublished data, and observational studies. We did not set language limitations to increase the number of eligible articles. **Supplementary Figure S1** illustrates the literature search and screening protocol.

Outcomes

The outcomes of interest in this study were the change in LVEF, 6-min walk distance, HF questionnaire score, change in brain natriuretic peptide (BNP), AF recurrence, HF hospitalization, and all-cause mortality.

Statistical analysis

The frequency of each evaluated outcome was extracted from each study, and the data were presented as cumulative rates. A random-effects model was employed to pool the individual odds ratio (OR), and all analyses were performed using Comprehensive Meta-Analysis software version 3 (Biostat, Englewood, NJ, United States). To assess the heterogeneity across trials, we used the chi-squared test (values of $p \leq 0.10$ were considered significant) and $I2$ statistics to examine each outcome from low to high heterogeneity (25%–75%, respectively). Potential publication bias was assessed using Egger's test *via* funnel plots, and statistical significance was set at $p \leq 0.10$. Statistical significance was set at $p < 0.05$ to compare the catheter ablation and medical treatment groups.

Results

Characteristics of included studies

The study selection process is illustrated in **Supplementary Figure S1**. Nine studies met our inclusion criteria. The study design, study period, participant characteristics, AF type, HF criteria, mean LVEF, and follow-up period are described in **Table 1**. A total of 2,074 participants (mean age, 65 ± 7.6 years; 70.9% men) were included. Most participants in these studies had nonparoxysmal AF (68%–100%). The enrollment criterion for HF trial patients in four studies was LVEF ≤ 35% (5, 6, 9, 11). In another three studies, different LVEF values were used to enroll HF patients, including ≤50% (7), ≤40% (8), and ≤45% (10). The remaining two studies did not declare the LVEF cutoff value for enrollment and used only a history of NYHA functional classification ≥II as the enrollment criteria (12, 13).

TABLE 1 Characteristics of the nine included studies.

First author (year)—study name	Patients number (male %)	Age (years)	Study period	Nonparoxysmal AF (%)	Enrollment criteria for HF	Mean LVEF of the two groups	Follow-up	Reference number
MacDonald MR (2011)	41 (78)	63 ± 7	January 2007–July 2009	100	NYHA class ≥ II and LVEF ≤ 35%	19.6 ± 5.5% vs. 16.1 ± 7.1%	6 months	5
Jones DG (2013)	52 (87)	63 ± 9	April 2009–June 2012	100	NYHA class ≥ II and LVEF ≤ 35%	25 ± 7% vs. 22 ± 8%	12 months	6
Hunter RJ (2014)—ARC AF	50 (96)	57 ± 11	N/A	92	NYHA class ≥ II and LVEF ≤ 50%	34 ± 12% vs. 32 ± 8%	12 months	7
Di Biase (2016)—CAMTAF	203 (74)	61 ± 11	N/A	100	NYHA class II, III, LVEF ≤ 40%, and an implanted defibrillator	30 ± 8% vs. 29 ± 5%	24 months	8
Marrouche NF (2018)—CASTLE-AF	363 (86)	64 ± 4	January 2008–January 2016	68	NYHA class ≥ II, LVEF ≤ 35%, and an implanted defibrillator	31.5 ± 2.5% vs. 32.5 ± 3.3%	37.8 months	9
Prabhu S (2018)—CAMERA MRI	36 (N/A)	61 ± 11	N/A	100	LVEF ≤ 45%	36 ± 8.2% vs. 33 ± 8.0%	6 months	10
Kuck KH (2021)—AMICA	140 (90)	65 ± 8	January 2008–June 2016	100	LVEF ≤ 35%	24.8 ± 8.8% vs. 27.8 ± 9.5%	12 months	11
Packer DL CABANA subgroup (2021)	778 (55)	67 ± 3	November 2009–April 2016	68	NYHA class ≥ II	56 ± 3% vs. 55 ± 3%	60 months	12
Parkash R (2022)—RAFTAF	411 (74)	67 ± 8	December 2011–January 2018	93	NYHA class II, III and elevated NT-proBNP	40.3 ± 14.6% vs. 41.0 ± 14.9%	24 months	13

HF, heart failure; AF, atrial fibrillation; LVEF, left ventricular ejection fraction; NYHA, New York Heart Association; N/A, not applicable; NT-proBNP; N-terminal pro-B-type natriuretic peptide.

Patient demographics

Table 2 describes the details of patients' demographics between the medical treatment and catheter ablation groups of the enrolled study patients. The mean age, sex, NYHA functional classification, prevalence of diabetes mellitus, hypertension, prior stroke, ischemic cardiomyopathy, implantable cardioverter defibrillator, cardiac resynchronization therapy placement, nonparoxysmal AF, AF duration, mean LVEF, and use of HF medications did not differ significantly between the medical treatment and catheter ablation groups.

TABLE 2 Patients' demographics.

	Medical treatment	Catheter ablation	*P* value
Number	1,041	1,033	
Age (years)	65 ± 7.4 (1,041)	65 ± 7.8 (1,033)	1.000
Male sex (%)	71.5 (731/1,023)	70.3 (714/1,015)	0.551
Diabetes mellitus (%)	29.2 (289/991)	27.4 (269/981)	0.375
Hypertension (%)	73.4 (745/1,015)	71.5 (720/1,007)	0.339
Nonparoxysmal AF (%)	79.1 (808/1,022)	81.8 (827/1,011)	0.125
ICM (%)	41.0 (214/522)	37.9 (203/535)	0.303
Coronary artery disease (%)	31.6 (293/927)	30.9 (285/921)	0.746
Prior stroke (%)	10.3 (84/818)	10.5 (85/811)	0.895
NYHA class ≥ III (%)	39.1 (204/522)	42.8 (229/535)	0.222
ICD and CRT (%)	57.2 (274/479)	57.1 (278/487)	0.975
LA dimension (mm)	48.2 ± 6.3 (548)	47.6 ± 6.4 (563)	0.116
LVEF (%)	41.7 ± 14.9 (1,041)	41.2 ± 14.1 (1,033)	0.433
CHA2DS2-VASc score	3.1 ± 1.2 (615)	3.1 ± 1.2 (610)	1.000
AF duration (months)	16.6 ± 21.3 (785)	15.7 ± 16.1 (786)	0.345
ACEI/ARB (%)	88.3 (545/617)	86.2 (542/629)	0.267
β-blocker (%)	84.4 (521/617)	82.7 (520/629)	0.419
MRA (%)	59.0 (364/617)	60.9 (383/629)	0.494

AF, atrial fibrillation; ICM, ischemic cardiomyopathy; NYHA, New York Heart Association; ICD, implantable cardioverter defibrillator; CRT, cardiac resynchronization therapy; LA, left atrium; LVEF, left ventricular ejection fraction; ACEI, angiotensin-converting enzyme inhibitor; ARB, angiotensin II receptor blocker; MRA, mineralocorticoid receptor antagonist.
Data are expressed as mean ± SD or number (percentage).

Pooled results of changes in LVEF, 6-min walk distance, HF questionnaire score, BNP level, AF recurrence, HF hospitalization, and all-cause mortality

Pooled results from the random-effects model showed that catheter ablation for AF, compared with medical treatment, was associated with an increased LVEF from baseline [mean difference 6.22%; 95% confidence interval (CI), 3.59%–8.86%] with high heterogeneity (Cochran's *Q*, 294.657; *df*, 7; I^2, 97.624%; $p < 0.001$) (Figure 1A). Egger's test revealed nonsignificant publication bias in the change in LVEF (*t*, 0.309; *df*, 6; $p = 0.767$). The funnel plot of the change in LVEF is shown in Supplementary Figure S2. Pooled results from the random-effects model showed that catheter ablation vs. medical treatment was associated with an increased 6-min walk distance from baseline (mean difference, 0.97 m; 95% CI, 0.27–1.67 m), with high heterogeneity (Cochran's *Q*, 94.559; *df*, 5; I^2, 94.712%; $p < 0.001$) (Figure 1B). Egger's test revealed a nonsignificant publication bias regarding the change in the 6-min walk distance (*t*, 0.782; *df*, 4; $p = 0.478$). The funnel plot for the change in the

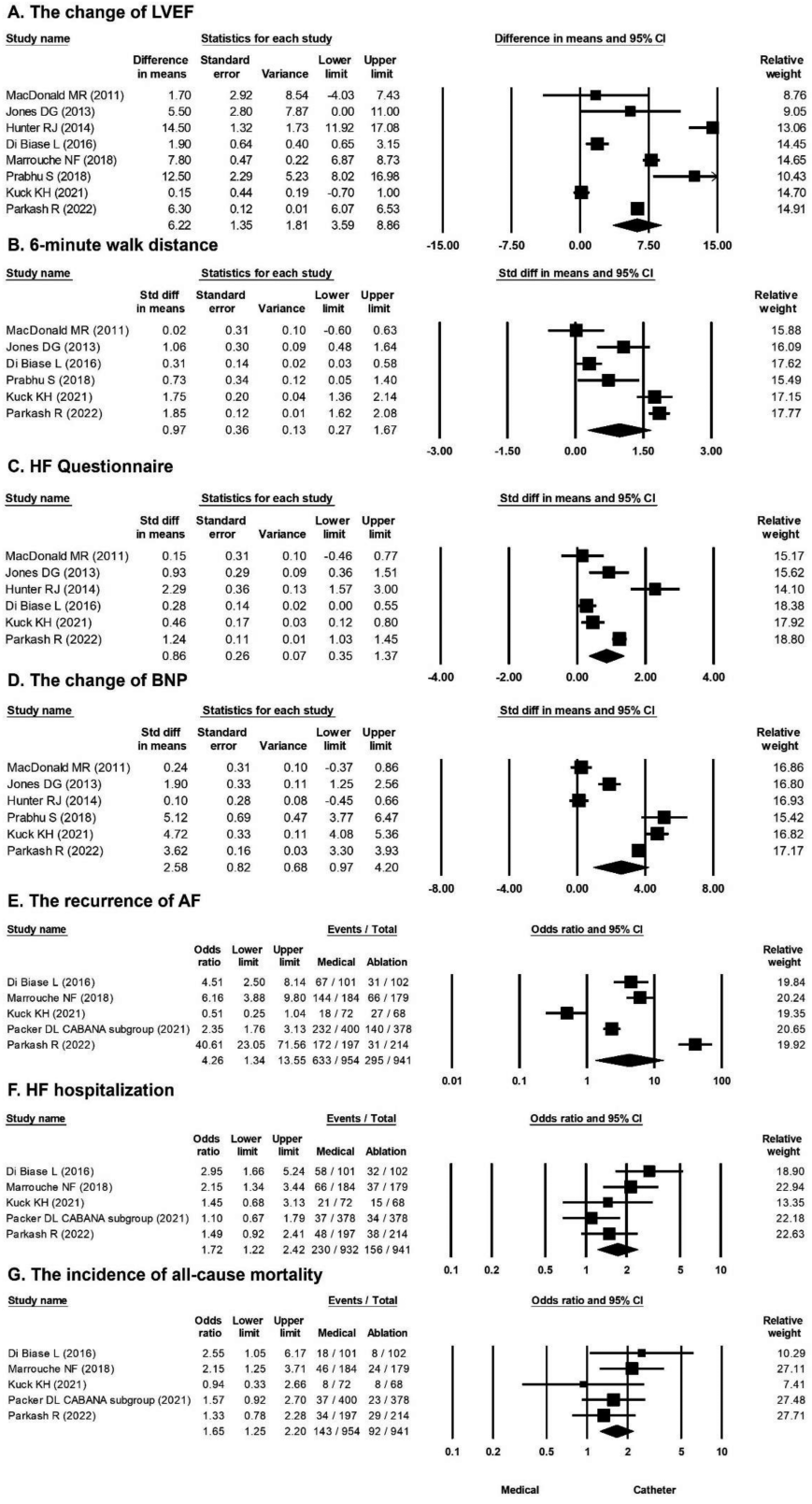

FIGURE 1
Forest plots comparing the changes in LVEF, 6-min walk distance, HF questionnaire score, BNP level, odds ratio for AF recurrence, odds ratio for HF hospitalization, and odds ratio for all-cause mortality of medical treatment versus catheter ablation. (**A**) Change of LVEF in eight studies. (**B**) 6-min walk distance in six studies. (**C**) HF questionnaire in six studies. (**D**) Change of BNP level in six studies. (**E**) AF recurrence rate in five studies. (**F**) HF hospitalization rate in five studies. (**G**) All-cause mortality rate in five studies. AF, atrial fibrillation; BNP, B-type natriuretic peptide; HF, heart failure; LVEF, left ventricular ejection fraction.

6-min walk distance is shown in Supplementary Figure S3. Pooled results from the random-effects model showed that catheter ablation vs. medical therapy was associated with an improved HF questionnaire score from baseline (mean difference, 0.86; 95% CI, 0.35–1.37) with high heterogeneity (Cochran's *Q*, 55.150; *df*, 5; I^2, 90.934%; $p < 0.001$) (Figure 1C). Egger's test showed a nonsignificant publication bias in the change in the HF questionnaire score (*t*, 0.028; *df*, 4; $p = 0.979$). The funnel plot for the change in HF questionnaire score is shown in Supplementary Figure S4. Pooled results from the random-effects model showed that catheter ablation vs. medical treatment was associated with significant change in the BNP level from baseline (mean difference, 2.58 pg/ml, 95% CI, 0.97–4.20 pg/ml) with high heterogeneity (Cochran's *Q*, 233.478; *df*, 5; I^2, 97.858%; $p < 0.001$) (Figure 1D). Egger's test revealed a nonsignificant publication bias for the change in the BNP level (*t*, 0.392; *df*, 4; $p = 0.715$). The funnel plot for the change in the BNP level is shown in Supplementary Figure S5. The overall OR of the recurrence of AF of the catheter ablation group vs. medical treatment was 4.26 (95% CI, 1.34–13.55) in favor of catheter ablation (Figure 1E) with high heterogeneity (Cochran's *Q*, 112.389; *df*, 4; I^2, 96.441%; $p < 0.001$). Egger's test revealed nonsignificant publication bias regarding the overall OR of AF recurrence (*t*, 0.382; *df*, 3; $p = 0.728$). A funnel plot for the log OR of AF recurrence is shown in Supplementary Figure S6. The overall OR of the HF hospitalization of catheter ablation vs. medical treatment was 1.72 (95% CI, 1.22–2.42) in favor of catheter ablation (Figure 1F) with moderate heterogeneity (Cochran's *Q*, 7.991; *df*, 4; I^2, 49.946%; $p = 0.092$). Egger's test revealed a nonsignificant publication bias regarding the overall OR of hospitalization for HF (*t*, 0.180; *df*, 3; $p = 0.869$). A funnel plot for the log OR of HF hospitalization is shown in Supplementary Figure S7. The overall OR of the incidence of all-cause mortality of catheter ablation vs. medical treatment was 1.65 (95% CI, 1.25–2.20) in favor of catheter ablation (Figure 1G) with low heterogeneity (Cochran's *Q*, 3.622; *df*, 4; I^2, 0%; $p = 0.460$). Egger's test revealed a nonsignificant publication bias regarding the overall OR of all-cause mortality (*t*, 0.215; *df*, 3; $p = 0.844$). The funnel plot for the log OR of all-cause mortality is shown in Supplementary Figure S8.

Pooled results of change in LVEF, 6-min walk distance, HF questionnaire score, BNP level, AF recurrence, HF hospitalization, and all-cause mortality stratified by different LVEFs

A greater improvement in LVEF in favor of catheter ablation vs. medical treatment was observed in the population with LVEF ≤50% (mean difference, 9.54%; 95% CI, 0.04%–19.04%) but not in the population with LVEF ≤35% (Figure 2A). A longer 6-min walk distance in favor of catheter ablation vs. medical treatment was observed in the population with LVEF ≤50% (mean difference, 0.40 m; 95% CI, 0.03–0.75 m), but not in the population with LVEF ≤35% (Figure 2B). Interestingly, a greater improvement in HF questionnaire scores in favor of catheter ablation vs. medical treatment was observed in the population with LVEF ≤35% (mean difference, 0.51; 95% CI, 0.14–0.89) but not in the population with LVEF ≤50% (Figure 2C). There was no significant difference in the change in the BNP level between catheter ablation and medical treatment in the population with LVEF ≤35% (mean difference, 2.29 pg/ml; 95% CI, −0.30 to 4.87 pg/ml) and in the population with LVEF ≤50% (mean difference, 2.57 pg/ml; 95% CI, −2.34 to 7.48 pg/ml) (Figure 2D). The risk of recurrence of AF was significantly lower by catheter ablation compared with medical treatment in the population with LVEF ≤50% (OR, 4.51; 95% CI, 2.50–8.14) but not in the population with LVEF ≤35% (Figure 2E). The overall OR values of HF hospitalization were 1.93 (95% CI, 1.29–2.88), in favor of catheter ablation vs. medical treatment in the population with LVEF ≤35%, and 2.95 (95% CI, 1.66–5.24), also in favor of catheter ablation vs. medical treatment in the population with LVEF ≤50% (Figure 2F). The incidence of all-cause mortality was significantly lower by catheter ablation compared with medical treatment in the population with LVEF ≤50% (OR, 2.55; 95% CI, 1.05–6.17) but not in the population with LVEF ≤35% (Figure 2G).

Pooled results of change in LVEF, 6-min walk distance, HF questionnaire score, BNP level, AF recurrence, HF hospitalization, and all-cause mortality stratified only by NYHA ≥II

A greater improvement in LVEF in favor of catheter ablation vs. medical treatment was observed in the population with HF history (mean difference, 6.30%; 95% CI, 6.07%–6.53%) (Figure 3A). A longer 6-min walk distance in favor of catheter ablation vs. medical treatment was observed in the population with HF history (mean difference, 1.85 m; 95% CI, 1.62–2.08 m) (Figure 3B). A greater improvement in HF questionnaire scores in favor of catheter ablation vs. medical treatment was observed in the population with HF history (mean difference, 1.24; 95% CI, 1.03–1.45) (Figure 3C). A significant difference in the change in the BNP level in favor of catheter ablation vs. medical treatment was observed in the population with HF history (mean difference, 3.62 pg/ml; 95% CI, 3.30–3.93 pg/ml) (Figure 3D). There was no significant difference in the recurrence of AF, HF hospitalization, and all-cause mortality between catheter ablation and medical treatment in the population with HF history of NYHA ≥II (Figures 3E–G).

Pooled results of change in LVEF, 6-min walk distance, HF questionnaire score, BNP level, AF recurrence, HF hospitalization, and all-cause mortality stratified by AF types

Mixed AF was defined as the study population with paroxysmal and persistent AF (14). A greater improvement in LVEF in favor of

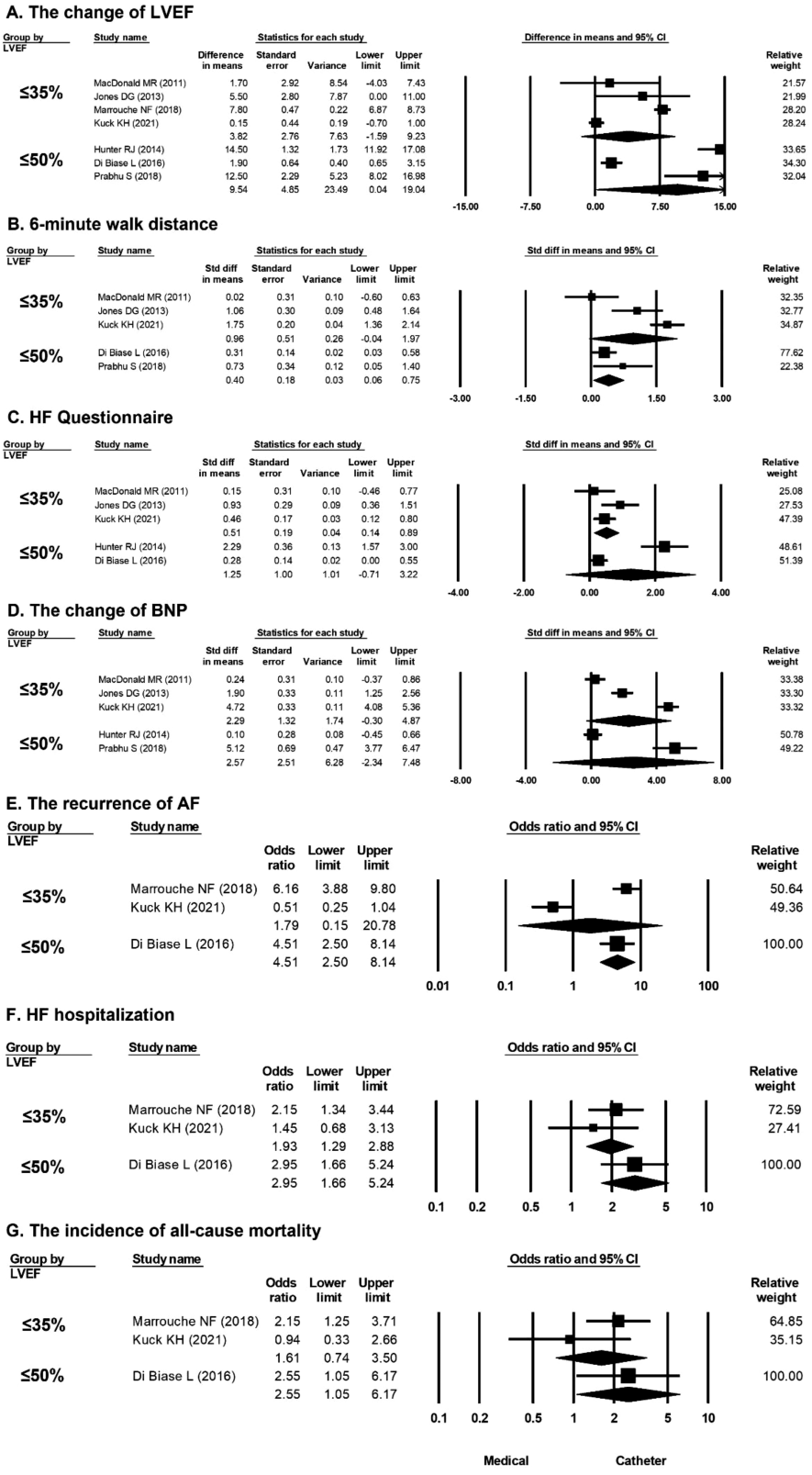

FIGURE 2
Forest plots comparing the changes in LVEF, 6-min walk distance, HF questionnaire score, BNP level, odds ratio for AF recurrence, odds ratio for HF hospitalization, and odds ratio for all-cause mortality of medical treatment versus catheter ablation in patients stratified by LVEF (LVEF ≤ 35% and LVEF ≤ 50%). (**A**) Change in LVEF in seven studies (≤35% in four, ≤50% in three). (**B**) 6-min walk distance in five studies (LVEF ≤ 35% in three, LVEF ≤ 50% in two). (**C**) HF questionnaire score in five studies (LVEF ≤ 35% in three, LVEF ≤ 50% in two). (**D**) BNP level in five studies (LVEF ≤ 35% in three, LVEF ≤ 50% in two). (**E**) AF recurrence in three studies (LVEF ≤ 35% in two, LVEF ≤ 50% in one). (**F**) HF hospitalization in three studies (LVEF ≤ 35% in two, LVEF ≤ 50% in one). (**G**) All-cause mortality rate in three studies (LVEF ≤ 35% in two, LVEF ≤ 50% in one). AF, atrial fibrillation; BNP, B-type natriuretic peptide; HF, heart failure; LVEF, left ventricular ejection fraction.

10.3389/fcvm.2023.1165011

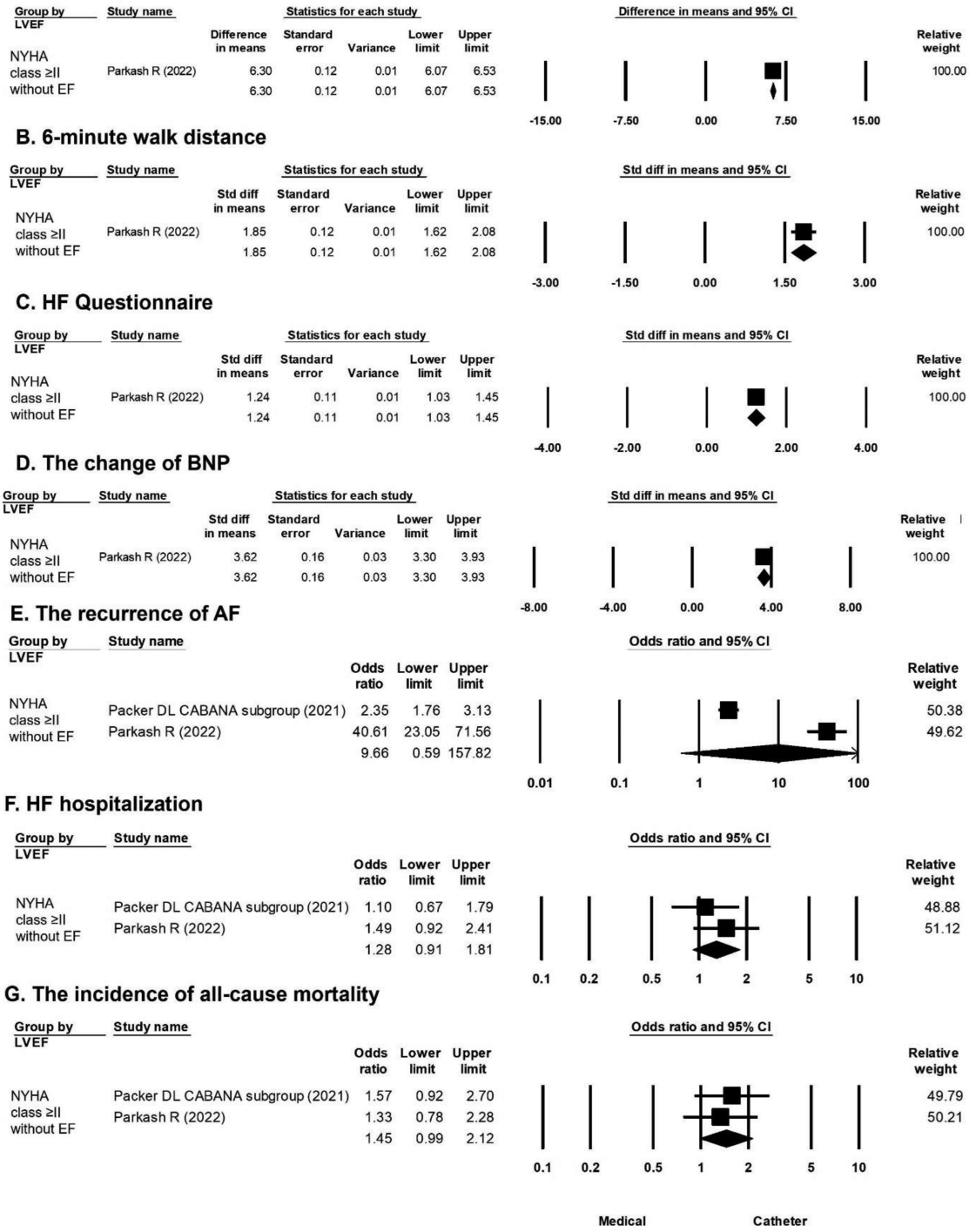

FIGURE 3
Forest plots comparing the changes in LVEF, 6-min walk distance, HF questionnaire score, BNP level, odds ratio for AF recurrence, odds ratio for HF hospitalization, and odds ratio for all-cause mortality of medical treatment versus catheter ablation in patients stratified by NYHA ≥ II without LVEF. (**A**) Change in LVEF in one study. (**B**) 6-min walk distance in one study. (**C**) HF questionnaire score in one study. (**D**) BNP level in one study. (**E**) AF recurrence in two studies. (**F**) HF hospitalization in two studies. (**G**) All-cause mortality rate in two studies. AF, atrial fibrillation; BNP, B-type natriuretic peptide; HF, heart failure; LVEF, left ventricular ejection fraction.

catheter ablation vs. medical treatment was observed in the population with nonparoxysmal AF (mean difference, 3.68%; 95% CI, 0.82%–6.54%) and mixed AF (mean difference, 9.07%; 95% CI, 6.46%–11.69%) (Figure 4A). A longer 6-min walk distance in favor of catheter ablation vs. medical treatment was observed in the population with nonparoxysmal AF (mean difference, 0.78 m; 95% CI, 0.11–1.45 m) and mixed AF (mean difference, 1.85 m; 95% CI, 1.62–2.08 m) (Figure 4B). A greater

10.3389/fcvm.2023.1165011

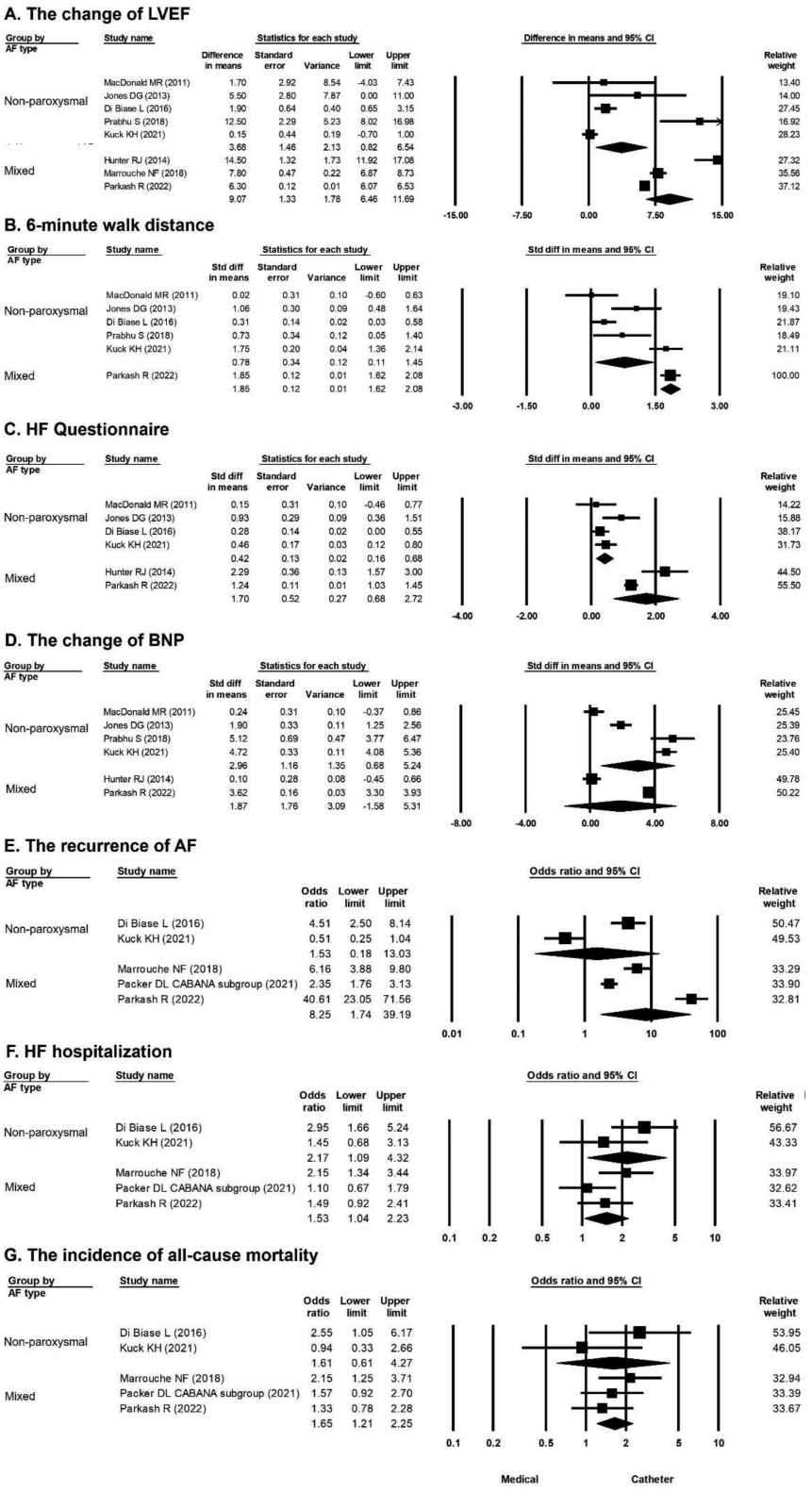

FIGURE 4
Forest plots comparing the changes of LVEF, 6-min walk distance, HF questionnaire score, BNP level, odds ratio for AF recurrence, odds ratio for HF hospitalization, and odds ratio for all-cause mortality of medical treatment versus catheter ablation in patients stratified by different AF types (nonparoxysmal and mixed AF). (**A**) Change in LVEF in eight studies (nonparoxysmal AF in five, mixed AF in three). (**B**) 6-min walk distance in six studies (nonparoxysmal AF in five, mixed AF in one). (**C**) HF questionnaire score in six studies (nonparoxysmal AF in four, mixed AF in two). (**D**) BNP level in six studies (nonparoxysmal AF in four, mixed AF in two). (**E**) AF recurrence rate in five studies (nonparoxysmal AF in two, mixed AF in three). (**F**) HF hospitalization rate in five studies (nonparoxysmal AF in two, mixed AF in three). (**G**) All-cause mortality rate in five studies (nonparoxysmal AF in two, mixed AF in three). AF, atrial fibrillation; BNP, B-type natriuretic peptide; HF, heart failure; LVEF, left ventricular ejection fraction.

improvement in HF questionnaire scores in favor of catheter ablation vs. medical treatment was observed in the population with nonparoxysmal AF (mean difference, 0.42; 95% CI, 0.16–0.68) and mixed AF (mean difference, 1.70; 95% CI, 0.68–2.72) (**Figure 4C**). A significant difference in the change in the BNP level in favor of catheter ablation vs. medical treatment was observed in the population with nonparoxysmal AF (mean difference, 2.96 pg/ml; 95% CI, 0.68–5.24 pg/ml) but not in the population with mixed AF (**Figure 4D**). The risk of recurrence of AF was significantly lower by catheter ablation compared with medical treatment in the population with mixed AF (OR, 8.25; 95% CI, 1.74–39.19) but not in the population with nonparoxysmal AF (**Figure 4E**). The overall OR values of HF hospitalization in favor of catheter ablation vs. medical treatment were 2.17 (95% CI, 1.09–4.32) in the population with nonparoxysmal AF and 1.53 (95% CI, 1.04–2.23) in the population with mixed AF (**Figure 4F**). The incidence of all-cause mortality was significantly lower by catheter ablation compared with medical treatment in the population with mixed AF (OR, 1.65; 95% CI, 1.21–2.25) but not in the population with nonparoxysmal AF (**Figure 4G**).

Discussion

In the whole study population of this meta-analysis, improved LVEF, improved 6-min walk distance, better HF questionnaire score, significantly decreased BNP level, less AF recurrence, less HF hospitalization, and lower all-cause mortality were observed after catheter ablation vs. medical treatment. When the study population was stratified by LVEF, improved LVEF, improved 6-min walk distance, less AF recurrence, and lower all-cause mortality in favor of catheter ablation vs. medical treatment were observed in the population with LVEF ≤50% but not in the population with LVEF ≤35%; however, less HF hospitalization was observed both in the population with LVEF ≤50% and LVEF ≤35%. When the study population was stratified by HF NYHA ≥II, improved LVEF, improved 6-min walk distance, and better HF questionnaire score in favor of catheter ablation vs. medical treatment were observed in the population with HF NYHA ≥II. When the study population was stratified by AF types, improved LVEF, improved 6-min walk distance, better HF questionnaire score, and less HF hospitalization in favor of catheter ablation vs. medical treatment were observed both in the population with nonparoxysmal AF and mixed AF; however, less AF recurrence and lower all-cause mortality in favor of catheter ablation vs. medical treatment were observed only in the population with mixed AF.

Population stratified by different LVEF criteria

The criteria for HF in the enrolled studies differed in LVEF cutoff values, ranging from LVEF ≤35% (5, 6, 9, 11) to ≤40% (8), ≤45% (10), and ≤50% (7) or differed in only enrolling patients with a history of HF with NYHA functional classification ≥II without mention LVEF (12, 13). According to our meta-analysis, improved LVEF, improved 6-min walk distance, less AF recurrence, and lower all-cause mortality in favor of catheter ablation vs. medical treatment were observed in the population with LVEF of 36%–50% and less HF hospitalization was observed both in the population with LVEF ≤ 50%, and LVEF ≤35%.

Population stratified by different AF types

In patients with HF and reduced LVEF, a high prevalence of persistent AF exists and is closely related to underlying heart disease severity and HF functional classes (15). In the enrolled studies of this meta-analysis, the prevalence of nonparoxysmal AF was 68%–100%. Previous meta-analyses comparing catheter ablation vs. medical treatment in terms of clinical outcomes in patients with AF and HF did not specifically stratify the study subjects by different AF types (16, 17). However, the long-term efficacy of catheter ablation vs. medical treatment for different AF types on clinical outcomes may differ and may require more than one catheter ablation procedure for different AF types (18). In this meta-analysis, improved LVEF, improved 6-min walk distance, better HF questionnaire score, and less HF hospitalization in favor of catheter ablation vs. medical treatment were observed both in the population with nonparoxysmal AF and mixed AF; however, AF recurrence and all-cause mortality in favor of catheter ablation vs. medical treatment were only observed in the population with mixed AF but not in the population with nonparoxysmal AF. Nonparoxysmal AF may contribute to more atrial and ventricular structural remodeling and atrial fibrosis, reducing the benefit of catheter ablation for AF, especially in HF patients. Therefore, catheter ablation could achieve more clinical benefits in patients with mixed AF than in patients with nonparoxysmal AF.

Limitations

This study had several limitations. First, the enrollment criteria for HF differed among the nine enrolled studies, and high heterogeneity was found in the analyses of the whole population. Therefore, we performed subgroup analyses, and patients were stratified by different LVEFs, HF history of NYHA ≥ II, and AF types. Second, the use of HF biomarkers differed among six studies, three (6, 7, 10) used serum BNP and the other three (5, 11, 13) used N-terminal proBNP. Third, although nine studies were included, over one-third of the 2,074 participants enrolled in this meta-analysis were derived from the HF subgroup of the CABANA study, which contributes a large number of patients with LVEF >50% (12). Fourth, the baseline characteristics of all participants in the enrolled studies were not completely available. Fifth, the enrolled studies had different follow-up periods, while HF hospitalization and all-cause mortality might need longer follow-up periods to show a significant difference between catheter ablation and medical treatment.

Conclusion

This meta-analysis showed improved LVEF, improved 6-min walk distance, less AF recurrence, and lower all-cause mortality in favor of catheter ablation vs. medical treatment in AF patients with HF and LVEF of 36%–50%, and less HF hospitalization was observed both in AF patients with HF and LVEF ≤50%, and LVEF ≤35%. Compared with medical treatment, catheter ablation improved LVEF, improved 6-min walk distance, and had better HF questionnaire score and less HF hospitalization in patients with nonparoxysmal AF and mixed AF; however, AF recurrence and all-cause mortality in favor of catheter ablation were observed only in HF patients with mixed AF.

Data availability statement

The original contributions presented in the study are included in the article/**Supplementary Material**, further inquiries can be directed to the corresponding author/s.

Author contributions

W-CL and P-JW reviewed the articles and wrote the manuscript. Y-NF and H-CC prepared figures. M-CC did the final revision. All authors contributed to the article and approved the submitted version.

Conflict of interest

The authors declare that the research was conducted in the absence of any commercial or financial relationships that could be construed as a potential conflict of interest.

Publisher's note

Supplementary material

The Supplementary Material for this article can be found online at: https://www.frontiersin.org/articles/10.3389/fcvm.2023.1165011/full#supplementary-material.

SUPPLEMENTARY FIGURE 1
Flowchart of the study selection strategy and inclusion and exclusion criteria for this meta-analysis. AF, atrial fibrillation; HF, heart failure

SUPPLEMENTARY FIGURE 2
Funnel plot showing non-significant publication bias using Egger's test (*t*, 0.309; *df*, 6; $p = 0.767$).

SUPPLEMENTARY FIGURE 3
Funnel plot showing non-significant publication bias using Egger's test (n *t*, 0.782; *df*, 4; $p = 0.478$).

SUPPLEMENTARY FIGURE 4
Funnel plot showing non-significant publication bias using Egger's test (*t*, 0.028; *df*, 4; $p = 0.979$).

SUPPLEMENTARY FIGURE 5
Funnel plot showing non-significant publication bias using Egger's test (*t*, 0.392; *df*, 4; $p = 0.715$).

SUPPLEMENTARY FIGURE 6
Funnel plot showing non-significant publication bias using Egger's test (*t*, 0.382; *df*, 3; $p = 0.728$).

SUPPLEMENTARY FIGURE 7
Funnel plot showing non-significant publication bias using Egger's test (*t*, 0.180; *df*, 3; $p = 0.869$).

SUPPLEMENTARY FIGURE 8
Funnel plot showing non-significant publication bias using Egger's test (*t*, 0.215; *df*, 3; $p = 0.844$).

References

1. Anter E, Jessup M, Callans DJ. Atrial fibrillation and heart failure: treatment considerations for a dual epidemic. *Circulation*. (2009) 119(18):2516–25. doi: 10.1161/CIRCULATIONAHA.108.821306

2. Heck PM, Lee JM, Kistler PM. Atrial fibrillation in heart failure in the older population. *Heart Fail Clin*. (2013) 9(4):451–9, viii–ix. doi: 10.1016/j.hfc.2013.07.007

3. Batul SA, Gopinathannair R. Atrial fibrillation in heart failure: a therapeutic challenge of our times. *Korean Circ J*. (2017) 47(5):644–62. doi: 10.4070/kcj.2017.0040

4. Gopinathannair R, Chen LY, Chung MK, Cornwell WK, Furie KL, Lakkireddy DR, et al. Managing atrial fibrillation in patients with heart failure and reduced ejection fraction: a scientific statement from the American heart association. *Circ Arrhythm Electrophysiol*. (2021) 14(6):HAE0000000000000078. doi: 10.1161/HAE.0000000000000078

5. MacDonald MR, Connelly DT, Hawkins NM, Steedman T, Payne J, Shaw M, et al. Radiofrequency ablation for persistent atrial fibrillation in patients with advanced heart failure and severe left ventricular systolic dysfunction: a randomised controlled trial. *Heart*. (2011) 97(9):740–7. doi: 10.1136/hrt.2010.207340

6. Jones DG, Haldar SK, Hussain W, Sharma R, Francis DP, Rahman-Haley SL, et al. A randomized trial to assess catheter ablation versus rate control in the management of persistent atrial fibrillation in heart failure. *J Am Coll Cardiol*. (2013) 61(18):1894–903. doi: 10.1016/j.jacc.2013.01.069

7. Hunter RJ, Berriman TJ, Diab I, Kamdar R, Richmond L, Baker V, et al. A randomized controlled trial of catheter ablation versus medical treatment of atrial fibrillation in heart failure (the CAMTAF trial). *Circ Arrhythm Electrophysiol*. (2014) 7(1):31–8. doi: 10.1161/CIRCEP.113.000806

8. Di Biase L, Mohanty P, Mohanty S, Santangeli P, Trivedi C, Lakkireddy D, et al. Ablation versus amiodarone for treatment of persistent atrial fibrillation in patients with congestive heart failure and an implanted device: results from the AATAC multicenter randomized trial. *Circulation*. (2016) 133(17):1637–44. doi: 10.1161/CIRCULATIONAHA.115.019406

9. Marrouche NF, Brachmann J, Andresen D, Siebels J, Boersma L, Jordaens L, et al. Catheter ablation for atrial fibrillation with heart failure. *N Engl J Med*. (2018) 378(5):417–27. doi: 10.1056/NEJMoa1707855

10. Prabhu S, Costello BT, Taylor AJ, Gutman SJ, Voskoboinik A, McLellan AJA, et al. Regression of diffuse ventricular fibrosis following restoration of sinus rhythm with catheter ablation in patients with atrial fibrillation and systolic dysfunction: a substudy of the CAMERA MRI trial. *JACC Clin Electrophysiol*. (2018) 4 (8):999–1007. doi: 10.1016/j.jacep.2018.04.013

11. Kuck KH, Merkely B, Zahn R, Arentz T, Seidl K, Schlüter M, et al. Catheter ablation versus best medical therapy in patients with persistent atrial fibrillation and congestive heart failure: the randomized AMICA trial. *Circ Arrhythm Electrophysiol*. (2019) 12(12):e007731. doi: 10.1161/CIRCEP.119.007731

12. Packer DL, Piccini JP, Monahan KH, Al-Khalidi HR, Silverstein AP, Noseworthy PA, et al. Ablation versus drug therapy for atrial fibrillation in heart failure: results from the CABANA trial. *Circulation*. (2021) 143(14):1377–90. doi: 10.1161/CIRCULATIONAHA.120.050991

13. Parkash R, Wells GA, Rouleau J, Talajic M, Essebag V, Skanes A, et al. Randomized ablation-based rhythm-control versus rate-control trial in patients with heart failure and atrial fibrillation: results from the RAFT-AF trial. *Circulation*. (2022) 145(23):1693–1704. doi: 10.1161/CIRCULATIONAHA.121.057095

14. Weinmann K, Aktolga D, Pott A, Bothner C, Rattka M, Stephan T, et al. Impact of re-definition of paroxysmal and persistent atrial fibrillation in the 2012 and 2016 European society of cardiology atrial fibrillation guidelines on outcomes after pulmonary vein isolation. *J Interv Card Electrophysiol*. (2021) 60(1):115–23. doi: 10.1007/s10840-020-00710-4

15. Schönbauer R, Duca F, Kammerlander AA, Aschauer S, Binder C, Zotter-Tufaro C, et al. Persistent atrial fibrillation in heart failure with preserved ejection fraction: prognostic relevance and association with clinical, imaging and invasive haemodynamic parameters. *Eur J Clin Invest*. (2020) 50(2):e13184. doi: 10.1111/eci.13184

16. Chen S, Pürerfellner H, Meyer C, Acou WJ, Schratter A, Ling Z, et al. Rhythm control for patients with atrial fibrillation complicated with heart failure in the contemporary era of catheter ablation: a stratified pooled analysis of randomized data. *Eur Heart J*. (2020) 41(30):2863–73. doi: 10.1093/eurheartj/ehz443

17. Pan KL, Wu YL, Lee M, Ovbiagele B. Catheter ablation compared with medical therapy for atrial fibrillation with heart failure: a systematic review and meta-analysis of randomized controlled trials. *Int J Med Sci*. (2021) 18(6):1325–31. doi: 10.7150/ijms.52257

18. Mujović N, Marinković M, Lenarczyk R, Tilz R, Potpara TS. Catheter ablation of atrial fibrillation: an overview for clinicians. *Adv Ther*. (2017) 34(8):1897–917. doi: 10.1007/s12325-017-0590-z

frontiers | Frontiers in Cardiovascular Medicine

TYPE Original Research
PUBLISHED 22 May 2023
DOI 10.3389/fcvm.2023.1187169

OPEN ACCESS

EDITED BY
Robert Sheldon,
University of Calgary, Canada

REVIEWED BY
Glen Sumner,
University of Calgary, Canada
Derek Chew,
University of Calgary, Canada

*CORRESPONDENCE
Yingxue Dong
dong_yignxue@126.com

†These authors have contributed equally to this work

RECEIVED 15 March 2023
ACCEPTED 05 May 2023
PUBLISHED 22 May 2023

CITATION
Ma C, Wang Z, Ma Z, Ma P, Dai S, Wang N, Yang Y, Li G, Gao L, Xia Y, Xiao X and Dong Y (2023) The feasibility and safety of his-purkinje conduction system pacing in patients with heart failure with severely reduced ejection fraction. Front. Cardiovasc. Med. 10:1187169. doi: 10.3389/fcvm.2023.1187169

The feasibility and safety of his-purkinje conduction system pacing in patients with heart failure with severely reduced ejection fraction

Chengming Ma[1†], Zhongzhen Wang[1†], Zhulin Ma[2], Peipei Ma[1], Shiyu Dai[1], Nan Wang[1], Yiheng Yang[1], Guocao Li[1], Lianjun Gao[1], Yunlong Xia[1], Xianjie Xiao[1] and Yingxue Dong[1*]

[1]Department of Cardiology, Institute of Cardiovascular Diseases, First Affiliated Hospital of Dalian Medical University, Dalian, China, [2]Department of Graduate School, Dalian Medical University, Dalian, China

Objective: The purpose of this study was to evaluate the feasibility and outcomes of conduction system pacing (CSP) in patients with heart failure (HF) who had a severely reduced left ventricular ejection fraction (LVEF) of less than 30% (HFsrEF).
Methods: Between January 2018 and December 2020, all consecutive HF patients with LVEF < 30% who underwent CSP at our center were evaluated. Clinical outcomes and echocardiographic data [LVEF and left ventricular end-systolic volume (LVESV)], and complications were all recorded. In addition, clinical and echocardiographic (≥5% improvement in LVEF or ≥15% decrease in LVESV) responses were assessed. The patients were classified into a complete left bundle branch block (CLBBB) morphology group and a non-CLBBB morphology group according to the baseline QRS configuration.
Results: Seventy patients (66 ± 8.84 years; 55.7% male) with a mean LVEF of 23.2 ± 3.23%, LVEDd of 67.33 ± 7.47 mm and LVESV of 212.08 ± 39.74 ml were included. QRS configuration at baseline was CLBBB in 67.1% (47/70) of patients and non-CLBBB in 32.9%. At implantation, the CSP threshold was 0.6 ± 0.3 V @ 0.4 ms and remained stable during a mean follow-up of 23.43 ± 11.44 months. CSP resulted in significant LVEF improvement from 23.2 ± 3.23% to 34.93 ± 10.34% ($P < 0.001$) and significant QRS narrowing from 154.99 ± 34.42 to 130.81 ± 25.18 ms ($P < 0.001$). Clinical and echocardiographic responses were observed in 91.4% (64/70) and 77.1% (54/70) of patients. Super-response to CSP (≥15% improvement in LVEF or ≥30% decrease in LVESV) was observed in 52.9% (37/70) of patients. One patient died due to acute HF and following severe metabolic disorders. Baseline BNP (odds ratio: 0.969; 95% confidence interval: 0.939–0.989; $P = 0.045$) was associated with echocardiographic response. The proportions of clinical and echocardiographic responses in the CLBBB group were higher than those in the non-CLBBB group but without significant statistical differences.
Conclusions: CSP is feasible and safe in patients with HFsrEF. CSP is associated with a significant improvement in clinical and echocardiographic outcomes, even for patients with non-CLBBB widened QRS.

KEYWORDS

his-purkinje conduction system pacing, heart failure, severely reduced ejection fraction, his-bundle pacing, left bundle branch pacing

Introduction

Heart failure (HF) remains a major health and economic burden worldwide with high incidence, hospitalizations, and mortality (1, 2). HF patients with a severely reduced left ventricular ejection fraction (LVEF) of less than 30% (HFsrEF) are not rare. These patients have a high risk of admission, progression to advanced HF, and mortality even after receiving maximal and optimal pharmacological therapy. Patients with HFsrEF are becoming more prevalent due to the ageing population, increasing number of HF patients, and improved treatment (3). Providing a better treatment is crucial to improving prognosis and lowing medical costs for these patients.

Conduction system pacing (CSP), including His bundle pacing (HBP) and left bundle branch pacing (LBBP), is an alternative strategy for achieving cardiac resynchronization therapy (CRT) in HF patients with reduced EF (HFrEF) and ventricular desynchrony (4, 5). Most guidelines recommended LVEF $\leq$ 35% as a crucial inclusion criterion for CRT selection, and the LVEF values in most randomized controlled trials (RCTs) focusing on CSP ranged from 30% to 40%. However, due to limited clinical trials, the feasibility, safety and benefits of CSP in patients with HFsrEF (<30%) remains unknown. Furthermore, patients with typical complete left bundle branch block (CLBBB) QRS morphology show a better CRT response than patients with non-CLBBB morphology (6). However, CRT response in patients with a non-CLBBB widened QRS remains uncertain.

This research aimed to describe the feasibility and safety of CSP in patients with HFsrEF and evaluate the clinical and echocardiographic responses to CSP.

Materials and methods

This was a retrospective, single-center and observational study. Written informed consent was obtained from all enrolled patients. The local ethics committee approved this study. The data from our research are available from the corresponding author upon request.

Study patients

All consecutive HF patients with LVEF < 30% treated with CSP in our center from January 2018 to December 2020 were collected, and all the patients met the CRT indication (**Figure 1**). All patients received guideline-directed medical treatment for at least three months before implantation. Patients who lost follow-up or could not perform device programming after the CSP procedure were excluded from this study.

Implant procedure

The detailed implant procedure was found in this article (7). In brief, a pre-shaped sheathing canal was inserted into the superior vena cava via the left or right subclavian vein approach. A Select Secure pacing lead (Model 3,830–69 cm, Medtronic, Minneapolis, Minnesota, USA) was introduced into the right atrium via a fixed curve sheathing canal (C315HIS; Medtronic, Minneapolis, Minnesota, USA). Endocardial mapping was performed using a unipolar mapping technique with the pacing lead. During the HBP procedure, the pacing lead initially obtained the HB potential. The preferred site was defined as a narrow paced QRS with the same QRS morphology as the intrinsic QRS and successful correction of LBBB with satisfactory pacing thresholds. During the LBBP procedure, the initial site of LBBP at the right ventricular septum was advanced 1–2 cm anteriorly and inferiorly into the ventricle along an imaginary line between the His and the right ventricle apex in the right anterior oblique projection. The location of the LBBP site was guided using the distal HBP location or the paced QRS morphology ("W" pattern with a notch at the nadir of the QRS in lead V1). Subsequently, the lead was inserted deeply into the muscular interventricular septum with caution. When LBB capture was confirmed with a low threshold, additional rotations were stopped. The preferred location was determined using criteria that had already been disclosed. An abrupt reduction in the stim to LV active time (LVAT) of longer than 10 ms and the morphologies of qR, Qr, or rSR′ in lead V1 was the criteria for the LBBB correct in the LBBP procedure.

Follow-up

All patients were followed up at the clinic 1-month, 6-month, and 12-month following the CSP procedure and then every 6 months after that. The device programming was performed at the time of discharge and each subsequent visit. The pacing parameters were collected, including bipolar R-wave amplitude, bipolar capture threshold and impedance. All transthoracic echocardiography (TTE) parameters at pre-implantation and post-implantation were collected, including LVEF, left ventricular end-diastolic diameter (LVEDd), left ventricular end-systolic volume (LVESV), and emerging or worsening tricuspid regurgitation (TR). Post-implantation echocardiographic outcomes were based on the last available follow-up. The baseline and post-procedural ECGs were analyzed, including QRS duration, QRS pattern, and QRS axis. The New York Heart Association (NYHA) cardiac function classification was documented. The following complications were recorded: a significant increase in pacing threshold (defined as a >1 V increase in capture threshold after implantation or capture threshold >5 V @ 0.4 ms at any follow-up visit), loss of capture, lead dislodgement, and cardiac perforation. All patients received guideline-directed medical treatment.

Response to CSP

The primary outcome was the clinical and echocardiographic responses to CSP. The secondary outcome was rehospitalization for HF and all-cause death. The definition of response to CSP was consistent with most studies in the literature, including the

following: (1) the documentation of an increase in LVEF ≥ 5% or decrease in LVESV ≥ 15% after 6 months relative to baseline, (2) clinical improvement in NYHA class ≥1 or NHYA class Ⅰ at last observation carried forward, or a ≥25% increase in 6-MWD (8–10). The super-response to CSP was defined as a ≥15% improvement in the LVEF or a ≥30% decrease in the LVESV with clinical improvements after 6 months relative to baseline. A non-responder was classified as a patient who had worsened HF, no improvement in clinical features, or a <5% increase in LVEF.

CLBBB morphology vs. non-CLBBB morphology

According to the baseline QRS configuration, the patients were classified into a CLBBB morphology (CLBBB + RVP) group and a non-CLBBB morphology group. RVP causes an CLBBB type QRS pattern and results in LV desynchrony; thus, patients who upgraded from RVP were assigned to the CLBBB morphology group. The clinical and echocardiographic responses to CSP were compared.

Statistical analysis

The data analysis was performed using SPSS 22.0 (SPSS Inc., Chicago, USA). The quantitative data were expressed as the mean ± standard deviation (SD) if normally distributed; they were described by median [25th quarter, 75th quarter] if non-normally distributed. The homogeneity of variance was tested by Kolmogorov–Smirnov Goodness. The categorical data were expressed in terms of frequency and percentage. An unpaired t-test or nonparametric Mann–Whitney *U* test was performed for comparison between groups for quantitative data. For categorical variables, chi-square tests or Fisher's exact tests were used. A 2-tailed *P*–value <0.05 was considered statistically significant.

Results

Baseline characteristics of study patients

Between January 2018 to December 2021, 70 patients (66 ± 8.84 years; 55.7% male) were included in this study. The mean baseline LVEF of these patients was 23.2 ± 3.23%, and their mean baseline LVEDd and LVESV were 67.33 ± 7.47 mm, and 212.08 ± 39.74 ml, respectively. The mean NYHA class was 3.46 ± 0.55 (NYHA Ⅱ in 2 (2.9%) patients, Ⅲ in 33 (47.1%) patients, Ⅲ-Ⅳ in 1 (1.4%) patient, and Ⅳ in 34 (48.6%) patients) with a baseline BNP of 787.63 pg/ml. The mean QRS duration was154.99 ± 34.42 ms. Among them, CRT indicated for HFrEF with CLBBB in 48 (68.6%) patients, HFrEF with inner-ventricular conduct delay (IVCD) in 7 (10%) patients, HFrEF with permanent atrial fibrillation (AF) being eligible for atrioventricular junction (AVJ) ablation in 4 (5.7%) patients, expected high ventricular pacing (VP) burden in 7 (10%) patients and upgrading for low LVEF due to RV pacing in the remaining 4 (5.7%) patients (**Figure 1**). Other baseline characteristics of the enrolled patients are shown in **Table 1**.

CSP implantation

The CSP procedure was successfully performed in all patients. Among them, 52 (74.29%) patients received HBP, and 18 (25.71%) patients received LBBP. After the implantation, all patients with widened QRS (CLBBB + RVP) were corrected, and the mean

TABLE 1 Baseline characteristics of enrolled patients.

	n = 70
Age (years), mean ± SD	66 ± 8.84
Male, *n* (%)	39 (55.7%)
ICM, *n* (%)	18 (25.7%)
Hypertension, *n* (%)	32 (45.7%)
Diabetes mellitus, *n* (%)	18 (25.7%)
DCM, *n* (%)	30 (42.9%)
Atrial fibrillation, *n* (%)	30 (42.9%)
CKD, *n* (%)	7 (10%)
Valve replacement, *n* (%)	9 (12.9%)
Mitral valve	5 (7.1%)
Aortic valve	3 (4.3%)
Mitral valve replacement + tricuspid annuloplasty	1 (1.4%)
Tricuspid regurgitation	43 (61.4%)
NYHA class	3.46 ± 0.55
Ⅰ	0
Ⅱ	2 (2.9%)
Ⅲ	33 (47.1%)
Ⅲ–Ⅳ	1 (1.4%)
Ⅳ	34 (48.6%)
6-MWD (m), mean ± SD	166.14 ± 54.52
BNP (pg/ml), median, [25% percentile,75% percentile] IQR1854	787.63 [402.83, 1686.63]
LVEF (%), mean ± SD	23.2 ± 3.23
LVEDd (mm), mean ± SD	67.33 ± 7.47
LVESV (ml), mean ± SD	212.08 ± 39.74
QRS duration (ms), mean ± SD	154.99 ± 34.42
QRS axis (°), median, [25% percentile,75% percentile] IQR75	−7, [−33.25, 35.5]
CLBBB	48 (68.6%)
IVCD	7 (10%)
Expected high VP burden	7 (10%)
Upgrade from RVP	4 (5.7%)
AF + AVJ ablation	4 (5.7%)
Previous implanted pacemakers, *n* (%)	14 (20%)
CRT	13 (16.5%)
RVP	4 (5.7%)
Pharmacological therapy for HF	
ACE inhibitors/ARB/ARNI	25 (35.7%)
Beta blockers	39 (55.7%)
MRA	60 (85.7%)
Diuretics	54 (77.1%)

DCM, dilated cardiomyopathy; ICM, Ischemic cardiomyopathy; CKD, chronic kidney disease; 6-MWD, 6 min' walk distance; BNP, brain natriuretic peptide; LVEF, left ventricular ejection fraction; LVEDd, left ventricular end-diastolic diameter; LVESV, left ventricular end-systolic volume; NYHA, New York Heart Association; CLBBB, complete left branch bundle block; IVCD, inner-ventricular conduct delay; CRT, cardiac resynchronization therapy; RVP, right ventricular pacing; MRA, mineralocorticoid receptor antagonists; ACE, angiotensin-converting enzyme; ARB, angiotensin receptor blockers; ARNI, angiotensin receptor neprilysin inhibitors; AVJ, atrioventricular junction.

TABLE 2 Clinical outcomes of the patients and changes in TTE.

	Baseline	Post-implantation	*P*
NYHA classification	3.46 ± 0.55	1.87 ± 0.92	<0.001
None	0	8 (11.4%)	
I	0	10 (14.3%)	
II	2 (2.9%)	35 (50%)	
III	33 (47.1%)	17 (24.3%)	
III–IV	1 (1.4%)	0	
IV	34 (48.6%)	0	
6-MWD (m)	166.14 ± 54.52	474.29 ± 293.38	<0.001
LVEF (%)	23.2 ± 3.23	34.93 ± 10.34	<0.001
LVEDd (mm)	67.33 ± 7.47	61.4 ± 8.9	<0.001
LVESV (ml)	212.08 ± 39.74	119.08 ± 64.09	<0.001
QRS duration (ms)	154.99 ± 34.42	130.81 ± 25.18	<0.001
QRS axis (°)	−7, [−33.25, 35.5]	12.5, [−11.5, 33]	0.578

LVEF, left ventricular ejection fraction; LVEDd, left ventricular end-diastolic diameter; LVESV, left ventricular end-systolic volume; NYHA, New York Heart Association.

postprocedural QRS duration was 131.75 ± 22.29 ms, significantly narrower than baseline (166.52 ± 23.99 ms, $P < 0.001$).

The mean capture threshold at implantation was 0.63 ± 0.31 V@ 0.4 ms, slightly decreased at 1-month post-implantation, and no increase was observed during the 1-year follow-up period. The R-wave amplitudes were 4.10 [2.73, 7.07] mV and impedance were 635.90 ± 141.73 Ω, with no significant increase noted during the follow-up. Capture threshold increase >1 V was noted in 4 (5.71%) patients. No dislodgments were observed. Other procedure related complications, such as thrombosis, infection, perforation, and stroke, were also not detected during the follow-up.

Clinical outcomes

During the mean follow-up period of 23.43 ± 11.44 months, compared with pre-implantation, a significant increase in LVEF

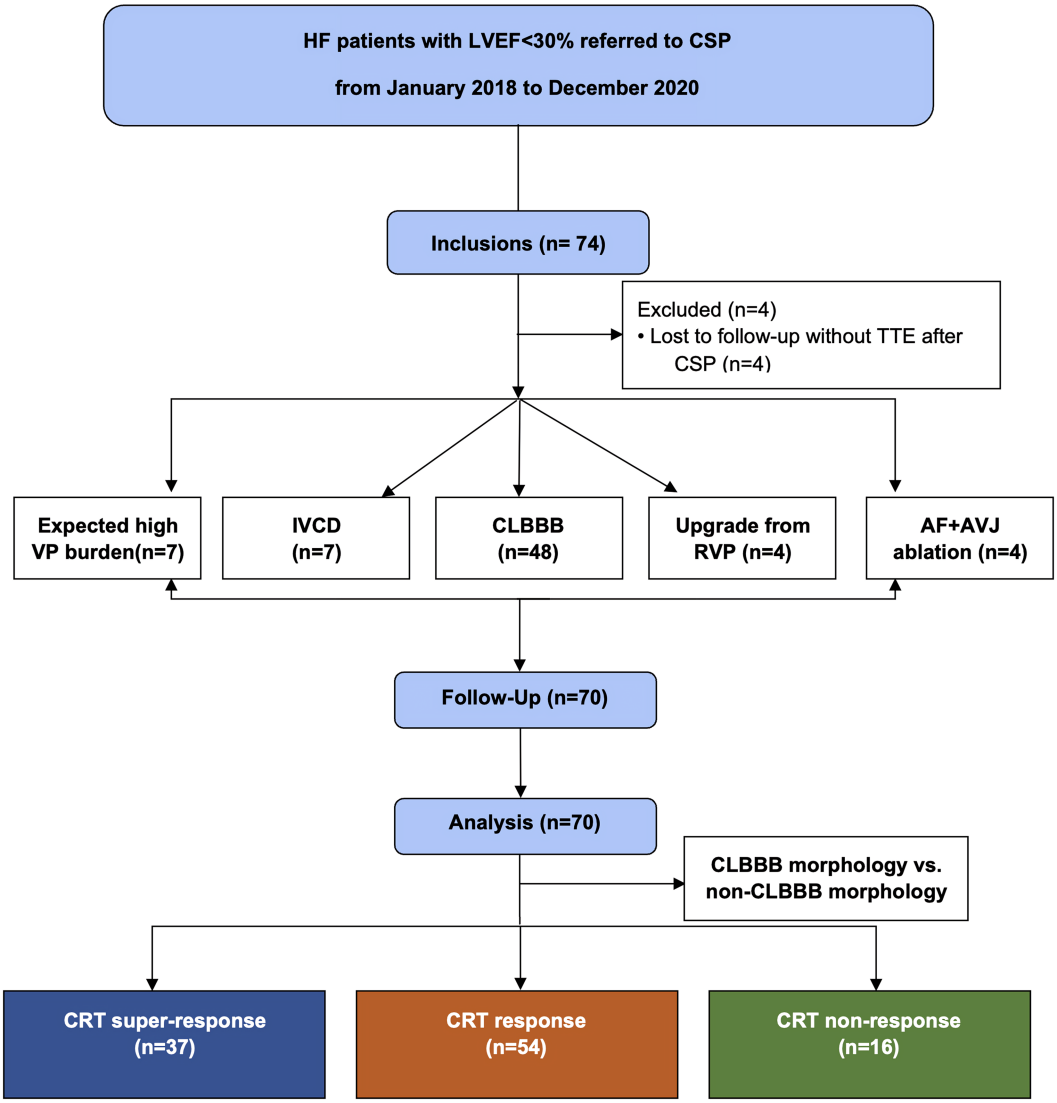

FIGURE 1
Flow chart of patients screened for inclusion in this study. IVCD, inner-ventricular conduct delay; CRT, cardiac resynchronization therapy; VP, ventricular pacing; CSP, conduction system pacing; CLBBB, complete left branch bundle block; RVP, right ventricular pacing; AF, atrial fibrillation; AVJ, atrioventricular junction; TTE, transthoracic echocardiography.

10.3389/fcvm.2023.1187169

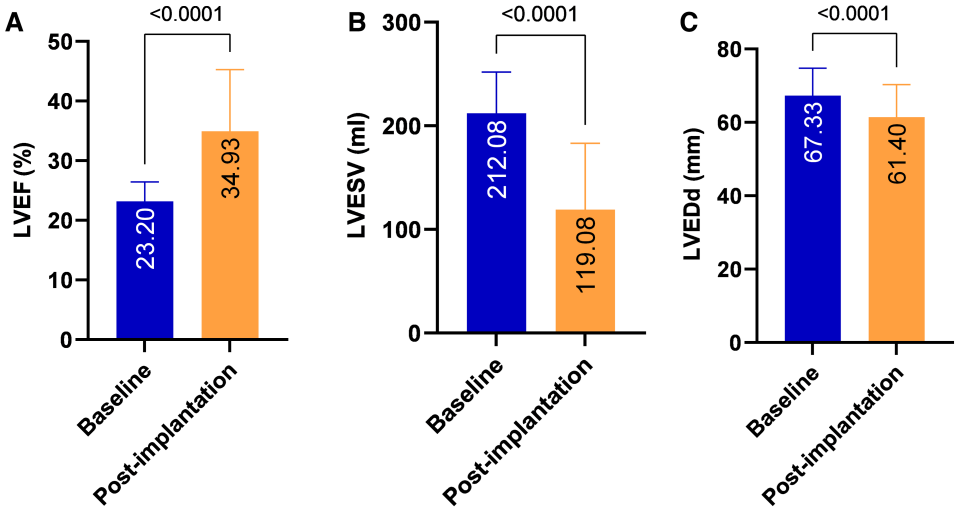

FIGURE 2
Echocardiographic performance after CSP. Significant improvements in LVEF (A), LVESV (B) and LVEDd (C) were observed after CSP in all patients. LVEF, left ventricular ejection fraction; LVEDd, left ventricular end-diastolic diameter; LVESV, left ventricular end-systolic volume; CSP, conduction system pacing.

(23.2 ± 3.23% vs. 034.93 ± 10.34%, $P < 0.001$), a decrease in LVESV (212.08 ± 39.74 vs. 119.08 ± 64.09 ml, $P < 0.001$) and a reduction in LVEDd (67.33 ± 7.47 vs. 61.4 ± 8.9 mm, $P < 0.001$) were observed (Table 2 and Figure 2). A significant improvement in the NYHA class and 6-MWD post-implantation was observed in all patients (3.46 ± 0.55 vs. 1.87 ± 0.92, $P < 0.001$; 166.14 ± 54.52 m vs. 474.29 ± 293.38 m, $P < 0.001$, Table 2 and Figure 3). A significant QRS narrowing from 154.99 ± 34.42 to 130.81 ± 25.18 ms ($P < 0.001$) was observed after the CSP (Figure 3). In addition, the mean number of rehospitalizations was 0.53 ± 0.28, and one patient died 13 months after implantation due to acute HF and subsequently severe metabolic disorders.

Of 70 patients in the study, 37 (52.9%) patients achieved a mean increase of 17.78 ± 10.4% in LVEF and were categorized as super-responders (Figure 4A). There were 43 (61.4%) patients who achieved a >10% increase in LVEF. In addition, a positive echocardiographic response to CRT was detected in 54 (77.1%) patients with a mean LVEF increase of 14.61 ± 9.89%. Sixteen (22.9%) patients had a <5% increase in LVEF; however, no patient had a decrease in LVEF during the follow-up. Sixty-four (91.4%) patients obtained a clinical improvement.

After multivariable logistic regression analysis, only baseline BNP (odds ratio: 0.969; 95% confidence interval: 0.939 to 0.989; $P = 0.045$) was associated with CRT response (Table 3).

CLBBB morphology vs. non-CLBBB morphology

Among all the enrolled patients, 52 patients (48 patients with CLBBB and 4 patients upgraded to CSP from RVP) were in the CLBBB morphology group, and 18 patients were in the non-CLBBB morphology. No significant differences in sex, age, HF duration, and baseline BNP were detected between the two groups.

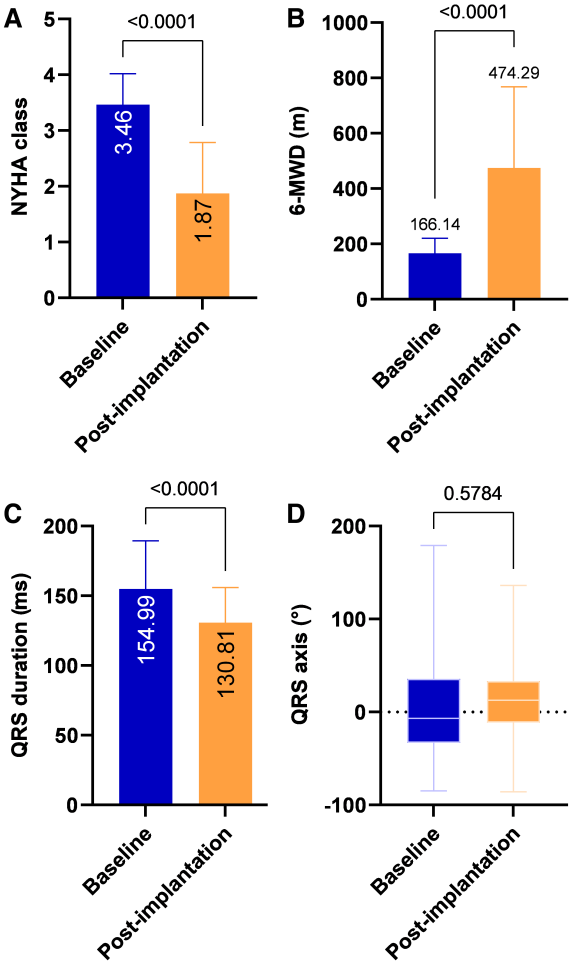

FIGURE 3
Clinical outcomes after CSP. Compared with pre-implantation, NYHA class and 6-MWD improved significantly at post-implantation (A, B). QRS duration after CSP was significantly reduced (C) with no apparent change in QRS axis (D). 6-MWD, 6-minute walk distance; NYHA, New York Heart Association.

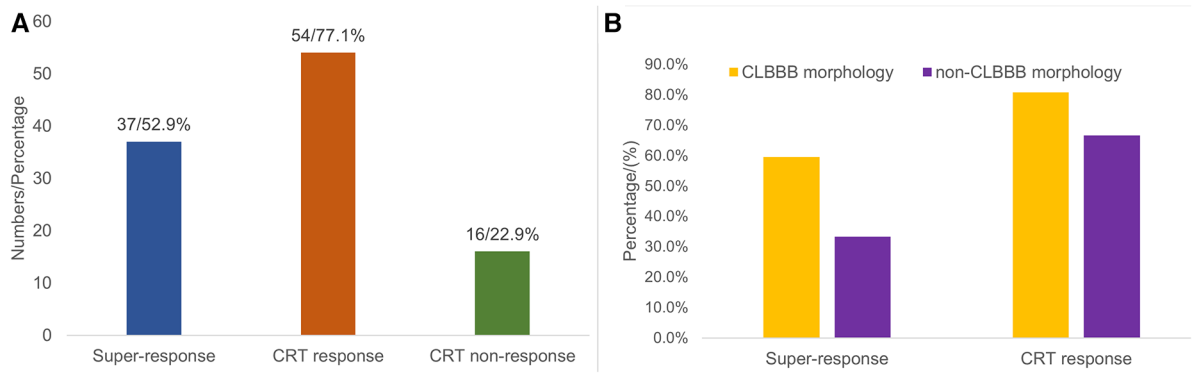

FIGURE 4
Distribution chart of CRT response. Among all 70 patients, 37 (52.9%) patients were classified as super-responders, 54 (77.1%) patients were classified as CRT-responders, and 16 (22.9%) patients had no response to CRT (A). The proportion of super-response (59.6% vs. 33.3%, $P = 0.054$) and response to CRT (80.8% vs. 66.7%, $P = 0.219$) in the CLBBB group were higher than those in the non-CLBBB group but without significant statistical differences (B). CRT, cardiac resynchronization therapy; CLBBB, complete left branch bundle block.

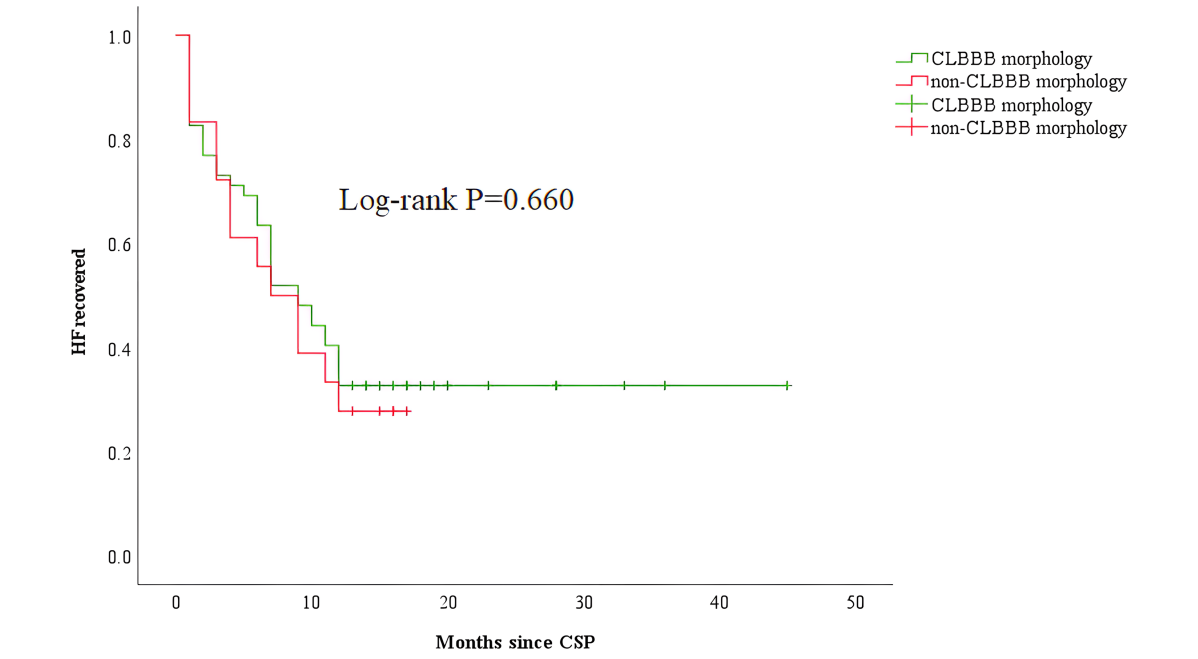

FIGURE 5
Kaplan–Meier curve comparing HF recovered between patients with CLBBB and non-CLBBB morphology. CSP, conduction system pacing; CLBBB, complete left branch bundle block; HF, heart failure.

The baseline characteristics of the two groups were summarized in Supplementary Table S1. The baseline QRS duration in the CLBBB morphology group was wider than that in the non-CLBBB morphology group. The baseline NYHA class, LVEF, LVEDd, and LVESV in the CLBBB morphology group were more severe than those in the non-CLBBB morphology group. There was no significant statistical difference in post-procedural NYHA class, 6-MWD, LVEF, LVEDd, LVESV, and QRS duration between the two groups (Supplementary Table S2). The proportion of super-response and response to CRT in the CLBBB group were higher than those in the non-CLBBB group but without significant statistical differences (Super-response: 59.6% vs. 33.3%, $P = 0.054$; CRT response: 80.8% vs. 66.7%, $P = 0.219$, Supplementary Table S2 and Figure 4B). No difference in time to HF recovered between the two groups (Figure 5).

Discussion

The present study found that CSP is feasible and safe and improves LV function for HF patients with LVEF < 30%. Furthermore, CSP is associated with significantly improving clinical and echocardiographic outcomes, even for patients with non-CLBBB widened QRS.

TABLE 3 Independent predictors of CSP response.

Variables	Univariate analysis		Multivariable analysis	
	OR (95%CI)	*P*	OR (95%CI)	*P*
Sex (male)	0.696 (0.222–2.187)	0.535	0.56 (0.101–3.103)	0.507
Age	1.007 (0.946–1.073)	0.82	1.07 (0.974v1.175)	0.158
CLBBB	1.847 (0.586–5.819)	0.295	3.174 (0.303–33.31)	0.335
ICM	0.476 (0.144–1.578)	0.225	0.272 (0.036–2.055)	0.207
Hypertension	2.2 (0.673–7.189)	0.192	10.274 (1.176–13.531)	0.083
Diabetes mellitus	1.05 (0.291–3.795)	0.941	0.862 (0.147–5.044)	0.869
DCM	0.954 (0.31–2.939)	0.935	4.72 (0.621–6.220)	0.134
AF	0.688 (0.224–2.108)	0.512	0.870 (0.155–4.874)	0.874
CKD	0.347 (0.069–1.746)	0.199	0.173 (0.023–1.316)	0.090
LVEF	1.002 (0.842–1.192)	0.986	0.942 (0.727–1.22)	0.648
LVEDd	0.947 (0.876–1.025)	0.176	0.992 (0.872–1.129)	0.907
LVESV	0.355 (0.068–1.841)	0.218	1.007 (0.975–1.041)	0.666
BNP	0.969 (0.939–0.999)	0.045	0.969 (0.939–0.989)	0.045
NYHA class	1.121 (0.409–3.076)	0.824	1.452 (0.125–16.87)	0.766
6-MWD	1.24 (0.414–3.716)	0.701	1.108 (0.062–19.73)	0.944
QRS duration	1.007 (0.856–1.186)	0.929	1.108(0.874–1.406)	0.397

DCM, dilated cardiomyopathy; ICM, Ischemic cardiomyopathy; CKD, chronic kidney disease; 6-MWD, 6 min walk distance; BNP, brain natriuretic peptide; LVEF, left ventricular ejection fraction; LVEDd, left ventricular end-diastolic diameter; LVESV, left ventricular end-systolic volume; NYHA, New York Heart Association; CLBBB, complete left branch bundle block; IVCD, inner-ventricular conduct delay; CRT, cardiac resynchronization therapy; RVP, right ventricular pacing.

HF with severely reduced EF

Patients with HFsrEF are not uncommon in clinical practice and frequently present with advanced HF, particularly in elderly patients (11). Many patients have poor prognoses, persistent symptoms, and a high rehospitalization rate despite receiving optimal drug treatment. To the best of our knowledge, there is no consensus on the definition of severely reduced EF. LVEF ≤ 30% is a criterion for diagnosing advanced HF in ESC guidelines and is used as a severity partition cut-off value for 2-dimensional echocardiography-derived LVEF (12, 13). Our study's baseline LVEF of enrolled patients ranged from 15% to 27%, with considerably enlarged LVEDd and LVESV. The median baseline NHYA class was at grade 3.46, with 97.1% of patients in NHYA class above grade 3, demonstrating the severity of these patients.

Patients with HFsrEF are becoming more prevalent due to the ageing population, increasing number of HF patients, and improved treatment (3). A large study of patients with chronic HF demonstrated that improving LVEF was associated with better outcomes and a lower risk for cardiovascular events (14). However, although optimal medical therapies have been thoroughly studied to improve cardiac function, managing the severely reduced EF in patients with HF remains a therapeutic challenge. CSP may provide a practical treatment choice to improve clinical outcomes for these patients.

CSP in patients with HFsrEF

To date, most guidelines recommend CRT in patients with LBBB and LVEF ≤ 35%, for those who subsequently develop symptomatic HF with decreased LV function following right ventricular (RV) pacing, and for atrioventricular (AV) block with poor LV function. CRT should also be considered for patients with AF who are candidates for AV node ablation, irrespective of QRS duration. CSP is an alternative strategy for achieving CRT. Several RCTs have demonstrated that CSP is superior to RV pacing in improving quality of life, NYHA class, and LV function in patients with HFrEF. However, the data on the benefit of CSP in patients with severely reduced EF was limited. The mean baseline LVEF values in several early small-sample studies focusing on HBP in HFrEF and LBB were less than 30% (15–17). The HBP was successful in 56%–76% of enrolled patients, achieving significant improvements in clinical outcomes and an approximately 5% increase in LVEF. Vijayaraman et al. evaluated His-Optimized CRT in 27 HF patients with a baseline LVEF of 24 ± 7% (NYHA class Ⅲ-Ⅳ). They reported a favorable clinical responder (NYHA class decreased to 2.04) in 84% and an echocardiographic response (LVEF grew to 38 ± 10%) in 92% of patients (18). Our study also demonstrated that CSP significantly improves HF symptoms, 6-MWD and NYHA classifications in patients with HFsrEF. Most patients had an echocardiographic response, and LV function improved significantly. Additionally, 77.1% of patients were CRT responders, 52.9% were CRT super-responder, and no patient had a reduction in LVEF during the follow-up. This satisfactory response rate to CSP provides us confidence in treating patients with HFsrEF with CSP.

Moreover, CSP has significantly facilitated implantation compared to CRT and has become more extensively employed in well-established centers. And, in our experience, with an experienced operator, CSP could be completed in a reasonably short time (in 2 h) and significantly decreased the duration of device implantation. Finally, even for patients with HFsrEF in the present study, none suffered from intraprocedural acute HF, and no severe complication was detected. Therefore, CSP may also be appropriate for patients with advanced HF.

In fact, CRT may be underutilized in these patients due to concerns about severe symptoms, a poor prognosis, and questionable improvement. Recently, a position statement on CRT by the Heart Failure Association (HFA) with several other European associations indicated that many HF patients are not exposed to the full potential benefit of CRT (19). They advocated for enhanced patient screening to identify potential eligible CRT candidates, ECG surveillance in HF patients, and comprehensive CRT education in primary and secondary care settings.

CRT response in patients with HFsrEF

In our study, CRT response was observed in 77.1% of enrolled patients, indicating CSP was highly effective for patients with severely impaired systolic. On the other hand, the patients who had no response to CRT presented with a 2% increase in LVEF and a significant improvement in HF symptoms. In addition, symptom improvement was more pronounced and occurred earlier than echocardiographic improvement. This finding was

consistent with most other studies, demonstrating that the proportion of super- and non-responders is low and that even non-responders are likely to obtain a clinical improvement (16, 20, 21). There is no consensus regarding the definition of CRT response or whether the echocardiographic response is a decisive criterion for CRT response (22). It is well known that LV reverse remodeling is poorly related to symptom improvement. LV remodeling is a long-term process and is likely to be maximal more than 2 years following CRT (23). Furthermore, patients with advanced decompensated HF who fail to achieve significant LV reverse remodeling in the early CRT post-implantation may still obtain hemodynamic benefits (24). Indeed, patients assessed as "non-responders" may have benefited symptomatically in NYHA class and 6-MWD. Thus, we believe that using echocardiographic response to evaluate CRT response may underestimate the benefits of CRT. HF is incurable, and the goal of treatment is to slow the disease progression. As CRT is a treatment for "disease modification", the concept of "remission" and "non-remission" may be more appropriate for assessing the effect of CRT rather than "response" and "non-response" (19).

Predictors of response to CRT

Several characteristics have been proven to predict a favorable CRT response. The patients with wide QRS and LBBB morphology, echocardiographic evidence of desynchrony, non-ischemic cardiomyopathy (ICM), and female sex responded favorably to CRT. In a meta-analysis of 5 randomized trials using individual patient data, QRS width was found to be a powerful predictor of response to CRT (25). In most guidelines, QRS duration ≥150 ms is listed as an inclusion criterion of recommendation for CRT. In contrast, CRT is not suggested in patients with a QRS duration <130 ms who are not candidates for RVP (26). Patients with typical LBBB QRS morphology show a better CRT response than patients with non-LBBB morphology (6). However, CRT response in patients with a non-CLBBB widened QRS remains uncertain. In our study, compared to patients with non-CLBBB, patients with CLBBB obtained more significant clinical and echocardiographic improvements from CSP.

The association between the etiology of HF and CRT response is also unclear. The magnitude of the echocardiographic response to CRT in patients with non-ICM is significantly higher than in those with ICM (27). Moreover, QRS narrowing after CRT was associated with clinical and echocardiographic CRT response (28). CRT response predictors are similar to those for reverse LV remodeling (29). A prospective registry study of outpatients with HFrEF found that shorter HF duration, no implantable cardioverter, lower LVEF, non-ICM, and no coronary disease were associated with significantly LVEF increase (30). However, only baseline BNP was associated with CRT response after multivariable analysis in our study.

This study has several limitations. First, this is a retrospective study with some patients without strict Strauss criteria for CLBBB. However, these patients represented only about 30% of this study and were compared with true CLBBB in terms of clinical outcomes. Moreover, most of the enrolled patients underwent the CSP procedure within the last 4 years. The CSP was performed mainly through one experienced operator, and only 4 patients were lost to follow-up, which helped to minimize bias. Second, the sample size was limited, but HF patients with LVEF < 30% who underwent CSP were relatively few. Third, the NYHA class is based on patients' symptoms. It is worth noting that when a patient feels significantly better after CSP, their attention may be directed towards less frequent admission to the hospital. However, 6-MWD is an objective indicator of HF symptoms. Fourth, we could not completely exclude that pharmacological therapy for HF contributed to the favorable prognosis. However, due to the low blood pressure, most HF patients with very low EF are intolerant to these drugs. In our analysis, there was no difference in drug use between CSP responders and non-responders. Finally, as a retrospective study, this study lacked intraprocedural ECG data.

Conclusions

CSP is feasible and safe in patients with HFsrEF, and it is associated with significantly better clinical and echocardiographic outcomes.

Data availability statement

The original contributions presented in the study are included in the article/**Supplementary Material**, further inquiries can be directed to the corresponding authors.

Ethics statement

The studies involving human participants were reviewed and approved by First affiliated hospital of Dalian medical university. The patients/participants provided their written informed consent to participate in this study.

Author contributions

CM and ZW contributed equally to this article. XX and YD contributed to the conception and design of the study. CM and ZW searched literatures and were major contributors in writing the manuscript. CM, ZM, and PM performed data acquisition and analysis. ZM, SD, YY, and NW followed up with the patients. GL, LG, and YX reviewed the manuscript. All authors contributed to the article and approved the submitted version.

Funding

This work was supported by the Scientific and Technological Innovation Foundation of Dalian City (2020JJ26SN055).

Acknowledgments

We greatly appreciate all the participants in the study.

Conflict of interest

The authors declare that the research was conducted in the absence of any commercial or financial relationships that could be construed as a potential conflict of interest.

Publisher's note

Supplementary material

The Supplementary Material for this article can be found online at: https://www.frontiersin.org/articles/10.3389/fcvm.2023.1187169/full#supplementary-material.

References

1. Tomasoni D, Adamo M, Anker MS, von Haehling S, Coats AJS, Metra M. Heart failure in the last year: progress and perspective. *ESC Heart Fail* (2020) 7(6):3505–30. doi: 10.1002/ehf2.13124

2. Wang H, Chai K, Du M, Wang S, Cai JP, Li Y, et al. Prevalence and incidence of heart failure among urban patients in China: a national population-based analysis. *Circ Heart Fail* (2021) 14(10):e008406. doi: 10.1161/circheartfailure.121.008406

3. Truby LK, Rogers JG. Advanced heart failure: epidemiology, diagnosis, and therapeutic approaches. *JACC Heart Fail* (2020) 8(7):523–36. doi: 10.1016/j.jchf.2020.01.014

4. Vijayaraman P, Ponnusamy S, Cano Ó, Sharma PS, Naperkowski A, Subsposh FA, et al. Left bundle branch area pacing for cardiac resynchronization therapy: results from the international lbbap collaborative study group. *Jacc Clin Electrophysiol* (2021) 7(2):135–47. doi: 10.1016/j.jacep.2020.08.015

5. Abdelrahman M, Subzposh FA, Beer D, Durr B, Naperkowski A, Sun H, et al. Clinical outcomes of his bundle pacing compared to right ventricular pacing. *J Am Coll Cardiol* (2018) 71(20):2319–30. doi: 10.1016/j.jacc.2018.02.048

6. Cunnington C, Kwok CS, Satchithananda DK, Patwala A, Khan MA, Zaidi A, et al. Cardiac resynchronisation therapy is not associated with a reduction in mortality or heart failure hospitalisation in patients with non-left bundle branch block qrs morphology: meta-analysis of randomised controlled trials. *Heart*. (2015) 101(18):1456–62. doi: 10.1136/heartjnl-2014-306811

7. Huang W, Chen X, Su L, Wu S, Xia X, Vijayaraman P. A beginner's guide to permanent left bundle branch pacing. *Heart Rhythm* (2019) 16(12):1791–6. doi: 10.1016/j.hrthm.2019.06.016

8. Chung ES, Leon AR, Tavazzi L, Sun J-P, Nihoyannopoulos P, Merlino J, et al. Results of the predictors of response to crt (prospect) trial. *Circulation*. (2008) 117 (20):2608–16. doi: 10.1161/circulationaha.107.743120

9. Daubert JC, Saxon L, Adamson PB, Auricchio A, Berger RD, Beshai JF, et al. 2012 Ehra/hrs expert consensus statement on cardiac resynchronization therapy in heart failure: implant and follow-up recommendations and management: a registered branch of the European society of cardiology (esc), and the heart rhythm society; and in col. *Europace*. (2012) 14(9):1236–86. doi: 10.1093/europace/eus222

10. Hsu JC, Solomon SD, Bourgoun M, McNitt S, Goldenberg I, Klein H, et al. Predictors of super-response to cardiac resynchronization therapy and associated improvement in clinical outcome: the madit-crt (multicenter automatic defibrillator implantation trial with cardiac resynchronization therapy) study. *J Am Coll Cardiol*. (2012) 59(25):2366–73. doi: 10.1016/j.jacc.2012.01.065

11. Dunlay SM, Roger VL, Killian JM, Weston SA, Schulte PJ, Subramaniam AV, et al. Advanced heart failure epidemiology and outcomes: a population-based study. *JACC Heart Fail* (2021) 9(10):722–32. doi: 10.1016/j.jchf.2021.05.009

12. McDonagh TA, Metra M, Adamo M, Gardner RS, Baumbach A, Böhm M, et al. 2021 Esc guidelines for the diagnosis and treatment of acute and chronic heart failure. *Eur Heart J*. (2021) 42(36):3599–726. doi: 10.1093/eurheartj/ehab368

13. Lang RM, Badano LP, Mor-Avi V, Afilalo J, Armstrong A, Ernande L, et al. Recommendations for cardiac chamber quantification by echocardiography in adults: an update from the American society of echocardiography and the European association of cardiovascular imaging. *Eur Heart J Cardiovasc Imaging*. (2015) 16 (3):233–71. doi: 10.1093/ehjci/jev014

14. DeVore AD, Hellkamp AS, Thomas L, Albert NM, Butler J, Patterson JH, et al. The association of improvement in left ventricular ejection fraction with outcomes in patients with heart failure with reduced ejection fraction: data from champ-hf. *Eur J Heart Fail* (2022) 24(5):762–70. doi: 10.1002/ejhf.2486

15. Lustgarten DL, Crespo EM, Arkhipova-Jenkins I, Lobel R, Winget J, Koehler J, et al. His-bundle pacing versus biventricular pacing in cardiac resynchronization therapy patients: a crossover design comparison. *Heart Rhythm*. (2015) 12 (7):1548–57. doi: 10.1016/j.hrthm.2015.03.048

16. Ajijola OA, Upadhyay GA, Macias C, Shivkumar K, Tung R. Permanent his-bundle pacing for cardiac resynchronization therapy: initial feasibility study in lieu of left ventricular lead. *Heart Rhythm*. (2017) 14(9):1353–61. doi: 10.1016/j.hrthm.2017.04.003

17. Upadhyay GA, Vijayaraman P, Nayak HM, Verma N, Dandamudi G, Sharma PS, et al. His corrective pacing or biventricular pacing for cardiac resynchronization in heart failure. *J Am Coll Cardiol*. (2019) 74(1):157–9. doi: 10.1016/j.jacc.2019.04.026

18. Vijayaraman P, Herweg B, Ellenbogen KA, Gajek J. His-optimized cardiac resynchronization therapy to maximize electrical resynchronization: a feasibility study. *Circ Arrhythm Electrophysiol*. (2019) 12(2):e006934. doi: 10.1161/CIRCEP.118.006934

19. Mullens W, Auricchio A, Martens P, Witte K, Cowie MR, Delgado V, et al. Optimized implementation of cardiac resynchronization therapy: a call for action for referral and optimization of care. *Eur J Heart Fail*. (2020) 22(12):2349–69. doi: 10.1002/ejhf.2046

20. Sharma PS, Dandamudi G, Herweg B, Wilson D, Singh R, Naperkowski A, et al. Permanent his-bundle pacing as an alternative to biventricular pacing for cardiac resynchronization therapy: a multicenter experience. *Heart Rhythm*. (2018) 15 (3):413–20. doi: 10.1016/j.hrthm.2017.10.014

21. Shan P, Su L, Zhou X, Wu S, Xu L, Xiao F, et al. Beneficial effects of upgrading to his bundle pacing in chronically paced patients with left ventricular ejection fraction <50%. *Heart Rhythm*. (2018) 15(3):405–12. doi: 10.1016/j.hrthm.2017.10.031

22. Steffel J, Ruschitzka F. Superresponse to cardiac resynchronization therapy. *Circ*. (2014) 130(1):87–90. doi: 10.1161/circulationaha.113.006124

23. Linde C, Gold MR, Abraham WT, St John Sutton M, Ghio S, Cerkvenik J, et al. Long-term impact of cardiac resynchronization therapy in mild heart failure: 5-year results from the resynchronization reverses remodeling in systolic left ventricular dysfunction (reverse) study. *Eur Heart J* (2013) 34(33):2592–9. doi: 10.1093/eurheartj/eht160

24. Mullens W, Verga T, Grimm RA, Starling RC, Wilkoff BL, Tang WHW. Persistent hemodynamic benefits of cardiac resynchronization therapy with disease progression in advanced heart failure. *J Am Coll Cardiol*. (2009) 53(7):600–7. doi: 10.1016/j.jacc.2008.08.079

25. Cleland JG, Abraham WT, Linde C, Gold MR, Young JB, Claude Daubert J, et al. An individual patient meta-analysis of five randomized trials assessing the effects of cardiac resynchronization therapy on morbidity and mortality in patients with symptomatic heart failure. *Eur Heart J* (2013) 34(46):3547–56. doi: 10.1093/eurheartj/eht290

26. Tan NY, Witt CM, Oh JK, Cha Y-M. Left bundle branch block. *Circ: Arrhythm Electrophysiol*. (2020) 13(4):364–77. doi: 10.1161/circep.119.008239

27. Barsheshet A, Goldenberg I, Moss AJ, Eldar M, Huang DT, McNitt S, et al. Response to preventive cardiac resynchronization therapy in patients with ischaemic

and nonischaemic cardiomyopathy in MADIT-CRT. *Eur Heart J*. (2011) 32 (13):1622–30. doi: 10.1093/eurheartj/ehq407

28. Bazoukis G, Naka KK, Alsheikh-Ali A, Tse G, Letsas KP, Korantzopoulos P, et al. Association of qrs narrowing with response to cardiac resynchronization therapy—a systematic review and meta-analysis of observational studies. *Heart Fail Rev*. (2020) 25(5):745–56. doi: 10.1007/s10741-019-09839-5

29. Wilcox JE, Fang JC, Margulies KB, Mann DL. Heart failure with recovered left ventricular ejection fraction: JACC scientific expert panel. *J Am Coll Cardiol*. (2020) 76 (6):719–34. doi: 10.1016/j.jacc.2020.05.075

30. Devore AD, Hellkamp AS, Thomas L, Albert NM, Butler J, Patterson JH, et al. Improvement in left ventricular ejection fraction in outpatients with heart failure with reduced ejection fraction. *Circ: Heart Failure*. (2020) 13(7):116–22. doi: 10.1161/circheartfailure.119.006833

frontiers | Frontiers in Cardiovascular Medicine

TYPE Original Research
PUBLISHED 25 May 2023
DOI 10.3389/fcvm.2023.1158509

OPEN ACCESS

EDITED BY
Alexander E. Berezin,
Zaporizhia State Medical University, Ukraine

REVIEWED BY
Peter Kokol,
University of Maribor, Slovenia
Liam Butler,
Wake Forest University, United States

*CORRESPONDENCE
Wei Liang
✉ weiliang@csu.edu.cn
Suzhen Huang
✉ huangsuzhen@csu.edu.cn

†These authors have contributed equally to this work and share first authorship

RECEIVED 04 February 2023
ACCEPTED 03 May 2023
PUBLISHED 25 May 2023

CITATION
Kuang X, Zhong Z, Liang W, Huang S, Luo R, Luo H and Li Y (2023) Bibliometric analysis of 100 top cited articles of heart failure–associated diseases in combination with machine learning.
Front. Cardiovasc. Med. 10:1158509.
doi: 10.3389/fcvm.2023.1158509

Bibliometric analysis of 100 top cited articles of heart failure–associated diseases in combination with machine learning

Xuyuan Kuang[1,2†], Zihao Zhong[3†], Wei Liang[3*], Suzhen Huang[4*], Renji Luo[3], Hui Luo[2,5] and Yongheng Li[3]

[1]Department of Hyperbaric Oxygen, Xiangya Hospital, Changsha, China, [2]National Research Center of Geriatric Diseases (Xiangya Hospital), Changsha, China, [3]Changsha Social Laboratory of Artificial Intelligence, Hunan University of Technology and Business, Changsha, China, [4]The Big Data Institute, Central South University, Changsha, China, [5]Department of Anesthesiology, Xiangya Hospital, Changsha, China

Objective: The aim of this paper is to analyze the application of machine learning in heart failure-associated diseases using bibliometric methods and to provide a dynamic and longitudinal bibliometric analysis of heart failure–related machine learning publications.

Materials and methods: Web of Science was screened to gather the articles for the study. Based on bibliometric indicators, a search strategy was developed to screen the title for eligibility. Intuitive data analysis was employed to analyze the top-100 cited articles and VOSViewer was used to analyze the relevance and impact of all articles. The two analysis methods were then compared to get conclusions.

Results: The search identified 3,312 articles. In the end, 2,392 papers were included in the study, which were published between 1985 and 2023. All articles were analyzed using VOSViewer. Key points of the analysis included the co-authorship map of authors, countries and organizations, the citation map of journal and documents and a visualization of keyword co-occurrence analysis. Among these 100 top-cited papers, with a mean of 122.9 citations, the most-cited article had 1,189, and the least cited article had 47. Harvard University and the University of California topped the list among all institutes with 10 papers each. More than one-ninth of the authors of these 100 top-cited papers wrote three or more articles. The 100 articles came from 49 journals. The articles were divided into seven areas according to the type of machine learning approach employed: Support Vector Machines, Convolutional Neural Networks, Logistic Regression, Recurrent Neural Networks, Random Forest, Naive Bayes, and Decision Tree. Support Vector Machines were the most popular method.

Conclusions: This analysis provides a comprehensive overview of the artificial intelligence (AI)-related research conducted in the field of heart failure, which helps healthcare institutions and researchers better understand the prospects of AI in heart failure and formulate more scientific and effective research plans. In addition, our bibliometric evaluation can assist healthcare institutions and researchers in determining the advantages, sustainability, risks, and potential impacts of AI technology in heart failure.

KEYWORDS

machine learning, heart failure, bibliometric analysis, VOSviewer, artificial intelligence, heart diseases

1. Introduction

The explosive growth in the research literature production has led to the need for new approaches to structure knowledge (1). Citations in the medicinal field can reflect the impact of an article in its field, which show that the number of citations is directly related to its worth (2). Bibliometric analysis provides the opportunity to gain an informative understanding of the field of study and promotes interdisciplinary collaboration (3). Bibliometrics is a measurable approach to informatics that analyzes emerging trends and knowledge structures in a field to obtain quantifiable, repeatable, and objective data (4). Top-cited publications in medical journals are also crucial in educating and advancing the next generation of technology (5).

There is a lack of literature on the top heart failure (HF)–related articles, despite the fact that the study of heart disease in recent decades has remained a very popular research topic (6). The epidemiology, pathophysiology, and development of heart failure are complex, and as a result, it can be difficult to determine its origin as well as its diagnosis, prognosis, and course of treatment (7). Artificial Intelligence (AI) is a technology that enables computer systems to simulate, understand, and execute tasks similar to human intelligence. The goal of AI is to create a machine that can think, learn, and adapt to new environments autonomously, handling complex problems and making accurate decisions like a human. Machine learning (ML) has recently been applied in heart failure treatment and it has contributed to the diagnosis, categorization, and prediction of the disease (8).

The aim of the present paper is to propose certain machine learning concepts and provide advice for cardiologists with no machine learning background to participate in the integration of machine learning and medicine and help them conduct research in this area. This paper is also an essential resource for people who are less familiar with the field but are interested in machine learning applications in the field of heart failure.

These excellent articles (9–14) are a good introduction to AI and machine learning–related technologies.

In addition, we provide some key machine learning concepts for busy clinicians.

1.1. Traditional rule-based algorithms apply rules to data, while machine learning algorithms learn patterns from data

The main difference between machine learning algorithms and traditional algorithms lies in their input and output. Traditional algorithms are based on rules and logical statements written by programmers that require precise definition of input and expected output. For example, a sorting algorithm requires an unordered list as input to generate a sorted list in ascending order as output.

In contrast, machine learning algorithms are based on statistics and data analysis and can automatically learn patterns and rules from data. Machine learning algorithms can handle raw or unclassified data and learn and adapt from it. The input for machine learning algorithms can be large datasets, and the output is typically a prediction or classification. For example, machine learning algorithms can learn natural language processing rules from large amounts of natural language data to perform natural language understanding or generation tasks more accurately (15).

Another difference is that traditional algorithms are usually deterministic, meaning they always produce the same output for a given input. In contrast, machine learning algorithms can be stochastic or probabilistic, meaning they may produce different output results for a given input because they are based on probabilistic models.

Finally, machine learning algorithms typically require a large amount of data to train the model to improve the accuracy of prediction or classification, whereas traditional algorithms typically use less data. There are several types of machine learning algorithms, from decision trees and support vector machines (SVMs), to highly complex, data-hungry algorithms called neural networks. Neural networks are used in deep machine learning (deep learning or DL), and their ability to analyze large amounts of highly complex data—electronic health record (EHR) data, for example, or the collection of pixels that make up medical images—are especially exciting for cardiology applications (16).

1.2. ML algorithms can learn patterns from labeled examples: supervised learning

Supervised learning algorithms need to be trained using existing datasets in order to learn regularity and patterns. These datasets are typically from hospitals or research institutions and include medical images, medical records, and experimental data. The accuracy of supervised learning algorithms depends on the quality and quantity of the datasets used, so a large amount of high-quality data is required to train the model (17).

The advantage of supervised learning algorithms is that they have a clear goal: to predict the labels of interest. But the downside of supervised ML algorithms is that their ability to find interesting patterns in the data is also limited by these labels. Training the right data and deciding on the right answer or label is critical to training and requires a lot of work. Similarly, a major challenge in supervised machine learning is the availability of datasets of sufficient size that have properly annotated labels of interest. However, this is also not necessarily accurate. Therefore, proper labeling of datasets requires active management by physicians and often requires consensus from more than one physician.

1.3. ML algorithms can learn patterns without labeled examples: unsupervised learning

Unsupervised learning is a machine learning method that uses unlabeled data for training to discover regularity and patterns in the data without first having labeled data. Unlike supervised

learning, unsupervised learning does not require predefined inputs and outputs, but instead lets the algorithm learn the structure and features of the data on its own. The main goal of unsupervised learning is to discover hidden structures in data in order to better understand the data and extract useful information.

The advantages of unsupervised learning include the following:

(i) No need to label data: Unlike supervised learning, unsupervised learning does not require labeled data for training, so it is easier to obtain a large amount of unlabeled data.
(ii) Discover hidden structures: Unsupervised learning can help discover hidden structures and patterns in data to provide better data understanding and analysis.
(iii) More comprehensive data analysis: Unsupervised learning can use a variety of algorithms to analyze data from different perspectives, so as to be able to understand the data more comprehensively.
(iv) Applicable to a variety of fields: Unsupervised learning can be applied to a variety of fields, such as image processing, natural language processing, data mining, etc. (11).

1.4. A hot branch of the AI field: deep learning

With the development of medical informatization and digital diagnosis, medical monitoring indicators continue to grow, and the amount of data is getting larger and larger; strong data processing capabilities are urgently needed to provide strong support to the medical field. Deep learning, as a hot branch of the AI field, has developed rapidly in speech recognition and computer vision, and its application in the medical field is increasingly used.

The reason why deep learning is suitable for application in the field of medicine is that it can automatically learn and extract hidden patterns and features from data. This automated process can reduce human interference and errors, and improve the accuracy and efficiency of disease diagnosis and treatment.

2. Materials and methods

Two researchers examined the core collection database Web of Science (WOS) on December 15, 2022. They identified 3,312 articles. In the end, 2,392 papers were included in the study. The papers related to heart failure and machine learning were identified by combing keywords with Boolean operators in the search engine: "heart failure" and "machine learning, AI, Support Vector Machine, Convolutional Neural Networks, Logistic Regression, Recurrent Neural Networks, Random Forest, Naive Bayes, or Decision Tree". As the search results settled at 2,392 papers, on this basis, we further selected the 100 top-cited articles. **Figure 1** shows the selected process. The 100 top-cited articles were compared with the analysis results of all searched articles, and their similarities and differences were analyzed.

The abstract or full text of 100 top-cited articles was read by two independent researchers who manually extracted information about the first and second authors, the journal name, the institute, and other details after evaluating the pertinent articles in accordance with the inclusion and exclusion criteria (18). Exclusion criteria included (i) articles unrelated to heart failure or machine learning and (ii) articles about heart transplantation and blood pressure measurement. Data were extracted from each of the articles by the two researchers and then analyzed by other researchers. The first draft was written by two researchers and all authors commented on the previous editions of the manuscript.

3. Results

3.1. The basic characteristics of 100 top-cited articles and all articles

In Online Resource 1 (**Supplementary Table S1**), the final top-100 cited articles were given in order of decreasing number of citations per article. The 2015 article about machine learning in medicine had the most citations, totaling 1,189 (19). The 2019 article about cardiac tissue engineering: state-of-the-art methods and outlook had the fewest citations (47 times) (20).

The 100 top-cited articles were all published from 2009 to 2021. The timeline diagram in **Figure 2A** shows that the period between 2017 and 2022 contains one peak. The majority (68%) of highly cited articles on heart failure were published between 2017 and 2020. All of the articles were published between 1999 and 2023. **Figure 2B** shows a peak in 2020–2022 and a trend to continue to rise. It can reflect the development history and important nodes in the field of machine learning and heart failure. The growth rate of publications over time was calculated by raising the rate of the number of publications in 2022 over the number of publications in 1999 to the power of 1/23, as shown below. The growth rate is a very important indicator that reflects the development trend in the field. The publication trends of the number of publications each year were also reported (21).

$$\text{Growth rate} = ((\text{number of publications in the last year} \div \text{number of publications in the first year})^{1/(\text{last year}-\text{first year})} - 1) \times 100$$

3.2. Distribution by journal and author

Table 1 lists the journals of the top 100 cited papers in descending order, with the number of articles, average number of citations per publication, and impact factor (2021). In total, 49 journals were included. The following journals had >3 instances: *Artificial Intelligence in Medicine* ($n = 5$), *Journal of the American College of Cardiology* ($n = 5$), *Computer Methods and Programs in Biomedicine* ($n = 4$), *BMC Medical Informatics and Decision Making* ($n = 3$), *European Heart Journal* ($n = 3$), *European Journal of Heart Failure* ($n = 3$), *JACC-Basic to Translational Science* ($n = 3$), and *American Journal of Surgical Pathology* ($n = 3$). A total of 206 authors participated in the preparation of these

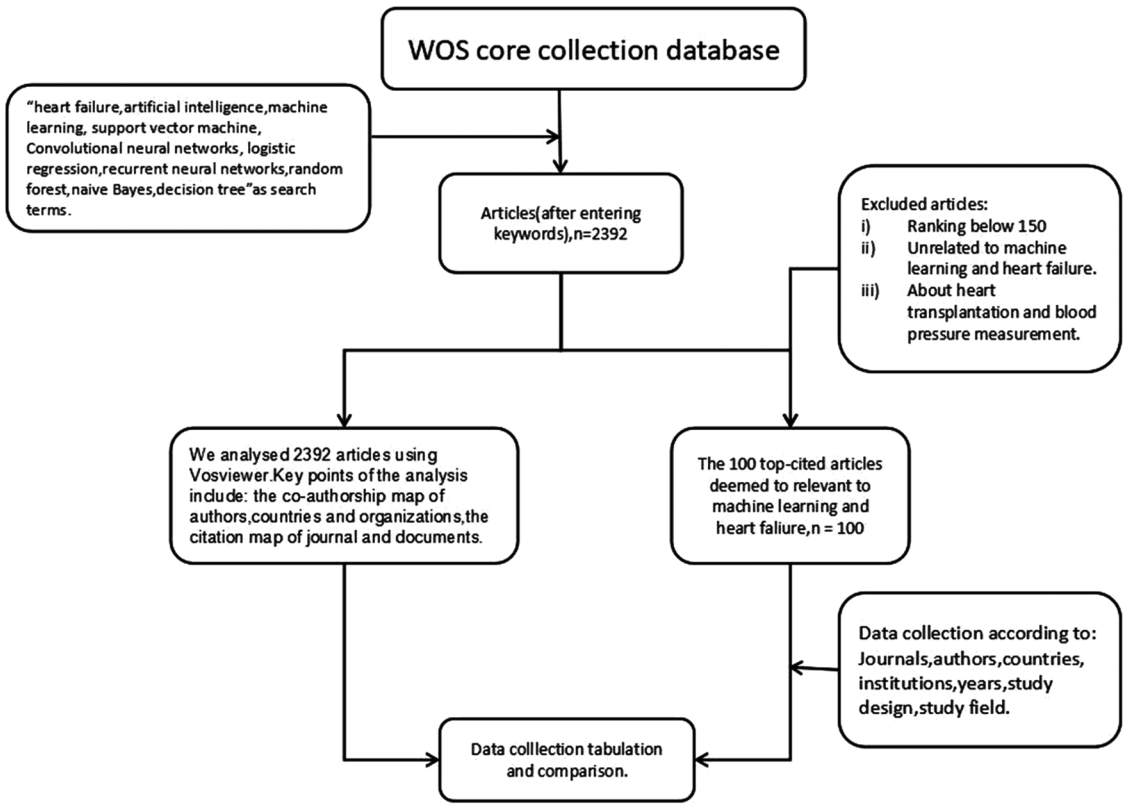

FIGURE 1
Flow chart showing the methodology used in the study.

most-cited articles, and 15 authors participated in the preparation of three or more articles. Daniel Rueckert wrote 5 of the 100 top-cited articles, topping this list. **Table 2** includes a list of these 15 authors.

Analyses of the data were descriptive in nature (22). According to the total link strength (TLS), which measures the overall strength of connections between a certain researcher and the co-authors of other articles, projects were divided into clusters. The citation map of journals and the co-authorship map of authors for the 2,392 articles are shown in **Figures 3A**, **4A**. A total of 43 journals have contributed to machine learning in heart failure. Among them, *Frontiers in Cardiovascular Medicine* was the leading journal with 78 documents, followed by *Circulation* with 58 documents, and *PLoS One* with 52 documents. The top three co-authorship triads of authors were Pandey Ambarish (TLS = 38), Segar Matthew W. (TLS = 36), and Acharya U. Rajendra (TLS = 35). In comparing highly cited articles to all articles, we found a big difference. The impact rankings for each country and each journal provided are based on citation rates (23).

3.3. Analysis of high-cited references

The most-cited reference was published in the *New England Journal of Medicine* and authored by Alan S. Maisel in 2002. The second most-cited reference was published in *Circulation* and authored by Rahul C. Deo in 2015. The third most-cited reference was published in the *Cochrane Database of Systematic Reviews* and authored by Jasvinder A. Singh in 2011.

These top three articles were analyzed. The most-cited reference by A. S. Maisel in 2002 (24) reported that measurements of B-type natriuretic peptide added significant independent predictive power to other clinical variables in models predicting which patients had congestive heart failure, using multiple logistic regression analysis. Used in conjunction with other clinical information, rapid measurement of B-type natriuretic peptide is useful in establishing or excluding the diagnosis of congestive heart failure in patients with acute dyspnea.

The second most-cited reference by R. C. Deo in 2015 reported that part of its effort was to identify what obstacles there may be in the change of the practice of medicine through statistical learning approaches, and discuss how these might be overcome (19).

The third most-cited reference by J. A. Singh in 2011 used mixed-effects logistic regression using arm-based random-effects models within the empirical Bayesian framework, and planned to combine the results of biologics used in many conditions to obtain much-needed risk estimates (25). The citation map documents are shown in **Figure 3B**.

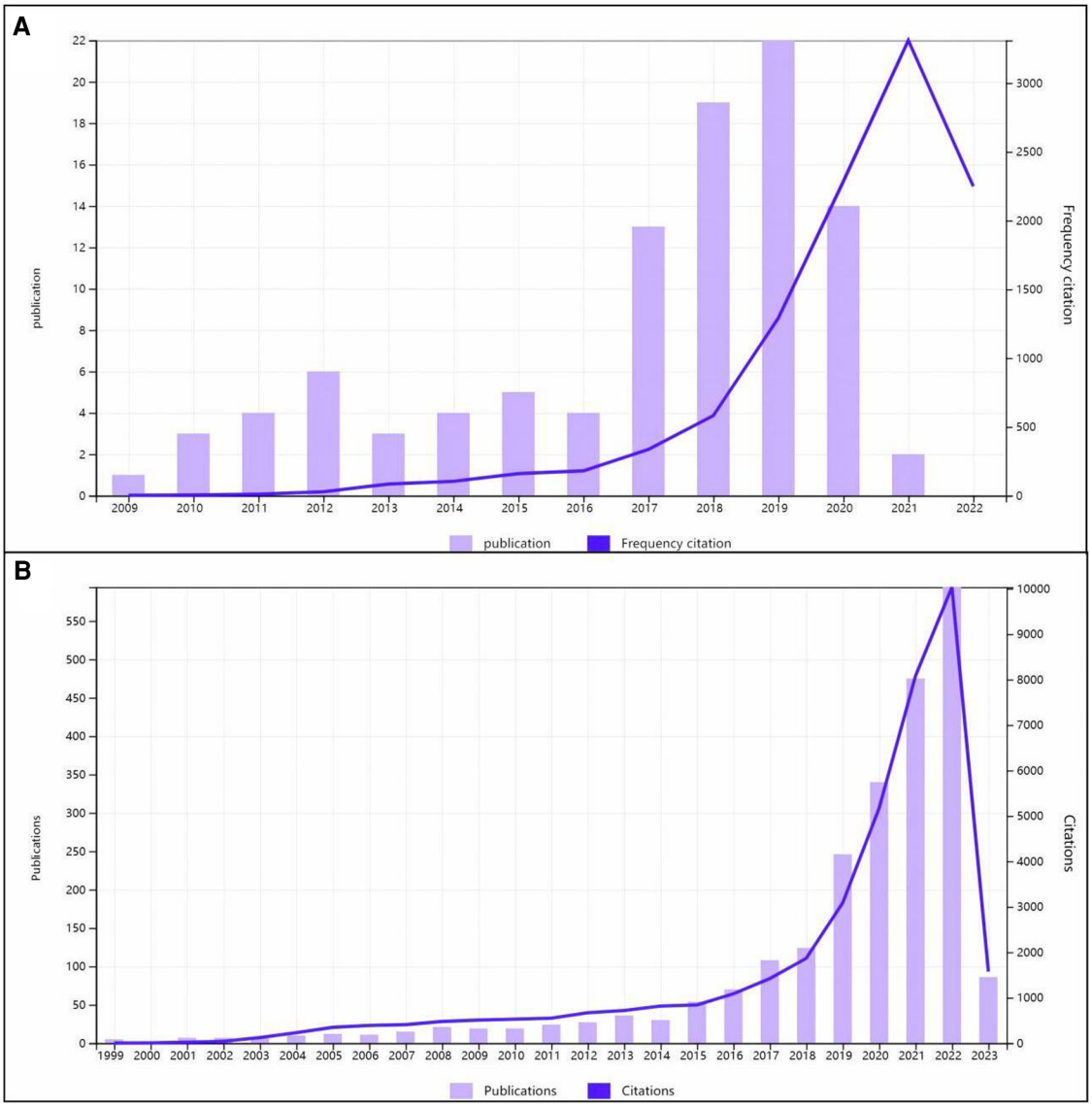

FIGURE 2
Times cited and publications over time (A) with the 100 top-cited articles and (B) with the 2,392 articles.

3.4. Countries and organizations of top 100 cited articles

Countries and institutes of origin of the top 100 cited articles are listed in Tables 3, 4. A total of 24 different countries contributed these 100 articles. The United States ($n = 50$) with half of the articles was the most prolific country, followed by China ($n = 7$), England ($n = 5$), Singapore ($n = 4$), Canada ($n = 4$), Spain ($n = 4$), Australia ($n = 3$), Turkey ($n = 3$), Italy ($n = 3$), and others. The institutes with the largest number of publications were Harvard University in the United States ($n = 17$) and University of California in the United States ($n = 10$). Icahn School of Medicine at Mount Sinai in Egypt produced eight articles. Two institutes produced seven articles: Mayo Clinic in the United States and Stanford University in the United States. As for all the articles, the co-authorship map of countries and institutes is summarized in Figures 4B,C. The top three countries in co-authorship were the United States, China, and England. The top three institutes in co-authorship were Harvard Medical School in the United States, Duke University in the United States, and University of Toronto in Canada. The field of AI healthcare attracts research from all over the world, but high-income countries are a major force in healthcare-related AI research. The United States alone contributes about half of the research in healthcare-related AI research (26), staying far ahead of other countries in terms of both quantity and quality of its contribution in this area. For researchers, understanding the ranking results can help them better choose suitable research partners, publish research results in appropriate journals, and participate in academic conferences.

TABLE 1 Journals in which the top 100 cited heart diseases articles were published.

Rank	Journals	Number of articles (%)	Average number of citations per paper	Impact factor[a] (2021)
1a	*Artificial Intelligence in Medicine*	5	59.2	7.011
1b	*Journal of the American College of Cardiology*	5	199.7	27.203
2	*Computer Methods and Programs in Biomedicine*	4	88	7.027
3a	*BMC Medical Informatics and Decision Making*	3	133.7	3.298
3b	*European Heart Journal*	3	107.3	35.855
3c	*European Journal of Heart Failure*	3	83.7	17.349
3d	*JACC-Basic to Translational Science*	3	50.7	9.531
4a	*Circulation*	2	528.5	39.918
4b	*Circulation-Cardiovascular Imaging*	2	62.5	8.589
4c	*Circulation-Heart Failure*	2	71	10.447
4d	*Computers in Biology and Medicine*	2	50.5	6.698
4e	*Critical Care*	2	70	19.334
4f	*Expert Systems With Applications*	2	70	8.093
4g	*IEEE Access*	2	57.5	3.476
4h	*IEEE Journal of Biomedical and Health Informatics*	2	93	7.021
4i	*IEEE Transactions on Biomedical Engineering*	2	141.5	4.756
4j	*IEEE Transactions on Visualization and Computer Graphics*	2	80	5.226
4k	*International Journal of Medical Informatics*	2	123.5	4.73
4l	*Journal of Biomedical Informatics*	2	63.5	8
4m	*Journal of the American Society of Echocardiography*	2	52.2	7.722

[a]Journal impact factor is based on Thomson Reuters Web of Knowledge Journal Citation Reports Ranking (2021).

TABLE 2 Authors with three or more top-cited articles.

Rank	Author	Number of articles
1	Ruecker D	5
2a	Acharya UR	4
2b	Johnson KW	4
2c	Sengupta PP	4
2d	Stewart WF	4
3a	Cook SA	3
3b	Dawes TJW	3
3c	De Marvao A	3
3d	Dudley JT	3
3e	Krittanawong C	3
3f	Melillo P	3
3g	Sanchez-martinez S	3
3h	Shameer K	3
3i	Tang WHW	3
3j	Wang Z	3

3.5. Heart diseases and machine learning methods of the top-cited articles

Causes of heart failure included atrial fibrillation ($n = 8$), cardiomyopathy ($n = 20$), cardiovascular disorders ($n = 22$), and coronary artery disease ($n = 6$). Moreover, we discovered that SVM appeared 22 times and SVM utilized in the 100 publications accounted for the majority. Numerous deep learning techniques, including Recurrent Neural Networks, Convolutional Neural Networks, and others, were also utilized. Heart disorders frequently had certain consequences or causative diseases in addition to the link to machine learning, for example, pneumonia ($n = 2$), diabetes ($n = 5$), hypertension ($n = 5$), and stroke ($n = 5$). The 100 studies suggest that machine learning techniques can be used to discover interactions between heart failure and other diseases.

Figure 5 shows the co-occurrence map of keywords and four research directions. The blue cluster includes heart failure, machine learning, AI, and precision medicine. The red cluster includes risk score, risk prediction, in-hospital mortality, and hospitalization. The green cluster includes prediction, classification, electronic health records, feature selection, and identification. Finally, the yellow cluster includes electrocardiograph, biomarker, and recommendations. AI technology research in recent years has involved more healthcare fields and produced more diverse keywords. It is possible that the higher diversity of keywords of healthcare-related AI research diluted the citation bursts. From the perspective of citation rates, deep learning, SVM, big data, and electronic health records have the greatest impact on heart failure research. We have realized that deep learning has been gradually applied to the medical field, surpassing traditional machine learning methods frequently mentioned in the 100 top-cited articles.

4. Discussion

4.1. Bibliometrics is of significance in promoting scientific development and progress

Bibliometrics not only demonstrates trends in heart failure research but also shows historical promises for scientific growth (27). Moreover, bibliometric analysis might shed light on the most popular subjects in heart disease (28).

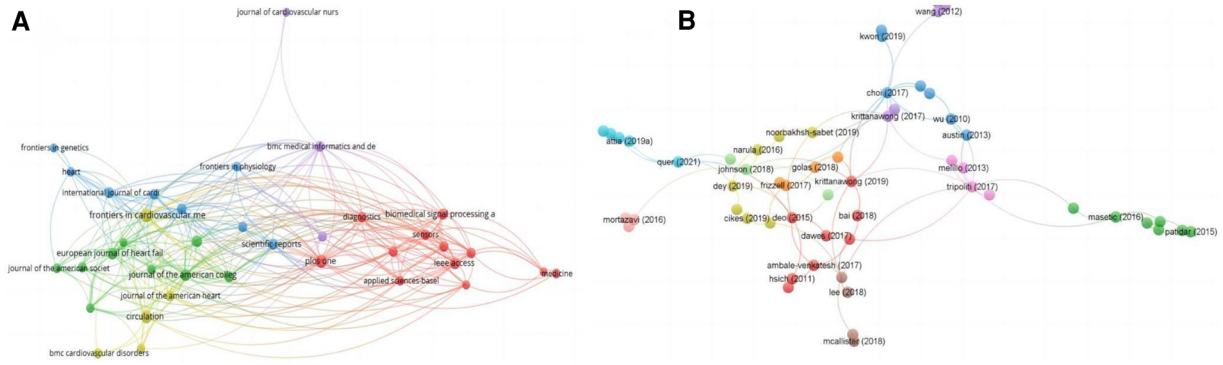

FIGURE 3
Visualization knowledge maps of citation. (A) Citation map of journal; (B) citation map of documents. Different color indicates different clusters. The size of the nodes represents the count of citations. The distance between the two nodes indicates their correlation.

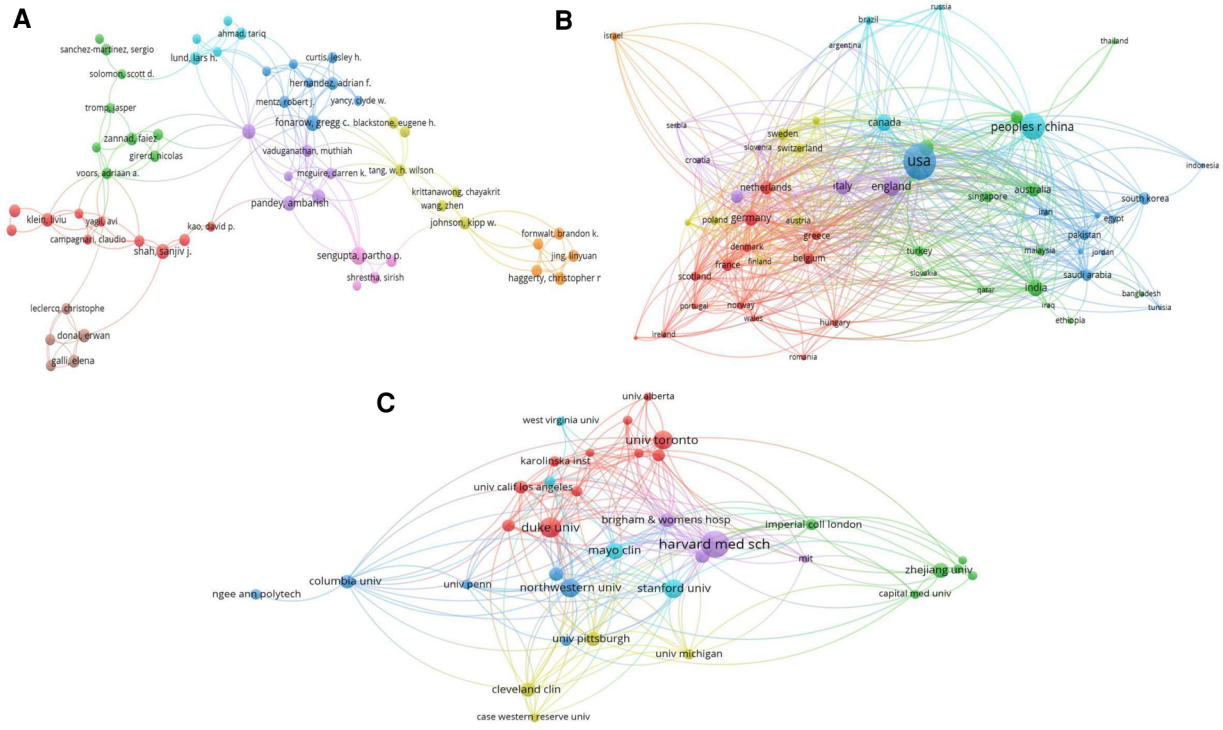

FIGURE 4
Visualization knowledge maps of the co-authorship. (A) Co-authorship map of authors that indicates the authors that cooperate in the field of heart failure. (B) Co-authorship map of countries. (C) Co-authorship map of organizations. Different colors indicate different clusters and the size of nodes indicates the number of publications. Thickness of the lines represents link strength of the countries.

The most citations that the top 100 journal papers from 1988 to 2022 ranged from 47 to 1,189. The collection of publications identifies topics that mirror the development of research on cardiac disorders throughout this 34-year span. Even though it might not be possible to thoroughly evaluate every one of these highly referenced papers, certain findings can be made. The characteristics of these important articles on heart problems are summed up in our current research.

4.2. The United States is leading the way in the area of heart failure and machine learning

The United States accounts for 50 of the 100 top-cited articles globally, which confirms the tremendous impact on medical science research in the United States with its large scientific population and the sufficient financial resources which are

TABLE 3 Original countries of the top-cited articles.

Rank	Countries	Number of article
1	United States	50
2	China	7
3	England	5
4a	Singapore	4
4b	Canada	4
4c	Spain	4
5a	Australia	3
5b	Turkey	3
5c	Italy	3

TABLE 4 Original institutions with two or more top-cited articles.

Rank	Institutions	No. of articles
1a	Harvard University, United States	17
1b	University of California System, United States	10
2	Icahn School of Medicine at Mount Sinai, Egypt	8
3b	Mayo Clinic, United States	7
3c	Stanford University, United States	7
4a	Brigham Women's Hospital, United States	6
4b	National Heart Centre Singapore, Singapore	6
5a	Columbia University	5
5b	Imperial College London, United Kingdom	5
5c	National University of Singapore, Singapore	5
5d	Northwestern University, United States	5
5e	University of California Sanfrancisco, United States	5
5f	University of Texas System, United States	5
6a	Cleveland Clinic Foundation, United States	4
6b	Ngee Ann Polytech, Singapore, Singapore	4
6c	Siemens Ag University of Texas, United States	4
6d	Yale University, United States	4
6e	Southwestern Medical Center Dallas, United States	4

available to the scientific communities, demonstrating its dominance in the fields of research, technology, and medicine. The United States is a pioneer in many other fields as well (29). The United States hosts many prestigious journals, which may be the reason why publications there account for the vast majority. Nevertheless, researchers prefer to cite papers from their own countries. American researchers may similarly favor papers from their own country (30, 31). For papers published in WOS, this work is with significant per-capita contributions from all industrialized nations as well as work in the majority of developing nations. Global and similarly multi-institutional collaborations in cardiac AI/ML exist within the United States.

It is undeniable that citation analysis within a specific subject may always provide a wealth of information about journals, organizations, and authors that is useful for identifying important publications and high-impact journals. It shows the trajectory of heart failure research as well as a historical perspective on scientific advancement in the subject. Through the analysis of the statistics of the journals, authors, and countries of the first 100 citations, we can learn advanced medical technologies and concepts, learn the advanced nature of the country that plays a leading position in this field, understand the future development trend of the field, and timely improve the shortcomings and shortcomings of the data analysis methods used by medical scientists. Most importantly, our statistical results are intended to provide these healers with the direction and orientation to solve problems (32).

4.3. Range of machine learning methods in heart diseases in United States, Europe, and Asia

We divided the 100 articles based on their original countries for analysis: the United States, Europe, and a few Asian countries (mainly from China). **Figure 6** displays the articles from the three areas that examine the main cardiac conditions and machine learning techniques. The tables on the left of the three regions show heart failure and its common causes (33). It demonstrates that the worldwide research results about origins of heart diseases are much the same. SVM, a binary classification method that uses machine learning techniques, occurs most frequently. Its basic model is defined in the feature space of the largest interval linear classifier. Its advantage is that only a small number of support vectors determine the outcome, which not only helps identify important samples but also eliminates redundant samples (34). These techniques have been widely adopted by medical research to predict disease and survival.

However, the interesting thing is that in the article "Comparing different supervised machine learning algorithms for disease prediction," we found the following description. They discovered that the SVM algorithm is applied most frequently (in 29 studies) followed by the Naïve Bayes algorithm (in 23 studies). However, the Random Forest (RF) algorithm showed superior accuracy comparatively. Of the 17 studies where it was applied, RF showed the highest accuracy in 9 of them, i.e., 53%. This was followed by SVM which topped in 41% of the studies it was considered (35). We also found that different diseases use different machine learning models to achieve different accuracy.

4.4. Analysis of the application of machine learning in heart failure

Millions of individuals die from cardiovascular disease yearly worldwide. Heart attack (induced by obstruction of blood vessels), stroke (caused by occlusion or rupture of cerebral blood vessels), and heart failure are the three main heart and blood vessel diseases (caused by the inability of the heart to pump enough blood to the body). Prediction of patients' status and prognosis based on clinical and laboratory data is crucial since severe heart failure can result in mortality (36).

Using machine learning, heart failure may be predicted, detected, and treated with high reliability and accuracy. Among these, data analysis and model building for heart failure frequently use methods like Neural Networks, Support Vector Machines, Decision Tree, and Random Forests. Physiological data, electrocardiograms, medical records, and images are just a

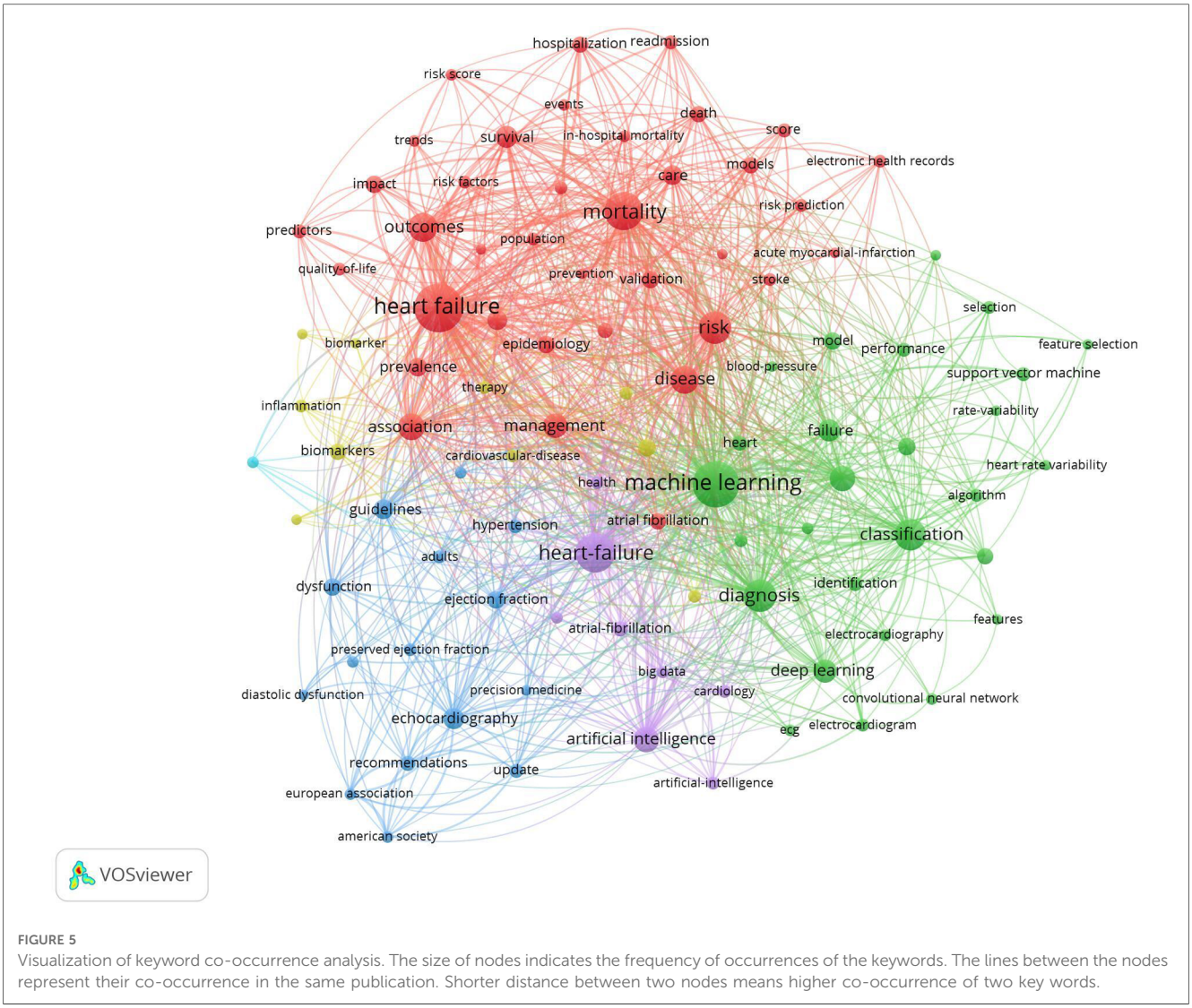

FIGURE 5
Visualization of keyword co-occurrence analysis. The size of nodes indicates the frequency of occurrences of the keywords. The lines between the nodes represent their co-occurrence in the same publication. Shorter distance between two nodes means higher co-occurrence of two key words.

few of the numerous data sources that offer rich data resources and research foundations for application of machine learning in heart failure (37).

Since SVM appears the most, we analyzed the articles in which this keyword appeared. We found that most of the SVM used by these authors are not traditional SVM models. Here are some examples: (i) SVM and boosting algorithms (38); (ii) an expert system that stacks two (SVM) models. The first SVM model is linear and L-1 regularized and the second SVM model is L-2 regularized (39); (iii) RBF kernel-based SVM (40); (iv) a boosted C5.0 tree, as the base classifier, was ensembled with a SVM, as a secondary classifier (41); (v) the proposed prediction SVM model with particle swarm parameter (42). These are some of the representatives of the 100 top-cited articles. It is all known to us that just building a working AI model does not make it usable. We have to combine and compare different models to improve our accuracy, and we have to pay attention to the development of technology and update our technology, because each model has its advantages and disadvantages. For example, random forests are suitable for handling large datasets, and this ensemble-based classifier may outperform a single classifier, while SVM is less prone to overfitting and performs well in classifying semistructured or unstructured data such as text, images, etc. (35). We can learn more about the differences from this paper.

4.5. Specific applications of machine learning

As most machine learning algorithms are "data agnostic" (43), the case studies are organized not by clinical data types or disorders, but rather by machine learning use cases.

Machine learning has some of the following key capabilities

Denoising and image enhancement: Machine learning has been used to address the clinical issue of image post-processing and denoising across a variety of modalities. For ultrasound, CT, MRI, and clinical imaging, neural network-based denoising has proven beneficial due to the complicated patterns of noise found in clinical imaging (44). In terms of clinical utility, machine

FIGURE 6
Major heart diseases and machine learning methods in the United States (A), Europe (B), and Asia (C).

learning has the ability to reduce the time and effort required for image post-processing as well as the discrepancies in data processing between operators, vendors, and institutes (45). Most machine learning denoising techniques now employ supervised learning techniques, where the model is trained to approximately represent proprietary denoising software as a real label (46). A crucial next step to demonstrate its usefulness in clinical practice is the use of machine learning–based image denoising to monitor changes in diagnostic performance. To test image denoising on a broader scale, several clinical trials are now underway (47).

Feature extraction, feature selection, and feature representation: Feature selection is the process of choosing the most pertinent characteristics from a vast number of features, aiming to increase the precision and interpretability of the prediction model. For instance, feature selection techniques based on Decision Trees or Logistic Regression algorithms might be used. Representing important features in a simpler and more unified form is called feature extraction. For example, myocardial wall thickness measurement is a crucial diagnostic, monitoring, and therapeutic tool for the identification of coronary heart disease and cardiomyopathy. The outlines and thickness of the myocardial wall can be automatically extracted and determined using feature extraction methods in medical image analysis (48).

Measuring cardiac flow is vital for evaluating cardiac function and lesions as it provides important diagnostic information about the volume of blood the heart pumps each minute (49). Heart disorders including coronary artery disease and heart failure may be diagnosed and treated using feature extraction algorithms. These algorithms can automatically extract the contours of the ventricles and blood arteries and determine the flow rate and velocity (50).

Deep learning algorithms achieve higher classification performance through automatic extraction of these characteristics through intricate nonlinear combinations of input data (51). Data may be compared between institutes using these extracted features, and by integrating features from various data types, it is possible to create a multimodal image of a specific patient or disease by integrating features from various data types. This study will continue to benefit from concurrent experiments using small datasets as well as synthesizing larger datasets from smaller datasets, because training a model to execute these fundamental tasks frequently requires a lot of data labeling.

With a small amount of data available, synthetic knowledge synthesis (SKS) can be a useful tool for heart failure feature extraction. Existing data can be combined with domain expertise to create more data samples, enlarging the dataset and enhancing

the model's performance. Synthetic knowledge synthesis can also aid in avoiding issues such as overfitting. However, SKS cannot deal with all issues. There is just one viable answer and more experimental testing is needed to determine whether it applies to certain datasets. For effectiveness, it is necessary to combine SKS with other machine learning approaches, such as feature selection, classifier selection, and so on (52).

4.6. Strength and limitations in our analysis process

4.6.1. Strength

The Web of Science database is an authoritative citation database with a worldwide scope. It includes the core journals with the greatest academic influence across a range of disciplines and the literature can, to a certain extent, reflect cutting-edge global development trends in certain discipline or field. Objective assessment of the current state and level of scientific advancement is possible through observing quantity and quality of the produced scientific materials.

The 100 top-cited articles were compared with all articles retrieved. Readers can find suitable and commonly used methods as well as valuable conclusions from their comparison and analysis. They can also learn development laws from the present paper and realize better combination of medicine and machine learning.

4.6.2. Limitations

Some pertinent articles might have been overlooked due to the keywords used. Second, the citation count could be inflated by self-citations, errors, or insufficient statistics. Because of this, older articles may receive more citations at the time of retrieval and study because they have received more citations over a longer period of time (53). The Web of Science core collection database was used as the literature source. Various databases have significant disparities and if the literature was procured from another database, even more variations would be observed in the citations or articles (54). Most importantly, some keywords, although they were ranked as top keywords, were uninformative by themselves (risk, model, and system) and *could not be analyzed*.

Notwithstanding the potential of machine learning in the study and treatment of heart failure, there are a number of problems and difficulties that must be resolved. For instance, gathering a sufficient amount of high-quality data to train and verify machine learning algorithms can be challenging. On the other hand, heart failure is a complicated disease and involves interaction of multiple tissues and organ systems. Therefore, data integration and model interpretability are the major challenges preventing widespread assimilation into clinical practice (55), which might lead to practical application issues, particularly in clinical decision-making.

5. Conclusion

Our analysis also depicted research trends of AI-related health research: (i) the growth rate of heart failure–related ML publications has grown rapidly in the past two decades and the rate showed a trend of continuous growth; (ii) high-income countries are the main force of HF-related AI research; (iii) ML is being increasingly employed in the field of heart failure. Future research trends will most likely include more accurate predictive models, personalized treatment, real-time monitoring, and early warning systems; (iv) although SVM appears the most, what cannot be ignored is the combination of different models. Improving accuracy and reducing complexity is the goal of doctors.

Data availability statement

The original contributions presented in the study are included in the article/Supplementary Materials, further inquiries can be directed to the corresponding authors.

Ethics statement

Ethical review and approval was not required for the study on human participants in accordance with the local legislation and institutional requirements. The patients/participants provided their written informed consent to participate in this study. Written informed consent was obtained from the individual(s) for the publication of any potentially identifiable images or data included in this article.

Author contributions

ZZ, RL, and YL were responsible for data collection, investigation, figure and table construction, and original draft writing. XK, WL, SH, and HL contributed to discussion and final review and editing. All authors contributed to the article and approved the submitted version.

Funding

The work was supported in part by the National Natural Science Foundation of China under Grant Nos. 62072171, 72091515, 82000388 and 82170291 and in part by the Hunan Provincial Science and Technology Fund under Grant No. 2021JJ40962; Hunan Health Commission Science and Technology Program under Grant No. B20231901922; and in part by Hunan Provincial Innovation Foundation For Postgraduate under Grant No. CX20211102.

Conflict of interest

The authors declare that the research was conducted in the absence of any commercial or financial relationships that could be construed as a potential conflict of interest.

Publisher's note

All claims expressed in this article are solely those of the authors and do not necessarily represent those of their affiliated organizations, or those of the publisher, the editors and the reviewers. Any product that may be evaluated in this article, or claim that may be made by its manufacturer, is not guaranteed or endorsed by the publisher.

Supplementary material

The Supplementary Material for this article can be found online at: https://www.frontiersin.org/articles/10.3389/fcvm.2023.1158509/full#supplementary-material.

References

1. Kokol P, Blažun Vošner H, Završnik J. Application of bibliometrics in medicine: a historical bibliometrics analysis. *Health Info Libr J*. (2021) 38:125–38. doi: 10.1111/hir.12295

2. Cao F, Li J, Li A, Fang Y, Li F. Citation classics in acute pancreatitis. *Pancreatology*. (2012) 12:325–30. doi: 10.1016/j.pan.2012.05.001

3. Niu BB, Hong S, Yuan JF, Peng S, Wang Z, Zhang X. Global trends in sediment-related research in earth science during 1992-2011: a bibliometric analysis. *Scientometrics*. (2014) 98:511–29. doi: 10.1007/s11192-013-1065-x

4. Kreps GL, Neuhauser L. Artificial intelligence and immediacy: designing health communication to personally engage consumers and providers. *Patient Educ Couns*. (2013) 92:205–10. doi: 10.1016/j.pec.2013.04.014

5. Muhammad G, Alhussein M. Convergence of artificial intelligence and internet of things in smart healthcare: a case study of voice pathology detection. *IEEE Access*. (2021) 9:89198–209. doi: 10.1109/ACCESS.2021.3090317

6. Dickstein K. ESC guidelines for the diagnosis and treatment of acute and chronic heart failure 2008: application of natriuretic peptides: reply. *Eur Heart J*. (2009) 30:383. doi: 10.1093/eurheartj/ehn561

7. Isomi M, Sadahiro T, Ieda M. Progress and challenge of cardiac regeneration to treat heart failure. *J Cardiol*. (2019) 73:97–101. doi: 10.1016/j.jjcc.2018.10.002

8. Olsen CR, Mentz RJ, Anstrom KJ, Page D, Patel PA. Clinical applications of machine learning in the diagnosis, classification, and prediction of heart failure. *Am Heart J*. (2020) 229:1–17. doi: 10.1016/j.ahj.2020.07.009

9. Sardar P, Abbott JD, Kundu A, Aronow HD, Granada JF, Giri J. Impact of artificial intelligence on interventional cardiology from decision-making aid to advanced interventional procedure assistance. *JACC Cardiovasc Interv*. (2019) 12:1293–303. doi: 10.1016/j.jcin.2019.04.048

10. Litjens G, Ciompi F, Wolterink JM, de Vos BD, Leiner T, Teuwen J, et al. State-of-the-art deep learning in cardiovascular image analysis. *JACC Cardiovasc Imaging*. (2019) 12:1549–65. doi: 10.1016/j.jcmg.2019.06.009

11. Johnson KW, Soto JT, Glicksberg BS, Shameer K, Miotto R, Ali M, et al. Artificial intelligence in cardiology. *J Am Coll Cardiol*. (2018) 71:2668–79. doi: 10.1016/j.jacc.2018.03.521

12. Krittanawong C, Zhang HJ, Wang Z, Aydar M, Kitai T. Artificial intelligence in precision cardiovascular medicine. *J Am Coll Cardiol*. (2017) 69:2657–64. doi: 10.1016/j.jacc.2017.03.571

13. Dey D, Slomka PJ, Leeson P, Comaniciu D, Shrestha S, Sengupta PP, et al. Artificial intelligence in cardiovascular imaging JACC state-of-the-art review. *J Am Coll Cardiol*. (2019) 73:1317–35. doi: 10.1016/j.jacc.2018.12.054

14. Al'Aref SJ, Anchouche K, Singh G, Slomka PJ, Kolli KK, Kumar A, et al. Clinical applications of machine learning in cardiovascular disease and its relevance to cardiac imaging. *Eur Heart J*. (2019) 40:1975. doi: 10.1093/eurheartj/ehy404

15. Frizzell JD, Liang L, Schulte PJ, Yancy CW, Heidenreich PA, Hernandez AF, et al. Prediction of 30-day all-cause readmissions in patients hospitalized for heart failure comparison of machine learning and other statistical approaches. *JAMA Cardiol*. (2017) 2:204–9. doi: 10.1001/jamacardio.2016.3956

16. Quer G, Arnaout R, Henne M, Arnaout R. Machine learning and the future of cardiovascular care JACC state-of-the-art review. *J Am Coll Cardiol*. (2021) 77:300–13. doi: 10.1016/j.jacc.2020.11.030

17. Attia ZI, Kapa S, Lopez-Jimenez F, McKie PM, Ladewig DJ, Satam G, et al. Screening for cardiac contractile dysfunction using an artificial intelligence-enabled electrocardiogram. *Nat Med*. (2019) 25:70. doi: 10.1038/s41591-018-0240-2

18. Yuan F, Cai J, Liu B, Tang X. Bibliometric analysis of 100 top-cited articles in gastric disease. *Biomed Res Int*. (2020) 2020:2672373. doi: 10.1155/2020/2672373

19. Deo RC. Machine learning in medicine. *Circulation*. (2015) 132:1920–30. doi: 10.1161/CIRCULATIONAHA.115.001593

20. Bal-Ozturk A, Miccoli B, Avci-Adali M, Mogtader F, Sharifi F, Cecen B, et al. Current strategies and future perspectives of skin-on-a-chip platforms: innovations, technical challenges and commercial outlook. *Curr Pharm Design*. (2018) 24:5437–57. doi: 10.2174/1381612825666190206195304

21. Guo Y, Hao Z, Zhao S, Gong J, Yang F. Artificial intelligence in health care: bibliometric analysis. *J Med Internet Res*. (2020) 22:18228. doi: 10.2196/18228

22. van Eck NJ, Waltman L. Citation-based clustering of publications using CitNetExplorer and VOSviewer. *Scientometrics*. (2017) 111:1053–70. doi: 10.1007/s11192-017-2300-7

23. Shi L, Mai YP, Wu YJ. Digital transformation: a bibliometric analysis. *J Organ End User Com*. (2022) 37:302637. doi: 10.4018/JOEUC.302637

24. Maisel AS, Krishnaswamy P, Nowak RM, McCord J, Hollander JE, Duc P, et al. Rapid measurement of B-type natriuretic peptide in the emergency diagnosis of heart failure. *New Engl J Med*. (2002) 347:161–7. doi: 10.1056/NEJMoa020233

25. Singh JA, Wells GA, Christensen R, Ghogomu TE, Maxwell L, MacDonald JK, et al.. Adverse effects of biologics: a network meta-analysis and Cochrane overview. *Cochrane Database Syst Rev*. (2011) 2:14651858. doi: 10.1002/14651858.CD008794.pub2

26. Reis RS, Salvo D, Ogilvie D, Lambert EV, Goenka S, Brownson RC, et al. Scaling up physical activity interventions worldwide: stepping up to larger and smarter approaches to get people moving. *Lancet*. (2016) 388:1337–48. doi: 10.1016/S0140-6736(16)30728-0

27. Boyd CJ, Patel JJ, Soto E, Kurapati S, Martin KD, King TW. Differences in highly-cited and lowly-cited manuscripts in plastic surgery. *J Surg Res*. (2020) 255:641–6. doi: 10.1016/j.jss.2020.02.009

28. Wang S, Wang D, Li C, Li Y, Ding G. Clustering by fast search and find of density peaks with data field. *Chinese J Electron*. (2016) 25:397–402. doi: 10.1049/cje.2016.05.001

29. Subroto I, Haviana S, Fatmawati W. Analysis and measurement of scientific collaboration networks performance. *Indones J Electr Eng Informatics*. (2020) 8:1145. doi: 10.11591/ijeei.v8i3.1145

30. Lum ZC, Pereira GC, Giordani M, Meehan JP. Top 100 most cited articles in orthopaedic surgery: an update. *J Orthop*. (2020) 19:132–7. doi: 10.1016/j.jor.2019.11.039

31. Hirt J, Meichlinger J, Schumacher P, Mueller G. Agreement in risk of bias assessment between RobotReviewer and human reviewers: an evaluation study on randomised controlled trials in nursing-related Cochrane reviews. *J Nurs Scholarship*. (2021) 53:246–54. doi: 10.1111/jnu.12628

32. Zhou WT, Deng ZH, Liu Y, Shen H, Deng HW, Xiao HM. Global research trends of artificial intelligence on histopathological images: a 20-Year bibliometric analysis. *Int J Env Res Pub Health*. (2022) 19:191811597. doi: 10.3390/ijerph191811597

33. Cooper LT, Baughman KL, Feldman AM, Frustaci A, Jessup M, Kuhl U, et al. The role of endomyocardial biopsy in the management of cardiovascular disease. *Eur Heart J*. (2007) 28:3076–93. doi: 10.1093/eurheartj/ehm456

34. Verma A, Chitalia VC, Waikar SS, Kolachalama VB. Machine learning applications in nephrology: a bibliometric analysis comparing kidney studies to other medicine subspecialities. *Kidney Med*. (2021) 3:762–7. doi: 10.1016/j.xkme.2021.04.012

35. Uddin S, Khan A, Hossain ME, Moni MA. Comparing different supervised machine learning algorithms for disease prediction. *BMC Med Inform Decis*. (2019) 19:s12911–9. doi: 10.1186/s12911-019-1004-8

36. Fiani B, Pasko KBD, Sarhadi K, Covarrubias C. Current uses, emerging applications, and clinical integration of artificial intelligence in neuroradiology. *Rev Neurosci*. (2022) 33:383–95. doi: 10.1515/revneuro-2021-0101

37. Lee J, Jun S, Cho Y, Lee H, Kim GB, Seo JB, et al. Deep learning in medical imaging: general overview. *Korean J Radiol*. (2017) 18:570–84. doi: 10.3348/kjr.2017.18.4.570

38. Krittanawong C, Virk H, Bangalore S, Wang Z, Johnson KW, Pinotti R, et al.. Machine learning prediction in cardiovascular diseases: a meta-analysis. *Sci Rep*. (2020) 10:s41520–98. doi: 10.1038/s41598-020-72685-1

39. Ali L, Niamat A, Khan JA, Golilarz NA, Xiong XZ, Noor A, et al. An optimized stacked support vector machines based expert system for the effective prediction of heart failure. *IEEE Access*. (2019) 7:54007–14. doi: 10.1109/ACCESS.2019.2909969

40. Saqlain SM, Sher M, Shah FA, Khan I, Ashraf MU, Awais M, et al. Fisher score and Matthews correlation coefficient-based feature subset selection for heart disease diagnosis using support vector machines. *Knowl Inf Syst*. (2019) 58:139–67. doi: 10.1007/s10115-018-1185-y

41. Turgeman L, May JH. A mixed-ensemble model for hospital readmission. *Artif Intell Med*. (2016) 72:72–82. doi: 10.1016/j.artmed.2016.08.005

42. Zheng BC, Zhang JH, Yoon SW, Lam SS, Khasawneh M, Poranki S. Predictive modeling of hospital readmissions using metaheuristics and data mining. *Expert Syst Appl*. (2015) 42:7110–20. doi: 10.1016/j.eswa.2015.04.066

43. Madani A, Arnaout R, Mofrad M, Arnaout R. Fast and accurate view classification of echocardiograms using deep learning. *NPJ Digit Med*. (2018) 1: s41717–46. doi: 10.1038/s41746-017-0013-1

44. Shen DG, Wu GR, Suk HI. Deep learning in medical image analysis. *Annu Rev Biomed Eng*. (2017) 19:221–48. doi: 10.1146/annurev-bioeng-071516-044442

45. Quer G, Arnaout R, Henne M, Arnaout R. Machine learning and the future of cardiovascular care JACC state-of-the-art review. *J Am Coll Cardiol*. (2021) 77:300–13. doi: 10.1016/j.jacc.2020.11.030

46. Huang O, Long W, Bottenus N, Lerendegui M, Trahey GE, Farsiu S, et al. Mimicknet, mimicking clinical image post- processing under black-box constraints. *IEEE Trans Med Imaging*. (2020) 39:2277–86. doi: 10.1109/TMI.2020.2970867

47. Kaur P, Singh G, Kaur P. A review of denoising medical images using machine learning approaches. *Curr Med Imaging Rev*. (2018) 14:675–85. doi: 10.2174/1573405613666170428154156

48. Cao Y, Liu W, Zhang S, Xu L, Zhu B, Cui H, et al.. Detection and localization of myocardial infarction based on Multi-Scale ResNet and attention mechanism. *Front Physiol*. (2022) 13:783184. doi: 10.3389/fphys.2022.783184

49. Kohler B, Gasteiger R, Preim U, Theisel H, Gutberlet M, Preim B. Semi-automatic vortex extraction in 4D PC-MRI cardiac blood flow data using line predicates. *IEEE Trans Vis Comput Graph*. (2013) 19:2773–82. doi: 10.1109/TVCG.2013.189

50. Bibicu D, Moraru L. Cardiac cycle phase estimation in 2-D echocardiographic images using an artificial neural network. *IEEE Trans Biomed Eng*. (2013) 60:1273–9. doi: 10.1109/TBME.2012.2231864

51. Gadaleta M, Rossi M, Topol EJ, Steinhubl SR, Quer G. On the effectiveness of deep representation learning: the atrial fibrillation case. *Computer*. (2019) 52:18–29. doi: 10.1109/MC.2019.2932716

52. Kokol P, Kokol M, Zagoranski S. Machine learning on small size samples: A synthetic knowledge synthesis. *Sci Prog*. (2022) 105:00368504211029777. doi: 10.1177/00368504211029777

53. Mukherjee D, Lim WM, Kumar S, Donthu N. Guidelines for advancing theory and practice through bibliometric research. *J Bus Res*. (2022) 148:101–15. doi: 10.1016/j.jbusres.2022.04.042

54. Bayram B, Limon O, Limon G, Hanci V. Bibliometric analysis of top 100 most-cited clinical studies on ultrasound in the emergency department. *Am J Emerg Med*. (2016) 34:1210–6. doi: 10.1016/j.ajem.2016.03.033

55. Gautam N, Ghanta SN, Clausen A, Saluja P, Sivakumar K, Dhar G, et al. Contemporary applications of machine learning for device therapy in heart failure. *JACC Heart Fail*. (2022) 10:603–22. doi: 10.1016/j.jchf.2022.06.011

frontiers | Frontiers in Cardiovascular Medicine

TYPE Opinion
PUBLISHED 12 June 2023
DOI 10.3389/fcvm.2023.1193226

OPEN ACCESS

EDITED BY
Jamshid Karimov,
Cleveland Clinic, United States

REVIEWED BY
Eric Rytkin,
Northwestern University, United States

*CORRESPONDENCE
Ezra A. Amsterdam
✉ eaamsterdam@ucdavis.edu

RECEIVED 24 March 2023
ACCEPTED 16 May 2023
PUBLISHED 12 June 2023

CITATION
Dixit NM and Amsterdam EA (2023) Should GDMT be prioritized over revascularization in new onset HFrEF? Potential lessons from the REVIVED-BCIS2 and STRONG-HF trials. Front. Cardiovasc. Med. 10:1193226. doi: 10.3389/fcvm.2023.1193226

Should GDMT be prioritized over revascularization in new onset HFrEF? Potential lessons from the REVIVED-BCIS2 and STRONG-HF trials

Neal M. Dixit and Ezra A. Amsterdam*

Division of Cardiovascular Medicine, School of Medicine, University of California, Davis, Sacramento, CA, United States

KEYWORDS

guideline-directed medical therapy, heart failure, revascularization, cardiomyopathy, coronary artery bypass surgery, percutaneous coronary intervention

1. Introduction

Many patients with heart failure with reduced ejection fraction (HFrEF) are initially diagnosed at an index heart failure hospitalization. Nearly half of these patients have an ischemic etiology. In the latter group, the Surgical Treatment for Ischemic Heart Failure (STICH) trial was the first, and thus far, the only trial to show benefit of revascularization on survival in patients with left ventricular (LV) dysfunction (1). Revascularization by percutaneous coronary intervention (PCI) has also been applied to this population in anticipation of achieving similar benefit. The REVIVED-BCIS2 trial tested this hypothesis by randomizing patients with multivessel coronary artery disease (CAD) and a left ventricular ejection fraction (LVEF) $\leq$ 35% to PCI and guideline directed medical therapy (GDMT) vs. GDMT alone (2). However, no benefit on survival or LV function was found with PCI compared to GDMT during a mean follow-up interval of more than 3 years. Thus, for patients with HFrEF and stable multivessel CAD, coronary artery bypass graft surgery (CABG) is the only revascularization method with documented mortality benefit. GDMT remains the foundation of care for these patients.

This finding raises an important question: For newly diagnosed HFrEF patients at high risk for CAD not presenting with acute coronary syndrome, how should revascularization be prioritized at index hospitalization?

2. Discussion

2.1. GDMT should be the focus for newly diagnosed HFrEF

The 2022 ACC/AHA/HFSA Guidelines identify 4 pillars of GDMT for HFrEF (3). Each of these agents has shown reduction in heart failure hospitalization and cardiovascular death within 30 days of initiation (4). However, due to widespread underuse of GDMT, there have been considerable and potentially avoidable losses of life and function (5). The Guidelines suggest simultaneous initiation of this regimen at diagnosis with subsequent titration at regular intervals (3). This is a documented strategy to reduce both early and long-term mortality and morbidity in HFrEF, regardless of etiology.

In fact, the STRONG-HF trial randomized patients hospitalized with heart failure, a majority with HFrEF, to a strategy of aggressive initiation and titration of GDMT vs. usual care (6). The result was a notable 8.1% absolute risk reduction in the primary endpoint of 180-day readmission for heart failure or all-cause death. N-terminal pro-brain natriuretic peptide was also reduced by 23% at 90 days in the aggressively titrated arm compared to usual care despite no difference in doses of loop diuretics. The key to this success was targeted up-titration of GDMT peri-discharge, resulting in >80% of patients on half-target dose or greater of beta-blocker, renin-angiotensin-aldosterone system inhibitor, and mineralocorticoid receptor antagonist by 2 weeks post-discharge.

While an ischemic evaluation is a crucial aspect in the evaluation of newly diagnosed HFrEF, immediate revascularization may impede GDMT initiation. Percutaneous coronary intervention-induced acute kidney injury (AKI) occurs in up to 7%–10% of cases, which may prohibit initiation or continuation of GDMT agents, which often transiently reduce glomerular filtration rate (7). Moreover, the concern for contrast induced AKI from coronary angiography can render clinicians reluctant to titrate GDMT. Additionally,

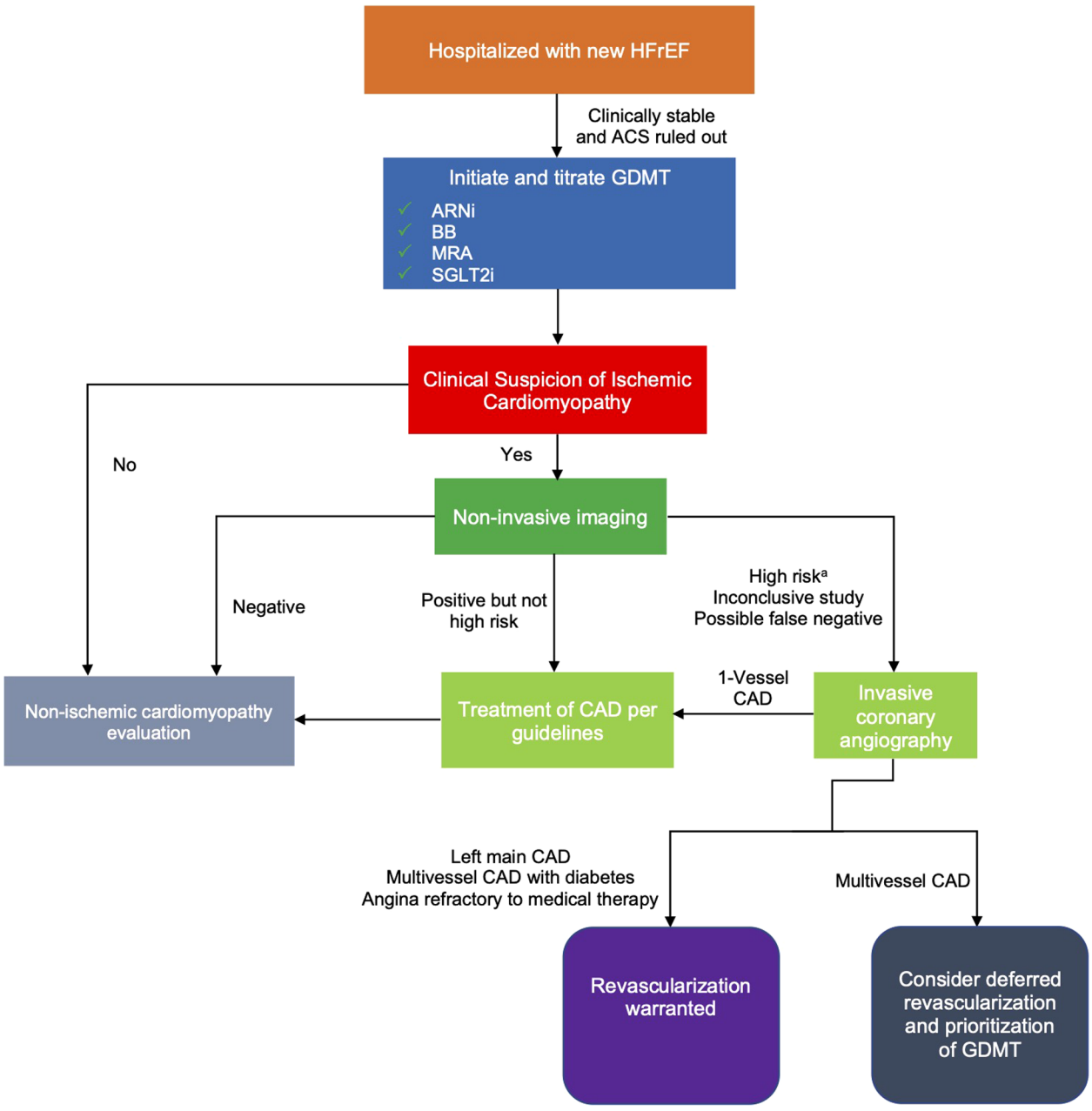

FIGURE 1
Proposed algorithm for evaluation of ischemic cardiomyopathy in hospitalized patients with newly diagnosed HFrEF. [a]Suggestive of LM or multivessel CAD. ACS, acute coronary syndrome; ARNi, angiotensin receptor-neprilysin inhibitor; BB, beta-blocker; CAD, coronary artery disease; GDMT, guideline-directed medical therapy; HFrEF, heart failure with reduced ejection fraction; MRA, mineralocorticoid receptor antagonist; SGLT2i, sodium/glucose cotransporter-2 inhibitors.

GDMT use after CABG has historically been lower than with PCI, presenting another barrier to medical optimization (8).

2.2. Could there be benefit to deferred revascularization of multivessel disease?

Guidelines provide a Class I indication for revascularization with CABG for patients with high risk left main (LM) CAD and multivessel CAD associated with diabetes or LVEF < 35% (9). However, as with candidacy for implantable cardiac defibrillators for primary prevention, consideration of revascularization may shift as a patient's LVEF improves after optimization of GDMT (10). Per Guidelines, a patient with an LVEF of 30% with multivessel disease and no diabetes has a Class I indication for CABG; however, in three months if the EF improves to 35%–50% with optimal GDMT, then the recommendation for CABG drops to Class 2a; if EF improves to >50% then it becomes 2b. Moreover, marked LV dysfunction is a leading reason for rejection of surgery due to the increased risk of surgical mortality (1, 5). Historically, many of these turndowns are sent for PCI. However, results of REVIVED-BCIS2 reveal that this approach may not have been beneficial (2). But even with high rates of surgical mortality, the STICH trial showed that the clinical benefits of CABG in LV dysfunction are eventually realized (1). Prioritization of optimal GDMT before revascularization in patients whose sole indication is LVEF < 35%, could result in increased LVEF at the time of consideration for CABG, which may obviate the need for CABG, or lower operative risk if the decision is made to proceed with CABG. Therefore, deferred, i.e., postponement of this decision to the outpatient setting, may be a preferred strategy for management of these patients.

2.3. Consider a non-invasive ischemic evaluation

While invasive coronary angiography has been the gold-standard for diagnosis of ischemic cardiomyopathy, the limited role of PCI in patients with LV dysfunction and stable CAD may limit its necessity. Non-invasive imaging minimizes procedural risk while maintaining diagnostic accuracy for high risk disease. Coronary computed tomography angiography (CCTA) has upwards of 90% sensitivity and specificity for identifying obstructive CAD (11). For certain patients in which CCTA may be impractical, such as those with elevated heart rates or marginal kidney function, non-invasive stress imaging can be used to detect LM and triple vessel CAD (3, 12). Patients with high risk, inconclusive, or high likelihood of false negative findings on non-invasive testing can be considered for invasive angiography, but the possible benefits of deferred revascularization should be considered as previously noted (**Figure 1**). Patients whose non-invasive testing is negative or not high risk have low annual rates of ischemic events and further invasive evaluation can be performed in the outpatient setting, if indicated (13, 14). In these cases, non-ischemic causes of cardiomyopathy should also be evaluated (15).

3. Conclusion

With the negative results of the REVIVED-BCIS2 trial, CABG remains the only method of revascularization in patients with ischemic cardiomyopathy to demonstrate morbidity and mortality benefit. However, deferred revascularization of multivessel disease in patients with new onset HFrEF should be considered to allow time for the impact of the rapid, beneficial effects of GDMT, which may lead to lower surgical risk or render CABG unnecessary. Additionally, an initial non-invasive ischemic evaluation reduces procedural risk and may better facilitate GDMT optimization than an initial invasive evaluation. Overall, for newly diagnosed HFrEF patients, a strategy prioritizing GDMT over revascularization may lead to greater long-term benefits. A randomized trial is required to provide further guidance on this approach.

Author contributions

ND: wrote the first draft of the manuscript. EA: reviewed and edited the manuscript. All authors contributed to the article and approved the submitted version.

Conflict of interest

The authors declare that the research was conducted in the absence of any commercial or financial relationships that could be construed as a potential conflict of interest.

Publisher's note

References

1. Velazquez EJ, Lee KL, Jones RH, Al-Khalidi HR, Hill JA, Panza JA, et al. Coronary-artery bypass surgery in patients with ischemic cardiomyopathy. *N Engl J Med.* (2016) 374(16):1511–20. doi: 10.1056/NEJMoa1602001

2. Perera D, Clayton T, O'Kane PD, Greenwood JP, Weerackody R, Ryan M, et al. Percutaneous revascularization for ischemic left ventricular dysfunction. *N Engl J Med.* (2022) 387(15):1351–60. doi: 10.1056/NEJMoa2206606

3. Heidenreich PA, Bozkurt B, Aguilar D, Allen LA, Byun JJ, Colvin MM, et al. 2022 AHA/ACC/HFSA guideline for the management of heart failure: a report of the American college of cardiology/American heart association joint committee on clinical practice guidelines. *Circulation*. published correction appears in Circulation. (2022) 145(18):e1033; (2022) 146(13):e185; (2023) 147(14):e674; (2022) 145(18): e895–e1032. doi: 10.1161/CIR.0000000000001063

4. Brownell NK, Ziaeian B, Fonarow GC. The gap to fill: rationale for rapid initiation and optimal titration of comprehensive disease-modifying medical therapy for heart failure with reduced ejection fraction. *Card Fail Rev*. (2021) 7:e18. doi: 10.15420/cfr.2021.18

5. Greene SJ, Butler J, Albert NM, DeVore AD, Sharma PP, Duffy CI, et al. Medical therapy for heart failure with reduced ejection fraction: the CHAMP-HF registry. *J Am Coll Cardiol*. (2018) 72(4):351–66. doi: 10.1016/j.jacc.2018.04.070

6. Mebazaa A, Davison B, Chioncel O, Cohen-Solal A, Diaz R, Filippatos G, et al. Safety, tolerability and efficacy of up-titration of guideline-directed medical therapies for acute heart failure (STRONG-HF): a multinational, open-label, randomised, trial. *Lancet*. (2022) 400(10367):1938–52. doi: 10.1016/S0140-6736(22)02076-1

7. Azzalini L, Candilio L, McCullough PA, Colombo A. Current risk of contrast-induced acute kidney injury after coronary angiography and intervention: a reappraisal of the literature. *Can J Cardiol*. (2017) 33(10):1225–8. doi: 10.1016/j.cjca.2017.07.482

8. Pinho-Gomes AC, Azevedo L, Ahn JM, Park SJ, Hamza TH, Farkouh ME, et al. Compliance with guideline-directed medical therapy in contemporary coronary revascularization trials. *J Am Coll Cardiol*. (2018) 71(6):591–602. doi: 10.1016/j.jacc.2017.11.068

9. Lawton JS, Tamis-Holland JE, Bangalore S, Bates ER, Beckie TM, Bischoff JM, et al. 2021 ACC/AHA/SCAI guideline for coronary artery revascularization: executive summary: a report of the American college of cardiology/American heart association joint committee on clinical practice guidelines. *Circulation*. published correction appears in Circulation. (2022) 145(11):e771; (2022) 145(3):e4–e17. doi: 10.1161/CIR.0000000000001039

10. Wilcox JE, Fang JC, Margulies KB, Mann DL. Heart failure with recovered left ventricular ejection fraction: JACC scientific expert panel. *J Am Coll Cardiol*. (2020) 76 (6):719–34. doi: 10.1016/j.jacc.2020.05.075

11. Paech DC, Weston AR. A systematic review of the clinical effectiveness of 64-slice or higher computed tomography angiography as an alternative to invasive coronary angiography in the investigation of suspected coronary artery disease. *BMC Cardiovasc Disord*. (2011) 11(1):32. doi: 10.1186/1471-2261-11-32

12. Mahajan N, Polavaram L, Vankayala H, Ference B, Wang Y, Ager J, et al. Diagnostic accuracy of myocardial perfusion imaging and stress echocardiography for the diagnosis of left main and triple vessel coronary artery disease: a comparative meta-analysis. *Heart*. (2010) 96(12):956–66. doi: 10.1136/hrt.2009.182295

13. Reynolds HR, Shaw LJ, Min JK, Page CB, Berman DS, Chaitman BR, et al. Outcomes in the ISCHEMIA trial based on coronary artery disease and ischemia severity. *Circulation*. (2021) 144(13):1024–38. doi: 10.1161/CIRCULATIONAHA.120.049755

14. Hoffmann U, Ferencik M, Udelson JE, Picard MH, Truong QA, Patel MR, et al. Prognostic value of noninvasive cardiovascular testing in patients with stable chest pain: insights from the PROMISE trial (prospective multicenter imaging study for evaluation of chest pain). *Circulation*. (2017) 135(24):2320–32. doi: 10.1161/CIRCULATIONAHA.116.024360

15. Bozkurt B, Colvin M, Cook J, Cooper LT, Deswal A, Fonarow GC, et al. Current diagnostic and treatment strategies for specific dilated cardiomyopathies: a scientific statement from the American heart association. *Circulation*. (2016) 134(23):134(23): e652; e579–e646.

frontiers | Frontiers in Cardiovascular Medicine

TYPE Case Report
PUBLISHED 23 June 2023
DOI 10.3389/fcvm.2023.1169165

OPEN ACCESS

EDITED BY
Jamshid Karimov,
Cleveland Clinic, United States

REVIEWED BY
Nagarajan Muthialu,
Great Ormond Street Hospital for Children NHS Foundation Trust, United Kingdom
Fabrizio De Rita,
Newcastle upon Tyne Hospitals NHS Foundation Trust, United Kingdom

*CORRESPONDENCE
Lukasz Pyka
✉ l.t.pyka@gmail.com

RECEIVED 18 February 2023
ACCEPTED 30 May 2023
PUBLISHED 23 June 2023

CITATION
Pyka L, Szkodzinski J, Piegza J, Swietlińska M and Gąsior M (2023) Case Report: do heart transplant candidates benefit from mechanically supported revascularization? Front. Cardiovasc. Med. 10:1169165. doi: 10.3389/fcvm.2023.1169165

Case Report: do heart transplant candidates benefit from mechanically supported revascularization?

Lukasz Pyka[1]*, Janusz Szkodzinski[1], Jacek Piegza[1], Malgorzata Swietlińska[2] and Mariusz Gąsior[1]

[1]3rd Department of Cardiology, Faculty of Medical Sciences in Zabrze, Medical University of Silesia, Katowice, Poland, [2]Department of Cardiology, Scanmed Center of Cardiology, Chorzow, Poland

Introduction: Recently published studies suggest that percutaneous coronary intervention (PCI) has no significant impact on outcomes in patients with heart failure and stable coronary artery disease. The use of percutaneous mechanical circulatory support is growing, but its value is still uncertain. If large areas of viable myocardium are ischemic, the benefit from revascularization should be evident. In such instances, we should strive for complete revascularization. The use of mechanical circulatory support in such cases is vital because it provides hemodynamic stability throughout the complex procedure.
Case report: We present a case of a 53-year-old male heart transplant candidate with type 1 diabetes mellitus, initially considered unsuitable for revascularization and qualified for heart transplantation, transferred to our center due to acute decompensated heart failure. At this time, the patient had temporary contraindications for heart transplantation. As the patient was considered no-option, we have decided to reassess the possibility of revascularization. The heart team opted for a high-risk mechanically supported PCI with the aim of complete revascularization. A complex multivessel PCI was performed with optimal effect. The patient was weaned off dobutamine on the second day post-PCI. Four months post-discharge, he remains stable, is in NYHA II class, and has no chest pain. Control echocardiography showed improved ejection fraction. The patient is not a heart transplant candidate anymore.
Conclusions: This case report shows that we must strive for revascularization in select heart failure cases. The outcome of this patient suggests that heart transplant candidates with potentially viable myocardium should be considered for revascularization, especially as the shortage of donors persists. In the most complex coronary anatomy and severe heart failure, mechanical support in the procedure might be essential.

KEYWORDS
heart transplant, revascularisation, congestive heart failure, mechanical circulatory support, outcomes, myocardial recovery

Introduction

Recently published studies suggest that percutaneous coronary intervention (PCI) has no significant impact on outcomes in patients with heart failure (HF) and stable coronary artery disease (CAD) (1, 2). In patients with severe CAD and HF, the use of percutaneous mechanical circulatory support (MCS) is growing. However, its impact on outcomes is

still uncertain, and, in many instances, the potential benefits are diminished by complications (3–5).

Nonetheless, we believe that a significant population of ischemic HF patients benefits from these interventions, especially when revascularization is achieved in large areas of viable myocardium. In such instances, we should strive for complete revascularization, including interventions on chronically occluded arteries (6, 7). MCS is vital because it provides hemodynamic stability throughout the complex procedure.

Case report

We present a case of a 53-year-old male heart transplant candidate with type 1 diabetes mellitus who was initially hospitalized at the intensive care unit in our center in March 2022 due to acute decompensated heart failure (ADHF). He was considered unsuitable for revascularization by the heart team, as his severe left ventricular impairment with a left ventricular ejection fraction (LVEF) of 15% and advanced multivessel coronary artery disease were considered extremely high risk and futile both for PCI and coronary artery bypass grafting. The patient was qualified for heart transplantation (OHT) by the heart transplant team. He was treated medically and discharged in stable condition.

In May 2022, the patient was transferred to our cardiology department due to a second ADHF episode, with severe congestion, hypotension, pleural effusion, severe asymmetric lower limb edema, and signs of infection. On admission, his echo showed a LVEF of 18% and an end-diastolic left ventricle dimension of 64 mm, with moderate mitral and tricuspid insufficiencies and good right ventricular function. The patient was stabilized with inotropes, intravenous diuretics, and pleurocentesis. As Doppler ultrasound and CT-angio confirmed lower limb deep vein thrombosis (DVT) with an infected ulceration, the patient was temporarily taken off the OHT list. Subsequently, after initial stabilization on oral medical treatment, he was transferred back to the referring cardiology department for further observation and rehabilitation. He was readmitted after 25 days in deteriorated clinical condition, on dobutamine support, hypotensive, in NYHA III/IV class. At this time, an urgent heart transplant was considered the only option. Therefore, he underwent right heart catheterization (cardiac output 3.55 L/min; cardiac index 1.92 L/min/m^2; pulmonary vascular resistance 2.25 Wood units). Nonetheless, after the heart transplant team reassessment, he was still deemed unsuitable for OHT (due to persistent significant DVT and unclear infectious status with significantly elevated inflammation markers despite treatment).

At this time, we have decided to reassess the possibility of revascularization, as the patient was considered no-option, dobutamine-dependent, unsuitable for urgent OHT. In our healthcare system, only OHT-qualified patients are potential candidates for long-term mechanical circulatory support; therefore, such treatment was not available. The patient's coronary angiography before initial OHT qualification revealed a critical, calcified proximal left anterior descending artery (LAD) lesion, a chronic total occlusion (CTO) of the circumflex artery (LCx), a significant left main stenosis, and diffuse disease of the right coronary artery (RCA) with a critical lesion at the crux cordis. The heart team opted for a high-risk MCS PCI with the aim of complete revascularization. As revascularization was considered the last viable treatment option, myocardial viability or ischemia testing was not performed.

At the beginning of the procedure, two Abbott Perclose ProGlide devices were inserted after an ultrasound-guided femoral puncture. The Abiomed Impella CP catheter was inserted into the left ventricle. With the single access technique (puncture of the Impella hemostatic sheath), we were able to engage the left coronary artery with an EBU 3.5 catheter and perform a control angiography, which revealed similar coronary artery status to that before OHT qualification. A Pilot 50 guidewire easily crossed the LAD lesion; however, we were unable to introduce the HD IVUS Acist Kodama catheter. After meticulous 2.5-mm × 20-mm NC balloon predilatation, two sirolimus-eluting stents were implanted up to the ostium of the LAD (Ultimaster Tansei 2.5 mm × 28 mm and 3.0 mm × 38 mm). As IVUS at this point revealed stent underexpansion and further postdilatation provided insufficient results, 70 impulses of intravascular lithotripsy (Shockwave 3.5 mm × 15 mm) were performed to very good effect.

Subsequently, the circumflex artery was recanalized using a microcatheter-supported Pilot 150 guidewire and followed by the implantation of three everolimus-eluting stents (Xience Pro 2.25 mm × 23 mm, 2.5 mm × 23 mm, 2.5 mm × 18 mm). TIMI 3 flow was restored with optimal angiographic and IVUS results. Finally, the left main PCI was performed using a provisional technique with implantation of a 4.0-mm × 12-mm sirolimus-eluting Ultimaster Tansei stent, postdilated with a 4.5-mm × 6-mm NC balloon. Optimal angiographic and IVUS results were achieved. The patient remained hemodynamically stable through the procedure. The Impella CP was removed in the cathlab, and the Proglide presuture device provided hemostasis.

After 6 days, the patient was taken back to the cathlab. Coronary angiography showed optimal results of the previous procedure. After predilatation, a PCI of the right coronary artery with the use of three sirolimus-eluting stents was performed (Ultimaster Tansei 3.5 × 38, 2.75 × 24, 2.5 × 33).

Initial and follow-up echocardiography is presented in **Supplementary Video 1**. The angiographic images of the procedures are presented in **Supplementary Video 2**. The IVUS images are presented in **Supplementary Video 3**. The summary of initial and final angiography and echocardiography is presented in **Figure 1**.

The patient was weaned off dobutamine on the second day post-PCI. The in-hospital stay was complicated by pneumonia, which was subsequently treated in the referring cardiology department. Four months post-discharge, he was controlled at the outpatient clinic. The patient remains stable, is in NYHA II class, and has no chest pain. Control echocardiography showed an LVEF of 37% and a mild mitral insufficiency. The patient is currently not an OHT candidate. Persistent DVT, despite

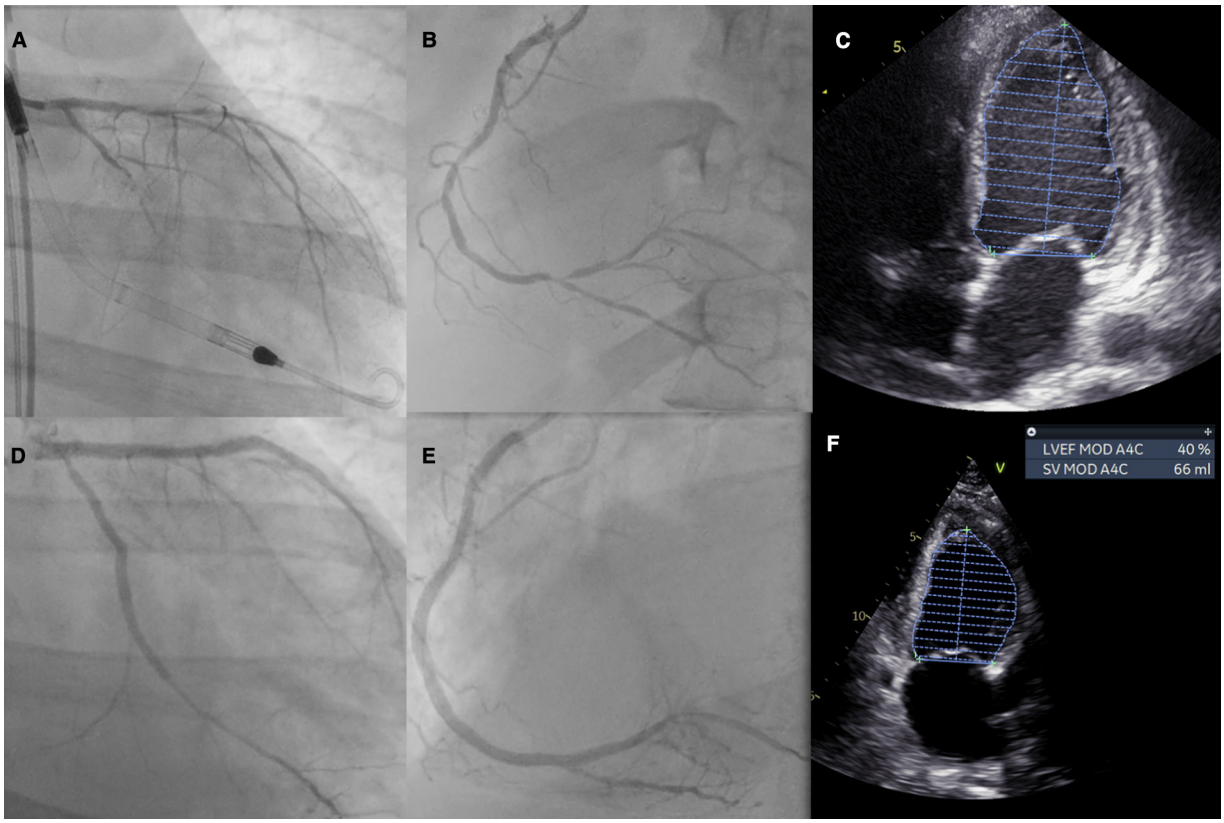

FIGURE 1
Patient summary: (A) initial left coronary artery anatomy with visible Impella support, (B) initial right coronary artery anatomy, (C) initial echocardiography with an LVEF of 18%, (D) final PCI effect of the left coronary artery, (E) final PCI effect of the right coronary artery, and (F) echocardiography on follow-up with an LVEF of 37%–38%. LVEF, left ventricular ejection fraction.

antithrombotic treatment, remains the most important clinical problem at the time of follow-up.

Discussion

In general, it is the policy at our center to utilize all of the available treatment methods for severe HF patient before OHT qualification. This includes almost routine revascularization. In these patients, long-term results are generally satisfactory, especially when complete revascularization is possible (6). There are, however, select cases when the patient is not revascularized. This concerns mostly patients with extremely complicated coronary anatomy and the most severe left ventricular impairment, especially when the benefit of revascularization is doubtful. In such cases, myocardial viability testing may be useful in the decision-making process. However, severe dilatation of the left ventricle and thinning of the myocardium may be considered surrogates for lack of viability. Moreover, in hemodynamically unstable patients, inotrope-dependent, when OHT is considered urgent (in-hospital), revascularization is rarely performed to avoid potential complications or the need for a dual (or triple) antithrombotic regimen. If the heart team decides to perform PCI in OHT candidates, especially in complex coronary anatomy (unprotected left main lesion, multivessel disease, last patent vessel), a periprocedural hemodynamic compromise might be expected. In such cases, MCS should be considered to provide patient stability throughout the procedure.

This case report presents the treatment and outcomes of a patient in whom, at an early stage of treatment, there was a decision to treat CAD conservatively. Such a decision, a premature one in our opinion, complicated the patient's further clinical course. Performing complete revascularization produced left ventricular improvement exceeding expectations, even with no initial proof of myocardial viability. MCS support enabled the operators to perform the procedure safely and optimally. In such complex HF cases, the ever-changing clinical scenario might compel the physicians to challenge initial treatment decisions in the best interest of the patient.

Conclusions

We have presented a case of a dramatic clinical and LVEF improvement in an OHT candidate with temporary contraindications after complete revascularization. High-risk PCI was the only viable option and provided results exceeding our

expectations. This case report shows that in select HF cases, we must strive for revascularization, despite recent trial results. The question remains whether revascularization during initial OHT qualification could have prevented the ADHF episodes. The patient should have never entered the OHT waiting list, especially with the significant comorbidities. The outcome of this patient suggests that OHT candidates with potentially viable myocardium should be considered for revascularization, especially as shortage of donors persists. In the most complex coronary anatomy and severe LVEF impairment, MCS might be essential.

Data availability statement

The datasets presented in this article are not readily available because this is a case report. Requests to access the datasets should be directed to the corresponding author.

Ethics statement

Written informed consent was obtained from the individual(s) for the publication of any potentially identifiable images or data included in this article.

Author contributions

LP contributed to the design of the manuscript, analyzed the data, prepared the manuscript, and contributed to the design of the case report study. JP, JS, and MS contributed to the design of the manuscript, design of the case report study, and reviewed the manuscript. MG contributed to the preparation of the manuscript, design of the case report study, and reviewed the manuscript. All authors contributed to the article and approved the submitted version.

Conflict of interest

The authors declare that the research was conducted in the absence of any commercial or financial relationships that could be construed as a potential conflict of interest.

Publisher's note

All claims expressed in this article are solely those of the authors and do not necessarily represent those of their affiliated organizations, or those of the publisher, the editors and the reviewers. Any product that may be evaluated in this article, or claim that may be made by its manufacturer, is not guaranteed or endorsed by the publisher.

Supplementary material

The Supplementary Material for this article can be found online at: https://www.frontiersin.org/articles/10.3389/fcvm.2023.1169165/full#supplementary-material

References

1. Maron DJ, Hochman JS, Reynolds HR, Bangalore S, O'Brien SM, Boden WE, et al. Initial invasive or conservative strategy for stable coronary disease. *N Engl J Med*. (2020) 382(15):1395–407. doi: 10.1056/NEJMoa1915922

2. Perera D, Clayton T, O'Kane PD, Greenwood JP, Weerackody R, Ryan M, et al. Percutaneous revascularization for ischemic left ventricular dysfunction. *N Engl J Med*. (2022) 387(15):1351–60. doi: 10.1056/NEJMoa2206606

3. O'Neill WW, Kleiman NS, Moses J, Henriques JP, Dixon S, Massaro J, et al. A prospective, randomized clinical trial of hemodynamic support with Impella 2.5 versus intra-aortic balloon pump in patients undergoing high-risk percutaneous coronary intervention: the PROTECT II study. *Circulation*. (2012) 126(14):1717–27. doi: 10.1161/CIRCULATIONAHA.112.098194

4. Protty M, Sharp ASP, Gallagher S, Farooq V, Spratt JC, Ludman P, et al. Defining percutaneous coronary intervention complexity and risk: an analysis of the United Kingdom BCIS database 2006–2016. *JACC Cardiovasc Interv*. (2022) 15 (1):39–49. doi: 10.1016/j.jcin.2021.09.039

5. Chieffo A, Burzotta F, Pappalardo F, Briguori C, Garbo R, Masiero G, et al. Clinical expert consensus document on the use of percutaneous left ventricular assist support devices during complex high-risk indicated PCI: Italian society of Interventional Cardiology Working Group Endorsed by Spanish and Portuguese Interventional Cardiology Societies. *Int J Cardiol*. (2019) 293:84–90. doi: 10.1016/j.ijcard.2019.05.065

6. Pyka Ł, Hawranek M, Tajstra M, Gorol J, Lekston A, Gąsior M. Complete percutaneous revascularisation feasibility in ischaemic heart failure is related to improved outcomes: insights from the COMMIT-HF registry. *Kardiol Pol*. (2017) 75(5):453–61. doi: 10.5603/KP.a2017.0018

7. Tajstra M, Pyka Ł, Gorol J, Pres D, Gierlotka M, Gadula-Gacek E, et al. Impact of chronic total occlusion of the coronary artery on long-term prognosis in patients with ischemic systolic heart failure: insights from the COMMIT-HF registry. *JACC Cardiovasc Interv*. (2016) 9(17):1790–7. doi: 10.1016/j.jcin.2016.06.007

frontiers | Frontiers in Cardiovascular Medicine

TYPE Brief Research Report
PUBLISHED 17 July 2023
DOI 10.3389/fcvm.2023.1193800

OPEN ACCESS

EDITED BY
Tomasz Zieliński,
National Institute of Cardiology, Poland

REVIEWED BY
Eric Rytkin,
Northwestern University, United States
Randy Stevens,
St. Christopher's Hospital for Children, United States

*CORRESPONDENCE
Kiyotaka Fukamachi
✉ fukamak@ccf.org

†These authors have contributed equally to this work and share first authorship

RECEIVED 25 March 2023
ACCEPTED 03 July 2023
PUBLISHED 17 July 2023

CITATION
Miyagi C, Ahmad M, Karimov JH, Polakowski AR, Karamlou T, Yaman M, Fukamachi K and Najm HK (2023) Human fitting of pediatric and infant continuous-flow total artificial heart: visual and virtual assessment.
Front. Cardiovasc. Med. 10:1193800.
doi: 10.3389/fcvm.2023.1193800

Human fitting of pediatric and infant continuous-flow total artificial heart: visual and virtual assessment

Chihiro Miyagi[1†], Munir Ahmad[2†], Jamshid H. Karimov[1,3], Anthony R. Polakowski[1], Tara Karamlou[2], Malek Yaman[4], Kiyotaka Fukamachi[1,3]* and Hani K. Najm[2]

[1]Department of Biomedical Engineering, Cleveland Clinic Lerner Research Institute, Cleveland, OH, United States, [2]Department of Thoracic and Cardiovascular Surgery, Cleveland Clinic, Cleveland, OH, United States, [3]Department of Biomedical Engineering, Cleveland Clinic Lerner College of Medicine of Case Western Reserve University, Cleveland, OH, United States, [4]Department of Pediatric Cardiology, Cleveland Clinic Children's Hospital, Cleveland, OH, United States

Background: This study aimed to determine the fit of two small-sized (pediatric and infant) continuous-flow total artificial heart pumps (CFTAHs) in congenital heart surgery patients.
Methods: This study was approved by Cleveland Clinic Institutional Review Board. Pediatric cardiac surgery patients ($n = 40$) were evaluated for anatomical and virtual device fitting (3D-printed models of pediatric [P-CFTAH] and infant [I-CFTAH] models). The virtual sub-study consisted of analysis of preoperative thoracic radiographs and computed tomography ($n = 3$; 4.2, 5.3, and 10.2 kg) imaging data.
Results: P-CFTAH pump fit in 21 out of 40 patients (fit group, 52.5%) but did not fit in 19 patients (non-fit group, 47.5%). I-CFTAH pump fit all of the 33 patients evaluated. There were critical differences due to dimensional variation ($p < 0.0001$) for the P-CFTAH, such as body weight (BW), height (Ht), and body surface area (BSA). The cutoff values were: BW: 5.71 kg, Ht: 59.0 cm, BSA: 0.31 m^2. These cutoff values were additionally confirmed to be optimal by CT imaging.
Conclusions: This study demonstrated the range of proper fit for the P-CFTAH and I-CFTAH in congenital heart disease patients. These data suggest the feasibility of both devices for fit in the small-patient population.

KEYWORDS

pediatric heart failure, congenital heart disease, mechanical circulatory support, pediatric total artificial heart, infant total artificial heart

1. Introduction

In the pediatric heart failure (HF) population, the need for long-term support therapies such as the use of mechanical circulatory support (MCS) devices has become more prevalent in the last decade. The ventricular assist device (VAD), a representative MCS device, has yielded better outcomes recently (1–4) and it is reported that nearly one-third of pediatric patients receiving heart transplantation surgery are on VAD support (5). However, the donor hearts available for these children remain scarcer than those for adults; waitlist of infant mortality remains high (17%–30%) (6) compared to adults (7%) (7).

As for the recipient characteristics of the pediatric population undergoing heart transplantation, dilated cardiomyopathy (DCM) is the most common diagnosis globally; in North America, however, DCM and congenital heart disease (CHD) were equally

prevalent as the diagnosis for heart transplantation recipients (both about 40%) (8). For this CHD population, both two-year survival post-device implantation and post-transplantation following VAD support are significantly worse compared with the DCM population (5). A probable explanation is the presence of anatomical and physiological challenges such as shunt-dependent circulations and/or single ventricle circulations, causing technical issues with a pump design that focuses only on biventricular circulation patients. Therefore, advanced-stage pediatric HF patients, especially CHD patients, might have benefited from replacement therapy, such as the total artificial heart (TAH) (9–12).

In particular, due to the specific developmental, anatomical, and morphological representations in the pediatric population (i.e., bilateral HF with single ventricular patients), the applications of currently available VADs are limited. In addition, due to the small size of the chest cavity, the applications and considerations are also limited to select patients. Therefore, more durable solutions are critical to address this clinical burden. Moreover, these patients need longer-term options even after the heart transplant, since the risk of chronic rejection or infection after a transplant is much higher.

Among viable clinical alternatives currently available, the only option as a pediatric TAH is the SynCardia 50 cc (SynCardia, Tucson, AZ). Although some space in the thoracic can be made after ventricular resection, the recommended patient size for this pump requires a body surface area (BSA) of 1.2–1.7 m^2 (9, 10, 13), leaving a large number of pediatric patients ineligible due to their body size.

The pediatric continuous-flow TAH (P-CFTAH) is a pediatric-size TAH that is being developed by scaling down the adult CFTAH. Using the same algorithm as the adult CFTAH, the P-CFTAH produces self-balancing left and right circulations without electronic intervention, and is currently at the *in vivo* experimental stage of development (14). We also have conceptualized an even smaller pump designated as the infant CFTAH (I-CFTAH). Here we report the results of our initial fitting study of the P-CFTAH and I-CFTAH that were designed to confirm the feasibility of anatomical implantation, and to explore the appropriate range of patient sizes that would permit the use of replacement MCS devices.

2. Materials and methods

2.1. Study design

This study was approved by the Cleveland Clinic's Institutional Review Board (#17-1706). A written consent for participation was obtained prior to the surgeries. Mean body weight (BW), height (Ht), and BSA were 8.2 ± 6.2 kg, 68.7 ± 22.8 cm, and 0.39 ± 0.21 m^2, respectively. The patients' diagnosis data are summarized in **Supplementary Table S1**.

2.2. Study inclusion criteria

The patients listed for surgery at the Cleveland Clinic Department of Thoracic and Cardiovascular Surgery from July 2019 to June 2021, with a confirmed CHD and a need for corrective surgery via a median sternotomy with pericardiotomy, were enrolled and included in this study after consent was obtained ($n = 40$, average age: 18.0 months, ranging from 5 days to 4 years). Both bi-ventricular and single-ventricular cases, in addition to palliative surgeries, were included in this study.

2.3. Study exclusion criteria

Patients over >30 kg, preterm infants, and those who were already on cardiopulmonary bypass support at the time of the fitting were excluded.

2.4. 3D-printed models of the P-CFTAH and I-CFTAH pumps

The P-CFTAH pump was derived from the adult CFTAH by downsizing with a scale factor of 0.70, or approximately 1/3 of the total adult volume (**Figure 1**). The 3D-printed prototypes of the P-CFTAH (**Supplementary Figures S1A–S1C**) and I-CFTAH (**Supplementary Figures S1D–1F**) were developed for the intraoperative fittings. The 3D-printed model of the P-CFTAH follows the exact dimensions of the working prototype and has adjustable inlet and outlet conduits; as a result, the angulation and length can be adjusted to each patients' anatomies per case. The

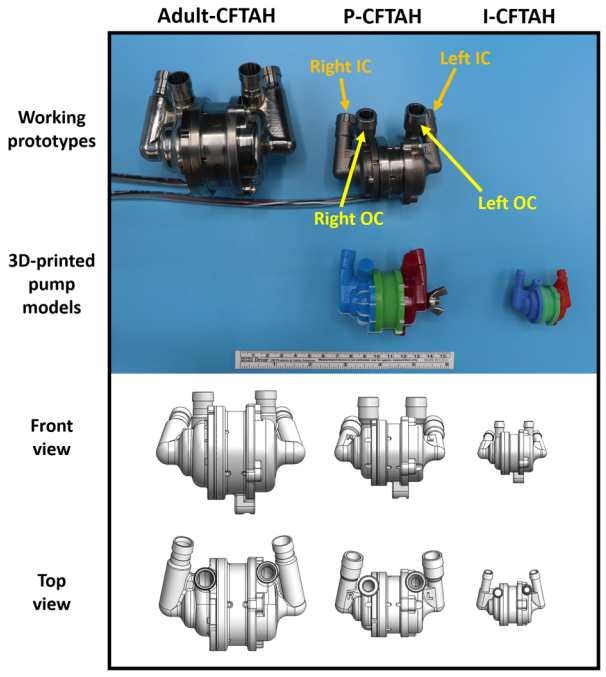

FIGURE 1
Size reference of three pumps (Adult CFTAH, P-CFTAH, and I-CFTAH). Top line: working pump prototypes of the adult CFTAH and P-CFTAH. Second line: 3D-printed models of the P-CFTAH and I-CFTAH used in intraoperative fitting studies. Third line: schematic illustrations of front view used for virtual fitting studies. Fourth line: schematic illustrations of top view used for virtual fitting studies. OC, outflow cannula; IC, inflow cannula.

size of outlet conduit is not true to size, but they are attached to the pump for length and angle evaluation. Dimensions of the 3D-printed model of the I-CFTAH were downsized with a scale factor of 0.65 of the P-CFTAH; therefore, the inlet and outlet conduits are not adjustable and are used for size evaluation only. An actual working prototype of the I-CFTAH is presently under development.

2.5. Intraoperative fitting

The 3D-printed models were sterilized through ethylene oxide gas sterilization. The sterilized models were used with a sterile plastic cover (iVAS Transducer Cover, CIVCO Medical Solutions, Kalona, IA), and the fitting procedure was performed from the first operator's position (patient right side). The size of the systemic ventricle was visually compared to the 3D-printed model, and the necessity of geometric adjustment to the inlet/outlet features of the P-CFTAH was also evaluated. If the model seemed to be of adequate size and implantable in the patient's thoracic cavity, the patient was assigned to the fit group (**Figure 2A**). If the ventricle seemed to be too small and not implantable for the pump, the patient was assigned to the non-fit group (**Figure 2B**). Since the concept of I-CFTAH was new, the first 7 cases were evaluated only for the P-CFTAH and in the remaining 33 studies, both P- and I-CFTAH were evaluated for fit.

2.6. Preoperative x-ray evaluation

For all patients enrolled in the fitting study ($n = 40$), their preoperative x-rays were evaluated besides the intraoperative fitting. From the front view (**Supplementary Figure S2A**): the thoracic width from left to right (A); the total heart size (B); the distance between the middle of vertebrae to apex (C); and the distance between the carina to apex (D) were measured. From the side view (**Supplementary Figure S2B**): the distance between sternum and middle of the vertebrae (E) was measured. Although a side view of x-rays is not always taken for all patients, those of 15 patients were available. All measurements were completed and recorded by one researcher, and the cardio-thoracic ratio (CTR) was also calculated as B/A.

2.7. Preoperative 3D-computed tomography image evaluation

Among the 40 patients, three had a contrast-enhanced computed tomography (CT) study performed prior to their intraoperative fitting study, which included a range of scans wide enough to evaluate the pump fitting. The CT datasets in the Digital Imaging and Communications in Medicine format were downloaded onto a computer workstation, and 3D on-screen models of the great vessels, rib cage, and heart without both ventricles were generated using Mimics Medical 22.0 software (Materialise, Leuven, Belgium) and exported in stereolithographic (STL) file format.

The anatomic models in STL format were then opened in the SOLIDWORKS application (Dassault Systèmes SOLIDWORKS Corporation, Waltham, MA), and the pump STL files, which were used to make the 3D-printed prototypes and were displayed with the anatomical models. The pump position was adjusted to determine an optimal pump fitting site (dependent on the

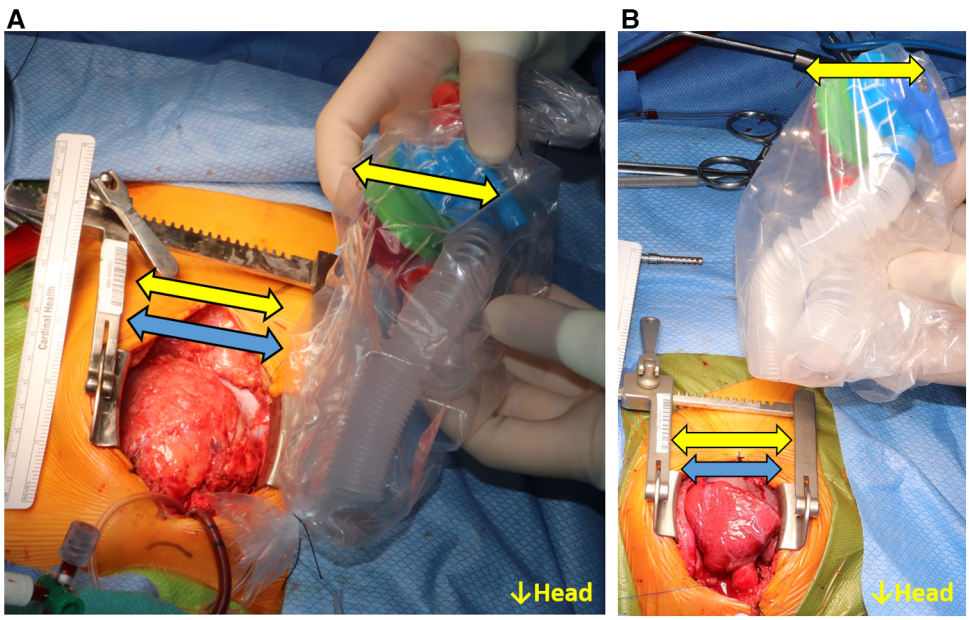

FIGURE 2
Intraoperative fittings for the P-CFTAH. (A) the patient categorized to the fit group, (B) the pump categorized to the non-fit group. Yellow arrow: size of the pump; blue arrow: size of the heart.

patient's anatomy), and device interference with the surrounding tissues and chest walls was assessed from all directions. For all three anatomical models from the different size patients' CT data, both P-CFTAH and I-CFTAH pump data were applied and evaluated, respectively.

2.8. Statistical analysis

Data are presented as mean values with standard deviation (mean ± SD). Differences among quantitative parameters between the fitting and non-fitting groups were assessed using the Mann-Whitney *U* test (U). To investigate the cutoff value of each parameter, receiver operating characteristic (ROC) curves were constructed, and area under curve (AUC) for each ROC curve was evaluated. In all analyses, a value of $p < 0.05$ was considered statistically significant. Statistical analysis was performed using JMP Pro 14.2.0 software (SAS Institute Inc., Cary, NC).

3. Results

The P-CFTAH pump model fit 21 patients ($n = 21$; 52.5%), with the remaining patients ($n = 19$; 47.5%) classified to the non-fit group. By using the flexible conduit in mating length and alignment to the vessels, for all patients in the fit group, there was no need to adjust any angles of the inlet/outlet features of the pump. The mean age and BW of the fit group were 32.9 ± 32.3 months and 12.0 ± 6.4 kg, and those of the non-fit group were 1.47 ± 1.14 months and 3.94 ± 0.97 kg, respectively. Each group had significant differences for the BW ($p < 0.0001$), Ht ($p < 0.0001$), BSA ($p < 0.0001$), and thoracic and heart sizes (A–D: $p < 0.0001$, E: $p < 0.05$) (**Table 1**). There were no differences in the CTR. The fitting in the rest of the patients was not deemed feasible ($n = 19$) without expanding the space for physical device fit.

The cutoff values of each parameter obtained from the ROC curves are shown in **Supplementary Table S2**. Those of BW, Ht, and BSA were calculated as 5.7 kg, 59 cm, and 0.31 m^2, with high AUCs of >0.95. These values are all relatively equivalent to the average size of 3–4 month-old children, and the BSA is much smaller than the minimum size reported by the SynCardia 50 cc case (0.9–1.1 m^2) (9). One of the ROC curves (BSA) is shown in **Supplementary Figure S3**. As for the parameters obtained from the x-rays, A, B, and D also had clear cut-off values, with a high of AUC > 0.95. The distance between the sternum and middle of the vertebrae (E, $n = 15$) had a relatively low AUC (0.820) compared with other values, but was still high enough to make the cut-off line useful.

TABLE 1 Mean values of 40 patients for each parameter measured.

	Total ($n = 40$)	Fit group ($n = 21$)	Non-fit group ($n = 19$)	
Age (month)	18.0 ± 28.2	32.9 ± 32.3	1.5 ± 1.1	$p < 0.0001$
BW (kg)	8.2 ± 6.2	12.0 ± 6.4	3.9 ± 1.0	$p < 0.0001$
Ht (cm)	68.7 ± 22.8	83.8 ± 21.8	52.1 ± 6.0	$p < 0.0001$
BSA (m^2)	0.39 ± 0.21	0.52 ± 0.21	0.23 ± 0.04	$p < 0.0001$
A (mm)	139.2 ± 30.8	160.6 ± 27.0	115.6 ± 11.4	$p < 0.0001$
B (mm)	81.8 ± 18.6	94.7 ± 16.2	67.5 ± 7.3	$p < 0.0001$
C (mm)	53.9 ± 15.2	62.3 ± 13.5	43.7 ± 10.3	$p < 0.0001$
D (mm)	75.8 ± 19.5	87.8 ± 18.0	61.2 ± 9.1	$p < 0.0001$
E (mm)	79.0 ± 14.6	82.1 ± 15.5	69.6 ± 4.7	$p < 0.05$
CTR (B/A)	0.59 ± 0.07	0.59 ± 0.07	0.59 ± 0.07	$p = 0.89$

BW, body weight; Ht, height; BSA, body surface area; CTR, cardio-thoracic ratio; A, the thoracic width from left to right; B, the total heart size; C, the distance between the middle of vertebrae to apex; D, the distance from the carina to the apex; E, the distance between the sternum and middle of the vertebrae in side view.

With regards to the I-CFTAH model, 33 out of 40 patients (range: 3.0–17.2 kg, mean: 7.10 ± 4.45 kg) underwent the intraoperative fitting evaluation following that of P-CFTAH. All showed an optimal anatomical fitting in the size of the chest and angles of the great vessels.

From the three preoperative 3D CT images, the combined views of the thoracic and the pump were obtained; the front, bottom, and left-side views are shown and compared in **Figure 3**. Patient #1 (10.2 kg, 16 months old) showed a proper fit for the P-CFTAH pump. Since this patient underwent heart transplantation, we were able to compare the pump prototype and the ventricles directly after resection of the ventricles. The images of patient #2 (5.3 kg, 4 months old) demonstrate how both the P-CFTAH and I-CFTAH pumps would be seen in the thoracic. According to the cutoff line of the BW obtained by the intraoperative fittings, the size of 5.3 kg is just below the line. Although the P-CFTAH in patient #2 looks much tighter than that in patient #1, it is still considered to be implantable with resection of the ventricles, and the intraoperative evaluation had actually assigned patient #2 to the fit group. Combined with the visual and virtual fitting, the cutoff line of 5.7 kg is considered to be probable and reasonable. Since the I-CFTAH model also showed an adequate fit in patient #2, this size patient (around 5.3–5.7 kg) could be a candidate for either pump. The 3D CT images of patient #3 (4.2 kg, 2 month-old) lack detail of the lowest part of the thoracic, including the diaphragm, but it is readily apparent that the I-CFTAH fits properly in this patient's chest cavity because size of the I-CFTAH is smaller than this patient's ventricles (**Figure 3**, bottom row).

4. Discussion

Children under 18 years old on the wait list for heart transplantation are known to experience some of the poorest mortality rates when compared to all other solid organ recipients in the United States (9, 15, 16). The outcomes of end-stage HF in the pediatric population have significantly improved recently due to the introduction of VADs (15, 17). When looking at their survival by age, however, the outcomes of the youngest group (age < 1year) have been the lowest. In the latest annual report of the Pediatric Interagency Registry for Mechanical Circulatory Support (Pedimacs), a strong appeal is made for better options for this population (18). This is largely because implantable continuous-flow VADs (IC-VADs), which have yielded superior results when compared to pulsatile VADs, are currently not available for infants and small children (19), and only 10% of IC-VADs were implanted in children under 20 kg (18).

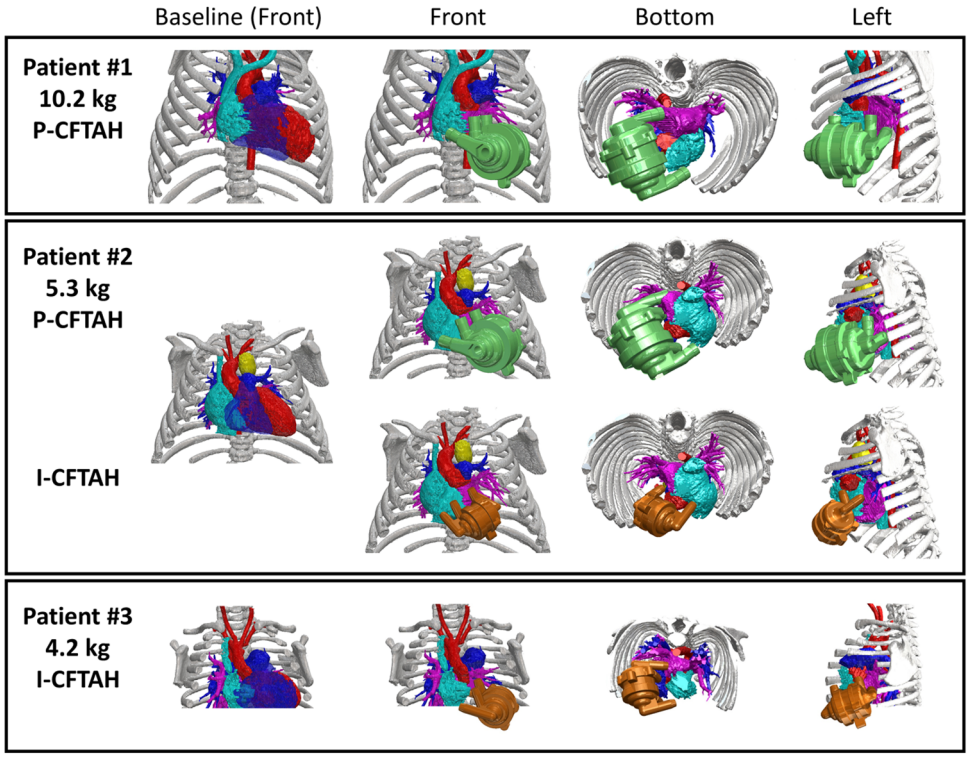

FIGURE 3
Combined views of three patients' 3D-computed tomography images with and without P-/I-CFTAH pumps.

As a result, the representative pulsatile VAD, the Berlin Heart EXCOR pediatric VAD (Berlin Heart GmbH, Berlin, Germany), tends to be used in younger, smaller patients with CHD. The Berlin Heart extracorporeal configuration with large-bore silicone cannulas, can carry blood across the abdominal wall and has less risk of lacking space in thoracic. However, the cannulas are prone to complications such as infection, cardiac tissue ischemia, and wound-healing problems in comparison with the smaller drivelines of implantable VADs. However, there are serious challenges to supporting patients with CHD with EXCOR VADs only, due to the complicated physiology, hemodynamics, and previous surgical interventions of CHD patients, in addition to the required hospital stay for the whole period while being treated with this device (2).

To resolve this critical deficiency, TAHs are getting more attention, since they enable biventricular support with a smaller size than VADs regardless of single- or bi-ventricle circulations. Especially in patients suffering from Fontan failure hemodynamics, VADs provide only systemic support that sometimes fails to benefit patients; thus, TAHs should be in consideration for improving hepatic congestion, renal insufficiency, or protein-losing enteropathy (17). However, only one TAH device, the SynCardia 50 cc, is currently approved by the Food and Drug Administration for pediatric use and even this cannot be considered for infants or small children with a BSA < 1.2 m^2. It is an urgent goal to develop a novel smaller TAH for this population. The P-CFTAH was developed with this understanding, and the main aim is to support children < 1 year old and, more specifically, patient groups under 10 kg.

The adult CFTAH is a double-ended centrifugal pump with single rotor. The device is a valveless, continuous-flow pump, capable of automatic self-regulation to balance the systemic and pulmonary circulation passively, depending on the preload (left and right atrial pressures) (20). To address the clinical needs of smaller patients, the core device design transfer to a smaller-sized blood pump has been proposed. All the critical CFTAH features, including self-regulation, were incorporated into the P-CFTAH design; therefore, this pediatric device is also fully capable of balancing systemic and pulmonary flows. For patients with CHD, one of the biggest advantages of this self-balancing concept is that it can compensate for flow differences between left and right circulations due to bronchial shunts, which are commonly seen in CHD patients, and the shunt flow in patients requiring a TAH is said to be up to one-third of the systemic output (21).

The P-CFTAH pump has undergone a series of acute *in vivo* studies with lambs (~30 kg), which confirmed that the prototype design has met the proposed performance parameters, including self-regulation and pulse modulation (14). The next step is to determine the feasibility and fit of this downsized device through intrathoracic human fitting studies, since the chest morphology and size of quadrupedal animals can differ largely from those of humans.

A similar fitting process had been conducted for the adult CFTAH, combining intraoperative and virtual fitting studies with CT scans (22), but for pediatric CHD patients, the number of available preoperative CT images with contrast was extremely small compared to those of adults. For evaluation, we accordingly attempted to use the x-ray images that are routinely

taken preoperatively for most pediatric patients before any cardiac procedures. Combined with the intraoperative evaluation, the thoracic dimensions and cardiac sizes obtained from x-rays showed clear cut-off values with a large AUC for the differentiation between fit and non-fit; therefore, a preoperative x-ray is useful for evaluating whether the P-CFTAH is implantable.

Data accuracy of these cut-off values were effectively confirmed, even with a limited number of 3D-CT images. The technique of creating and combining on-screen images through generating 3D-reconstructions of complex anatomy and medical devices has been widely applied in diagnosis, patient education, and operative planning for complicated surgical approaches (23–25). Other TAH development processes have utilized a similar method for evaluation of fitting (26–28); so far, our lab has also had several experiences of virtual fittings with other pumps, using the Mimic software (29, 30). Size and anatomical fitting (i.e., distances and angles to the great arteries and both atriums) can be evaluated through 3D-CT fitting. Although the inlet/outlet angles of the P-CFTAH prototype are adjustable, the default angles were confirmed to be suitable for all fitting group patients and there was no need to adjust them. Adjustable diameters, angles, and lengths of the pump conduits at distal anastomosis sites will give much more flexibility in mating alignment to various native vessels and atria.

There are several limitations in this study. The first is that the visual intraoperative fitting could be subjective, and thus cannot be totally free of bias. Also, in this study, we could not put the device model into the chest directly due to Institutional Review Board regulations that prevent any possible infections by the study. The evaluation was done with eye measurements and by consensus, and although the method of comparing the chest and the pump was stylized as well as possible, there is still room for improvement in order to be more objective.

The second limitation is that the number of patients around the cut-off value of 5 kg was limited. More cases representing this BW are required to establish a more closely defined cut-off value; in some cases, a patient over the proposed cut-off line was placed in the non-fit group, and a smaller patient under the cut-off line placed in the fit group. Also, our previous study that compared the vertebra-to-sternum distances (the same parameter as E in the **Supplemental Figure 2B**) to BSA (31), showed that the P-CFTAH could fit in patients with a BSA $\geq 0.3\ m^2$ (almost the same result as the current study), and that the parameter E was a good indicator for fitting. However, in this study, the AUC of parameter E was much less than other parameters. This can be explained by the fact that there are larger variations in the absolute values for vertebra-to-sternum distances than the not-CHD pediatric population due to the influence of previous surgeries for the CHD population. Recruitment of more CHD patients, ideally before VAD implantation or transplantation, is necessary. Since taking a CT scan with contrast before the surgery is not always a common strategy for most of the CHD population, related to this second limitation, we were only able to obtain three 3D-CT images from among the 40 patients. For the remaining patients, most of the imaging have been done by magnetic resonance imaging (MRI) if needed, but MRI has limited quality in resolution for fitting studies, and thus we decided not to use them.

The third limitation is that not all CHD patients require TAH implantation or transplantation, resulting in a discrepancy between the characteristics of the patient collection in this study when compared to the actual target population for the P-CFTAH/I-CFTAH pump. Among the 40 patients, simple CHD cases such as atrial septum defect patients are included, even though unlikely to experience severe HF, and only two DCM patients were included. However, these CHD patients' data were still useful in understanding the relationship between the actual heart size at surgery and the size shown in x-ray/CT, and we succeeded in confirming the reliability of x-ray measurements from them.

A final limitation is that this is merely a virtual or visual fitting. Careful evaluation of fit is still required at an actual implant surgery in the future. Also, even with careful preoperative evaluations, a risk of non-fit cannot be zero, so having some back-up plans, such as extracorporeal placement of a device would be necessary. Furthermore, since even the P-CFTAH pump cannot be used in patients smaller than 5 kg, the development of an actual working I-CFTAH prototype is needed as quickly as possible. This study's aim is only for size comparison. We did not intend to evaluate the sufficiency of cardiac output created by the pumps at this moment, but upcoming study will reveal these in near future.

5. Conclusion

This study demonstrated that the range of optimal dimensions for the P-CFTAH and I-CFTAH were feasible in pediatric CHD patients, including those who were under 10 kg at the time of evaluation. These results suggest the potential use of MCS devices is viable in small-sized pediatric HF patients. As a preoperative evaluation for fit, the BW, Ht BSA, and preoperative thoracic and cardiac dimensions obtained from thoracic radiography images were important parameters as a cutoff line for P-CFTAH and I-CFTAH implantation.

Data availability statement

The raw data supporting the conclusions of this article will be made available by the authors, without undue reservation.

Ethics statement

The studies involving human participants were reviewed and approved by Cleveland Clinic's Institutional Review Board (#17-1706). Written informed consent to participate in this study was provided by the participants' legal guardian/next of kin.

Author contributions

All authors contributed to the design and data collection of the study. CM and MA: contributed equally to this study, drafted the manuscript, and participated in patient selection. HN: is the clinical Principal Investigator of the study. HN and MA: obtained

patients' consent forms or IRB approval. All authors contributed to the article and approved the submitted version.

Funding

This study was supported by funding from the National Heart, Lung, and Blood Institute, National Institutes of Health (NIH), (R01HL139984). (PI: Fukamachi).

Conflict of interest

The authors declare that the research was conducted in the absence of any commercial or financial relationships that could be construed as a potential conflict of interest.

Publisher's note

Supplementary material

The Supplementary Material for this article can be found online at: https://www.frontiersin.org/articles/10.3389/fcvm.2023.1193800/full#supplementary-material

References

1. Conway J, Miera O, Adachi I, Maeda K, Eghtesady P, Henderson HT, et al. Worldwide experience of a durable centrifugal flow pump in pediatric patients. *Semin Thorac Cardiovasc Surg*. (2018) 30(3):327–35. doi: 10.1053/j.semtcvs.2018.03.003

2. Conway J, St Louis J, Morales DLS, Law S, Tjossem C, Humpl T. Delineating survival outcomes in children <10 kg bridged to transplant or recovery with the Berlin heart excor ventricular assist device. *JACC Heart Fail*. (2015) 3(1):70–7. doi: 10.1016/j.jchf.2014.07.011

3. Kreuziger LB, Massicotte MP. Adult and pediatric mechanical circulation: a guide for the hematologist. *Hematology Am Soc Hematol Educ Program*. (2018) 2018 (1):507–15. doi: 10.1182/asheducation-2018.1.507

4. Morales DLS, Adachi I, Peng DM, Sinha P, Lorts A, Fields K, et al. Fourth annual pediatric interagency registry for mechanical circulatory support (pedimacs) report. *Ann Thorac Surg*. (2020) 110(6):1819–31. doi: 10.1016/j.athoracsur.2020.09.003

5. Dipchand AI, Kirk R, Naftel DC, Pruitt E, Blume ED, Morrow R, et al. Ventricular assist device support as a bridge to transplantation in pediatric patients. *J Am Coll Cardiol*. (2018) 72(4):402–15. doi: 10.1016/j.jacc.2018.04.072

6. Deshpande S, Sparks JD, Alsoufi B. Pediatric heart transplantation: year in review 2020. *J Thorac Cardiovasc Surg*. (2021) 162(2):418–21. doi: 10.1016/j.jtcvs.2021.04.073

7. Bakhtiyar SS, Godfrey EL, Ahmed S, Lamba H, Morgan J, Loor G, et al. Survival on the heart transplant waiting list. *JAMA Cardiol*. (2020) 5(11):1227–35. doi: 10.1001/jamacardio.2020.2795

8. Singh TP, Cherikh WS, Hsich E, Chambers DC, Harhay MO, Hayes D Jr., et al. The international thoracic organ transplant registry of the international society for heart and lung transplantation: twenty-fourth pediatric heart transplantation report—2021; focus on recipient characteristics. *J Heart Lung Transplant*. (2021) 40 (10):1050–9. doi: 10.1016/j.healun.2021.07.022

9. Beasley GS, Allen K, Pahl E, Jackson L, Eltayeb O, Monge M, et al. Successful bridge to transplant in a pediatric patient using the syncardia 50 cc total artificial heart. *Asaio J*. (2020) 66(2):e33–e5. doi: 10.1097/MAT.0000000000000968

10. Kirklin JK. Advances in mechanical assist devices and artificial hearts for children. *Curr Opin Pediatr*. (2015) 27(5):597–603. doi: 10.1097/MOP.0000000000000273

11. Morales DLS, Lorts A, Rizwan R, Zafar F, Arabia FA, Villa CR. Worldwide experience with the syncardia total artificial heart in the pediatric population. *Asaio J*. (2017) 63(4):518–9. doi: 10.1097/MAT.0000000000000504

12. Rossano JW, Goldberg DJ, Fuller S, Ravishankar C, Montenegro LM, Gaynor JW. Successful use of the total artificial heart in the failing fontan circulation. *Ann Thorac Surg*. (2014) 97(4):1438–40. doi: 10.1016/j.athoracsur.2013.06.120

13. Devaney EJ. The total artificial heart in pediatrics: expanding the repertoire. *J Thorac Cardiovasc Surg*. (2016) 151(4):e73–4. doi: 10.1016/j.jtcvs.2015.12.039

14. Karimov JH, Horvath DJ, Byram N, Sunagawa G, Kuban BD, Gao S, et al. Early in vivo experience with the pediatric continuous-flow total artificial heart. *J Heart Lung Transplant*. (2018) 37(8):1029–34. doi: 10.1016/j.healun.2018.03.019

15. Zafar F, Castleberry C, Khan MS, Mehta V, Bryant R 3rd, Lorts A, et al. Pediatric heart transplant waiting list mortality in the era of ventricular assist devices. *J Heart Lung Transplant*. (2015) 34(1):82–8. doi: 10.1016/j.healun.2014.09.018

16. Almond CSD, Thiagarajan RR, Piercey GE, Gauvreau K, Blume ED, Bastardi HJ, et al. Waiting list mortality among children listed for heart transplantation in the United States. *Circulation*. (2009) 119(5):717–27. doi: 10.1161/CIRCULATIONAHA.108.815712

17. Shugh SB, Riggs KW, Morales DLS. Mechanical circulatory support in children: past, present and future. *Transl Pediatr*. (2019) 8(4):269–77. doi: 10.21037/tp.2019.07.14

18. Rossano JW, VanderPluym CJ, Peng DM, Hollander SA, Maeda K, Adachi I, et al. Fifth annual pediatric interagency registry for mechanical circulatory support (pedimacs) report. *Ann Thorac Surg*. (2021) 112(6):1763–74. doi: 10.1016/j.athoracsur.2021.10.001

19. Rossano JW, Lorts A, VanderPluym CJ, Jeewa A, Guleserian KJ, Bleiweis MS, et al. Outcomes of pediatric patients supported with continuous-flow ventricular assist devices: a report from the pediatric interagency registry for mechanical circulatory support (pedimacs). *J Heart Lung Transplant*. (2016) 35(5):585–90. doi: 10.1016/j.healun.2016.01.1228

20. Horvath D, Byram N, Karimov JH, Kuban B, Sunagawa G, Golding LAR, et al. Mechanism of self-regulation and in vivo performance of the Cleveland clinic continuous-flow total artificial heart. *Artif Organs*. (2017) 41(5):411–7. doi: 10.1111/aor.12780

21. Bhunia SK, Kung RT. Indirect bronchial shunt flow measurements in abiocor implantable replacement heart recipients. *Asaio J*. (2004) 50(3):211–4. doi: 10.1097/01.MAT.0000124101.70517.BF

22. Karimov JH, Steffen RJ, Byram N, Sunagawa G, Horvath D, Cruz V, et al. Human fitting studies of Cleveland clinic continuous-flow total artificial heart. *Asaio J*. (2015) 61(4):424–8. doi: 10.1097/MAT.0000000000000219

23. Chessa M, Van De Bruaene A, Farooqi K, Valverde I, Jung C, Votta E, et al. Three-dimensional printing, holograms, computational modelling, and artificial intelligence for adult congenital heart disease care: an exciting future. *Eur Heart J*. (2022) 43(28):2672–84. doi: 10.1093/eurheartj/ehac266

24. Goo HW, Park SJ, Yoo SJ. Advanced medical use of three-dimensional imaging in congenital heart disease: augmented reality, mixed reality, virtual reality, and three-dimensional printing. *Korean J Radiol*. (2020) 21(2):133–45. doi: 10.3348/kjr.2019.0625

25. Hell MM, Emrich T, Kreidel F, Kreitner KF, Schoepf UJ, Münzel T, et al. Computed tomography imaging needs for novel transcatheter tricuspid valve repair and replacement therapies. *Eur Heart J Cardiovasc Imaging*. (2021) 22(6):601–10. doi: 10.1093/ehjci/jeaa308

26. Alaeddine M, Ploutz M, Arabía FA, Velez DA. Implantation of total artificial heart in a 10-year-old after support with a temporary perventricular assist device. *J Thorac Cardiovasc Surg*. (2020) 159(3):e227–e9. doi: 10.1016/j.jtcvs.2019.07.101

27. Ferng AS, Oliva I, Jokerst C, Avery R, Connell AM, Tran PL, et al. Translation of first north American 50 and 70 cc total artificial heart virtual and clinical implantations: utility of 3d computed tomography to test fit devices. *Artif Organs*. (2017) 41(8):727–34. doi: 10.1111/aor.12854

28. Moore RA, Lorts A, Madueme PC, Taylor MD, Morales DL. Virtual implantation of the 50cc syncardia total artificial heart. *J Heart Lung Transplant*. (2016) 35(6):824–7. doi: 10.1016/j.healun.2015.12.026

29. Noecker AM, Chen JF, Zhou Q, White RD, Kopcak MW, Arruda MJ, et al. Development of patient-specific three-dimensional pediatric cardiac models. *Asaio J*. (2006) 52(3):349–53. doi: 10.1097/01.mat.0000217962.98619.ab

30. Noecker AM, Cingoz F, Ootaki Y, Liu J, Kuzmiak S, Kopcak MW, et al. The Cleveland clinic pedipump: anatomic modeling and virtual fitting studies in a lamb model. *Asaio J*. (2007) 53(6):716–9. doi: 10.1097/MAT.0b013e31805fe98b

31. Fukamachi K, Karimov JH, Byram NA, Sunagawa G, Dessoffy R, Miyamoto T, et al. Anatomical study of the Cleveland clinic continuous-flow total artificial heart in adult and pediatric configurations. *J Artif Organs*. (2018) 21(3):383–6. doi: 10.1007/s10047-018-1039-0

frontiers | Frontiers in Cardiovascular Medicine

TYPE Original Research
PUBLISHED 07 September 2023
DOI 10.3389/fcvm.2023.1210278

OPEN ACCESS

EDITED BY
Jamshid Karimov,
Cleveland Clinic, United States

REVIEWED BY
Dorin Ionescu,
Carol Davila University of Medicine and Pharmacy, Romania
Tahir Yagdi,
EGE University, Türkiye

*CORRESPONDENCE
Si Chen
✉ Sichen@hust.edu.cn
Jiawei Shi
✉ 1999xh0522@hust.edu.cn
Nianguo Dong
✉ 1986xh0694@hust.edu.cn

†These authors have contributed equally to this work

RECEIVED 22 April 2023
ACCEPTED 22 August 2023
PUBLISHED 07 September 2023

CITATION
Shen Q, Yao D, Zhao Y, Qian X, Zheng Y, Xu L, Jiang C, Zheng Q, Chen S, Shi J and Dong N (2023) Elevated serum albumin-to-creatinine ratio as a protective factor on outcomes after heart transplantation.
Front. Cardiovasc. Med. 10:1210278.
doi: 10.3389/fcvm.2023.1210278

Elevated serum albumin-to-creatinine ratio as a protective factor on outcomes after heart transplantation

Qiang Shen[1†], Dingyi Yao[1†], Yang Zhao[1,2†], Xingyu Qian[1], Yidan Zheng[1], Li Xu[1,2,3,4], Chen Jiang[1,2,3,4], Qiang Zheng[1], Si Chen[1,2,3,4*], Jiawei Shi[1,2,3,4*] and Nianguo Dong[1,2,3,4*]

[1]Department of Cardiovascular Surgery, Union Hospital, Tongji Medical College, Huazhong University of Science and Technology, Wuhan, China, [2]Key Laboratory of Organ Transplantation, Ministry of Education, Wuhan, China, [3]NHC Key Laboratory of Organ Transplantation, Wuhan, China, [4]Key Laboratory of Organ Transplantation, Chinese Academy of Medical Sciences, Wuhan, China

Background: The purpose of this study was to investigate the prognostic significance of serum albumin to creatinine ratio (ACR) in patients receiving heart transplantation of end-stage heart failure.
Methods: From January 2015 to December 2020, a total of 460 patients who underwent heart transplantation were included in this retrospective analysis. According to the maximum Youden index, the optimal cut-off value was identified. Kaplan-Meier methods were used to describe survival rates, and multivariable analyses were conducted with Cox proportional hazard models. Meanwhile, logistic regression analysis was applied to evaluate predictors for postoperative complications. The accuracy of risk prediction was evaluated by using the concordance index (C-index) and calibration plots.
Results: The optimal cut-off value was 37.54 for ACR. Univariable analysis indicated that recipient age, IABP, RAAS, BB, Hb, urea nitrogen, D-dimer, troponin, TG, and ACR were significant prognostic factors of overall survival (OS). Multivariate analysis showed that preoperative ACR (HR: 0.504, 95% = 0.352–0.722, $P < 0.001$) was still an independent prognostic factor of OS. The nomogram for predicting 1-year and 5-year OS in patients who underwent heart transplantation without ACR (C-index = 0.631) and with ACR (C-index = 0.671). Besides, preoperative ACR level was a significant independent predictor of postoperative respiratory complications, renal complications, liver injury, infection and in-hospital death. Moreover, the calibration plot showed good consistency between the predictions by the nomogram for OS and the actual outcomes.
Conclusion: Our research showed that ACR is a favorable prognostic indicator in patients of heart transplantation.

KEYWORDS
heart failure, heart transplantation, albumin/creatinine ratio, prognosis, nomogram

1. Introduction

Heart failure is one of the most common cardiovascular manifestations (1). More than 26 million people worldwide are affected by heart failure (2). Heart transplantation (HTx) is the most effective and reliable treatment for end-stage heart failure (3). Over the past decades, the selection of HTx candidates and improvements in preoperative care have led

to a steady improvement in outcomes after early HTx. Meanwhile, studies have shown that preoperative specific risk factors can predict survival after HTx, such as preoperative obesity, single-ventricle congenital heart disease, history of multiple thoracotomies, and renal replacement therapy (4–6). Therefore, it is very meaningful to study predictors of adverse HTx outcomes, as they may allow for closer monitoring and early intervention of patients at risk.

Human serum albumin is a key plasma protein and has important physiological functions such as immune regulation, endothelial stability, antioxidant effects, and binding to a variety of drugs, toxins, and other molecules (7). There is increasing evidence that serum albumin levels are closely associated with cardiovascular diseases, such as myocardial fibrosis, adverse pulsing aortic hemodynamics, heart failure, and coronary heart disease (8, 9). Furthermore, the serum albumin level before HTx is a useful marker for estimating post-transplantation survival (10). In addition, previous studies have pointed out that serum creatinine levels can affect prognosis in cardiac surgery (11). Importantly, glomerular filtration rate (GFR) is also often measured by serum creatinine level and can affect the prognosis of heart transplantation (9).

The definition of the ratio of serum albumin to creatinine (ACR) was proposed by Liu H (12). Recent studies have pointed out that it can be used to predict renal outcomes in diabetic patients. Meanwhile, ACR is also used in predicting the outcome of cardiovascular diseases, such as asymptomatic coronary artery disease and acute myocardial infarction (12–14). Nevertheless, its role in heart transplantation has not been investigated.

Therefore, in this retrospective study, we aimed to analyze the association of preoperative ACR levels with complications and overall survival (OS) after HTx.

2. Methods

2.1. Patients

Between 2015 and 2020, a total of 568 patients scheduled to undergo heart transplantation at Wuhan Union Medical College Hospital were included in this study. Age less than 18 years, retransplants, and patients with missing data were excluded. Ultimately 460 patients were recruited to the study and were divided into two groups of ACR > 37.54 ($n = 262$), and ACR ≤ 37.54 ($n = 198$), according to the optimal cut-off value of ACR (**Figure 1**). This retrospective study has been approved by the Committee of Tongji Medical College. The use and collection of patient data complied with the Declaration of Helsinki principles in our study.

2.2. Follow-up

Information on all survivors was collected through visits and telephone calls. OS was defined as the interval between surgery and death or last contact. The follow-up ended on December 31, 2020.

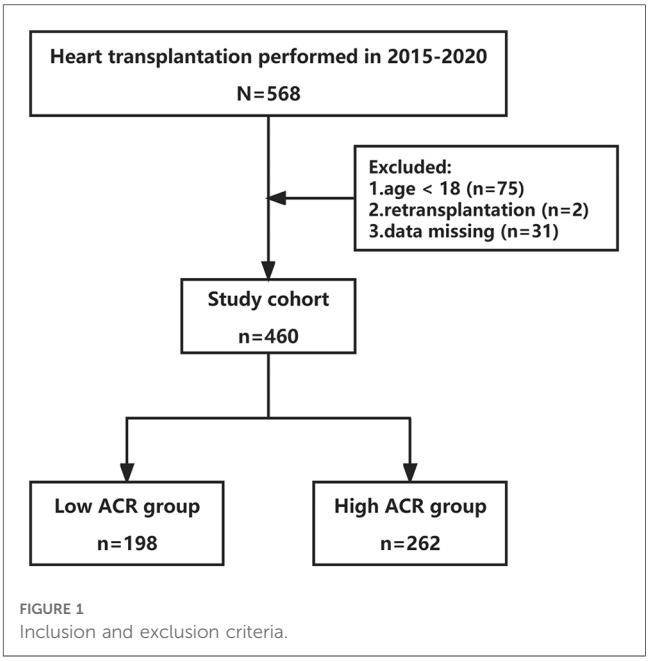

FIGURE 1
Inclusion and exclusion criteria.

2.3. Demographic and clinical variables

Demographic variables of all patients included sex, age, blood type, body mass index (BMI), and diagnosis. Additionally, the recipients' information also included the history of smoking, diabetes mellitus, previous cardiac surgery, hypertension, left ventricular ejection fraction (LVEF), and waiting time. The preoperative therapy data included extracorporeal membrane oxygenation (ECMO), implantable intra-aortic balloon pump (IABP), renin-angiotensin-aldosterone system (RAAS) antagonist, beta-blockers (BB), calcium channel blocker (CCB) and diuretics. Preoperative blood biochemical indexes included hemoglobin (Hb), white blood cell count (WBC), blood platelet (PLT), albumin, creatinine (Cr), bilirubin, glutamic oxaloacetic transaminase (AST), alanine aminotransferase (ALT), low-density lipoprotein (LDL), troponin and triglyceride (TG). Preoperative hematological and biochemical indicators are the first results of the first admission of a heart transplant patient.

2.4. Postoperative clinical events

We compared several postoperative clinical events between the high and low ACR groups, including postoperative ICU stay time, total postoperative hospital stay time, the use of postoperative CRRT, IABP, and ECMO, respiratory complications, neurological complications, hematological complications, hyperglycemia, hypertension, infection, renal injury, liver injury, septic shock, secondary thoracotomy, and death in hospital.

2.5. Definition

As previously reported in the literature, ACR was calculated from the ratio of serum albumin (mg/dl) to creatinine (mg/dl) (15). Postoperative infection is defined as an infection of soft tissues and organs after surgery and arises when the balance between host defense mechanisms and bacterial load or virulence is disrupted (16, 17).

2.6. Statistical analysis

In this study, continuous variables are expressed as mean ± standard deviation or median [interquartile range] according to their normality, whereas categorical variables are expressed as percentages. Different ACR groups were compared at baseline concerning participants' characteristics and outcome measures using Mann–Whitney U tests for continuous variables, which were tested to be non-normal distributions, and χ^2 tests for categorical variables. The Cox proportional hazards regression model was used to determine independent predictors of mortality after heart transplantation. Besides, univariate and multivariable logistic regression was employed to identify predictors of postoperative clinical events. Survival analysis was performed using the Kaplan-Meier method, and significance was assessed by the log-rank test. Two-tailed P values < 0.05 were considered significant. The statistical analysis was performed with SPSS 23.0 and R-software v.4.2.1.

3. Results

3.1. Population characteristics

According to the inclusion and exclusion criteria, a total of 460 patients were included in the study. The median age was 50.00 years (38.00–57.00) and 359 (78%) of the patients were male. The median ACR of the samples was 39.32 (31.96–47.95). The histogram curve of ACR distribution is shown in **Figure 2**.

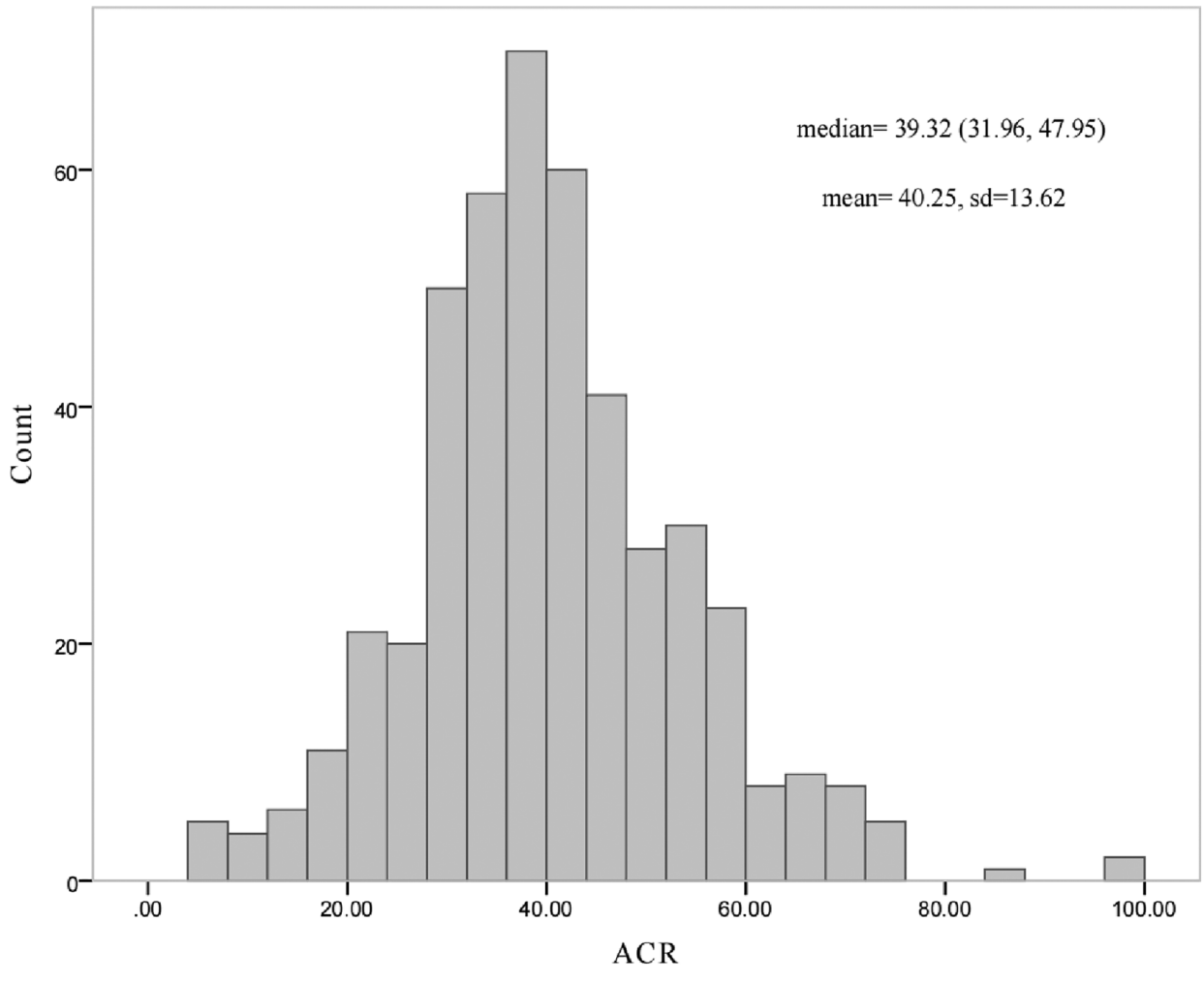

FIGURE 2
Histogram plot of ACR. ACR, serum albumin to creatinine ratio.

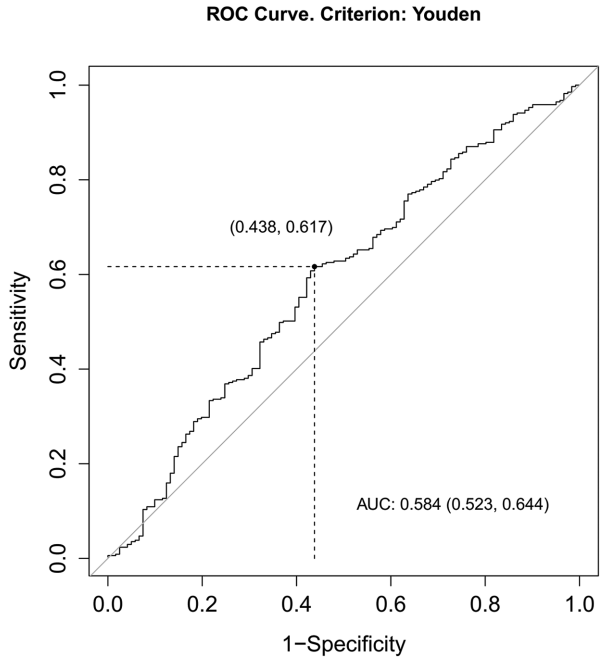

FIGURE 3
Receiver operating characteristic curves for pretreatment ACR.

3.2. The optimal cut-off values for estimating prognosis

The association between ACR and survival is shown in the ROC curve (Figure 3). During the process, the area under the curve (AUC) for survival was 0.584 ($P = 0.006$). According to the maximum Youden index, it revealed that 37.54 was an optimal cut-off value of the ACR index for predicting the survival rate. By the optimal cut-off value of ACR, the patients were divided into two groups (high, ≥37.54, and low, <37.54).

3.3. Characteristics of patients

Table 1 showed baseline patients' characteristics based on ACR. Patients with higher ACR levels tended to have a less proportion of males ($P < 0.001$) and chronic kidney disease ($P < 0.001$), younger age ($P < 0.001$), less hypertension ($P = 0.017$), more use of spironolactone ($P = 0.002$) and thiazides ($P = 0.010$), higher preoperative level of blood platelet ($P = 0.033$) and albumin ($P < 0.001$), lower preoperative levels of white blood cells ($P = 0.001$), creatinine ($P < 0.001$) and AST ($P = 0.025$), and a different proportions of Donor/recipient sex ($P = 0.001$).

3.4. Univariate and multivariate analyses of Os

At the end of follow-up, 121 (26.3%) patients had died and 339 (73.7%) patients were alive. The Kaplan-Meier curve (Figure 4) shows the association between OS and ACR for all patients. Patients with high ACR levels had better survival than those with low ACR levels ($P < 0.001$). To identify the risk factors affecting postoperative OS, the Cox proportional hazard model was applied to the analysis. Univariable analysis indicated that recipient age ($P < 0.001$), the preoperative use of IABP ($P = 0.004$), RAAS ($P = 0.001$), and BB ($P = 0.016$), preoperative level of Hb ($P < 0.001$), BUN ($P = 0.004$), D-dimer ($P = 0.018$), Troponin ($P = 0.014$), TG ($P = 0.043$) and ACR ($P < 0.001$) were significant prognostic factors of OS (Table 2). Nextly, significant prognostic factors identified by univariate analysis were entered into the multivariate Cox proportional hazards model. The results showed that recipient age ($P = 0.005$), the use of IABP ($P = 0.008$) and RAAS ($P = 0.014$), preoperative level of D-dimer ($P = 0.041$) and ACR ($P = 0.019$) were significant independent predictors of OS (Table 2).

3.5. Univariate and multivariate analysis of postoperative clinical events

A total of 17 surgery-related adverse clinical events occurred during the in-hospital posttransplant period, listed in Table 3. The result showed that lower levels of ACR tended to lead to more use of postoperative CRRT ($P < 0.001$) and IABP ($P = 0.001$), more respiratory complications ($P = 0.001$), liver injury ($P = 0.005$), kidney injury ($P = 0.001$), postoperative infection ($P = 0.001$), septic shock ($P = 0.012$), and in-hospital death ($P = 0.001$). We next performed univariate logistic regression analysis for these adverse clinical events (Supplementary Schedules S1–S8), and then the factors with $P < 0.05$ in univariate analysis were applied to multivariate logistic regression analysis. The results showed that lower preoperative ACR level was a significantly independent predictor of respiratory complications ($P = 0.043$), renal complications ($P = 0.007$), liver injury ($P = 0.019$), postoperative infection ($P = 0.003$) and in-hospital death ($P = 0.028$) (Table 4). What's more, higher age, less preoperative RAAS use and lower TG were independent risk factors of respiratory complication. Women and less RAAS use were independent risk factors of kidney injury. And less preoperative RAAS use was also associated with postoperative liver injury. Longer waiting time, diabetes mellitus and preoperative IABP were independently associated with in-hospital death. Moveover, smoking was an independent risk factor postoperative infection.

3.6. Prognostic nomogram for OS

A nomogram (Figure 5) integrating was constructed based on five prognostic variables (age, IABP, RAAS, D-dimer, and ACR) from the univariate and multivariate Cox regression results. A Nomogram with ACR had a concordance index (C-index) of 0.671 compared with 0.631 without ACR. The calibration plot (Figure 6) showed good consistency between the nomogram predictions and actual observations of survival at 1- or 5- years.

TABLE 1 Baseline patient characteristics based on ACR.

Recipient		Low (<37.54)	High (>37.54)	*P*
	Male, %	173 (87.4)	186 (71.0)	<0.001
	Age, years	50.50 [39.25, 57.00]	46.00 [34.00, 53.00]	<0.001
	BMI, Kg/m^2	23.39 [20.50, 25.51]	22.73 [19.63, 25.39]	0.079
	History of smoking, %	87 (43.9)	105 (40.1)	0.405
	Diagnosis, %			0.091
	Non-Ischemic cardiomyopathy	134 (67.7)	156 (59.5)	
	Ischemic cardiomyopathy	38 (19.2)	48 (18.3)	
	Congenital	5 (2.5)	14 (5.3)	
	Others	21 (10.6)	44 (16.8)	
	Diabetes mellitus, %	27 (18.2)	39 (18.6)	0.937
	Previous cardiac surgery, %	53 (26.8)	76 (29.0)	0.596
	Hypertension, %	39 (21.8)	30 (12.9)	0.017
	chronic kidney disease, %	25 (12.7)	3 (1.2)	<0.001
	interventricular septum, cm	0.90 [0.80, 1.00]	0.90 [0.80, 1.00]	0.568
	LVEF, %	16.10 [12.00, 26.90]	16.25 [12.00, 22.38]	0.412
	Waiting time, days	26.00 [19.00, 37.00]	27.00 [19.00, 35.00]	0.700
	Recipient blood-type, %			0.621
	A	62 (31.3)	94 (35.9)	
	B	56 (28.3)	73 (27.9)	
	O	69 (34.8)	78 (29.8)	
	AB	11 (5.6)	17 (6.5)	
	Preoperative Therapy			
	ECMO, %	4 (2.0)	2 (0.8)	0.410
	IABP, %	4 (2.0)	4 (1.5)	0.730
	RAAS antagonist, %	84 (42.4)	102 (38.9)	0.450
	BB, %	135 (68.2)	179 (68.3)	0.975
	CCB, %	17 (15.7)	16 (10.9)	0.254
	Loop diuretics, %	188 (96.9)	247 (96.1)	0.650
	Spironolactone, %	142 (74.0)	216 (85.7)	0.002
	Thiazides, %	4 (2.2)	19 (8.0)	0.010
	Preoperative Blood Index			
	Hb, g/L	132.50 [120.25, 150.50]	140.00 [129.00, 148.00]	0.115
	WBC, G/L	6.70 [5.03, 8.76]	5.89 [4.56, 7.52]	0.001
	PLT, G/L	163.00 [129.75, 212.50]	178.50 [139.00, 222.25]	0.033
	Albumin, mg/dl	37.90 [35.83, 40.58]	40.70 [37.73, 42.90]	<0.001
	Creatinine, mg/dl	110.40 [97.80, 129.20]	76.45 [67.93, 85.98]	<0.001
	Bilirubin, mg/dl	21.50 [14.75, 33.15]	21.15 [13.83, 33.88]	0.267
	AST, IU/L	29.50 [21.00, 43.50]	28.00 [20.00, 35.50]	0.025
	ALT, IU/L	30.50 [17.00, 57.00]	25.00 [16.25, 42.00]	0.065
	LDL, mmol/L	2.19 [1.71, 2.85]	2.26 [1.72, 2.81]	0.982
	Troponin, ng/L	29.20 [0.01, 101.90]	16.00 [0.00, 95.23]	0.310
	TG, mmol/L	0.99 [0.73, 1.24]	1.09 [0.82, 1.49]	0.362
Donor	Age, years	38.00 [26.00, 45.00]	36.00 [24.00, 45.50]	0.599
	Male, %	175 (88.4)	225 (85.9)	0.429
	Ischemia time, min	358.00 [297.75, 396.25]	345.00 [290.50, 392.50]	0.257
Donor/recipient	Blood-type same, %	125 (63.1)	163 (62.2)	0.840
	Donor/recipient BMI	0.97 [0.86, 1.12]	1.00 [0.88, 1.17]	0.135
	Donor/recipient age	0.74 [0.53, 0.89]	0.77 [0.55, 1.00]	0.125
	Donor/recipient sex, %			0.001
	Male/male	157 (79.3)	169 (65.0)	
	Male/female	18 (9.1)	54 (20.8)	
	Female/male	16 (8.1)	16 (6.2)	
	Female/female	7 (3.5)	21 (8.1)	

Continuous variables are presented as median and interquartile range. Categorical variables are presented as number and percentage. *P* values are 2-sided, with $P < 0.05$ considered statistically significant.

BMI, body mass index; LVEF, left ventricular ejection fraction; ECMO, extracorporeal membrane oxygenation; IABP, implantable intra-aortic balloon pump; RAAS, renin-angiotensin-aldosterone system; BB, beta-blockers; CCB, calcium channel blocker; Hb, hemoglobin; WBC, white blood cell count; PLT, blood platelet; Cr, creatinine; AST, glutamic oxaloacetic transaminase; ALT, alanine aminotransferase; LDL, low-density lipoprotein; TG, triglyceride.

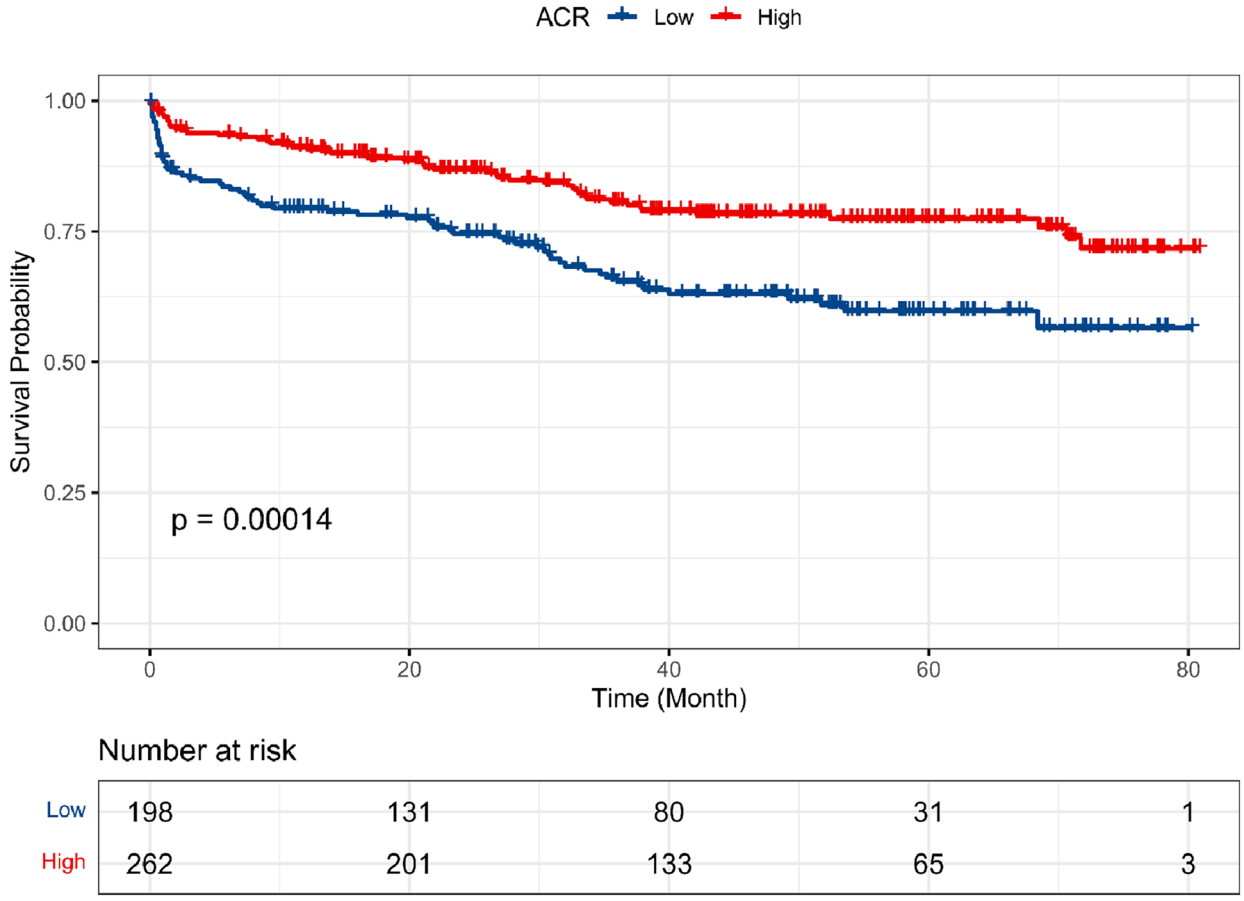

FIGURE 4
Kaplan–Meier survival curves for OS according to ACR. The low-ACR value group. Exhibited worse OS than high-ACR value group ($P < 0.001$).

4. Discussion

Heart failure is a common disease and the best treatment for patients with end-stage heart failure is HTx (1, 3). Meanwhile, many factors can predict the outcomes of HTx. For example, recent studies have pointed out that ACR as a preoperative indicator can predict the prognosis of cardiovascular disease (12–14). In this retrospective study, we evaluated the effect of ACR on the prognosis of HTx and found that high levels of ACR were a protective factor after HTx. Meanwhile, five possible prognostic factors (age, the use of IABP, RAAS, D-dimer, and ACR) were identified according to multivariable Cox regression analysis. Furthermore, multivariate logistic regression analysis showed that low levels of ACR are associated with several post-transplant complications, including respiratory complications, renal complications, liver injury, and in-hospital death. In addition, a visual nomogram was created in light of clinical variables and ACR, which helped to improve individual prognosis prediction accuracy.

Albumin is an important serum protein and has a wide range of physiological functions, such as immune regulation, endothelial stabilization, antioxidant effects, and binding to a variety of drugs, toxins, and other molecules (7). Albumin can also be used as a biomarker for many diseases, such as cancer, ischemia, obesity, severe acute graft-vs.-host disease, and diseases requiring monitoring of glycemic control (18). Specifically, numerous studies have demonstrated a strong association between serum albumin levels and the prognosis of cardiovascular diseases, such as atherosclerosis, myocardial infarction, and heart failure (19, 20). Moreover, Tomoko et al. proposed the effect of pre-transplant albumin levels on 1-year survival after heart transplantation in a retrospective study (21).

Creatinine was used as an index of renal function, which reflects not only renal excretion but also creatinine production (22, 23). In most genome-wide association studies, creatinine-based assessment of renal function (eGFR crea) has been used to define renal disease (24). Since the link between chronic kidney disease and cardiovascular disease was first described, numerous research suggested that chronic kidney disease greatly increases the risk of cardiovascular disease. This is partly because abnormal renal function leads to abnormal blood pressure, lipids, inflammatory responses, and increased activity of the renin-angiotensin system (25). Apart from preoperative renal disease, acute kidney injury is often a common complication after heart transplantation (26). It is associated with increased short- and long-term morbidity and mortality (27). Therefore, an important

TABLE 2 Univariate and multivariate Cox proportional hazards regression models for overall survival in patients with heart transplantation.

Variables	Univariate analysis		Multivariate analysis	
	HR (95%CI)	*P* value	HR (95%CI)	*P* value
Sex	1.458 (0.981–2.168)	0.062		
Age, years	1.030 (1.014–1.047)	<0.001	1.023 (1.006–1.040)	0.005
Recipient BMI, Kg/m^2	1.017 (0.989–1.046)	0.228		
History of smoking	0.778 (0.537–1.128)	0.185		
History of heavy drinking	0.740 (0.475–1.152)	0.182		
Waiting time, days	0.993 (0.980–1.005)	0.258		
Diagnosis		0.458		
Non-Ischemic cardiomyopathy	Reference			
Ischemic cardiomyopathy	0.755 (0.447–1.273)	0.291		
Congenital	0.558 (0.176–1.768)	0.321		
others	1.143 (0.700–1.865)	0.594		
Recipient blood-type		0.061		
A	Reference			
B	1.293 (0.804–2.080)	0.290		
O	1.680 (1.085–2.602)	0.020		
AB	0.664 (0.236–1.872)	0.439		
Donor/recipient BMI	1.528 (0.779–2.997)	0.218		
Donor/recipient age	0.684 (0.418–1.121)	0.132		
Donor/recipient sex		0.149		
Male/male	Reference			
Male/female	1.621 (1.031–2.548)	0.036		
Female/male	1.481 (0.765–2.865)	0.244		
Female/female	1.385 (0.694–2.765)	0.356		
Donor/recipient blood-type same	0.844 (0.581–1.227)	0.374		
Diabetes mellitus	1.366 (0.814–2.292)	0.237		
Previous cardiac surgery	1.314 (0.899–1.919)	0.158		
hypertension	0.981 (0.584–1.647)	0.942		
Ischemia time, min	1.000 (0.999–1.002)	0.590		
Preoperative Therapy				
ECMO	1.283 (0.178–9.227)	0.805		
IABP	4.333 (1.586–11.839)	0.004	4.086 (1.440–11.600)	0.008
ICD	1.182 (0.551–2.536)	0.668		
CRTD	0.856 (0.272–2.696)	0.791		
RAAS	0.527 (0.357–0.780)	0.001	0.593 (0.391–0.899)	0.014
BB	0.641 (0.446–0.922)	0.016	0.837 (0.568–1.234)	0.370
CCB	1.174 (0.581–2.374)	0.655		
Loop diuretics	0.725 (0.296–1.778)	0.483		
Spironolactone	0.826 (0.526–1.298)	0.407		
Thiazides	1.482 (0.687–3.201)	0.316		
Preoperative Blood Index				
Hb, g/L	0.989 (0.982–0.995)	<0.001	0.993 (0.985–1.000)	0.064
WBC, G/L	1.012 (0.988–1.037)	0.323		
Bilirubin, mg/dl	1.005 (0.997–1.013)	0.203		
BUN, mmol/L	1.054 (1.017–1.091)	0.004	1.004 (0.958–1.053)	0.856
AST, IU/L	1.000 (1.000–1.001)	0.216		
ALT, IU/L	1.000 (1.000–1.001)	0.903		
LDL, mmol/L	1.158 (0.958–1.399)	0.130		
D-dimer, mg/L	1.028 (1.005–1.052)	0.018	1.025 (1.001–1.049)	0.041
Troponin, ng/ml	1.000 (1.000–1.000)	0.014	1.000 (1.000–1.000)	0.094
TG, mmol/L	0.737 (0.549–0.991)	0.043	0.825 (0.606–1.122)	0.220
ACR level	0.504 (0.352–0.722)	<0.001	0.617 (0.412–0.923)	0.019

95%CI, 95% confidence interval; HR, hazard ratio.

Continuous variables are presented as median and interquartile range. Categorical variables are presented as numbers and percentages. *P* values are 2-sided, with $P < 0.05$ considered statistically significant.

BMI, body mass index; ECMO, extracorporeal membrane oxygenation; IABP, implantable intra-aortic balloon pump; ICD, implantable cardioverter defibrillator; CRTD, cardiac resynchronization therapy defibrillator; RAAS, renin-angiotensin-aldosterone system; BB, beta-blockers; CCB, calcium channel blocker; Hb, hemoglobin; WBC, white blood cell count; PLT, blood platelet; Cr, creatinine; AST, glutamic oxaloacetic transaminase; ALT, Alanine aminotransferase; LDL, low-density lipoprotein; TG, triglyceride; ACR, the ratio of serum albumin to creatinine.

TABLE 3 Early postoperative events in the in-hospital post-transplant period by pretransplant ACR.

Variables	All	Low (<37.54)	High (>37.54)	*P*
Postoperative ICU stay, hours	216 [162,294]	223 [168, 331]	213 [159, 275]	0.326
Total postoperative stay, days	35 [26,49]	35 [27, 54]	35 [26, 47]	0.076
Postoperative CRRT (%)	67 (14.6)	43 (22.3)	24 (9.3)	<0.001
Postoperative IABP (%)	191 (41.5)	99 (50.8)	92 (35.5)	0.001
Postoperative ECMO (%)	33 (7.2)	19 (9.9)	14 (5.4)	0.072
Respiratory complication (%)	278 (60.4)	137 (69.2)	141 (53.8)	0.001
Neurological complications (%)	33 (7.2)	17 (8.6)	16 (6.1)	0.308
Hematological complications (%)	19 (4.1)	11 (5.6)	8 (3.1)	0.182
Kidney injury (%)	73 (15.9)	44 (22.2)	29 (11.1)	0.001
Liver injury (%)	35 (7.6)	23 (11.6)	12 (4.6)	0.005
Infection (%)	234 (50.9)	116 (64.4)	118 (48.6)	0.001
Hyperglucosemia (%)	42 (9.1)	20 (10.1)	22 (8.4)	0.530
Hypertension (%)	25 (5.4)	11 (5.6)	14 (5.3)	0.921
Septic shock (%)	13 (2.8)	10 (5.1)	3 (1.1)	0.012
Secondary thoracotomy (%)	19 (4.1)	11 (5.7)	8 (3.1)	0.178
Acute rejection (%)	9 (2.0)	3 (1.5)	6 (2.3)	0.805
Death (%)	24 (5.2)	18 (9.1)	6 (2.3)	0.001

Continuous variables are presented as median and interquartile range. Categorical variables are presented as numbers and percentages. *P* values are 2-sided, with $P < 0.05$ considered statistically significant.
CRRT, continuous renal replacement therapy; IABP, implantable intra-aortic balloon pump; ECMO, extracorporeal membrane oxygenation; sACR, the ratio of serum albumin to creatinine.

TABLE 4 Multivariable analysis for early postoperative events following heart transplantation.

Early Postoperative Events	ACR	
	OR (95%CI)	*P* value
Prolonged Postoperative ICU Stay	0.835 (0.526–1.327)	0.446
Respiratory Complications	0.629 (0.402–0.985)	0.043
Kidney Complications	0.424 (0.227–0.790)	0.007
Infection	0.540 (0.358–0.816)	0.003
Liver Injury	0.394 (0.182–0.856)	0.019
Septic Shock	0.257 (0.059–1.117)	0.070
In-hospital death	0.250 (0.073–0.863)	0.028

ACR, the ratio of serum albumin to creatinine.

next step will be to investigate preoperative factors affecting AKI after heart transplantation.

The possibility of the correlation between ACR and the prognosis of HTx might be as follows: Firstly, Low serum albumin is often a marker of poor liver function (28). Likewise, in our study, we found that the preoperative ACR level was closely related to the occurrence of postoperative liver injury. In addition, albumin can improve the prognosis of heart transplantation by regulating systemic inflammatory response and immune response (7). Physiological concentrations of albumin attenuate inflammation by selectively inhibiting TNFα-induced upregulation of VCAM-1 expression and monocyte adhesion (29). Moreover,

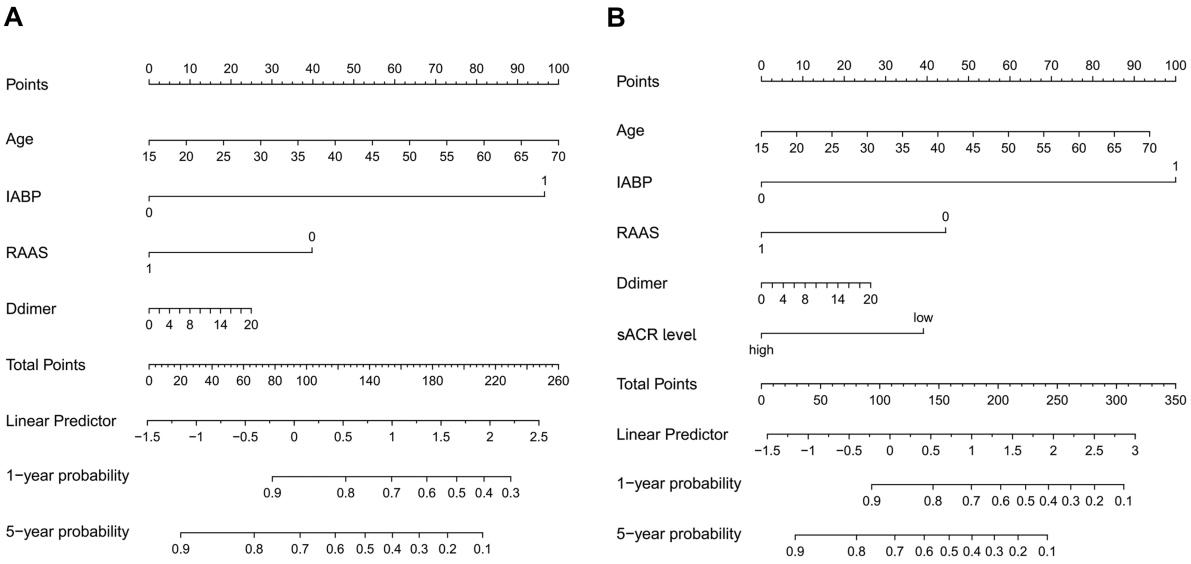

FIGURE 5
The nomogram for predicting 1-year and 5-year OS in patients who underwent HTx without ACR [(A), C-index = 0.631] and with ACR [(B), C-index = 0.671].

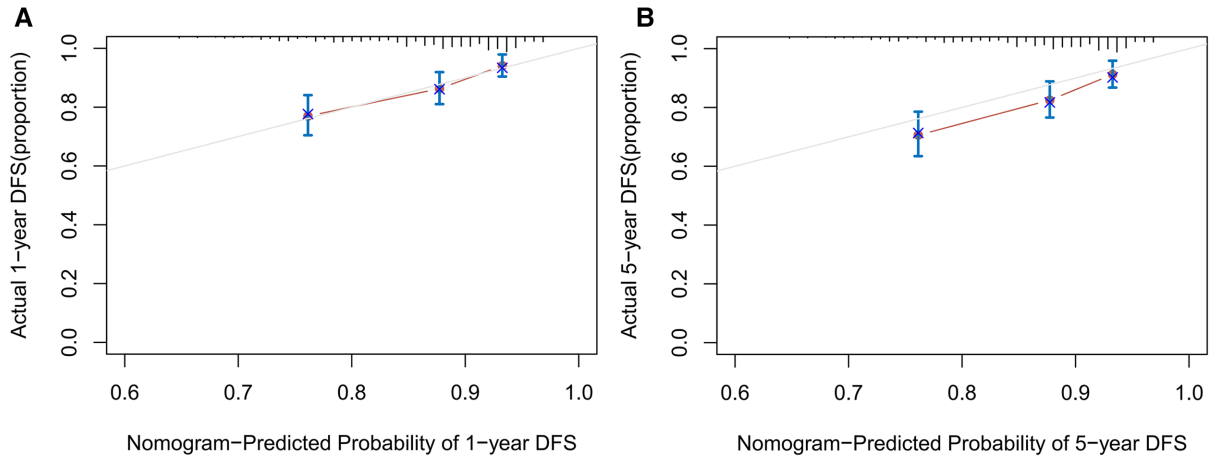

FIGURE 6
The calibration curves for predicting 1-year (A) and 5-year (B) OS of patients after HTx. Each point in the plot represents a group of patients, with the nomogram predicted probability of survival shown on x-axis and actual survival proportion shown on y-axis.

albumin inhibits histone-induced platelet aggregation and thrombus formation by binding to histones (30). These help explain why a low preoperative ACR level is associated with a higher incidence of septic shock. Besides, it is well established that oxidative stress is a common risk factor in various diseases, such as diabetes, inflammation, and cardiovascular disease. Oxidative stress generated by excessive reactive oxygen species (ROS) promotes cardiovascular disease (31). For example, starting point of atherosclerosis is considered to be oxidative stress, which facilitates key molecular events, such as oxidative modification of lipoproteins and phospholipids, endothelial cell activation, and macrophage infiltration/activation (32). Importantly, albumin exerts its antioxidant function by binding and neutralizing free metals such as copper and iron at its N-terminal site and specifically regulates cellular glutathione levels (7). Secondly, creatinine is a waste product of muscle metabolism (33). Produced at a continuous rate by creatine metabolism and excreted without tubular reabsorption, it is used as a marker of GFR (34). It is well-known that the reduction of GFR is now a recognized risk factor for cardiovascular disease (CVD) and chronic kidney disease (35, 36). Similarly, our results showed that low preoperative ACR levels are associated with a higher risk for postoperative Kidney Complications and In-hospital death. Besides, many studies have pointed out that chronic kidney disease often leads to dyslipidemia and inflammation, which leads to the hardening of the aorta and the reduction of coronary reserve (25, 37). Furthermore, kidney disease may cause remodeling of the ventricle through hypertension, renal anemia, and vascular stiffness, thus leading to hypertrophy of the left ventricle (25, 37). These biological processes may help explain associations between the level of ACR and the prognosis of HTx.

As far as we know, it is the first study to assess the role of ACR in HTx outcomes. Our study confirmed that preoperative ACR was a novel and promising indicator that independently predicts the outcomes of HTx. This investigation gives us some clues about preoperative interventions to reduce postoperative complications, such as albumin supplements (38–40).

However, there are some limitations of this study that should be considered. Firstly, this is a retrospective and observational study, which ignores the progression of the disease and has inherent risks of information bias. Secondly, the sample size of this study was small ($n = 460$) and the follow-up period was relatively short. Thirdly, preoperative frailty may have effect on the study results. Future studies about heart transplantation should consider this issue. What's more, null of the subjects in our study developed early graft failure, so the evaluation of early graft failure could not be performed. Lastly, we did not obtain cytokines, markers of glucose metabolism, or serum inflammatory markers, all of which may affect the prognosis of heart transplantation.

Data availability statement

The data analyzed in this study is subject to the following licenses/restrictions: a portion of the data, models, or code generated or used during the study is proprietary or confidential in nature and may only be provided with restrictions (e.g., anonymized data). Requests to access these datasets should be directed to ND, 1986xh0694@hust.edu.cn.

Ethics statement

This retrospective study has been approved by the Committee of Tongji Medical College. All patients signed the informed consent in light of the Declaration of Helsinki.

Author contribution

QS, DY and YZ: were in charge of collecting and analyzing data and writing this manuscript. XQ, YZ, LX, CJ and QZ: contributed to the discussion and provided additional advice. SC, JS and ND: gave their valuable and professional suggestions and guidance in

organizing and drafting this manuscript. All authors contributed to the article and approved the submitted version.

Funding

This study was supported by the National Natural Science Foundation of China (81974034).

Acknowledgments

This research is attributed to the Department of Cardiovascular Surgery, Union Hospital, Tongji Medical College, Huazhong University of Science and Technology. We are grateful to Guohua Wang, Jing Zhang, and Xiusi Xiongti for their generous assistance.

Conflict of interest

The authors declare that the research was conducted in the absence of any commercial or financial relationships that could be construed as a potential conflict of interest.

Publisher's note

Supplementary material

The Supplementary Material for this article can be found online at: https://www.frontiersin.org/articles/10.3389/fcvm.2023.1210278/full#supplementary-material

References

1. Bansal N, Szpiro A, Reynolds K, Smith DH, Magid DJ, Gurwitz JH, et al. Long-term outcomes associated with implantable cardioverter defibrillator in adults with chronic kidney disease. *JAMA Intern Med.* (2018) 178(3):390–8. doi: 10.1001/jamainternmed.2017.8462

2. Abraham WT, Ponikowski P, Brueckmann M, Zeller C, Macesic H, Peil B, et al. Rationale and design of the EMPERIAL-preserved and EMPERIAL-reduced trials of empagliflozin in patients with chronic heart failure. *Eur J Heart Fail.* (2019) 21 (7):932–42. doi: 10.1002/ejhf.1486

3. Tatum R, Briasoulis A, Tchantchaleishvili V, Massey HT. Evaluation of donor heart for transplantation. *Heart Fail Rev.* (2022) 27(5):1819–27. doi: 10.1007/s10741-021-10178-7

4. Grady KL, White-Williams C, Naftel D, Costanzo MR, Pitts D, Rayburn B, et al. Are preoperative obesity and cachexia risk factors for post heart transplant morbidity and mortality: a multi-institutional study of preoperative weight-height indices. Cardiac transplant research database (CTRD) group. *J Heart Lung Transplant.* (1999) 18(8):750–63. doi: 10.1016/S1053-2498(99)00035-2

5. O'Connor MJ, Glatz AC, Rossano JW, Shaddy RE, Ryan R, Ravishankar C, et al. Cumulative effect of preoperative risk factors on mortality after pediatric heart transplantation. *Ann Thorac Surg.* (2018) 106(2):561–6. doi: 10.1016/j.athoracsur.2018.03.044

6. Kim D, Choi JO, Cho YH, Sung K, Oh J, Cho HJ, et al. Impact of preoperative renal replacement therapy on the clinical outcome of heart transplant patients. *Sci Rep.* (2021) 11(1):13398. doi: 10.1038/s41598-021-92800-0

7. Spinella R, Sawhney R, Jalan R. Albumin in chronic liver disease: structure, functions and therapeutic implications. *Hepatol Int.* (2016) 10(1):124–32. doi: 10.1007/s12072-015-9665-6

8. Prenner SB, Pillutla R, Yenigalla S, Gaddam S, Lee J, Obeid MJ, et al. Serum albumin is a marker of myocardial fibrosis, adverse pulsatile aortic hemodynamics, and prognosis in heart failure with preserved ejection fraction. *J Am Heart Assoc.* (2020) 9(3):e014716. doi: 10.1161/JAHA.119.014716

9. Habib PJ, Patel PC, Hodge D, Chimato N, Yip DS, Hosenpud JD, et al. Pre-orthotopic heart transplant estimated glomerular filtration rate predicts post-transplant mortality and renal outcomes: an analysis of the UNOS database. *J Heart Lung Transplant.* (2016) 35(12):1471–9. doi: 10.1016/j.healun.2016.05.028

10. Kato TS, Lippel M, Naka Y, Mancini DM, Schulze PC. Post-transplant survival estimation using pre-operative albumin levels. *J Heart Lung Transplant.* (2014) 33 (5):547–8. doi: 10.1016/j.healun.2014.01.921

11. Lassnigg A, Schmidlin D, Mouhieddine M, Bachmann LM, Druml W, Bauer P, et al. Minimal changes of serum creatinine predict prognosis in patients after cardiothoracic surgery: a prospective cohort study. *J Am Soc Nephrol.* (2004) 15 (6):1597–605. doi: 10.1097/01.ASN.0000130340.93930.DD

12. Liu H, Zhang J, Yu J, Li D, Jia Y, Cheng Y, et al. Prognostic value of serum albumin-to-creatinine ratio in patients with acute myocardial infarction: results from the retrospective evaluation of acute chest pain study. *Medicine.* (2020) 99(35): e22049. doi: 10.1097/MD.0000000000022049

13. Sanchez RA, Sanchez MJ, Ramirez AJ. Renal function, albumin-creatinine ratio and pulse wave velocity predict silent coronary artery disease and renal outcome in type 2 diabetic and prediabetic subjects. *Curr Hypertens Rev.* (2021) 17(2):131–6. doi: 10.2174/1573402116999201210194817

14. Turkyilmaz E, Ozkalayci F, Birdal O, Karagoz A, Tanboga IH, Tanalp AC, et al. Serum albumin to creatinine ratio and short-term clinical outcomes in patients with ST-elevation myocardial infarction. *Angiology.* (2022) 73(9):809–17. doi: 10.1177/00033197221089423

15. Arar NH, Voruganti VS, Nath SD, Thameem F, Bauer R, Cole SA, et al. A genome-wide search for linkage to chronic kidney disease in a community-based sample: the SAFHS. *Nephrol Dial Transplant.* (2008) 23(10):3184–91. doi: 10.1093/ndt/gfn215

16. Alverdy JC, Hyman N, Gilbert J. Re-examining causes of surgical site infections following elective surgery in the era of asepsis. *Lancet Infect Dis.* (2020) 20(3):e38–43. doi: 10.1016/S1473-3099(19)30756-X

17. Steeg L T, Dominguez-Andres J, Netea MG, Joosten LAB, van Crevel R. Trained immunity as a preventive measure for surgical site infections. *Clin Microbiol Rev.* (2021) 34(4):e0004921. doi: 10.1128/CMR.00049-21

18. Fanali G, di Masi A, Trezza V, Marino M, Fasano M, Ascenzi P. Human serum albumin: from bench to bedside. *Mol Aspects Med.* (2012) 33(3):209–90. doi: 10.1016/j.mam.2011.12.002

19. Ronit A, Kirkegaard-Klitbo DM, Dohlmann TL, Lundgren J, Sabin CA, Phillips AN, et al. Plasma albumin and incident cardiovascular disease: results from the CGPS and an updated meta-analysis. *Arterioscler Thromb Vasc Biol.* (2020) 40(2):473–82. doi: 10.1161/ATVBAHA.119.313681

20. Deo R, Norby FL, Katz R, Sotoodehnia N, Adabag S, DeFilippi CR, et al. Development and validation of a sudden cardiac death prediction model for the general population. *Circulation.* (2016) 134(11):806–16. doi: 10.1161/CIRCULATIONAHA.116.023042

21. Kato TS, Cheema FH, Yang J, Kawano Y, Takayama H, Naka Y, et al. Preoperative serum albumin levels predict 1-year postoperative survival of patients undergoing heart transplantation. *Circ Heart Fail.* (2013) 6(4):785–91. doi: 10.1161/CIRCHEARTFAILURE.111.000358

22. Nielsen LR, Damm P, Mathiesen ER. Improved pregnancy outcome in type 1 diabetic women with microalbuminuria or diabetic nephropathy: effect of intensified antihypertensive therapy? *Diabetes Care.* (2009) 32(1):38–44. doi: 10.2337/dc08-1526

23. Levey AS, Perrone RD, Madias NE. Serum creatinine and renal function. *Annu Rev Med*. (1988) 39:465–90. doi: 10.1146/annurev.me.39.020188.002341

24. Ko YA, Yi H, Qiu C, Huang S, Park J, Ledo N, et al. Genetic-variation-driven gene-expression changes highlight genes with important functions for kidney disease. *Am J Hum Genet*. (2017) 100(6):940–53. doi: 10.1016/j.ajhg.2017.05.004

25. Gansevoort RT, Correa-Rotter R, Hemmelgarn BR, Jafar TH, Heerspink HJ, Mann JF, et al. Chronic kidney disease and cardiovascular risk: epidemiology, mechanisms, and prevention. *Lancet*. (2013) 382(9889):339–52. doi: 10.1016/S0140-6736(13)60595-4

26. Goren O, Matot I. Perioperative acute kidney injury. *Br J Anaesth*. (2015) 115 (Suppl 2):ii3–14. doi: 10.1093/bja/aev380

27. Lei C, Berra L, Rezoagli E, Yu B, Dong H, Yu S, et al. Nitric oxide decreases acute kidney injury and stage 3 chronic kidney disease after cardiac surgery. *Am J Respir Crit Care Med*. (2018) 198(10):1279–87. doi: 10.1164/rccm.201710-2150OC

28. Brahmer JR, Dahlberg SE, Gray RJ, Schiller JH, Perry MC, Sandler A, et al. Sex differences in outcome with bevacizumab therapy: analysis of patients with advanced-stage non-small cell lung cancer treated with or without bevacizumab in combination with paclitaxel and carboplatin in the eastern cooperative oncology group trial 4599. *J Thorac Oncol*. (2011) 6(1):103–8. doi: 10.1097/JTO.0b013e3181fa8efd

29. Zhang WJ, Frei B. Albumin selectively inhibits TNF alpha-induced expression of vascular cell adhesion molecule-1 in human aortic endothelial cells. *Cardiovasc Res*. (2002) 55(4):820–9. doi: 10.1016/S0008-6363(02)00492-3

30. Lam FW, Cruz MA, Leung HC, Parikh KS, Smith CW, Rumbaut RE. Histone induced platelet aggregation is inhibited by normal albumin. *Thromb Res*. (2013) 132(1):69–76. doi: 10.1016/j.thromres.2013.04.018

31. Shao D, Oka S, Liu T, Zhai P, Ago T, Sciarretta S, et al. A redox-dependent mechanism for regulation of AMPK activation by Thioredoxin1 during energy starvation. *Cell Metab*. (2014) 19(2):232–45. doi: 10.1016/j.cmet.2013.12.013

32. Forstermann U, Xia N, Li H. Roles of vascular oxidative stress and nitric oxide in the pathogenesis of atherosclerosis. *Circ Res*. (2017) 120(4):713–35. doi: 10.1161/CIRCRESAHA.116.309326

33. Bulka CM, Mabila SL, Lash JP, Turyk ME, Argos M. Arsenic and obesity: a comparison of urine dilution adjustment methods. *Environ Health Perspect*. (2017) 125(8):087020. doi: 10.1289/EHP1202

34. Nedergaard A, Sun S, Karsdal MA, Henriksen K, Kjaer M, Lou Y, et al. Type VI collagen turnover-related peptides-novel serological biomarkers of muscle mass and anabolic response to loading in young men. *J Cachexia Sarcopenia Muscle*. (2013) 4 (4):267–75. doi: 10.1007/s13539-013-0114-x

35. Chronic Kidney Disease Prognosis C, Matsushita K, van der Velde M, Astor BC, Woodward M, Levey AS, et al. Association of estimated glomerular filtration rate and albuminuria with all-cause and cardiovascular mortality in general population cohorts: a collaborative meta-analysis. *Lancet*. (2010) 375(9731):2073–81. doi: 10.1016/S0140-6736(10)60674-5

36. Levey AS, de Jong PE, Coresh J, El Nahas M, Astor BC, Matsushita K, et al. The definition, classification, and prognosis of chronic kidney disease: a KDIGO controversies conference report. *Kidney Int*. (2011) 80(1):17–28. doi: 10.1038/ki.2010.483

37. Pannier B, Guerin AP, Marchais SJ, Safar ME, London GM. Stiffness of capacitive and conduit arteries: prognostic significance for end-stage renal disease patients. *Hypertension*. (2005) 45(4):592–6. doi: 10.1161/01.HYP.0000159190.71253.c3

38. Hsich EM, Thuita L, McNamara DM, Rogers JG, Valapour M, Goldberg LR, et al. Variables of importance in the scientific registry of transplant recipients database predictive of heart transplant waitlist mortality. *Am J Transplant*. (2019) 19(7):2067–76. doi: 10.1111/ajt.15265

39. Lee EH, Kim WJ, Kim JY, Chin JH, Choi DK, Sim JY, et al. Effect of exogenous albumin on the incidence of postoperative acute kidney injury in patients undergoing off-pump coronary artery bypass surgery with a preoperative albumin level of less than 4.0 g/dl. *Anesthesiology*. (2016) 124(5):1001–11. doi: 10.1097/ALN.0000000000001051

40. Liang WQ, Zhang KC, Li H, Cui JX, Xi HQ, Li JY, et al. Preoperative albumin levels predict prolonged postoperative ileus in gastrointestinal surgery. *World J Gastroenterol*. (2020) 26(11):1185–96. doi: 10.3748/wjg.v26.i11.1185

Frontiers in
Cardiovascular Medicine

Innovations and improvements in cardiovascular treatment and practice

Focuses on research that challenges the status quo of cardiovascular care, or facilitates the translation of advances into new therapies and diagnostic tools.

Discover the latest Research Topics

See more →

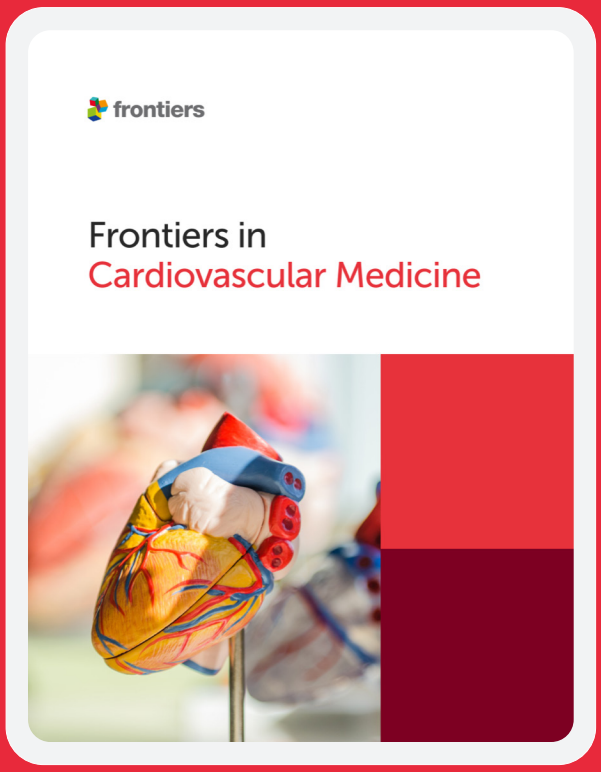

Frontiers

Avenue du Tribunal-Fédéral 34
1005 Lausanne, Switzerland
frontiersin.org

Contact us

+41 (0)21 510 17 00
frontiersin.org/about/contact